United States Department of the Interior

BUREAU OF RECLAMATION
P.O. Box 25007
Denver, CO 80225-0007

IN REPLY REFER TO:

86-68110
2.2.4.22

DEC 1 7 2018

MEMORANDUM

To: Technology Development Program Manager, Dam Safety Office
Attn: 84-44000 (LKrosley)

From: Hillery Venturini, P.E., Civil Engineer P.E.
Waterways and Concrete Dams Group 1

Subject: Transmittal of Dam Safety Report DSO-19-13: Evaluation of Numerical Models and Input Parameters in the Analysis of Concrete Dams, A Summary Report of the United States Society on Dams (USSD) Workshop

Attached for your use is Report DSO-19-13, Evaluation of Numerical Models and Input Parameters in the Analysis of Concrete Dams, A Summary Report of the USSD Workshop, that has been prepared by the Technical Service Center at the request of the Dam Safety Office. The report will be available in Adobe Acrobat Format on the Dam Safety website and will be loaded into DSDaMS.

If you have any questions, please contact me at 303-445-3281 or via email at hventurini@usbr.gov.

Hard copy CC recipients:
84-44000 (Dam Safety File Station)
(w/att)

Electronic copy CC recipients:
DSDaMS@usbr.gov
OfficialRecordsArchive@usbr.gov
KBartojay@usbr.gov
LKrosley@usbr.gov
DHanneman@usbr.gov
SDominic@usbr.gov
JSalamon@usbr.gov

RECLAMATION
Managing Water in the West

Report DSO-19-13

Evaluation of Numerical Models and Input Parameters in the Analysis of Concrete Dams

A Summary Report of the USSD Workshop, Miami, May 3, 2018

U.S. Department of the Interior
Bureau of Reclamation
Technical Service Center
Denver, Colorado

December 2018

MISSION STATEMENTS

The U.S. Department of the Interior protects America's natural resources and heritage, honors our cultures and tribal communities, and supplies the energy to power our future.

The mission of the Bureau of Reclamation is to manage, develop, and protect water and related resources in an environmentally and economically sound manner in the interest of the American public.

Disclaimer:

Any use of trade names and trademarks in this document is for descriptive purposes only and does not constitute endorsement. The information contained herein regarding commercial products or firms may not be used for advertising or promotional purposes and is not to be construed as an endorsement of any product or firm.

The public reporting burden for this collection of information is estimated to average 1 hour per response, including the time for reviewing instructions, searching existing data sources, gathering and maintaining the data needed, and completing and reviewing the collection of information. Send comments regarding this burden estimate or any other aspect of this collection of information, including suggestions for reducing the burden, to Department of Defense, Washington Headquarters Services, Directorate for Information Operations and Reports (0704-0188), 1215 Jefferson Davis Highway, Suite 1204, Arlington, VA 22202-4302. Respondents should be aware that notwithstanding any other provision of law, no person shall be subject to any penalty for failing to comply with a collection of information if it does not display a currently valid OMB control number.
PLEASE DO NOT RETURN YOUR FORM TO THE ABOVE ADDRESS.

1. REPORT DATE December 2018	**2. REPORT TYPE** Final	**3. DATES COVERED** *2018*

4. TITLE AND SUBTITLE **Evaluation of Numerical Models and Input Parameters in the Anlysis of Concrete Dams - A Summary Report of the USSD Workshop, Miami, May 3, 2018**	**5a. CONTRACT NUMBER** **5b. GRANT NUMBER** **5c. PROGRAM ELEMENT NUMBER**
6. AUTHOR(S) Jerzy Salamon, Ph.D., P.E.	**5d. PROJECT NUMBER** **5e. TASK NUMBER** **5f. WORK UNIT NUMBER**
7. PERFORMING ORGANIZATION NAME(S) AND ADDRESS(ES) Bureau of Reclamation, Denver Federal Center, P.O. Box 25007, D-86-68110, Denver, CO, 80225	**8. PERFORMING ORGANIZATION REPORT NUMBER**
9. SPONSORING/MONITORING AGENCY NAME(S) AND ADDRESS(ES) Dam Safety Office, Bureau of Reclamation, Denver Federal Center, P.O. Box 25007, Denver, CO, 80225	**10. SPONSOR/MONITOR'S ACRONYM(S)** **11. SPONSOR/MONITOR'S REPORT NUMBER(S)**

12. DISTRIBUTION/AVAILABILITY STATEMENT
Unrestricted

13. SUPPLEMENTARY NOTE

14. ABSTRACT
The report summarizes the results of the benchmark studies presented during the workshop titled, "*Evaluation of Numerical Models and Input Parameters in the Analysis of Concrete Dams*" during the USSD Annual Conference and Exhibition in Miami, Florida on May 3, 2018.
A series of case studies, based on Pine Flat Dam, included a time history analysis for a linear concrete dam-foundation-reservoir model.

15. SUBJECT TERMS
Reclamation, nonlinear material models, concrete material models, Finite Element Method

16. SECURITY CLASSIFICATION OF: For public use			**17. LIMITATION OF ABSTRACT**	**18. NUMBER OF PAGES**	**19a. NAME OF RESPONSIBLE PERSON**
				351	Jerzy Salamon
a. REPORT	**b. ABSTRACT**	**c. THIS PAGE**			**19b. TELEPHONE NUMBER**
U	U	U			303-445-3219

Standard Form 298 (Rev. 8/98)
Prescribed by ANSI Std. Z39.18

BUREAU OF RECLAMATION

DSO-19-13

Evaluation of Numerical Models and Input Parameters in the Analysis of Concrete Dams - A Summary Report of the USSD Workshop, Miami, May 3, 2018

JERZY SALAMON Digitally signed by JERZY SALAMON
Date: 2018.12.17 11:14:23 -07'00'

Prepared by: Jerzy Salamon, Ph.D., P.E.

Waterways & Concrete Dams Group 1, 86-68110

HILLERY VENTURINI Digitally signed by HILLERY VENTURINI
Date: 2018.12.17 12:36:21 -07'00'

Checked by: Hillery Venturini, P.E.

Waterways & Concrete Dams Group 1, 86-68110

JERZY SALAMON Digitally signed by JERZY SALAMON
Date: 2018.12.17 11:14:59 -07'00'

Technical Approval: Jerzy Salamon, Ph.D., P.E.

Waterways & Concrete Dams Group 1, 86-68110

STEPHEN DOMINIC Digitally signed by STEPHEN DOMINIC
Date: 2018.12.17 12:23:18 -07'00'

Peer Review: Steve Dominic, P.E. Date

Waterways & Concrete Dams Group 1, 86-68110

REVISIONS					
Date	Description	Prepared	Checked	Technical approval	Peer review

Contents

1. DESCRIPTION OF THE THEME

1.1. Introduction

The United States Society on Dams (USSD) Committee on Concrete Dams and Earthquakes Committee organized a workshop during the USSD Annual Conference and Exhibition in Miami, Florida on May 3, 2018 titled, "*Evaluation of Numerical Models and Input Parameters in the Analysis of Concrete Dams.*" The purpose of this workshop was to investigate uncertainties in finite element (FE) analyses of concrete dams in a focused, systematic and controlled approach with collaborative participation from the dam industry and academia. The workshop organizing committee (Committee) formulated a series of case studies, based on Pine Flat Dam, which initiated with linear analysis models for the 2018 workshop. Case studies for the workshop were comprised of a base case and several alternative analysis models. Load cases for static, pulse, harmonic, and dynamic time history were considered.

1.2. Purpose

The purpose of developing the case studies is to establish a process for evaluating the analysis methods and developing a common understanding regarding the sensitivity of the FE analysis for concrete dams. Benchmark studies, performed in an arbitrary manner, may not produce desired results or clear conclusions for advancement. Likewise, little is gained if participants perform analyses with widely varying input parameters and get widely varying answers so that key factors cannot be clearly identified.

The ultimate goal is to identify key uncertainties causing differences in numerical analyses results and develop best practices in the advanced analysis of concrete dams.

The outcome from this workshop will allow better planning the following workshops and will help to formulate the needs for future research. This and future workshops are intended to share and progress best practices in the seismic analysis of concrete dams.

1.3. Workshop

A one-day meeting, held in Miami on May 3, 2018, began at 8:00 am with an introduction and presentation of workshop goals (for the agenda refer to Appendix A). After a summary presentation of the results submitted by the workshop contributors (Contributors) and an overview of prior studies of Pine Flat Dam conducted at the University of California at Berkeley in the 1970's, eight Contributors presented the findings and key observations that they found interesting during the analysis, and issues identified to address in the future investigations. The workshop concluded with an open discussion summarized in Section 8.

1.4. Formulators

The workshop organizing committee included the following individuals:

Dr. Yusof Ghanaat (Quest Structures)

Dr. Mohammad Amin Hariri (University of Colorado at Boulder)

Mr. Vik Iso-Ahola (Stantec)

Dr. Lelio Mejia (Geosyntec Consultants)

Mr. Larry Nuss (Nuss Engineering, LLC)

Mr. David Queen (BC Hydro)

Dr. Jerzy Salamon (Bureau of Reclamation)

Ms. Hillery Venturini (Bureau of Reclamation)

1.5. Acknowledgement

The authors of the report would like to thank the Dam Safety Office at the Bureau of Reclamation for the constant support of the initiatives leading to better understanding and development of modern techniques in analyses of concrete dams.

We would like to express our sincere appreciation to the USSD Workshop Formulation Committee for the effort of formulating the analysis problems for the workshop and conducting constructive discussions during the conference. The contribution is greatly appreciated.

Moreover, the authors would like to thank Dr. Mohammad Amin Hariri-Ardebili at the University of Colorado Boulder for his helpful and general discussion, which have greatly contributed to improving the summary of the workshop results.

2. DESCRIPTION OF CASE STUDIES

2.1. Description of the Project

Pine Flat Dam, located on King's River 20 miles east of Fresno, California (Figure 2.1), was selected for the studies. The dam was constructed by the United States Army Corps of Engineers (USACE) in 1954. The dam consists of thirty-six 50-foot-wide monoliths and one 40-foot-wide monolith. The length of the straight gravity dam is 1,840 feet and the tallest non-overflow monolith is 400 feet high (Figure 2.2).

Figure 2.1 Downstream view of Pine Flat Dam [ref. Wikipedia.org]

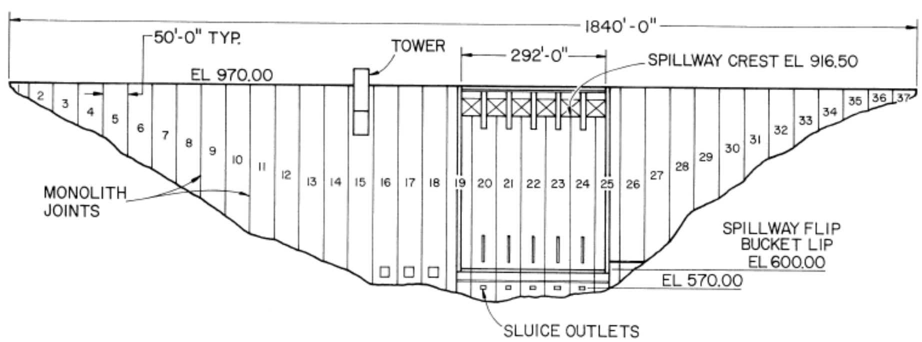

Figure 2.2 Downstream view of Pine Flat Dam [1]

The model selected for the workshop analysis includes the tallest non-overflow Monolith 16 (Figure 2.3). The block width is 50 feet. The Normal Reservoir Water Level (NRWL) is at El. 951.5 feet. The case is selected based on relatively simple geometry and extensive studies performed in the 1970's and 1980's at the University of California at Berkeley [1][2][3]. These past studies provide measured and calculated responses for correlation and comparison for the numerical analysis results from the workshop. The base case model (model) for the studies included the same dam monolith 16 as presented in the 1970's studies [1] in a linear analysis of the dam-foundation-reservoir system. Material properties for the case study are identical to the values used in the 1970's.

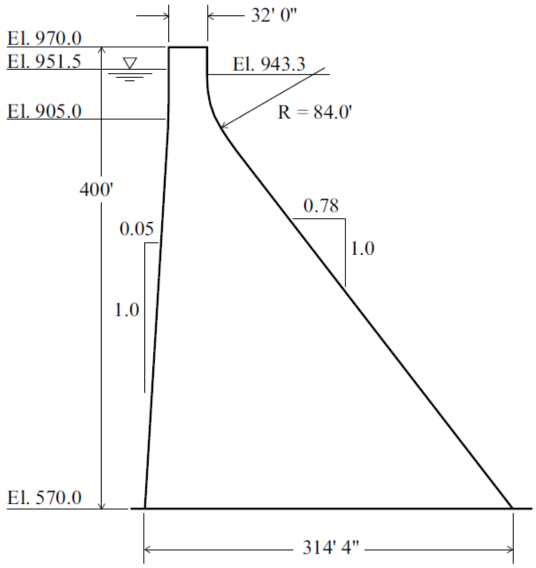

Figure 2.3 Cross Section Geometry of Monolith 16

2.2. Description of the Model

The model consists of a single 50-foot-wide dam monolith and a corresponding strip of the foundation. The coordinate system and key reference nodes are indicated in Figure 2.4 and were used for consistently reporting results of the analysis.

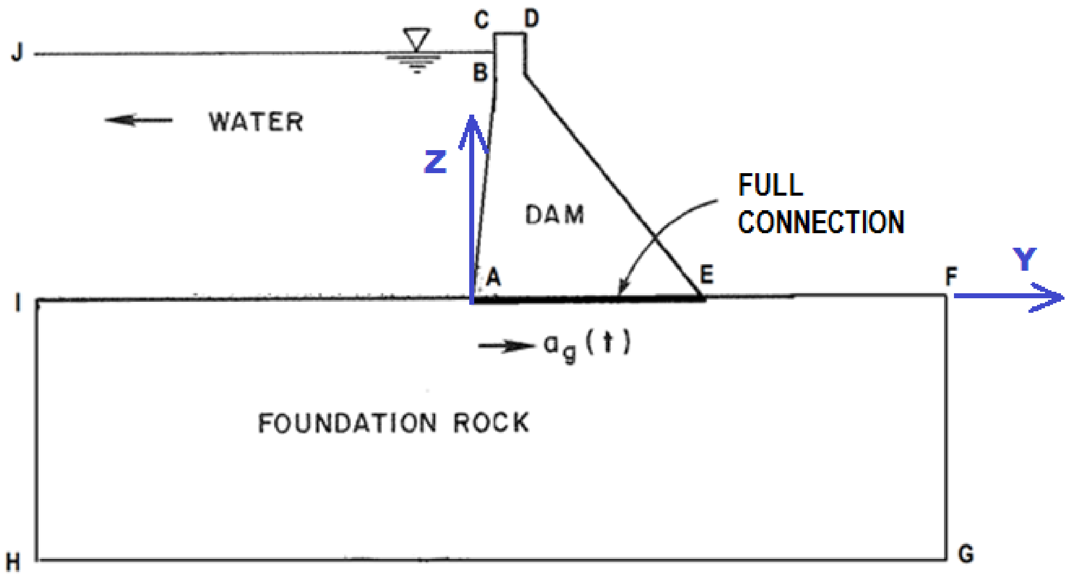

Figure 2.4 Cross Section of the Model

2.3. Material Properties

The concrete material properties are provided in Table 2.1. In Table 2.2. two sets of foundation properties are defined.

Table 2.1 Concrete Properties

Parameter	Properties	Units
Modulus of Elasticity	3,250,000	(lb/in^2)
Density	155	(lb/ft^3)
Poisson’s Ratio	0.20	

Table 2.2 Foundation Properties

Parameter	Properties I	Properties II	Units
Modulus of Elasticity	3,250,000	10,000,000	(lb/in^2)
Density	155	165	(lb/ft^3)
Poisson’s Ratio	0.2	0.33	
Shear Wave Velocity	6,350	10,280	(ft/sec)

Water is considered to have a unit weight of 62.5 lb/ft^3, compression wave velocity of 4,720 ft/sec., and bulk modulus of 300,000 lb/in^2.

2.4. Loads

The following loads are considered for various analysis cases.

2.4.1. Static Load

Static loads considered the weight of the dam (Table 2.1) and the weight of water.

2.4.2. Pulse Excitation

The pulse excitation in a form of velocity or acceleration time record for both the vertical and horizontal components is provided on Figure 2.5. An attempt to adjust the pulse load for a baseline correction was not pursued.

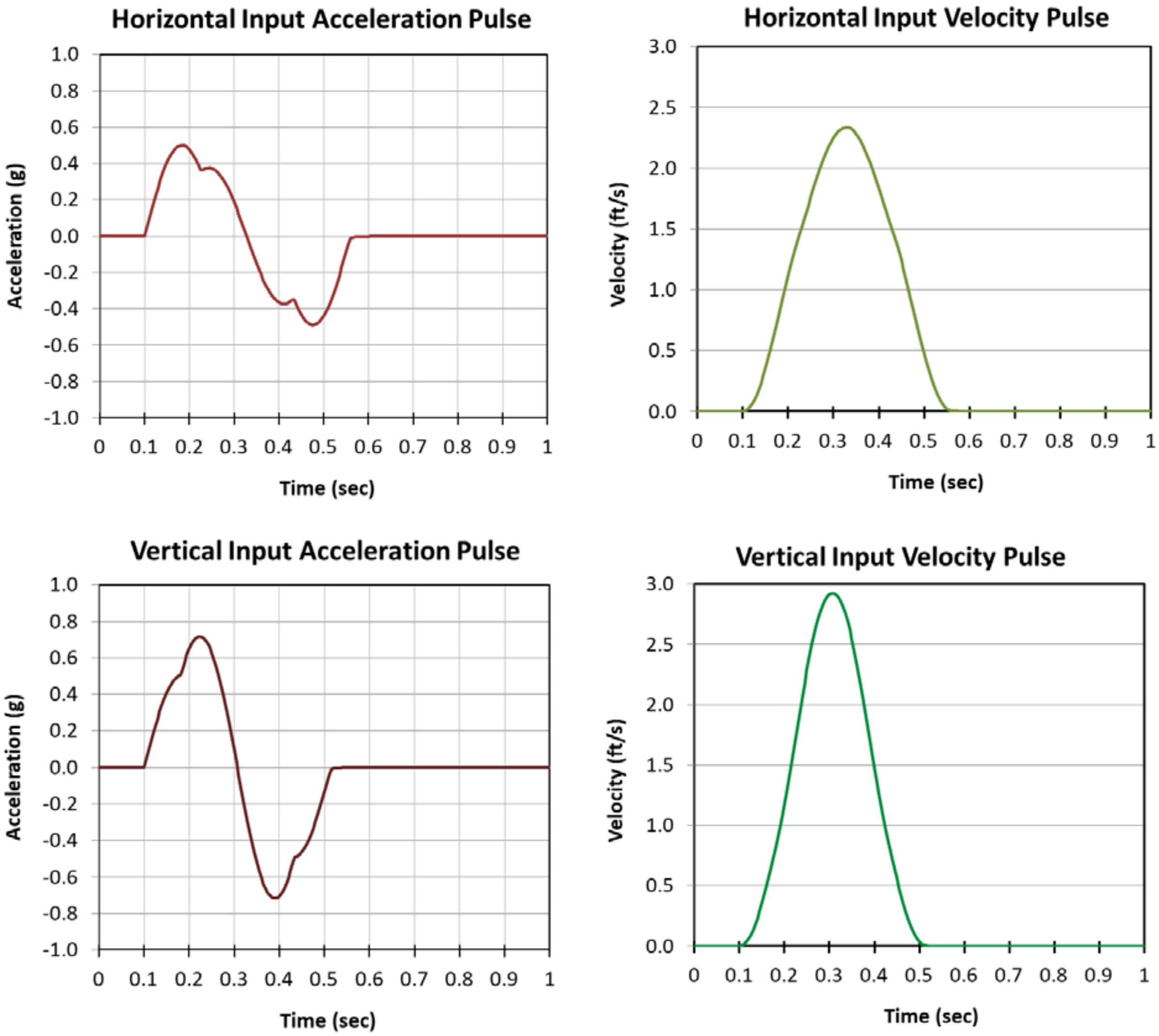

Figure 2.5 Acceleration and Velocity Pulse for Horizontal and Vertical Excitations

2.4.3. Taft Seismic Records

The Taft Lincoln School Tunnel (Taft), Kern County, California Earthquake occurred on July 21, 1952. Measured peak horizontal accelerations were 0.18g for the S69E component in the upstream to downstream direction and 0.11g for the vertical component.

The Taft time history records are given as free field ground motions at the surface of the foundation. The time step of the ground motion record is 0.01 seconds. The contributors were responsible to conduct deconvolution of the record. Taft Earthquake acceleration records are shown in Figure 2.6.a and Figure 2.6.b in the upstream/downstream and vertical direction, respectively. The acceleration time history records (*taftgm_Original tab*), as well as the baseline corrected acceleration, velocity and displacement time history records (*taftgm_BaselineCorrected tab)* were developed by Formulators. Of note, the original acceleration records and baseline corrected acceleration records result in minimal differences. The baseline corrected time history records were provided to the Contributors in the "**taftgm.xlsx**" Excel file with a note that the Taft Earthquake Upstream/Downstream and Vertical time history records should be applied together.

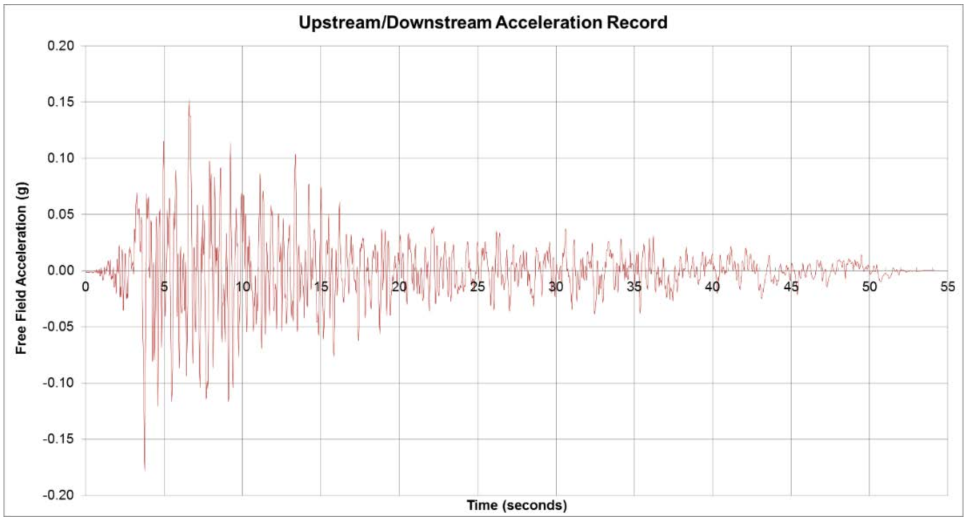

Figure 2.6.a Taft Upstream/Downstream Acceleration Record

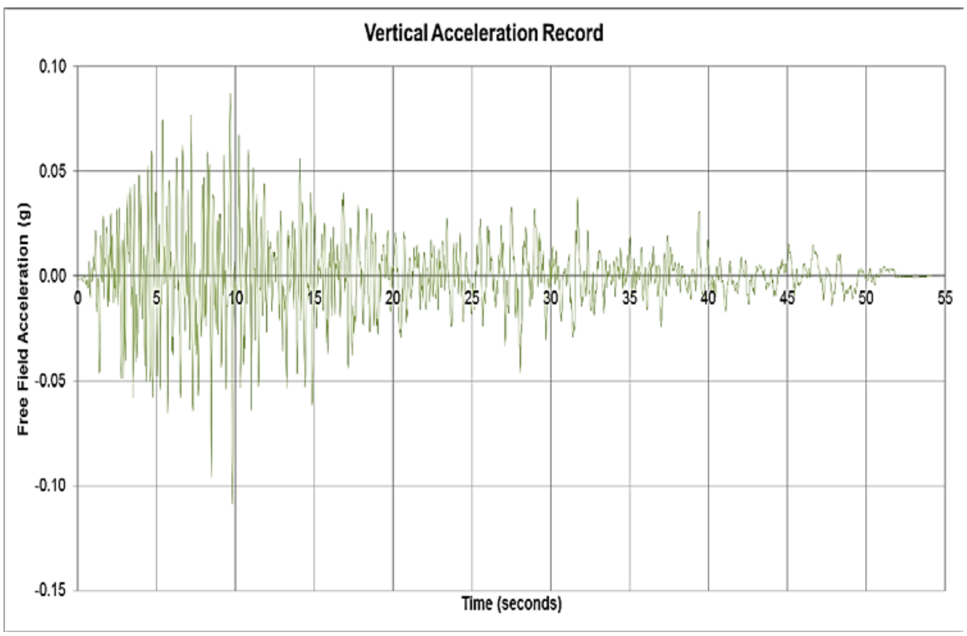

Figure 2.6.b Taft Vertical Acceleration Record

2.4.4. Endurance Time Acceleration Function

The Endurance Time Acceleration Function (ETAF) is a specially designed, intensifying acceleration time history record, where the response spectra of the ETAF linearly increases with time. Seismic performance is determined by the duration the structure can endure the dynamic input.

The ETAF time signal is applied as ground motions at the base of the foundation. The horizontal ETAF acceleration and velocity time history records are shown in Figure 2.7 and

Figure 2.8, respectively. The horizontal ETAF acceleration or velocity time history record is applied upstream/downstream. The acceleration and velocity time history records were provided to the Contributors in the "**ETAF_TimeSignal.xlsx**" Excel file.

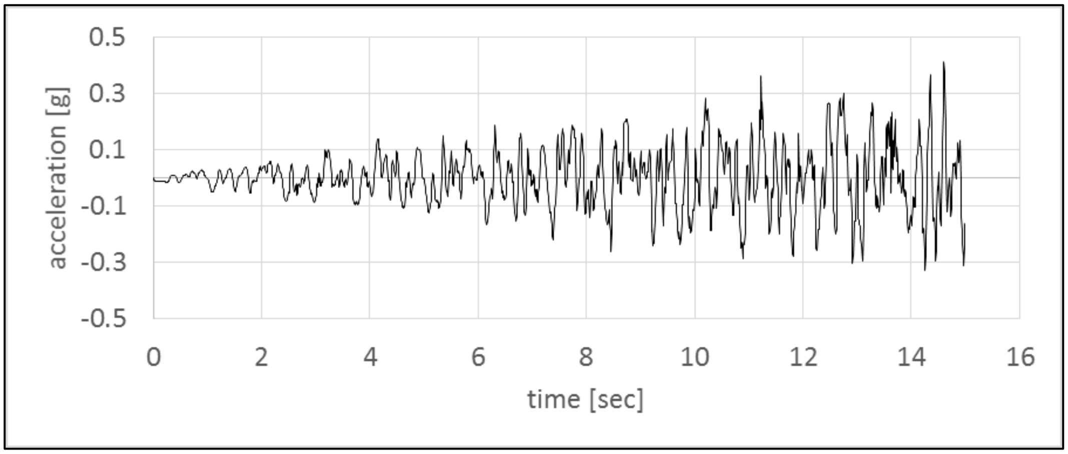

Figure 2.7 ETAF Acceleration Record

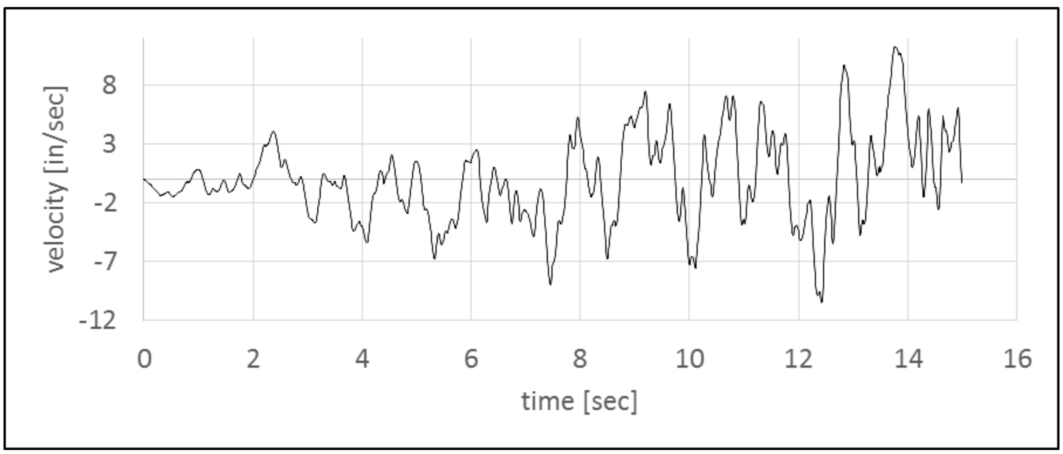

Figure 2.8 ETAF Velocity Record

2.4.5. Harmonic Excitation

The harmonic acceleration time excitation was applied at base of the dam with the period of oscillation defined for the 1st natural frequency of the dam/reservoir system determined by Contributors, and an amplitude of 0.1g, as shown in Figure 2.9. The record duration was specified to have 1 cycle at minimum.

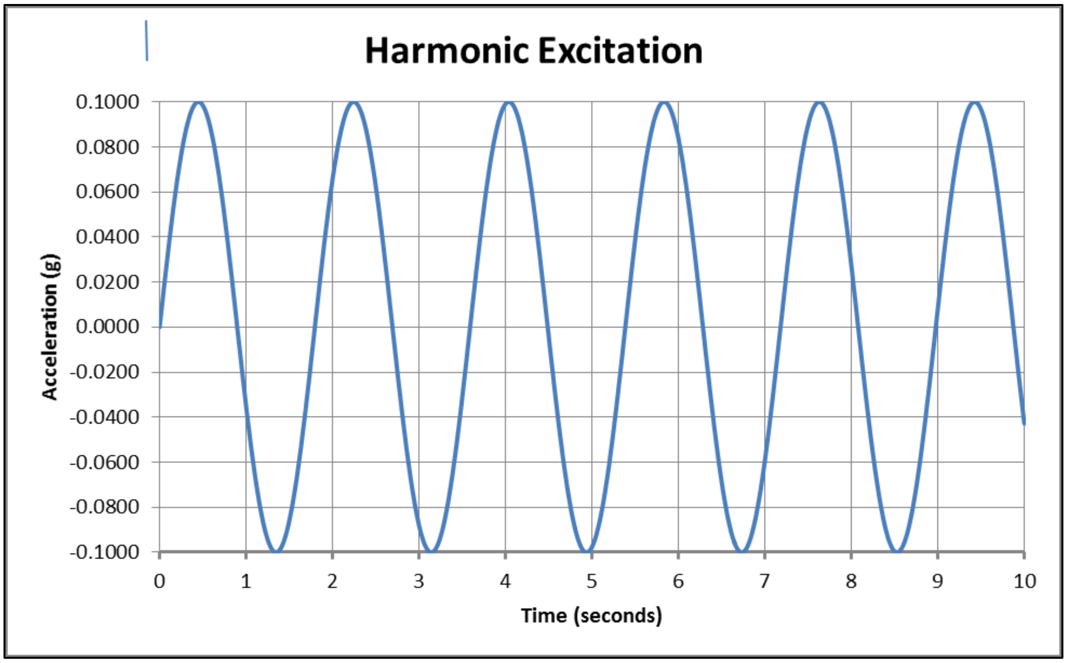

Figure 2.9 Harmonic Excitation

2.5. Damping

In the investigations, Contributors considered Rayleigh viscous damping (Rayleigh damping) proportional to a linear combination of mass matrix (M) and stiffness matrix (K), and constants of proportionality, α and β, respectively (Eq. 1):

$$C = \alpha M + \beta K \qquad \text{(Eq. 1)}$$

In reference to the values in Figure 2.10 for α and β, the value for Rayleigh damping can vary depending on the frequency, and matrix constants. For the purpose of the workshop study, a frequency between 1 and 3 Hz was considered. For this frequency range, the average Rayleigh damping equates to approximately 5 percent, using the input matrix constants as shown below. For consistency in the analysis between the participants, the constants of proportionality were assumed as **0.95** for alpha and **0.002** for beta.

Beta =	**0.002000**	(stiffness)	
Alpha =	**0.950000**	(mass)	
		Stiffness	**Mass**
Freq vs %	**Damping**	**Damping**	**Damping**
0.50	15.43	0.31	15.12
1.00	8.19	0.63	7.56
2.00	5.04	1.26	3.78
3.00	4.40	1.88	2.52
4.00	4.40	2.51	1.89
5.00	4.65	3.14	1.51
6.00	5.03	3.77	1.26
7.00	5.48	4.40	1.08
8.00	5.97	5.03	0.94
9.00	6.49	5.65	0.84
10.00	7.04	6.28	0.76
11.00	7.60	6.91	0.69
12.00	8.17	7.54	0.63
13.00	8.75	8.17	0.58
14.00	9.34	8.80	0.54
15.00	9.93	9.42	0.50
16.00	10.53	10.05	0.47
17.00	11.13	10.68	0.44
18.00	11.73	11.31	0.42
19.00	12.34	11.94	0.40

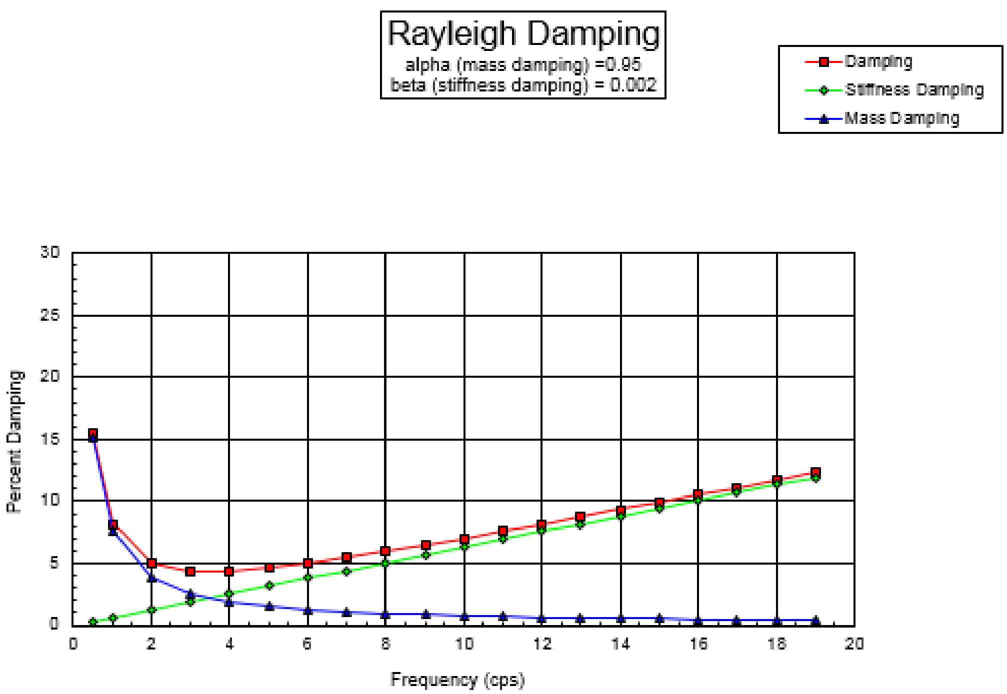

Figure 2.10 Damping Definition

Depending on the method of analysis chosen by the Contributors, the overall effects on dynamic response could vary among the analyses. Participants were encouraged to establish a clear understanding of how damping was applied and the parameters that were defined within the term. Behavior of the structure system was to be verified with fundamental principles, to ensure that the applied damping was reasonable.

3. CASE STUDIES

Five case studies, named Case A through Case E, were formulated considering the following model features:

Case A – Static Analysis

The primary focus of Case A was a static analysis of Monolith 16 considering NRWL. The model configuration consisted of the reservoir, dam, and foundation. The dimensions of the foundation were defined as: depth = 400 feet, length = 2,300 feet, and the distance from the dam heel to the upstream face of the foundation = 1,000 feet. The defined material properties can be referenced in Section 2.3.

The input parameters reference the values used in the Berkeley studies [2] and [3]. This is done to be able to compare the results obtained by Contributors with the original studies and to have consistency across the developed models.

Boundary conditions for the model were defined as follows:

- Displacements should be restrained in the perpendicular direction only at the side surfaces and at the bottom of the foundation block.
- No displacement restraints should be defined at the side faces (at contraction joins) of the 50-foot-wide monolith.
- When a 25-foot-wide FE model is analyzed to take advantage of monolith geometric symmetry, appropriate boundary conditions should be provided at the model symmetry plane.

Case B – Foundation

The purpose of the Case B (optional to Contributors) was to investigate the effect of the foundation size on the free-field ground motion in the dynamic analysis of dams. A dynamic analysis for a time-pulse loading of the foundation model (without the dam and the reservoir) is considered for various foundation extents. For consistency between Contributors the foundation depth is 400 feet and the horizontal dimensions for the foundation model are specified to be 2,300 feet and 12,300 feet. Contributors were requested to perform an additional analysis for other horizontal dimensions of their choice. Boundary conditions were defined and justified by the Contributors as appropriate for the analysis, and were as follows:

- A set of foundation properties defined similar to those specified in Table 2.2
- Mass type foundation should be considered in the analysis.
- This is a wave propagation analysis only. Static analysis due to weight of foundation material (gravity loads) should not be included in the analysis.
- Boundary conditions for the foundation block should resemble those used by the participant during dynamic analysis. The Contributors, however, can elect to perform additional runs with alternate boundary conditions and present separate sets of results accordingly.
- 1% viscous damping should be used for the foundation.

The load for Case B is defined by horizontal (Y axis) and vertical (Z axis) pulse acceleration or pulse velocity excitations shown in Figure 2.5. Depending on boundary conditions, the acceleration or velocity excitation should be applied uniformly at a level 30 feet or less above the bottom of the foundation model. Alternatively, for non-reflecting boundary condition, the velocity could be converted to traction and applied at the bottom of the foundation model.

Case C – Dam and Reservoir (Rigid Foundation)

The intent of Case C was to provide analysis results for a dam-reservoir system with a rigid foundation (or no foundation). Case C sought to examine effects of the reservoir on the behavior of a concrete dam founded on a rigid foundation. Two models for Case C include the dam with and without the reservoir. For analysis consistency the concrete and water properties were to be consistent with values referenced in Section 2.3. Loads included gravity and dam seismic excitation described by Figures 2.6 through Figure 2.9 and 5% damping was used for the dam only. The analysis included the modal analysis and the time history analysis for the Taft Earthquake and Harmonic Excitation.

Case D – Dam, Reservoir and Foundation Model I

The intent of Case D was to provide analysis results for two model configurations: the dam-foundation system (without reservoir) and the dam-reservoir-foundation system.

The Contributors were requested to define the boundary conditions used for the dynamic analysis. For consistency the following should be considered: concrete and water properties, and foundation properties – Properties I from Section 2.3.

The mass of the dam, reservoir and foundation together with the static weight of the dam and reservoir was considered without attention to the static weight of the foundation. A 5% damping value was applied to the dam and the foundation.

In Case D, static loads were applied as defined for Case A, as well as the time history records for the Taft earthquake and ETAF excitations, provided as both acceleration and velocity time history records applied in the upstream/downstream direction. The analysis included modal analysis and the linear dynamic analysis for the dam/reservoir/foundation system.

Case E – Dam, Reservoir and Foundation Model II

The intent of Case E was to perform the analysis using the model, configuration, input parameters, and loads as defined in Case D. The exception for Case E, is the use of foundation Properties II in Table 2.2 instead of Properties I used for Case D. Case E was optional for Contributors.

4. DESCRIPTION OF WORKSHOP CONTRIBUTORS

4.1. General Information

Eight Contributors from five countries submitted their solutions for the formulated workshop problems. Four various commercial software packages were used as chosen by the Contributors (Table 4.1). Table 4.2 list the study cases considered by each Contributor.

Table 4.1 Summary of Contributors Information

Contributor Name	Organizations Name (Country)	Presenter Name	Softwere Name
Giorgia Faggiani Piero Masarati	RSE SpA (Italy)	Faggiani	INDIA & ABAQUS
Arnkjell Loekke	Norwegian Univ. of Science & Technology / UC Berkeley (Norwey / USA)	Loekke	ABAQUS
Juan E Quiroz Nathan Grossmann Nedda Djavid	Stantec (USA)	Quiroz	ABAQUS
Jerzy Salamon Maziar Partovi	Bureau of Reclamation DIANA FEA / (USA / Holland)	Salamon	DIANA FEA
Yixing Yuan	GZA GeoEnvironmental, Inc.	Anonymous	Plaxis
Brent Bergman Osmar Penner Mina Shahbazi Jeff Yathon	BC Hydro (Canada)	Bergman	LS-DYNA
Sherry Hamedian Lan Nguyen Roman Koltuniuk	Bureau of Reclamation (USA)	Nguyen / Hamedian	LS-DYNA
Yusof Ghanaat Zachary Harper	Quest Structures, Inc. (USA)	Ghanaat	LS-DYNA

Table 4.2 Case Studies Submitted by Contributors

Contributor	Model A	Model B	Model C	Model D	Model E
1	X	X	X	X	X
2	X		X	X	
3	X		X	X	X
4	X		X	X	X
5	X	X		X (part)	
6	X		X (part)	X	X
7	X		X	X	
8	X	X		X	X

In Table 4.3, a description of the analysis types selected by each Contributor is provided.

Table 4.3 Type of Analysis Selected by Contributors

Contri-butor No.	FE Model Type / Width	Time Integration / Method - Convergence Norm	Element type/ size / nodes #	Non-reflecting Bundary Condtions	Fluid - Structure Interaction	Fluid type
1	3D / 50 ft	Implictit		Viscous-Spring Artificial Boundaries (VSAB)	Accustic - structural coupling	
2	2D	Implictit - HHT-alpha				
3	2D	Implicit		Far-field (Lysmer-Kuhlemayer)	Accustic - structural coupling	
4	3D / 25 ft	Implictit - Newton-Raphson / Force norm	8 noded linear / 12.5 ft / 27,777	Far-field (Lysmer-Kuhlemayer)	Accustic - structural coupling	In-compressible
5	3D	Implicit - Newmark type		Far-field (Lysmer-Kuhlemayer)	Fluid like structural elements	
6	3D	Explicit		Perfectly Matched Layer (PML)		Compressible
7	3D	Explicit				Compressible
8	3D	Explicit	8-node solid/ 6.5x6.5x12.5/ 46,335	PML	Fluid like structural elements	Compressible

Note: Five Contributors (1-5) used the implicit and three Contributors (6-8) explicit time integration method.

5. Overview of the Results

5.1. Case Study A

The Formulators made the results for Case A available to the Contributors before the workshop for the purpose of model verifications. The reason for this was to eliminate any potential modelling problems and verify that the formulations, descriptions and requirements were clear to all Contributors. Any deviations from the formulation would result in significant variations in results for dynamic analyses. Making the static results available prompted two Contributors to modify their FE model.

The results of the analysis were obtained at the monolith cross-section at the reference points identified in Figure 5.A.1.

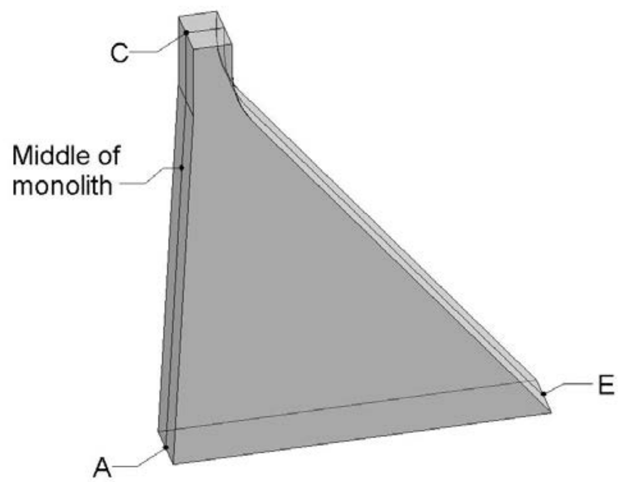

Figure 5.A.1 – Location of Reference Points for the Result Presentations

The relative displacements, measured as a difference between points at the crest and the heel, were in a range between 0.31 and 0.35 inches, or within a 10 percent range among Contributors. Most Contributors computed the same displacements for foundation material Properties I and II, with the exception of Contributors 4 and 8. Contributor 4 obtained larger relative horizontal displacement for Properties I (softer foundation) whereas Contributor 8 estimated larger values computed for Properties II (Figure 5.A.2). Rounding displacements to 0.01 inch made the picture less clear (more accurate results would be preferable for this comparison). The source of differences in displacement can be attributed to the 1) mesh size, 2) type of the elements used for discretization, and 3) type of numerical technique to solve the finite element formulation.

Vertical stresses at the dam-foundation interface shown in Figure 5.A.3 are in good agreement at the central part of the dam base, however, significant differences are observed at the heel and the toe of the dam. It appears that these differences are attributed to the various FE element sizes used by Contributors, reporting the stresses in Gauss points, or either averaging them or extrapolating them to the nearest element nodes.

In general, the stress concentration at the heel and toe can be due to the following factors, or a combination thereof. 1) different mesh sizes, 2) element types (plane stress, plane strain, or 3D solid), 3) computation of stresses with different numerical techniques, and 4) reporting the results at nodal points, integration points, or in elemental centers.

In conclusion, Case A allowed the Contributors to validate their FE models with other solutions, to eliminate potential errors in the model. Another observation from Case A is justifiable for a more precise request for the stress results, especially at the locations of stress singularities.

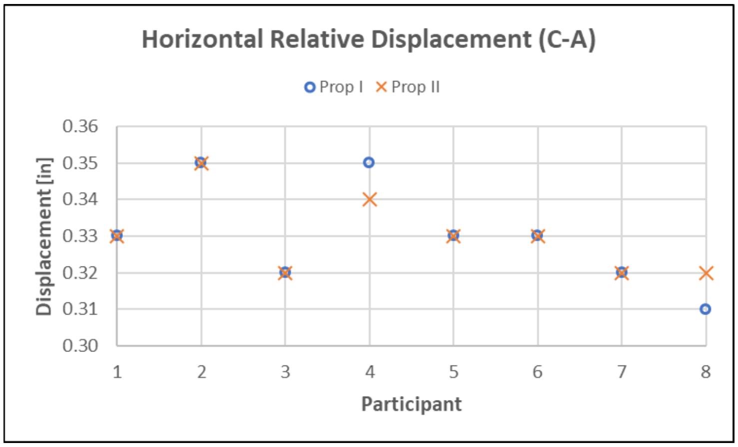

Figure 5.A.2 - Relative Horizontal Displacement between Dam Crest and Dam Heel (between Point C and Point A in Figure 5.1)

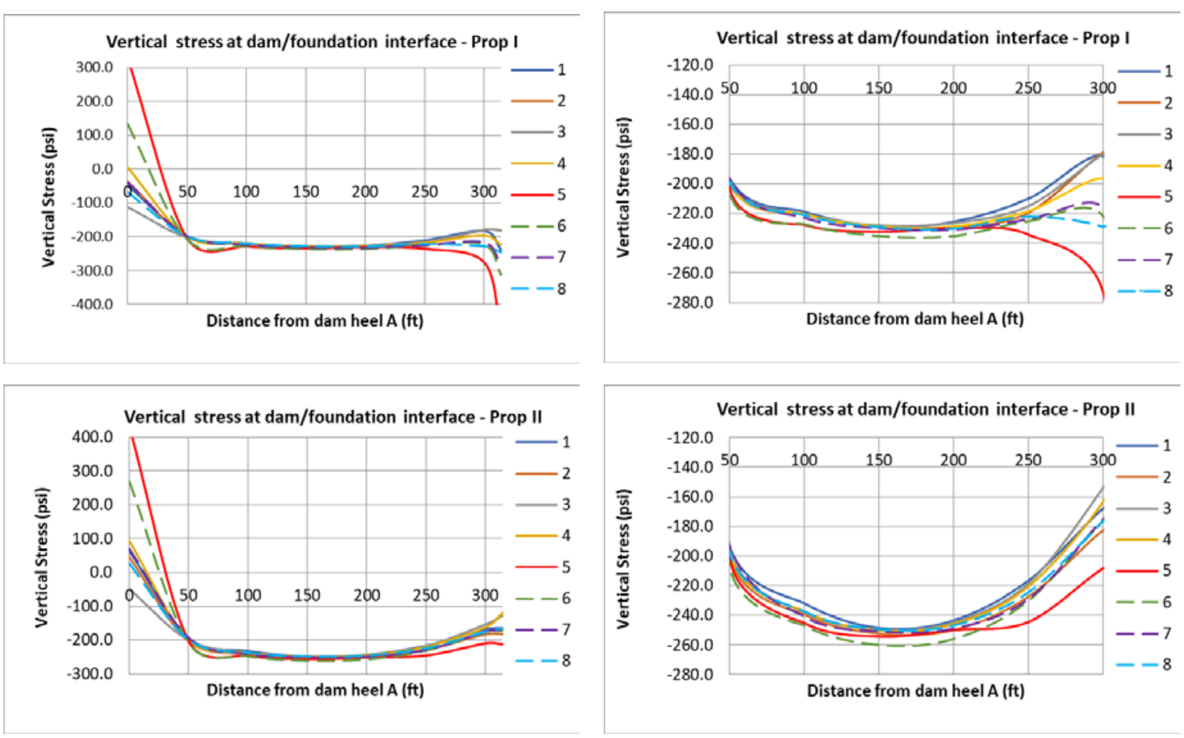

Figure 5.A.3 - Vertical Stress at the Dam Base for Foundation Properties Prop I and Prop II

5.2. Case Study B

Case B investigated the effect of the foundation size on the free-field ground motion in the dynamic analysis. A time-pulse applied at the base of a defined foundation block (no dam) was considered by the Contributors for foundation extents of 2,300 and 12,300 feet as shown in Figure 5.B.1. The Contributors were then asked to identify a third foundation size for additional comparison. All participating Contributors in this study chose the third foundation extend of 7,300 feet. The analysis results are compared at specified locations at the foundation block top surface (Figure 5.B.1).

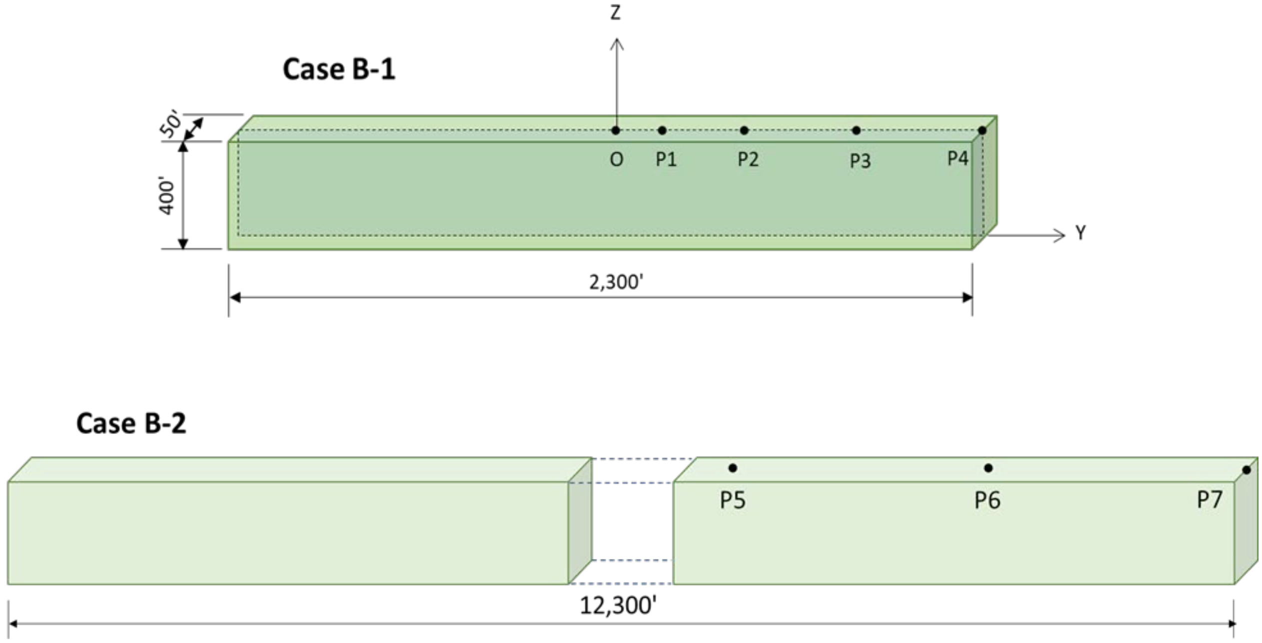

Figure 5.B.1. Location of Reference Points for Results Presentation

Figure 5.B.2 and Figure 5.B.3 show the acceleration plot at the block top surface for all three considered foundation sizes for the horizontal and vertical direction, respectively.

Figures 5.B.4, 5.B.6 and 5.B.8 show horizontal acceleration history responses at the ground surface of the foundation block. Figures 5.B.5, 5.B.7 and 5.B.9 show the vertical acceleration history responses at the ground surface of the foundation block.

The results confirm the edge effects of the model and a need for further investigation of the foundation model size in the analysis.

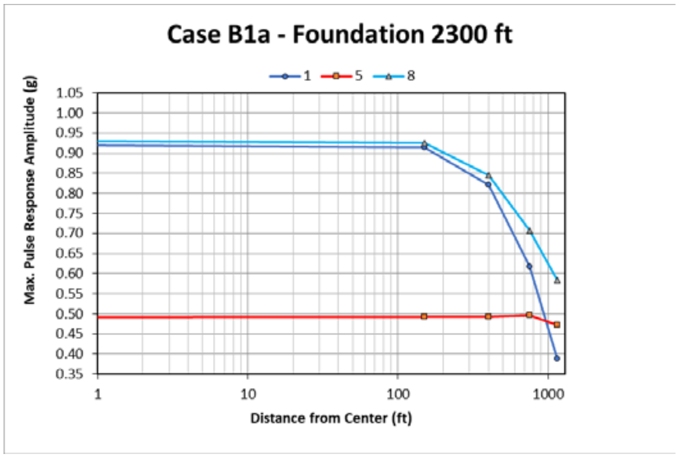

(a)

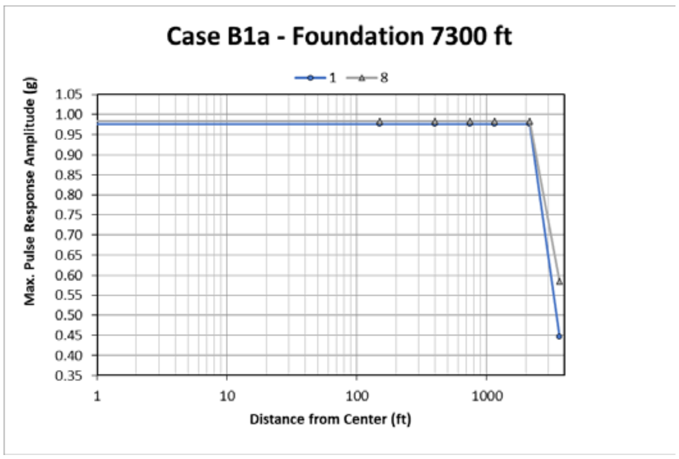

(b)

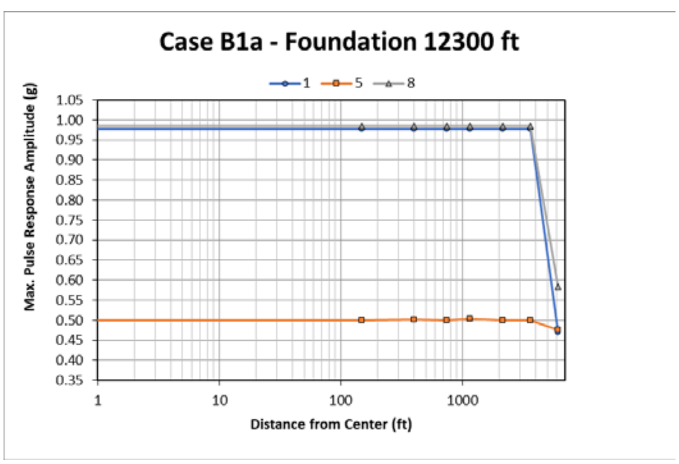

(c)

Figure 5.B.2. Results for Horizontal Pulse Excitation

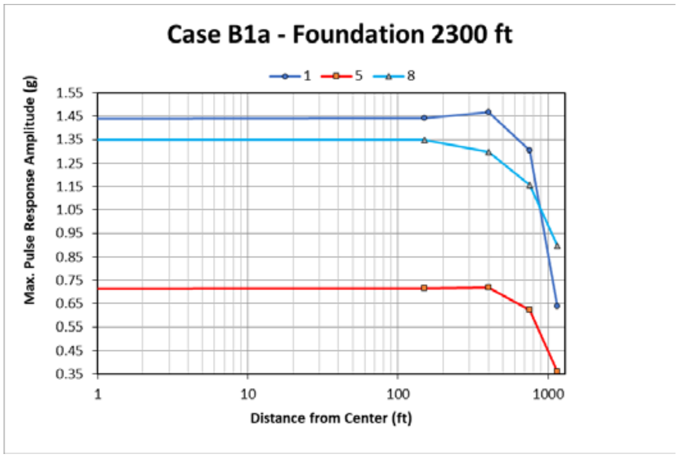

(a)

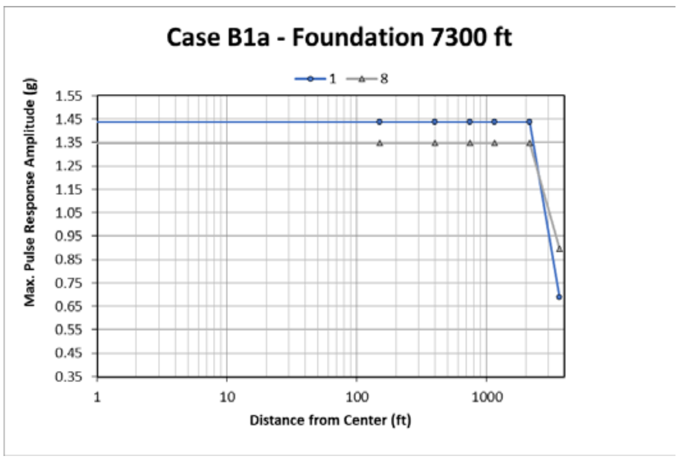

(b)

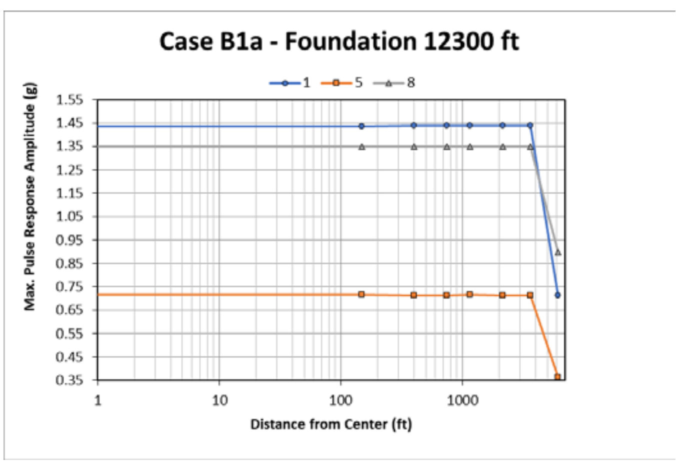

(c)

Figure 5.B.3 Results for Vertical Pulse Excitation

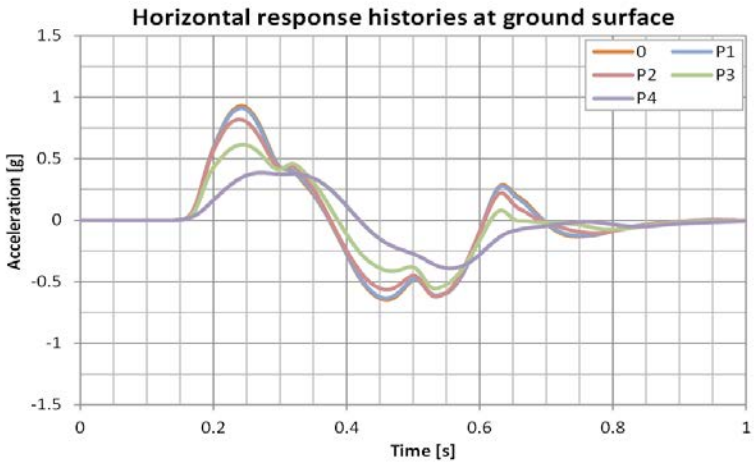

(a) Contributor 1

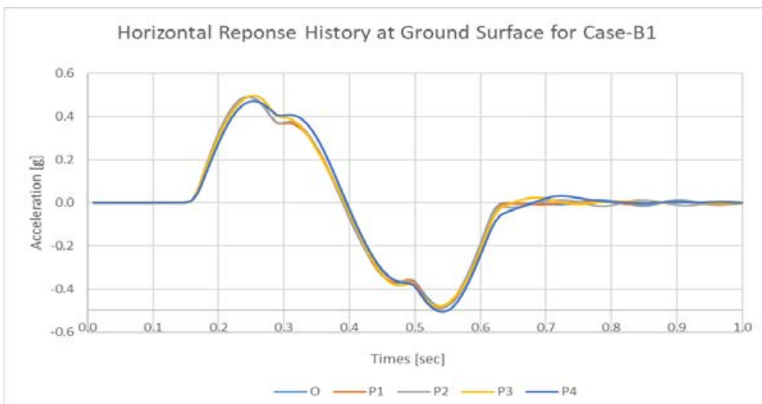

(b) Contributor 5

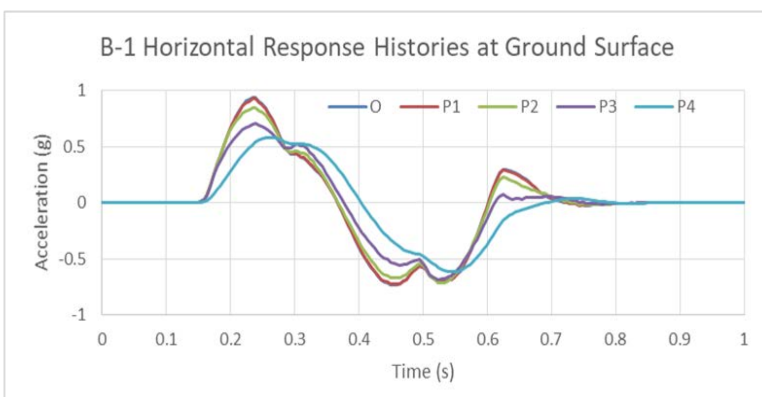

(c) Contributor 8

Figure 5.B.4 Horizontal Acceleration Response Histories at Ground Surface for 2,300 ft Long Foundation

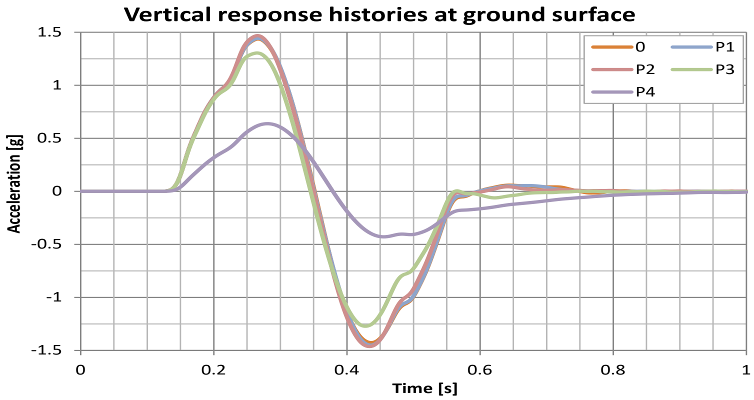

(a) Contributor 1

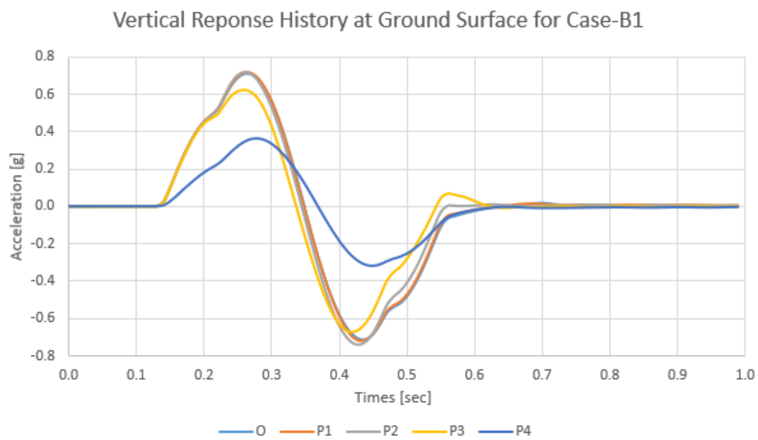

(b) Contributor 5

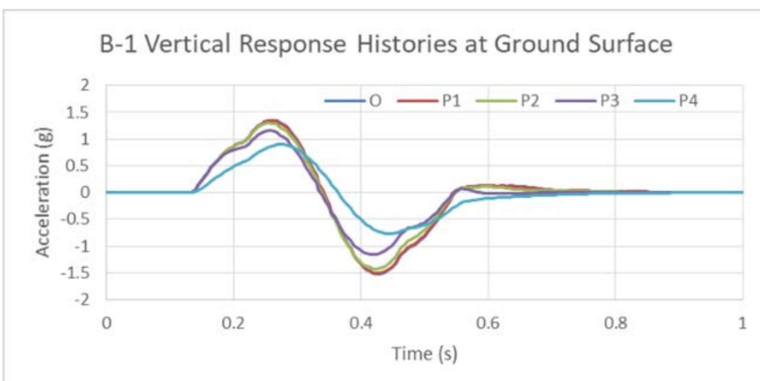

(c) Contributor 8

Figure 5.B.5 Vertical Acceleration Response Histories at Ground Surface for 2,300 ft Long Foundation

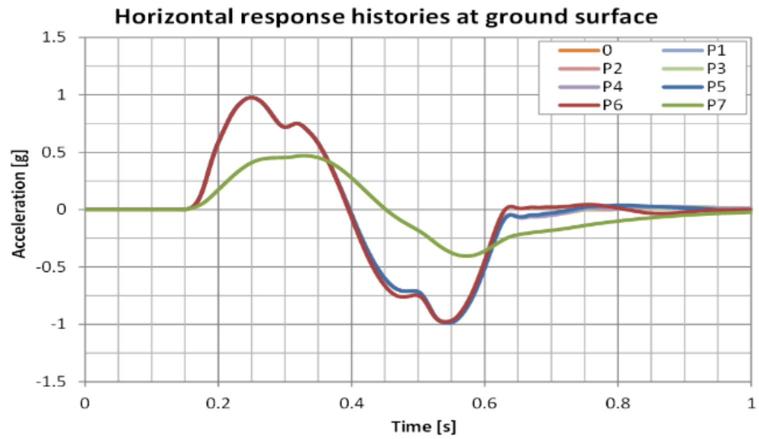

(a) Contributor 1

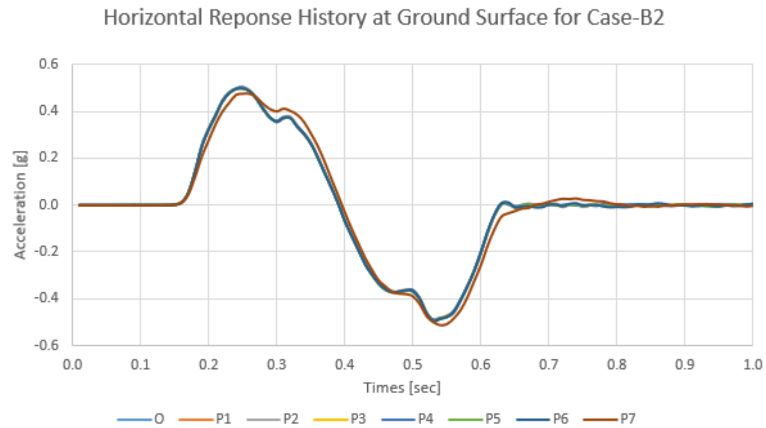

(b) Contributor 5

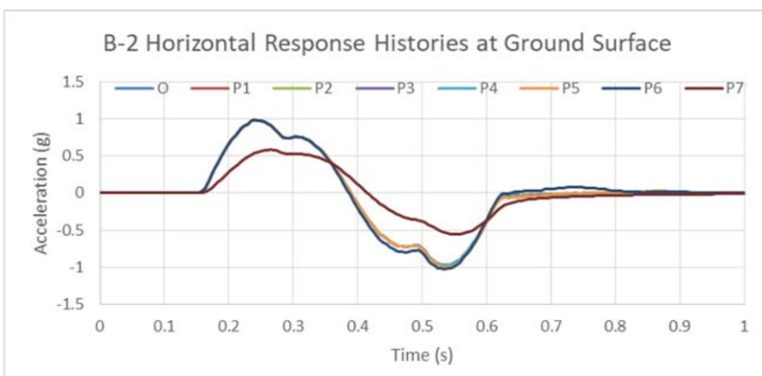

(c) Contributor 8

Figure 5.B.6 Horizontal Acceleration Response Histories at Ground Surface for 12,300 ft Long Foundation

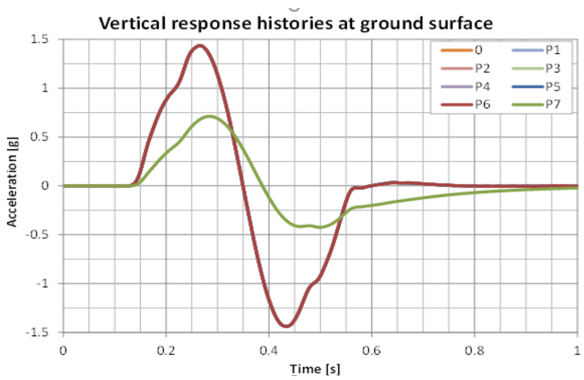

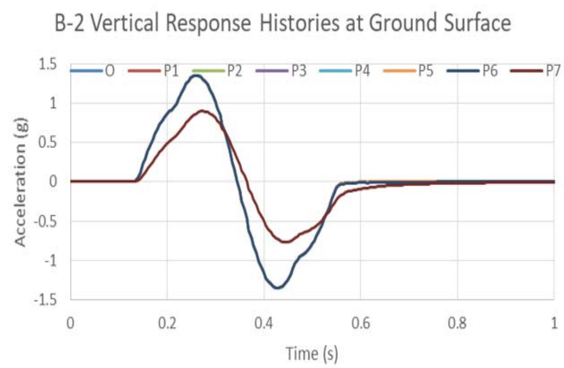

(a) Contributor 1 **(b) Contributor 8**

Figure 5.B.7 Vertical Acceleration Response Histories at Ground Surface for 12,300 ft long foundation

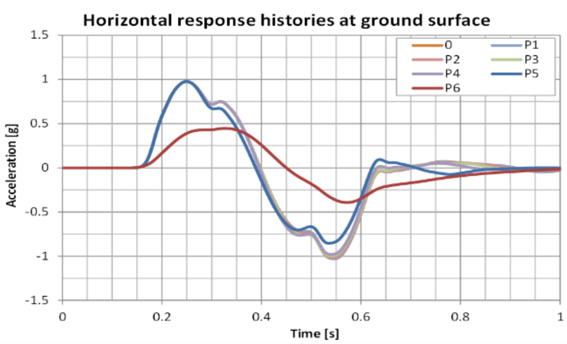

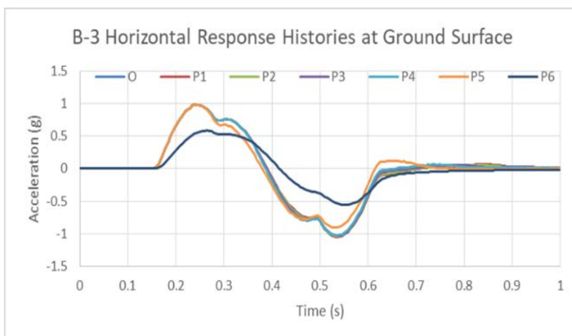

Contributor 1 **Contributor 8**

Figure 5.B.8 Horizontal Acceleration Response Histories at Ground Surface for 7,300 ft long foundation

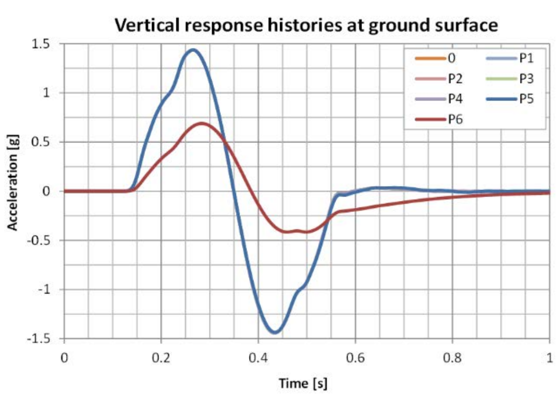

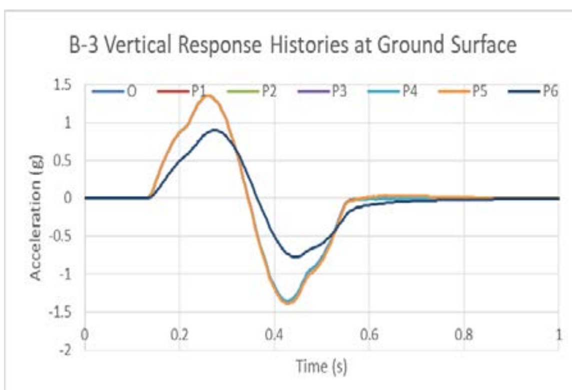

Contributor 1 **Contributor 8**

Figure 5.B.8 Vertical Acceleration Response Histories at Ground Surface for 7,300 ft long foundation

5.3. Case Study C

For Case C, the Contributors were requested to provide information on the first six natural frequencies, as well as, the associated modal shapes of the dam with and without the presence of the reservoir.

For the dam only, the first natural frequency was determined to be in a narrow range between 3.16 and 3.26 Hz. The difference among Contributor results was approximately 3 percent. The same narrow range of the higher five frequencies was determined by six Contributors (Fig. 5.C.1.a).

The first natural frequency for the dam-reservoir model was determined in seven solutions between 2.55 and 2.69 Hz. The difference among Contributor results was approximately 5 percent. The exception was Contributor 8 who determined this value to be 1.98 Hz, or approximately 25 percent below the range average. For higher natural frequencies, a good agreement is observed between Contributors 1 and 3 and separately between Contributors 2 and 4. Significant difference however, was observed when all Contributor results were compared (Fig. 5.C.1.b). The difference could be explained in that Contributors 1 and 3 reported the results for different natural frequency modes than Contributors 2 and 4.

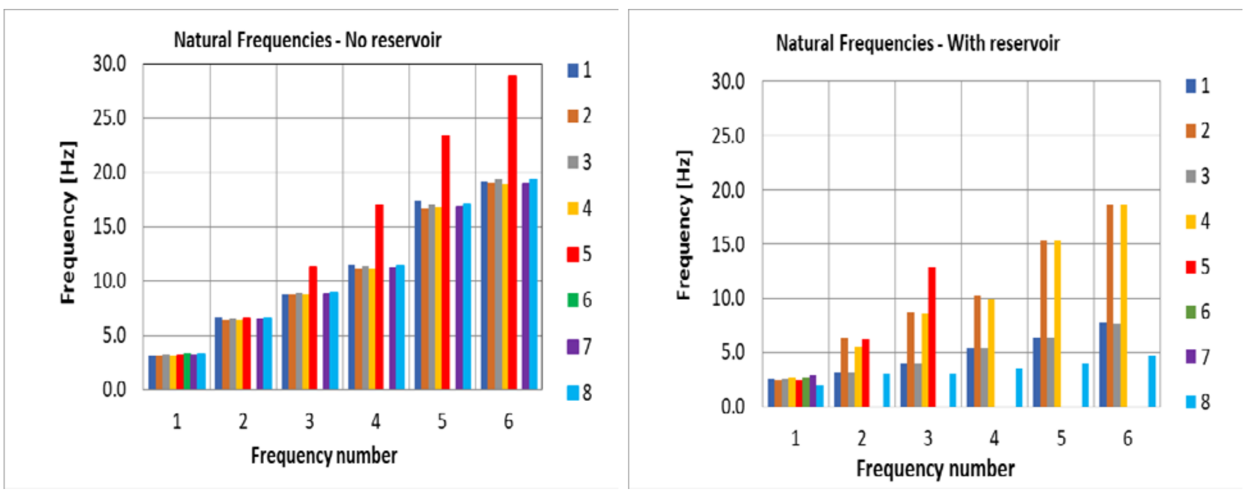

(a) **(b)**

Figure 5.C.1 - Natural frequencies (a) no reservoir (b) with reservoir

In the second part of Case C, the Contributors were requested to provide distributions of the hydrodynamic pressure and the total pressure at the upstream dam face (Line A-B-C, Figure 2.4) for the analysis time when the hydrodynamic pressure at the dam heel was at the maximum. Figures 5.C.2 through 5.C.4 show the total and hydrodynamic pressure for the Taft, ETAF, and Harmonic loads, respectively. Significant variations in the hydrodynamic pressure were observed at the dam heel ranging between 25.1 and 46.7 lb/in^2 for TAFT, 55.8 and 81.1 lb/in^2 for ETAF, and 33.7 and 72.2 lb/in^2 for the harmonic loads. Consequently, significant differences in the hydrodynamic pressure distribution at the dam face was observed between the submitted results.

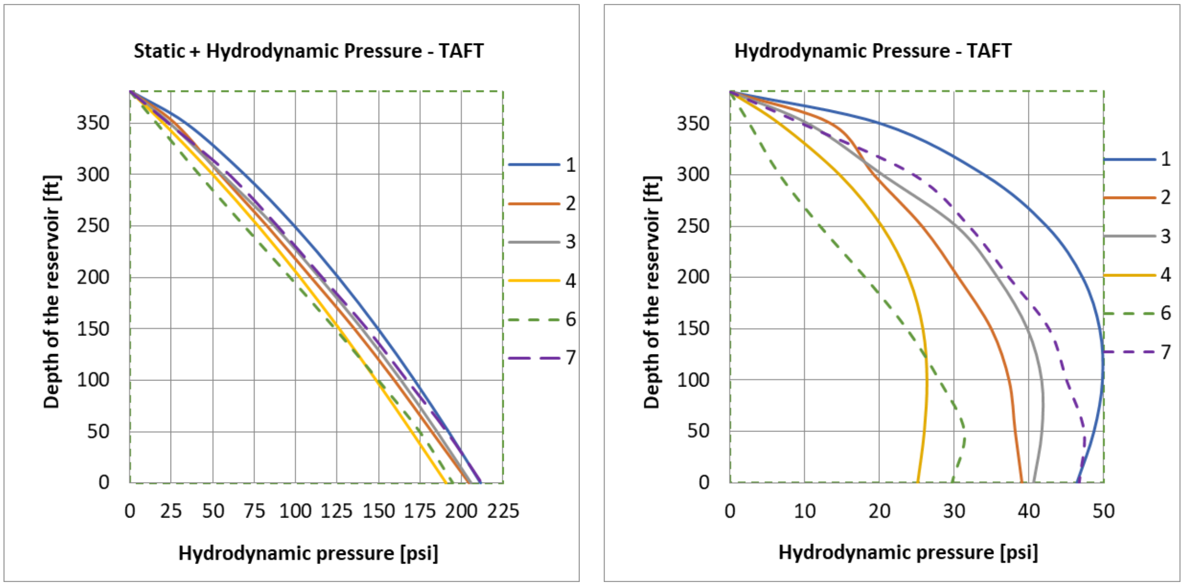

(a) **(b)**

Figure 5.C.2 - Taft Earthquake – Pressure at the dam face (a) total pressure; (b) hydrodynamic (only)

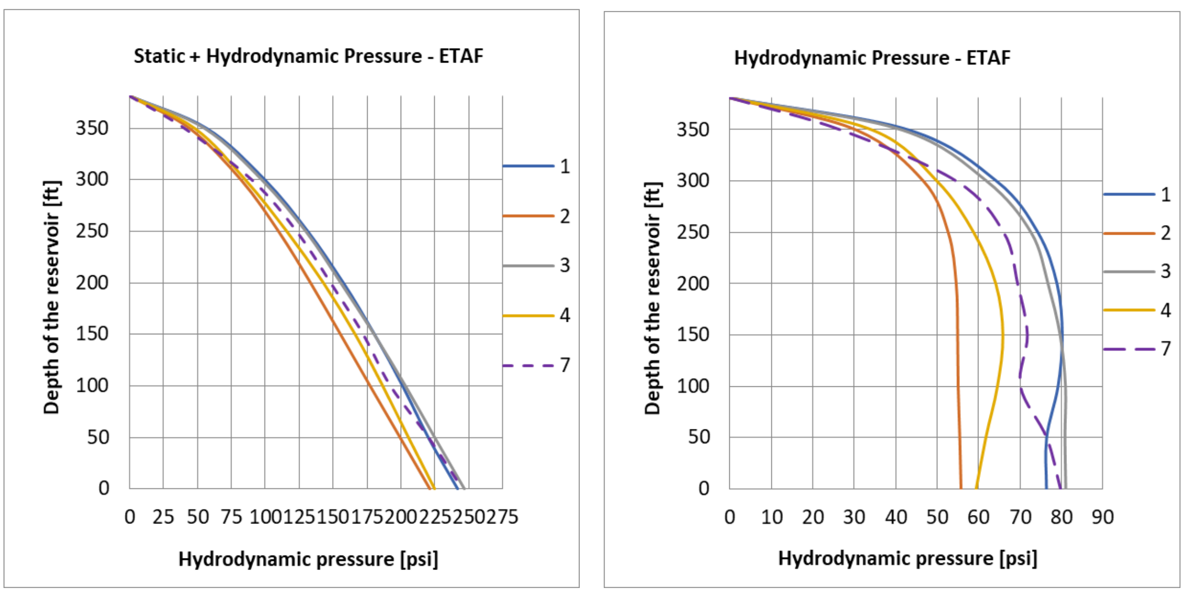

(a) **(b)**

Figure 5.C.3 - ETAF Excitation - Hydrodynamic Pressure (a) Total Pressure; (b) Hydrodynamic (only)

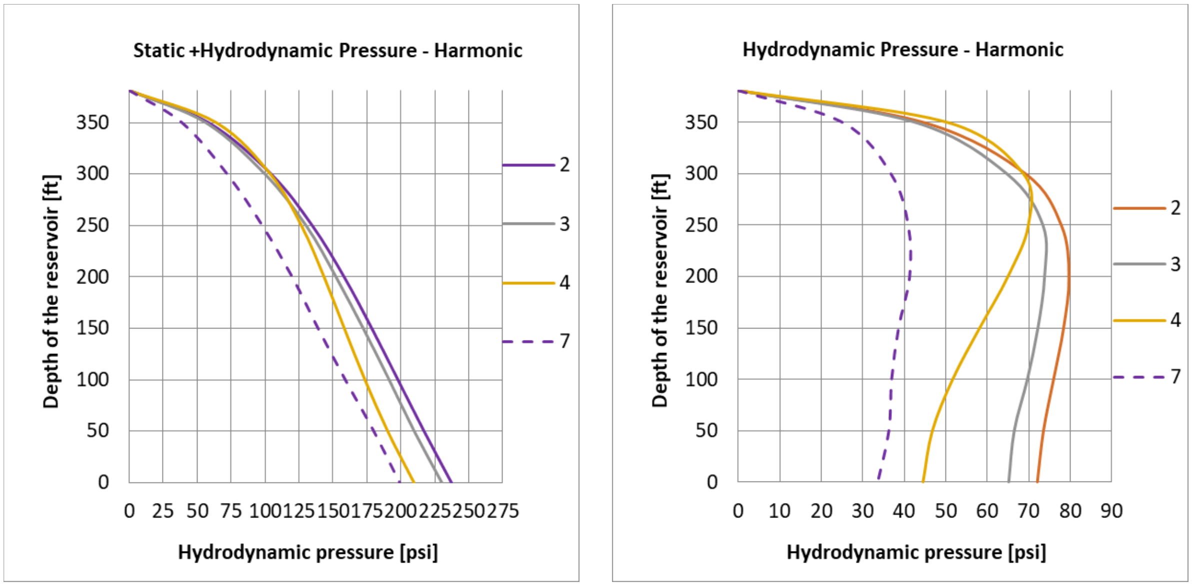

(a) (b)

Figure 5.C.4 - Harmonic Signal - Hydrodynamic Pressure (a) Total Pressure; (b) Hydrodynamic (only)

The reasons of differences in the hydrodynamic pressure distribution along the dam height can be attributed to:

1. Different formulations for the fluid-structure interaction and analysis techniques used by the Contributors,
2. Mesh size considerations,
3. Non-reflecting boundary conditions applied to the reservoir,
4. Correlation between the maximum pressure at the dam heel and the pressure distribution along the dam face.

5.4. Case Study D

For Case D, the Contributors were requested to provide information on the first six natural frequencies and the associated modal shapes of the dam-foundation system with and without presence of the reservoir, assuming the material properties for concrete in Table 2.1 and rock Table 2.2, Property I.

The first natural frequency of the system without reservoir was reported by three Contributors in a narrow range between 1.92 and 1.98 Hz. The difference among Contributor results was approximately 3 percent. The remaining four Contributors reported results in a range between 2.46 and 2.56. The difference among Contributor results was approximately 4 percent. Contributor 5 reported this value to be 2.88 Hz. The same relatively narrow range for the higher five frequencies was determined by five Contributors, however, larger differences are observed between these results for the second mode (Fig. 5.D.1.a).

The first natural frequency for the dam-foundation-reservoir model was determined in four solutions between 2.02 and 2.08 Hz. The difference among Contributor results was approximately 0.1 percent, however, two Contributors determined this value to be about 10 percent below, and a third Contributor about 18 percent above this narrow range. For higher natural frequencies, more variations in the results is observed between five Contributors providing the results (Fig. 5.D.1.b). The difference could be explained by reporting the results for different natural frequency modes identified by the Contributors.

Next, the Contributors were requested to provide the hydrodynamic pressure distributions and the total pressure distribution at the upstream face of the dam (along line A-B-C, Figure 2.4) for the maximum hydrodynamic pressure determined at the dam heel in the time analysis for TAFT and ETAF loads.

Figures 5.D.2 and 5.D.3 show the total and hydrodynamic pressure distributions at the dam face for TAFT and ETAF loads, respectively. The pressure distributions were selected, for the analysis time corresponding to the maximum hydrodynamic at the dam heel as shown in Figure 5.D.4 and Figure 5.D.6. Significant variations in the hydrodynamic pressure results was observed at the dam heel ranging between 25.1 - 46.7 lb/in^2 for TAFT, 55.8 - 81.1 lb/in^2 for ETAF, and 33.7 - 72.2 lb/in^2 for the harmonic loads.

Consequently, significant differences in the hydrodynamic pressure distribution at the dam face is observed between the submitted results.

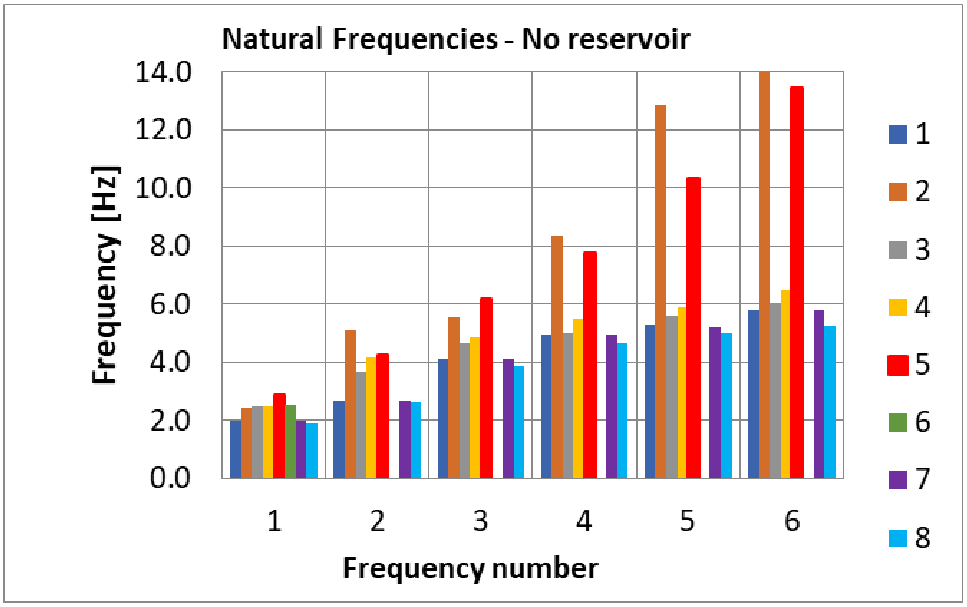

(a)

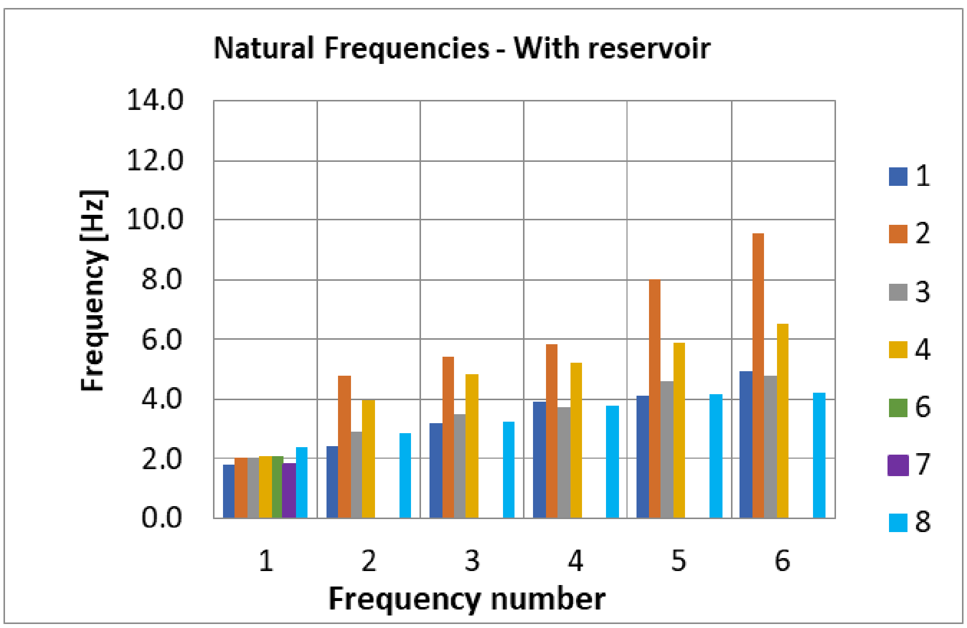

(b)

Figure 5.D.1 - Natural Frequencies (a) No Reservoir; (b) With Reservoir

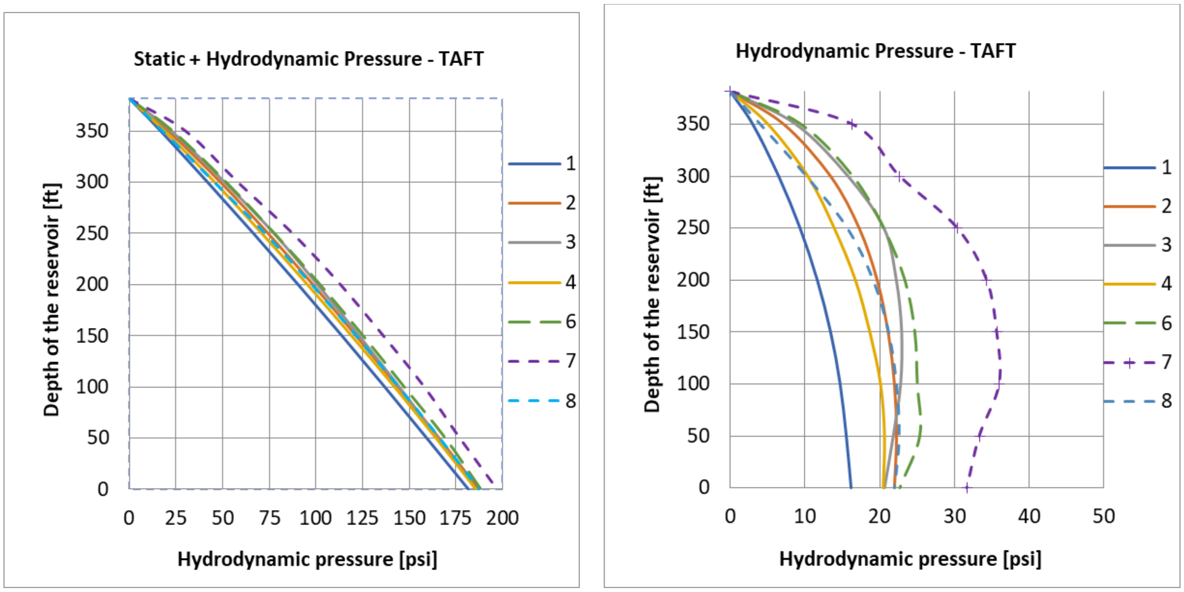

(a) (b)

Figure 5.D.2 - Taft Earthquake - Hydrodynamic Pressure (a) Total Pressure; (b) Hydrodynamic (only)

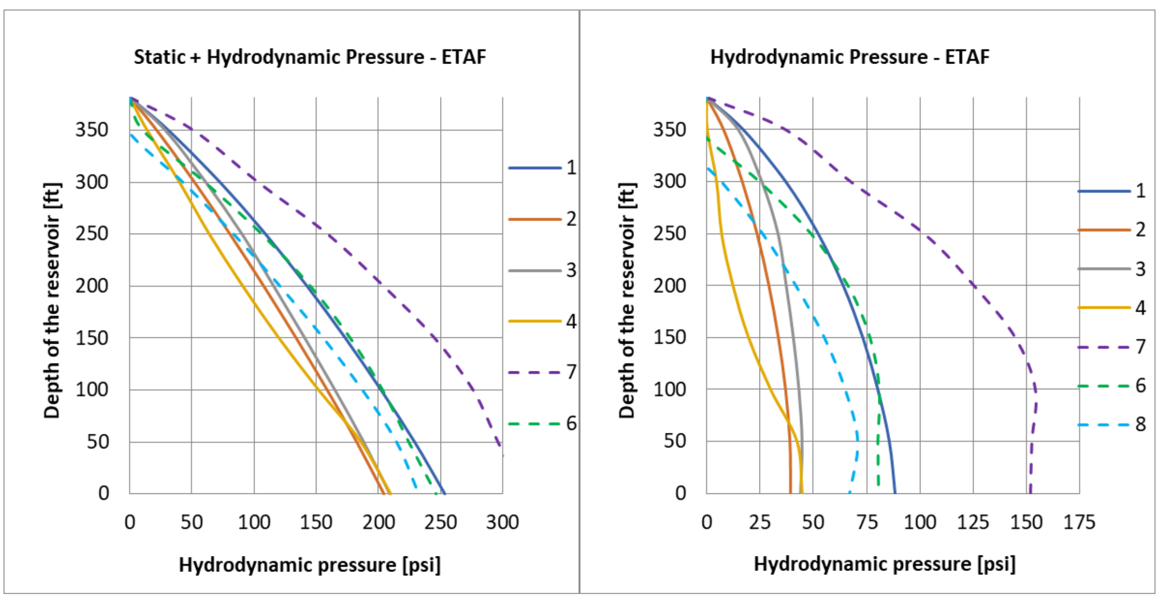

(a) **(b)**

Figure 5.D.3 - ETAF Excitation - Hydrodynamic Pressure (a) Total Pressure; (b) Hydrodynamic (only)

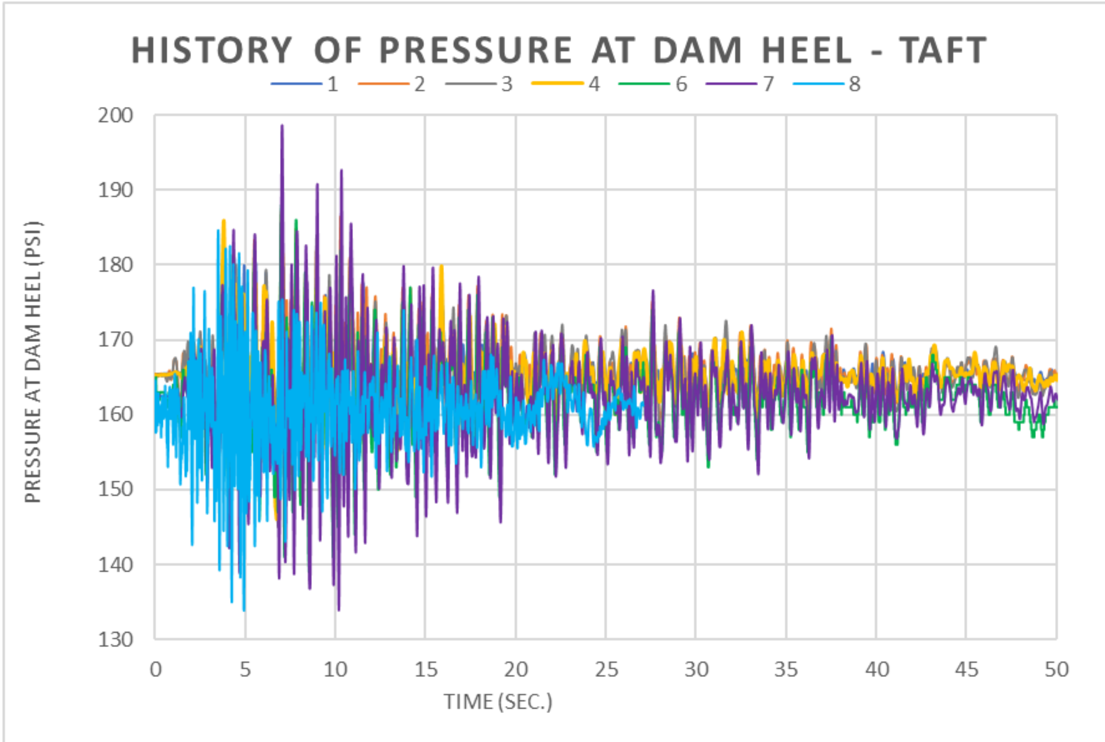
HISTORY OF PRESSURE AT DAM HEEL - TAFT
1
2
3
4
6
7
8
PRESSURE AT DAM HEEL (PSI)
200
190
180
170
160
150
140
130
0
5
10
15
20
25
30
35
40
45
50
TIME (SEC.)

(a)

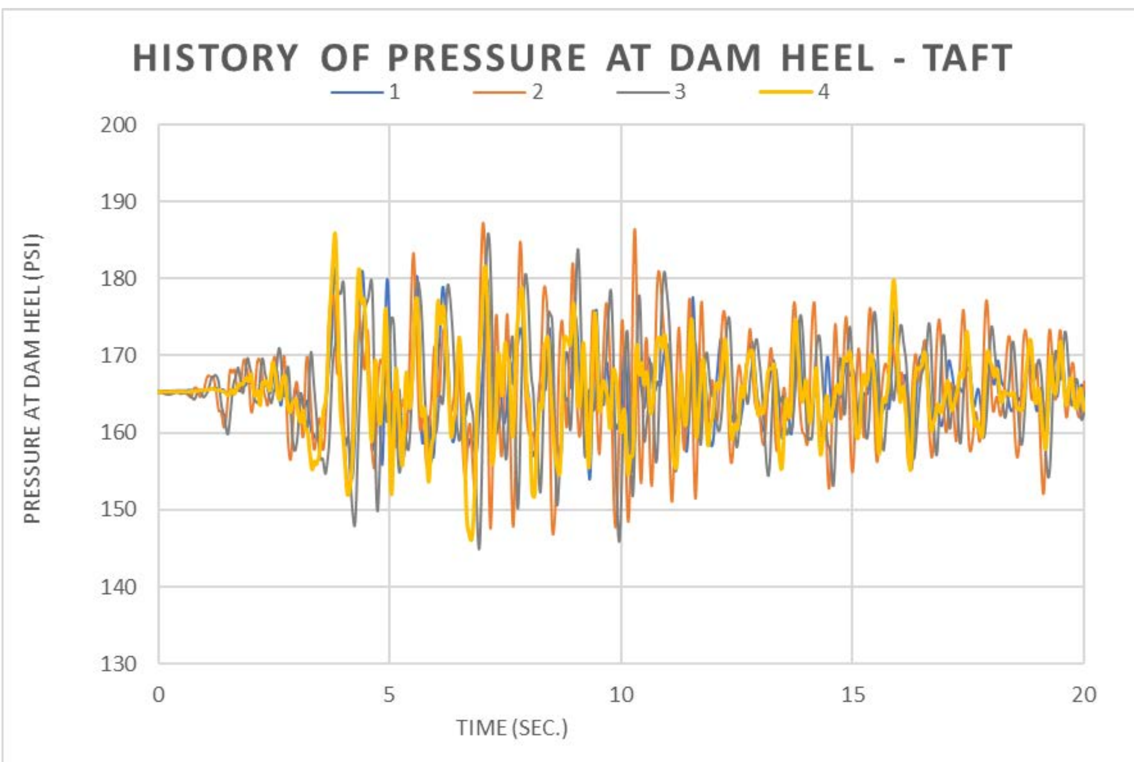
HISTORY OF PRESSURE AT DAM HEEL - TAFT
1
2
3
4
PRESSURE AT DAM HEEL (PSI)
200
190
180
170
160
150
140
130
0
5
10
15
20
TIME (SEC.)

(b)

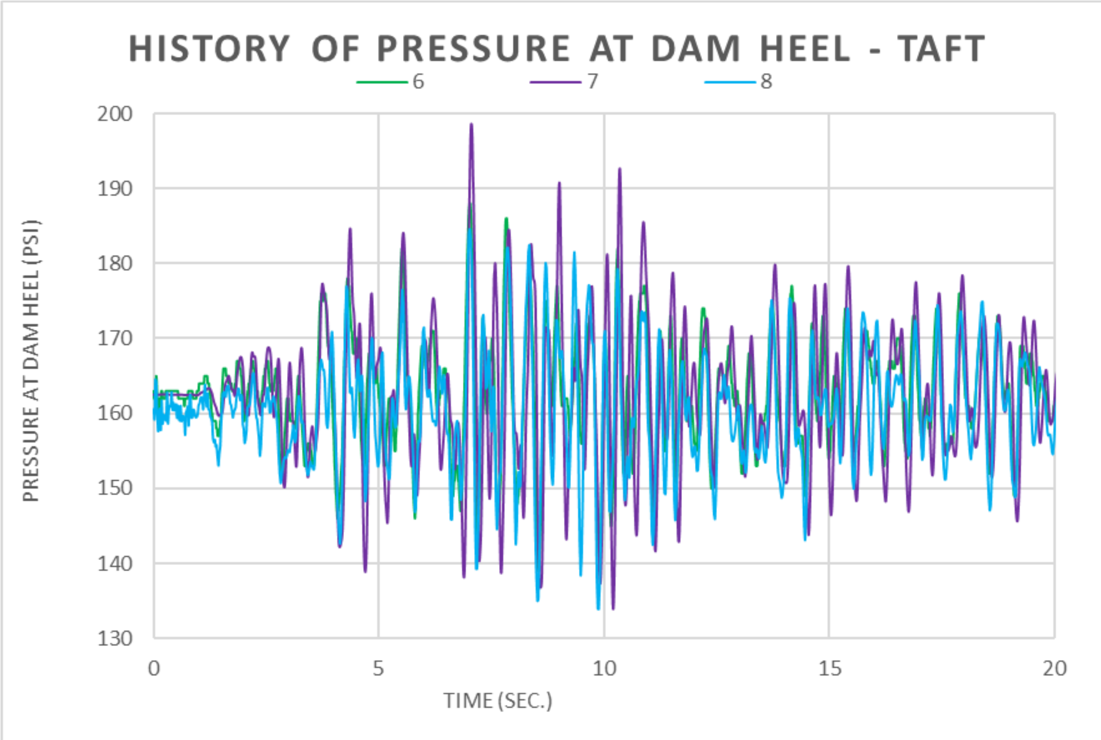

(c)

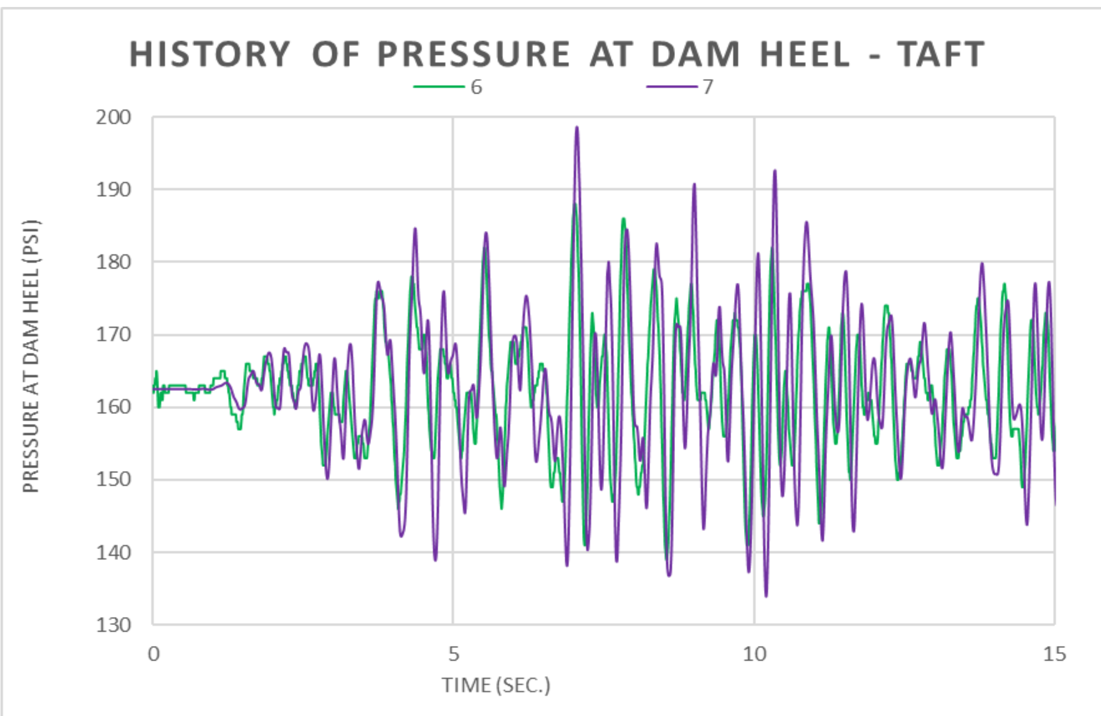

(d)

Figure 5.D.4 - TAFT Earthquake - Total Pressure at the Dam Heel

Table 5.D.1 – Extreme Total Pressures for Taft Load at the Dam Heel – Time Record 0 -50 sec.

Contributor	1	2	3	4	5	6	7	8
Max. Value	181.4	187.3	186.0	185.9	-	188.0	198.6	184.6
Min. Value	153.9	146.8	145.0	146.0	-	139.0	133.9	133.9

The peak maximum total pressure (Table 5.D.1) was determined by most Contributors to be between a range of 181.4 and 188 lb/in^2 (about 3.5 percent difference). The exception was Participant 7 who determined this value to be 198.6 lb/in^2 (approximately 7 percent above the range average).

Table 5.D.2 – Extreme Hydrodynamic Pressures for Taft Load at the Dam Heel – Time Record 0 -50 sec.

Contributor	1	2	3	4	5	6	7	8
Max. Value	16.3	22.2	20.8	20.8	-	22.9	33.5	19.5
Min. Value	-11.2	-18.3	-20.2	-19.1	-	-26.1	-31.2	-31.2

The positive hydrodynamic pressure (Table 5.D.2) was determined by five Contributors to be within a narrow range of 19.5 and 22.9 lb/in^2 (about 17 percent difference). Negative pressure of only three Contributors was within a range of 10 percent.

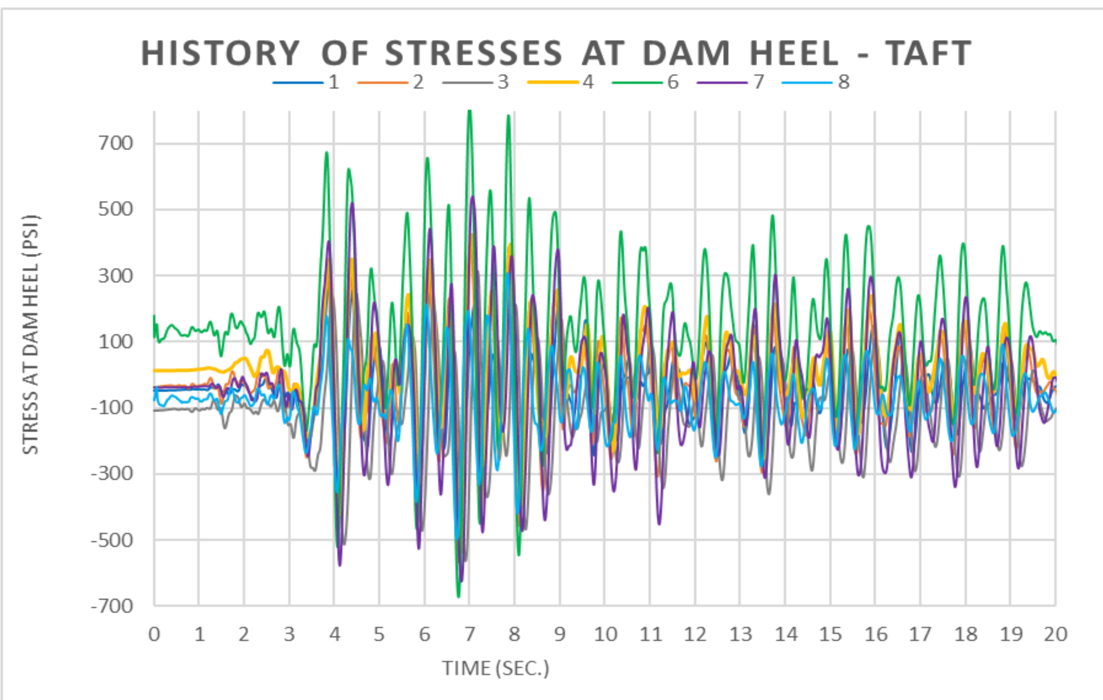

(a)

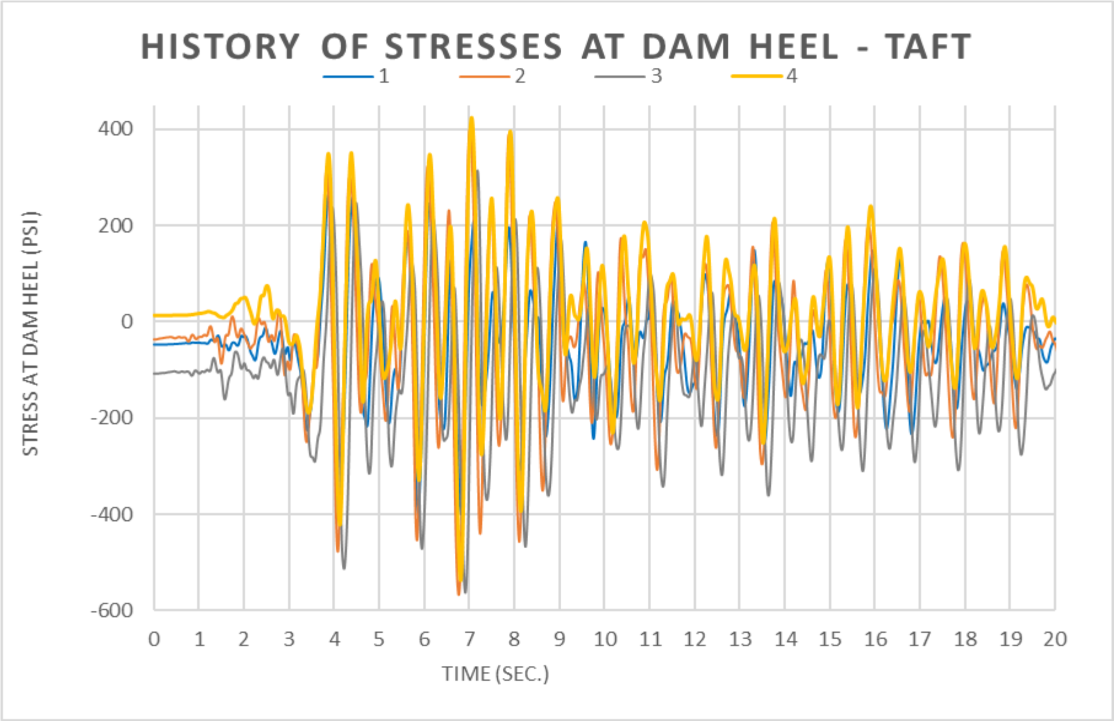

(b)

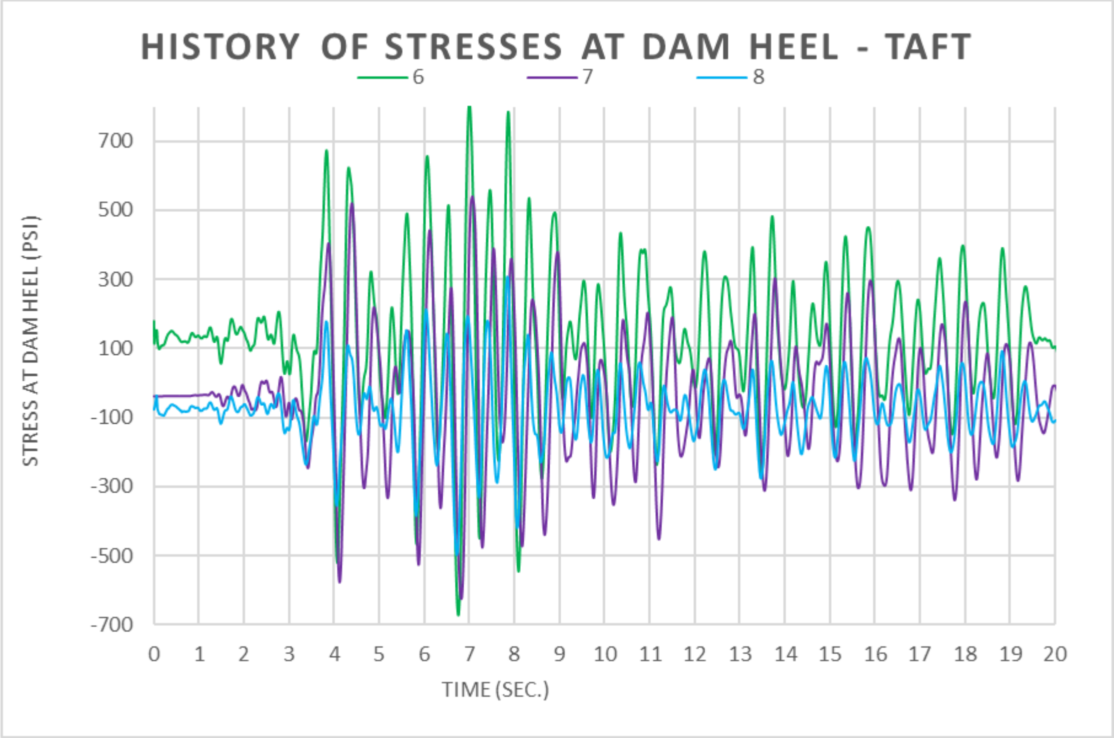

(c)

Figure 5.D.5 - TAFT Earthquake – Vertical Stress at the dam heel

Table 5.D.3 – Extreme Vertical Stress Values [lb/in^2] at the Dam Heel for Taft Load – Time Record 0 -50 seconds

Contributor	1	2	3	4	5	6	7	8
Max. Value	263.7	400.1	314.2	424.2	-	811.8	540.1	308.0
Min. Value	-407.5	-567.2	-563.1	-537.3	-	-672.3	-625.2	-497.7
Range	*671.2*	*967.2*	*877.3*	*961.5*		*1,484.1*	*1,165.3*	*805.7*

The maximum and minimum vertical stresses at the dam heel are shown in Table 5.D.3.

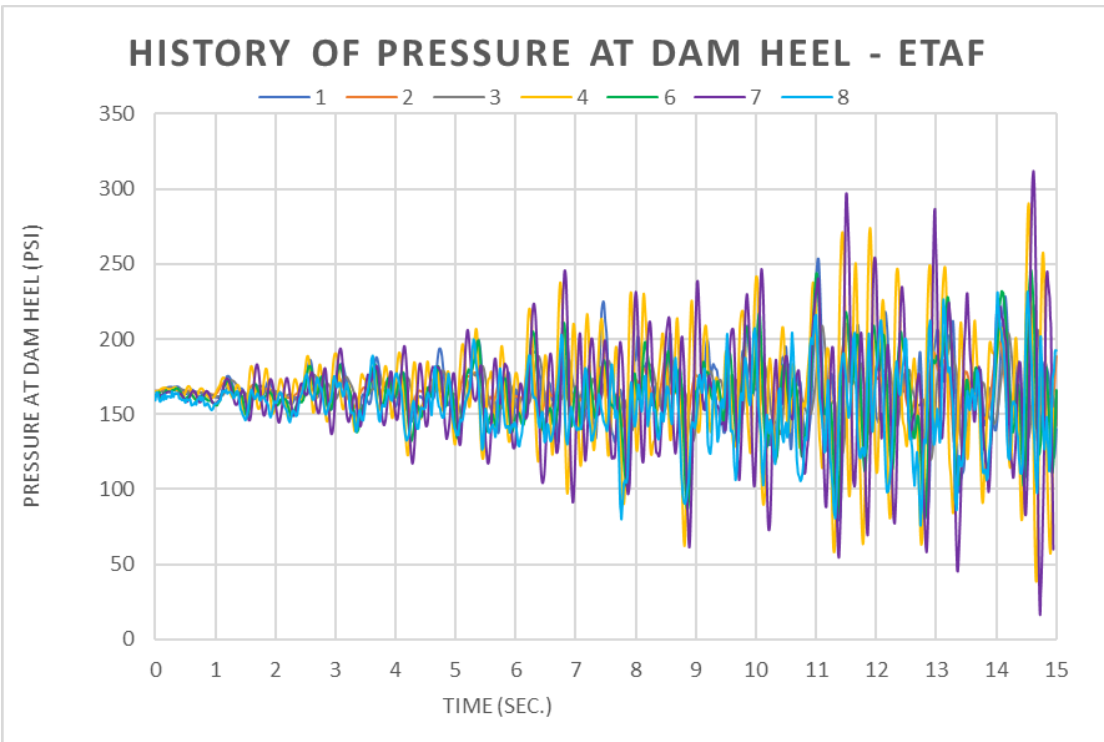

(a)

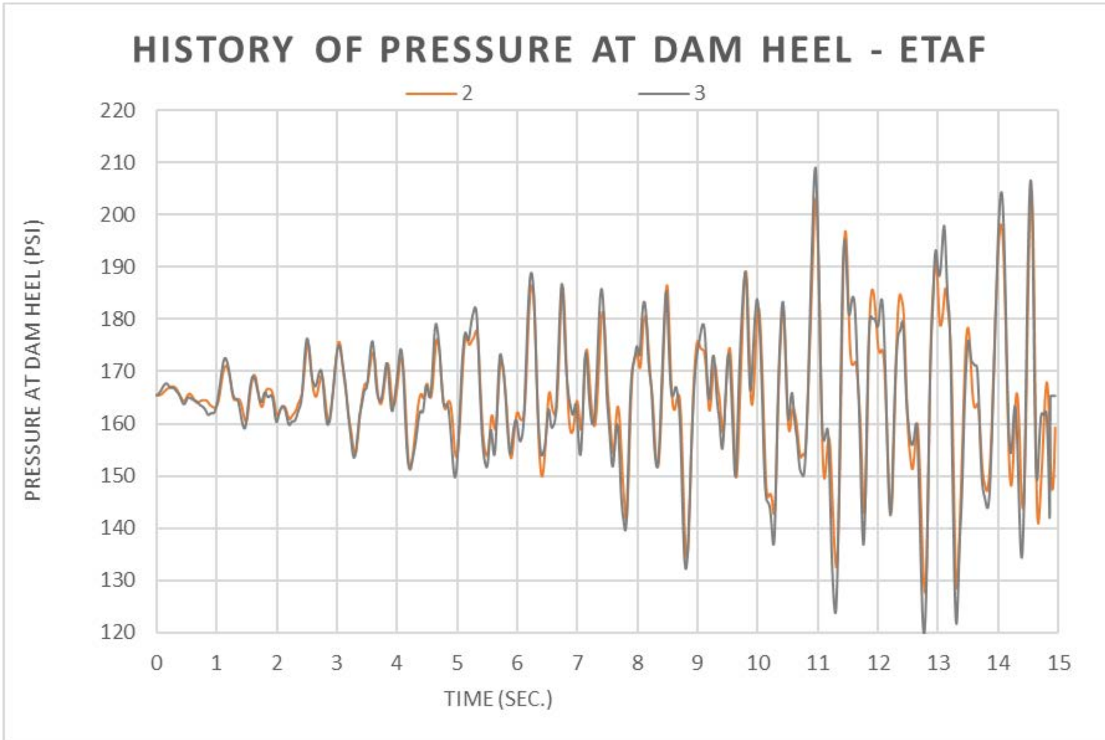
HISTORY OF PRESSURE AT DAM HEEL - ETAF
2
3
PRESSURE AT DAM HEEL (PSI)
TIME (SEC.)

(b)

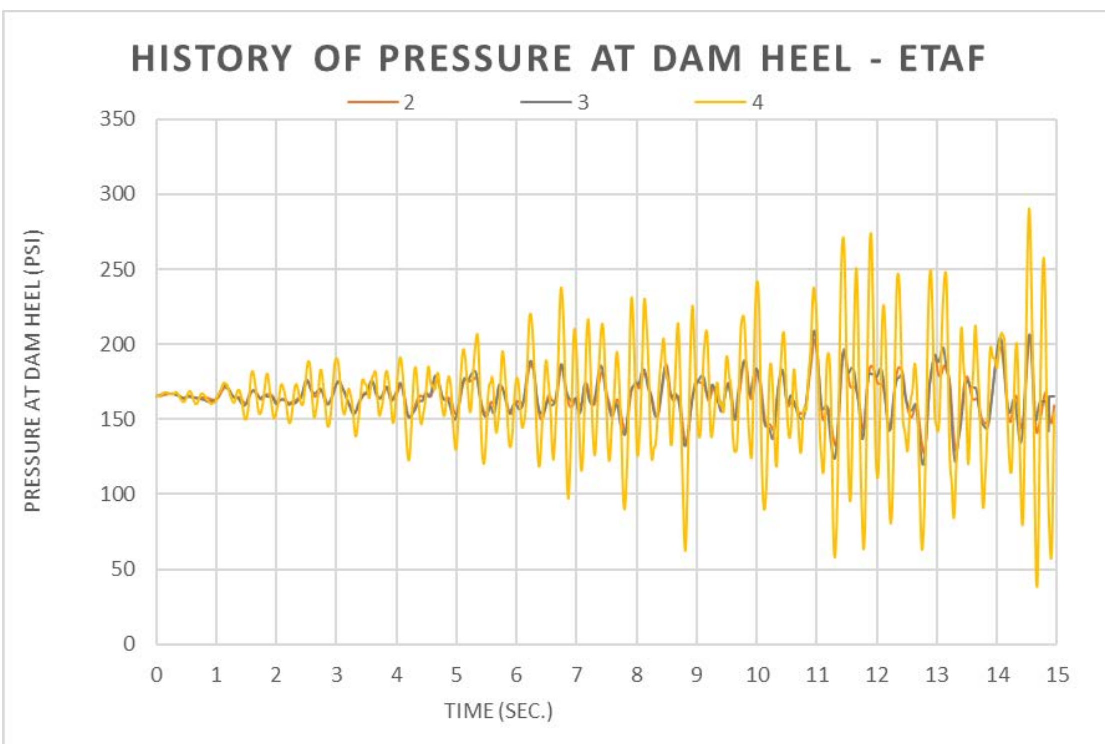
HISTORY OF PRESSURE AT DAM HEEL - ETAF
2
3
4
PRESSURE AT DAM HEEL (PSI)
TIME (SEC.)

(c)

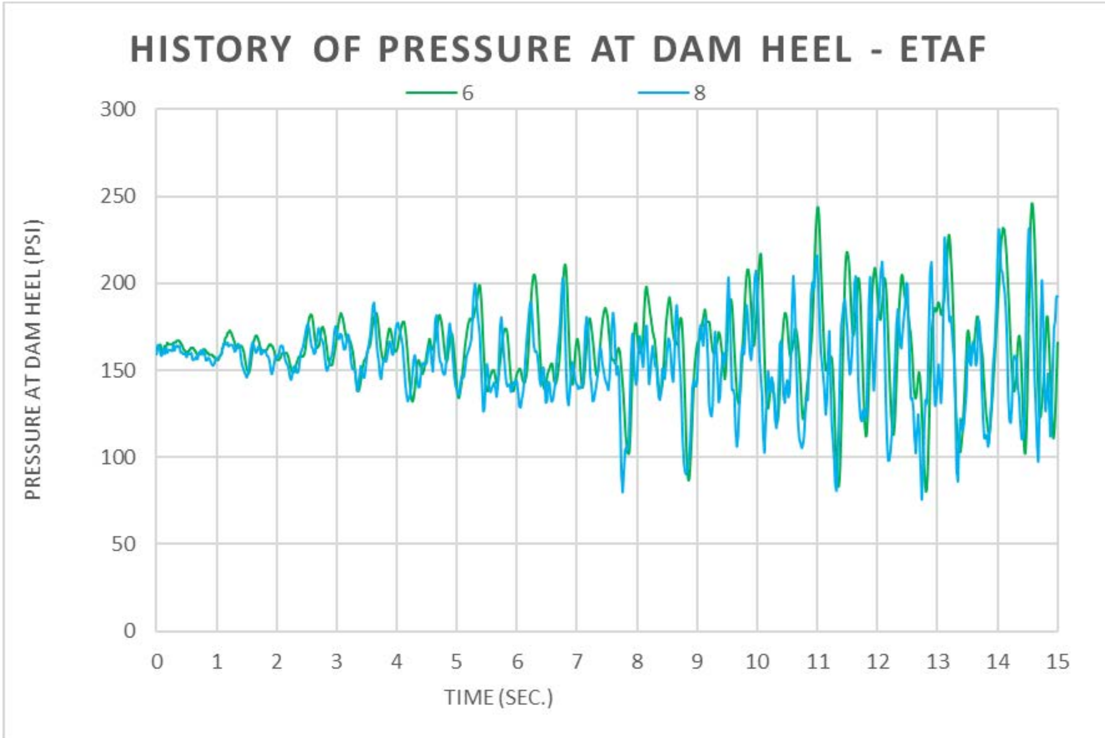

(d)

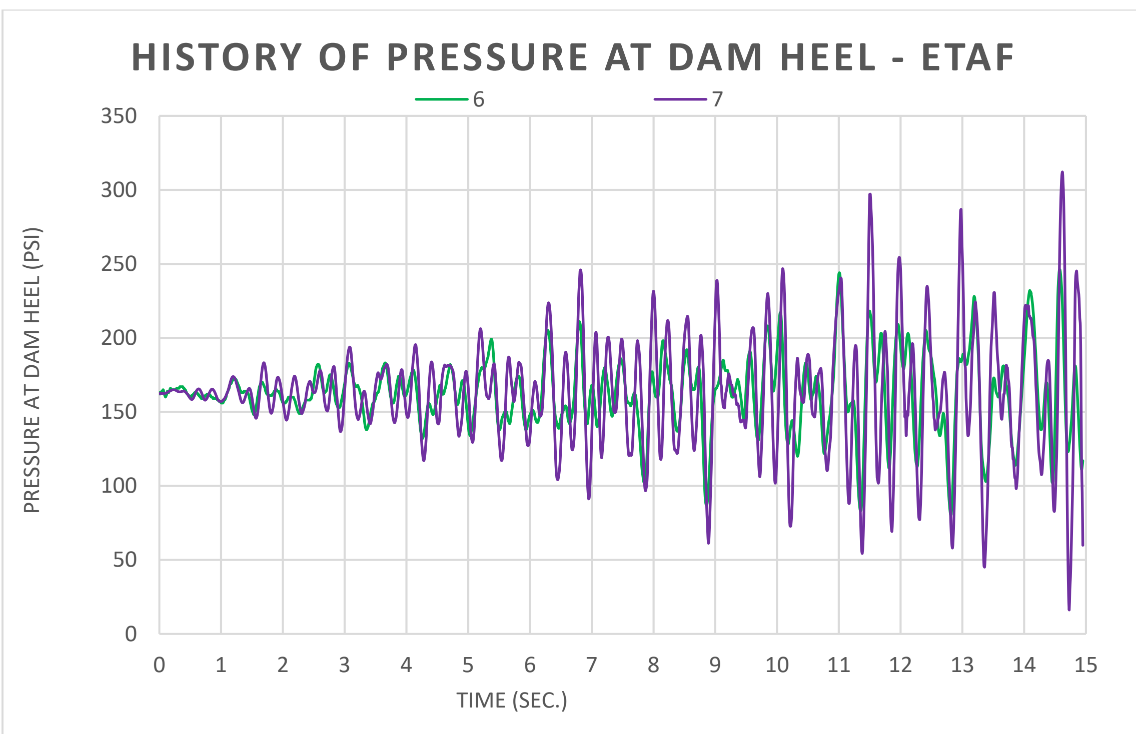

(e)

Figure 5.D.6 - ETAF Excitation - Total Pressure at the Dam Heel

Table 5.D.4– Extreme Total Pressure [lb/in^2] Values for ETAF Load - Time 0- 15 seconds

Participant	1	2	3	4	5	6	7	8
Max. Value	253.6	204.7	208.9	290.5	-	246.0	312.0	231.7
Min. Value	79.2	127.7	119.7	38.5	-	80.3	16.2	75.6

The peak maximum and minimum total pressure at the dam heel for ETAF load are shown in Table 5.D.4.

Table 5.D.5– Extreme Hydrodynamic Pressure [lb/in^2] Values for ETAF Load - Time 0- 15 seconds

Participant	1	2	3	4	5	6	7	8
Max. Value	88.5	39.6	43.8	125.4	-	80.9	146.9	66.6
Min. Value	-85.9	-37.4	-45.5	-126.6	-	-84.8	-148.9	-89.4

The maximum and minimum hydrodynamic pressure at the dam heel for ETAF load are shown in Table 5.D.5.

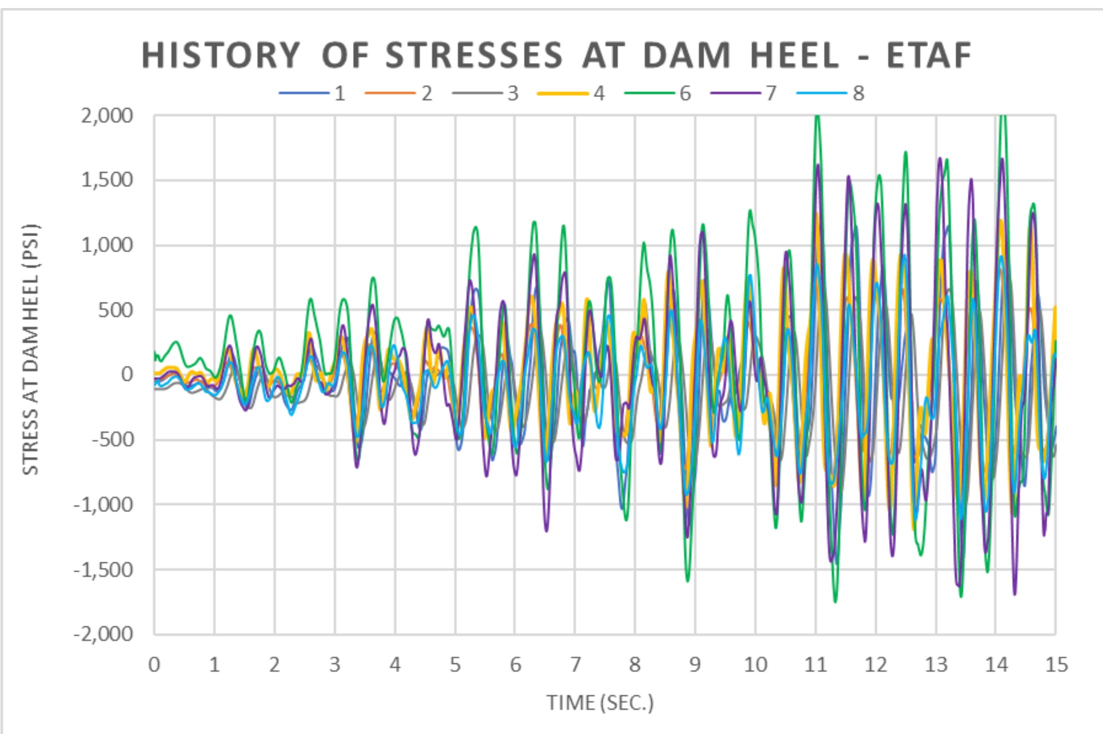

(a)

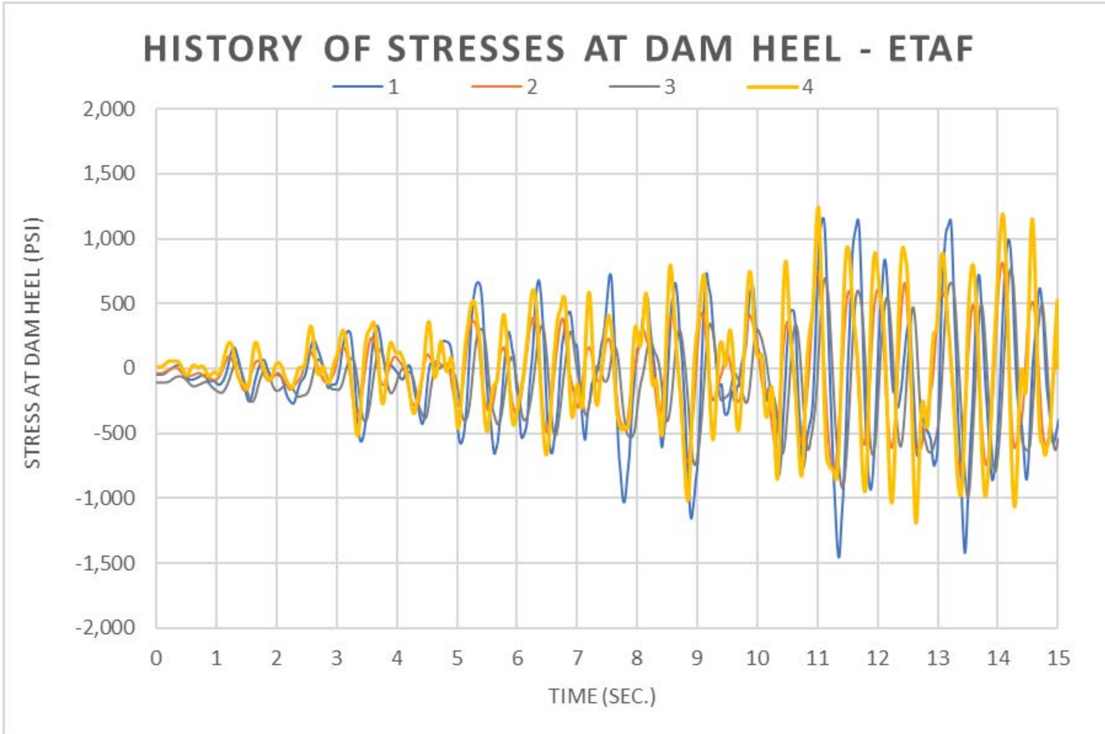

(b)

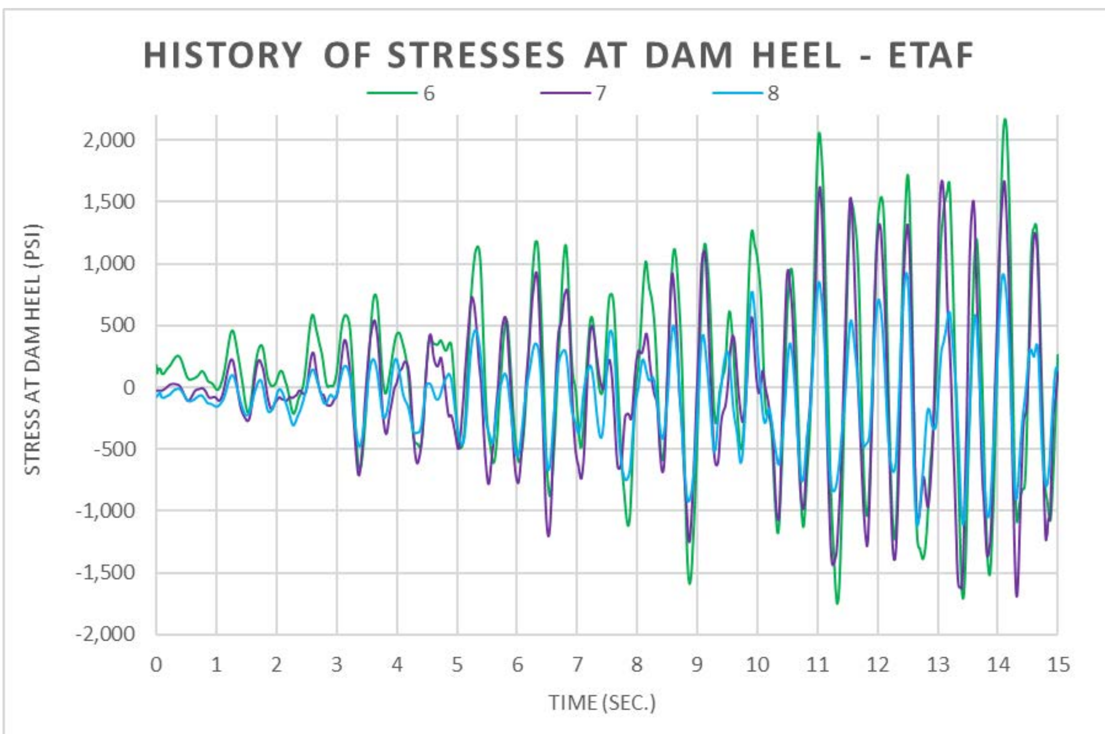

(c)

Figure 5.D.7 - ETAF Excitation – Vertical Stresses at the Dam Heel

Table 5.D.6 – Extreme Vertical Stress [lb/in^2] Values at the Dam Heel for ETAF Load – Time Record 0 -15 seconds

Contributor	1	2	3	4	5	6	7	8
Max. Value	1160.1	815.1	769.5	1244.1	-	2170.0	1672.6	925.9
Min. Value	-1455.3	-804.0	-986.3	-1190.0	-	-1750.0	-1692.0	-1120.4

The peak maximum and minimum vertical stresses at the dam heel are shown in Table 5.D.6.

5.5. Case Study E

Case E formulation is similar to Case D, except the foundation elastic modulus was about 3 times larger than one defined in Case D.

The first natural frequency of the system without reservoir was reported by four Contributors as 2.9 Hz, with a difference of 1 percent, while values from the other three Contributors were within a range difference of 7 percent. Of note, a relatively narrow range within about 10-15 percent for the higher five frequencies was determined by five Contributors (Fig. 5.E.1.a).

Very good agreement was observed for the first natural frequency of 2.43 Hz (± 0.01 Hz) of the dam-foundation-reservoir model determined by three Contributors, however, the remaining three solutions were within a 10 percent difference range. For higher natural frequencies, more variations in the results was observed between five Contributors providing the results (Fig. 5.E.1.b).

Next, the Contributors were requested to provide distributions of the hydrodynamic pressure and the total (static plus hydrodynamic) pressure at the upstream dam face (Line A-B-C, Figure 2.4) for the maximum hydrodynamic pressure determined at the dam heel in the time analysis for TAFT and ETAF loads.

Figures 5.E.2 and 5.E.3 show the total and hydrodynamic pressure distributions at the dam face for TAFT and ETAF loads, respectively. The pressure distributions correspond to the maximum hydrodynamic at the dam heel determined in the time analysis Figure 5.E.4 and Figure 5.E.6. Significant variations in the hydrodynamic pressure at the dam heel are observed ranging between 6.7 and 43.8 lb/in^2 for TAFT and between 49.8 and 131.6 lb/in^2 for ETAF loads. Consequently, significant differences in the hydrodynamic pressure distribution at the dam face were observed between the submitted results, Figure 5.E.2 and Figure 5.E.3.

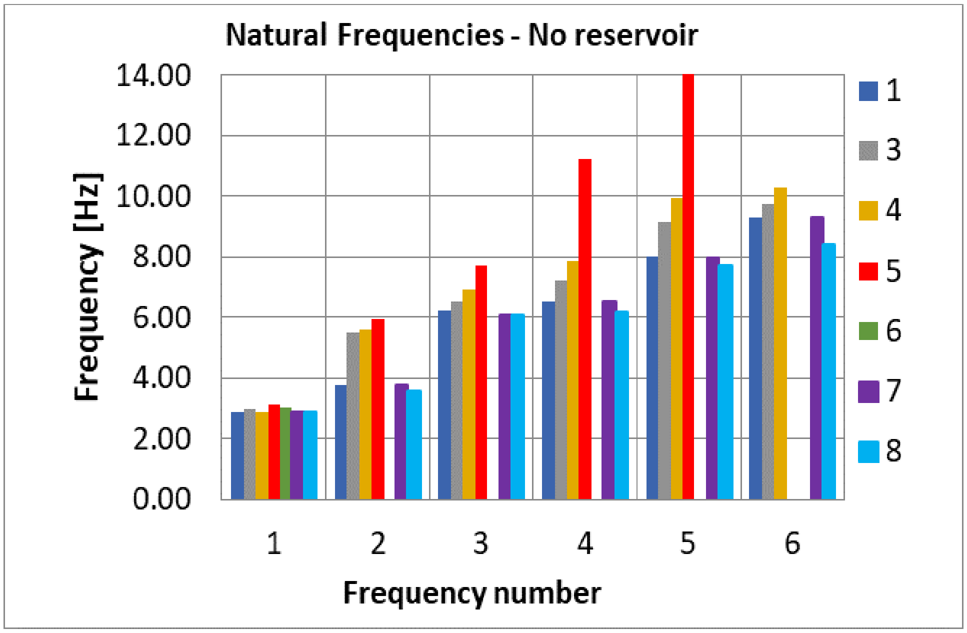

(a)

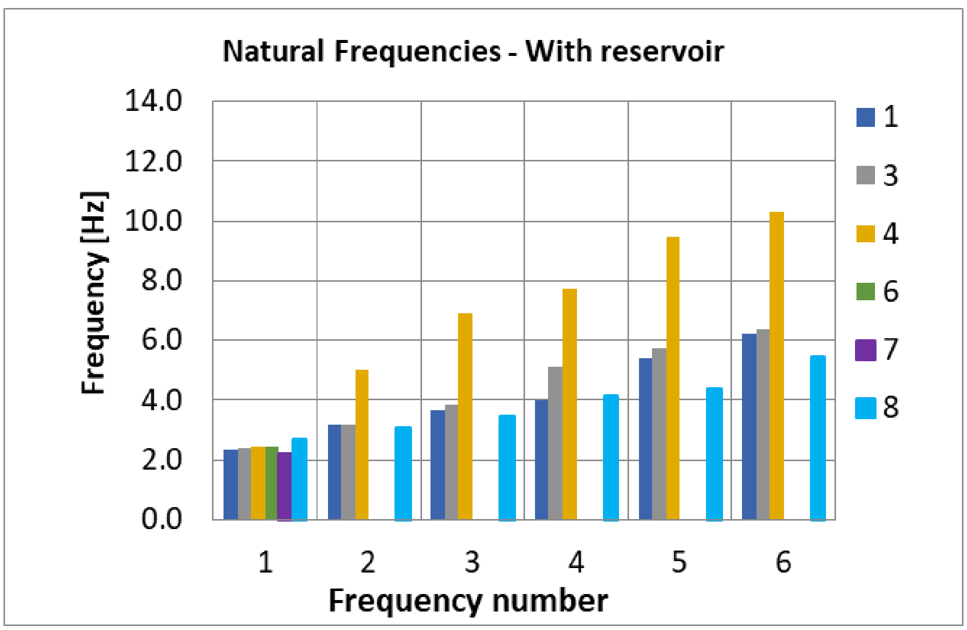

(b)

Figure 5.E.1 - Natural Frequencies (a) No Reservoir; (b) With Reservoir

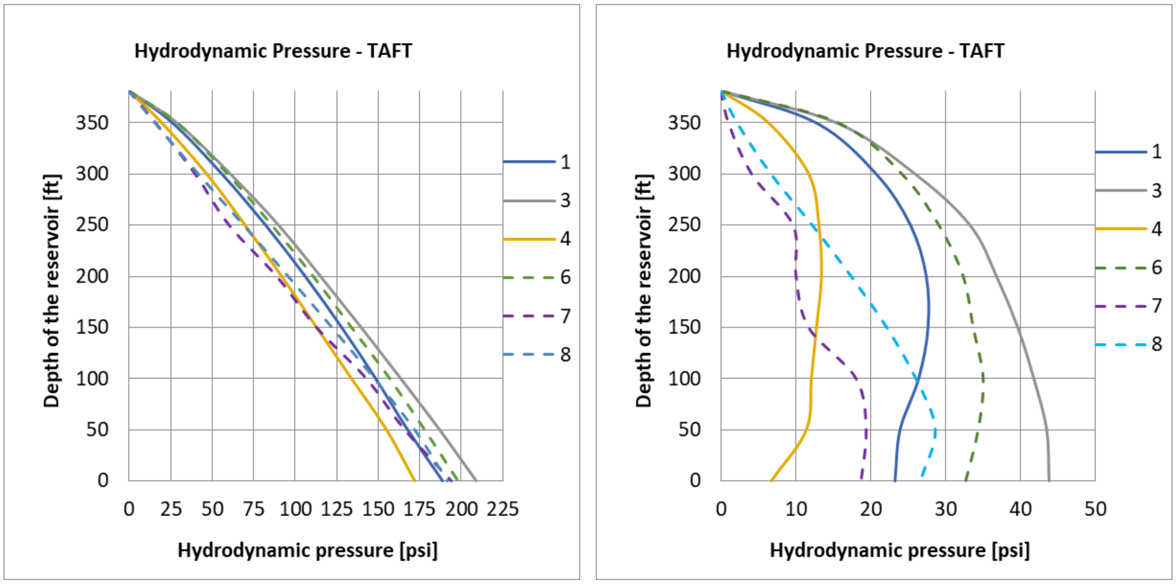

(a) (b)

Figure 5.E.2 - Taft Earthquake - Hydrodynamic Pressure (a) Total Pressure; (b) Hydrodynamic (only)

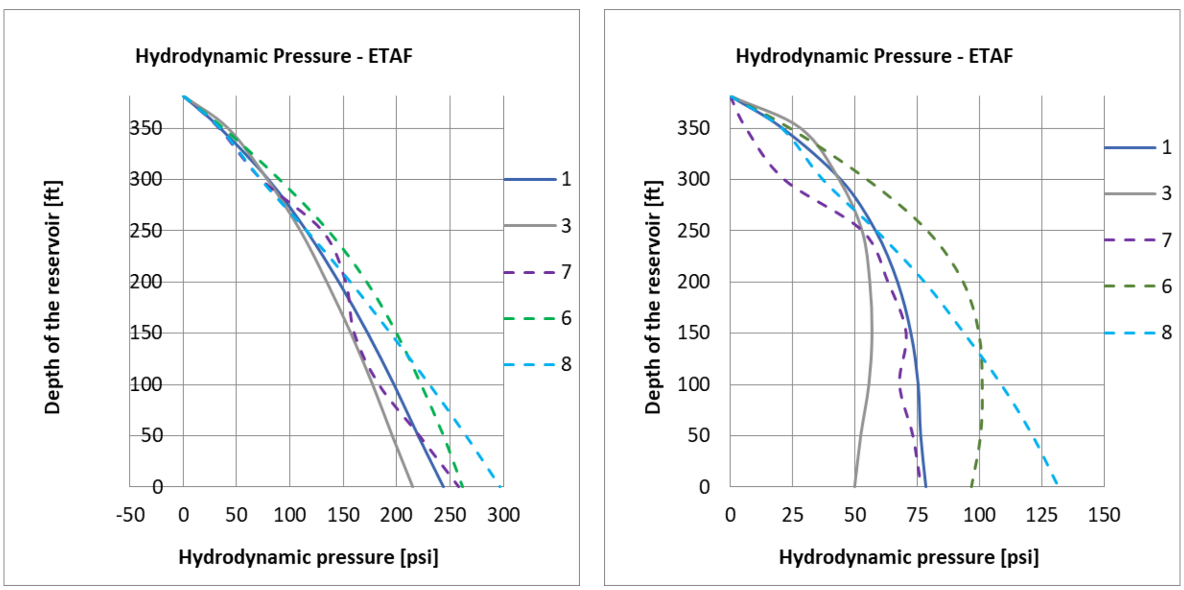

(a) (b)

Figure 5.E.3 - ETAF Excitation - Hydrodynamic Pressure (a) Total Pressure; (b) Hydrodynamic (only)

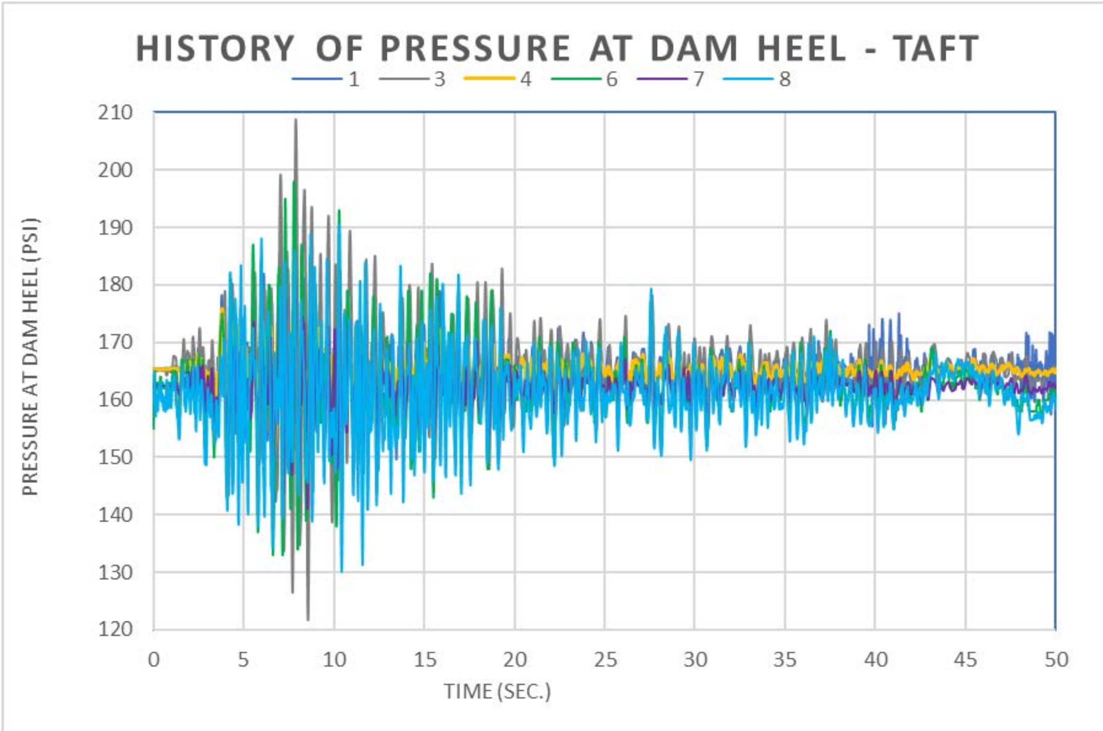
HISTORY OF PRESSURE AT DAM HEEL - TAFT
1
3
4
6
7
8
PRESSURE AT DAM HEEL (PSI)
210
200
190
180
170
160
150
140
130
120
0
5
10
15
20
25
30
35
40
45
50
TIME (SEC.)

(a)

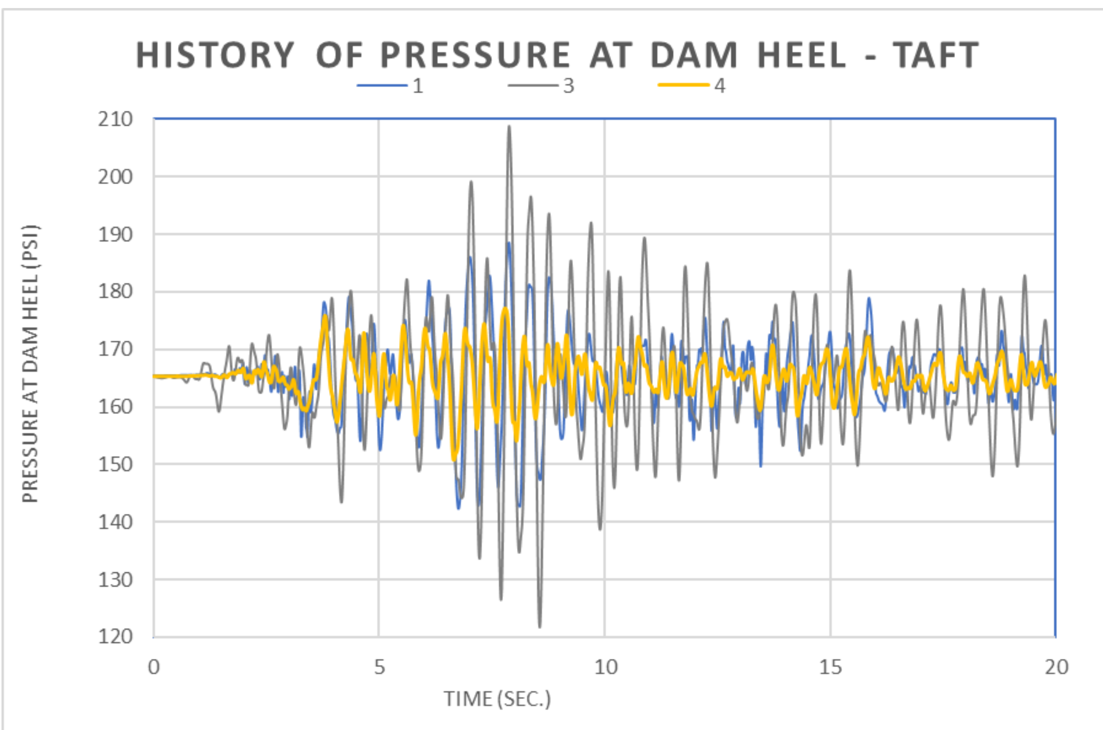
HISTORY OF PRESSURE AT DAM HEEL - TAFT
1
3
4
PRESSURE AT DAM HEEL (PSI)
210
200
190
180
170
160
150
140
130
120
0
5
10
15
20
TIME (SEC.)

(b)

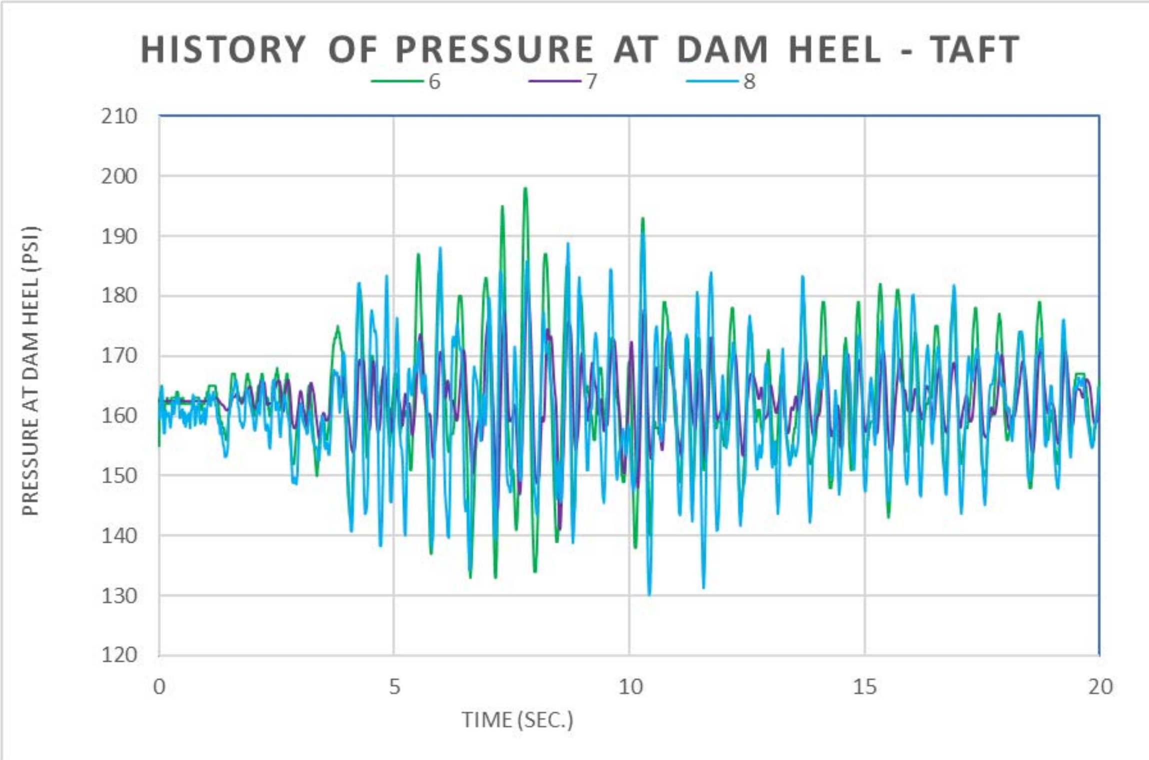

(c)

Figure 5.E.4 - TAFT Earthquake - Total Pressure at the Dam Heel

Table 5.E.1 – Extreme Total Pressure Values for Taft Load [lb/in^2] – Time Record 0 -50 seconds

Contributor	1	2	3	4	5	6	7	8
Max. Value	142.3	-	121.7	150.8	-	133.0	141.1	130.1
Min. Value	188.5	-	208.8	177.1	-	198.0	182.1	190.6
Variation	46.2		87.1	26.3		65.0	41.0	60.4

Table 5.E.2 – Extreme Hydrodynamic Pressure Values for Taft Load [lb/in^2] – Time Record 0 -50 seconds

Contributor	1	2	3	4	5	6	7	8
Max. Value	23.4	-	43.7	12.0	-	32.9	72.3	25.5
Min. Value	-22.8	-	-43.4	-14.3	-	-32.1	-76.0	-35.0

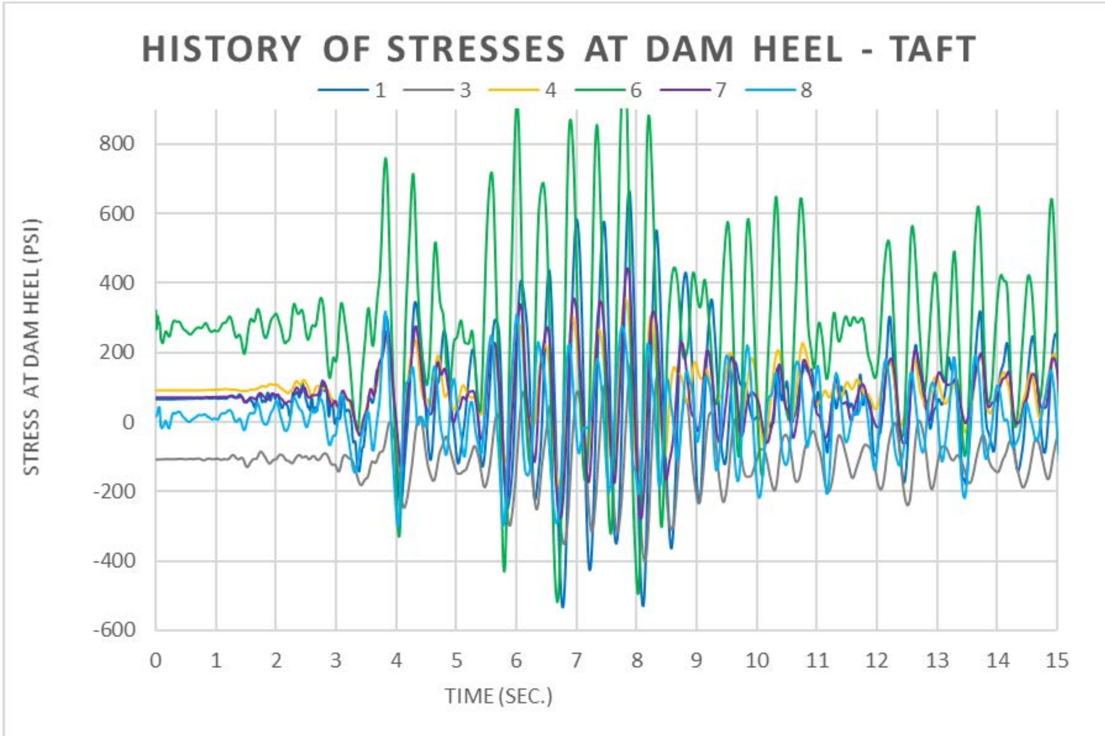
HISTORY OF STRESSES AT DAM HEEL - TAFT
1
3
4
6
7
8
STRESS AT DAM HEEL (PSI)
800
600
400
200
0
-200
-400
-600
0
1
2
3
4
5
6
7
8
9
10
11
12
13
14
15
TIME (SEC.)

(a)

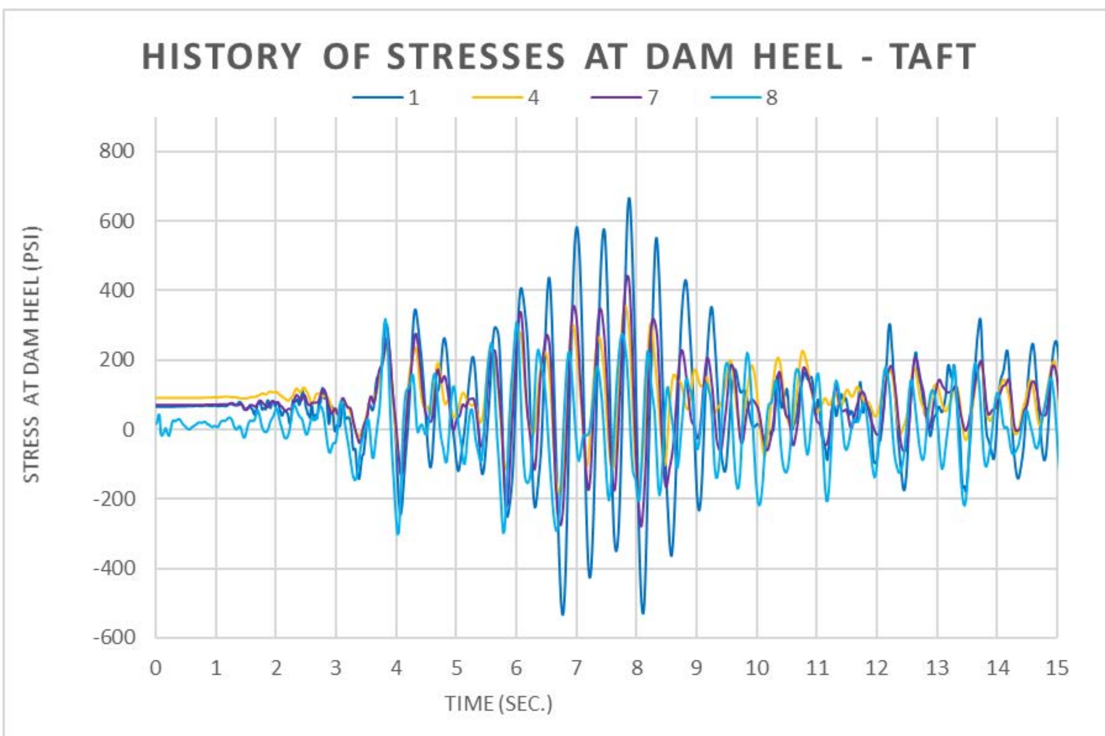
HISTORY OF STRESSES AT DAM HEEL - TAFT
1
4
7
8
STRESS AT DAM HEEL (PSI)
800
600
400
200
0
-200
-400
-600
0
1
2
3
4
5
6
7
8
9
10
11
12
13
14
15
TIME (SEC.)

(b)

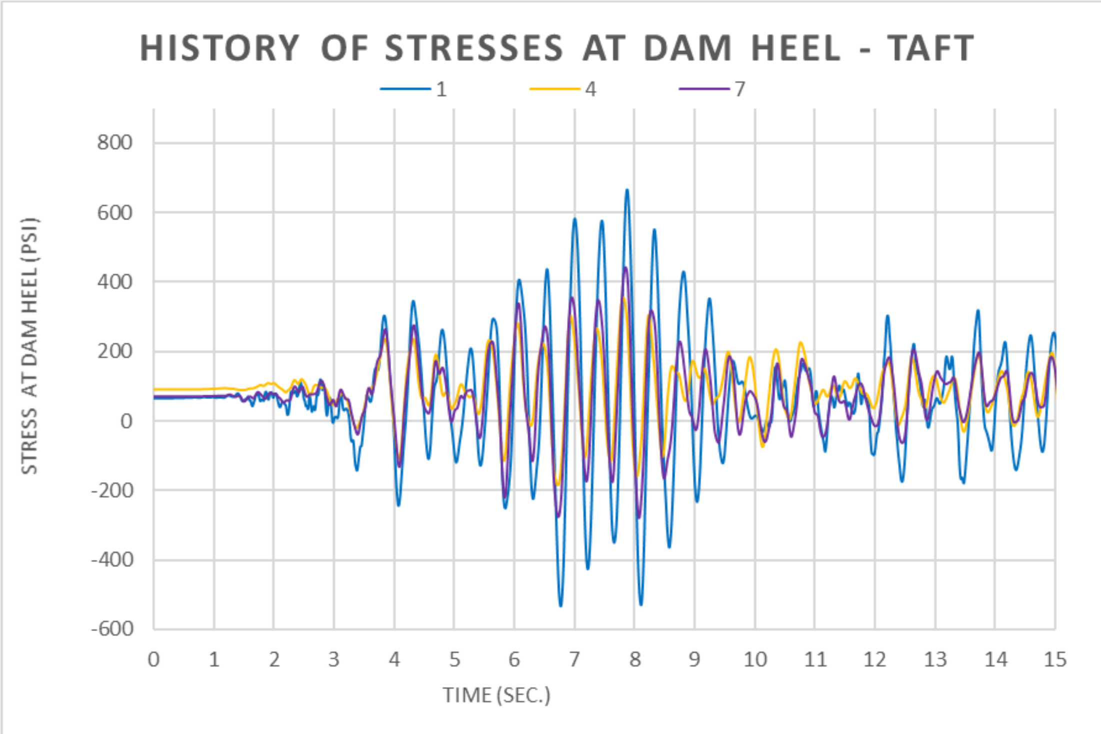

(c)

Figure 5.E.5 - TAFT Earthquake – Vertical Stresses at the Dam Heel

Table 5.E.3 – Extreme Stress Values for Taft Load [lb/in^2] – Time Record 0 -50 seconds

Contributor	1	2	3	4	5	6	7	8
Min. Value	-533.5	-	-400.8	356.2	-	-518.0	-279.0	-301.3
Max. Value	666.1	-	172.7	-184.5	-	1030.0	442.8	318.0
Variations	1,199.6	-	573.6	540.7	-	1,548.0	721.9	619.3

The peak maximum and minimum vertical stresses at the dam heel are shown in Table 5.E.3.

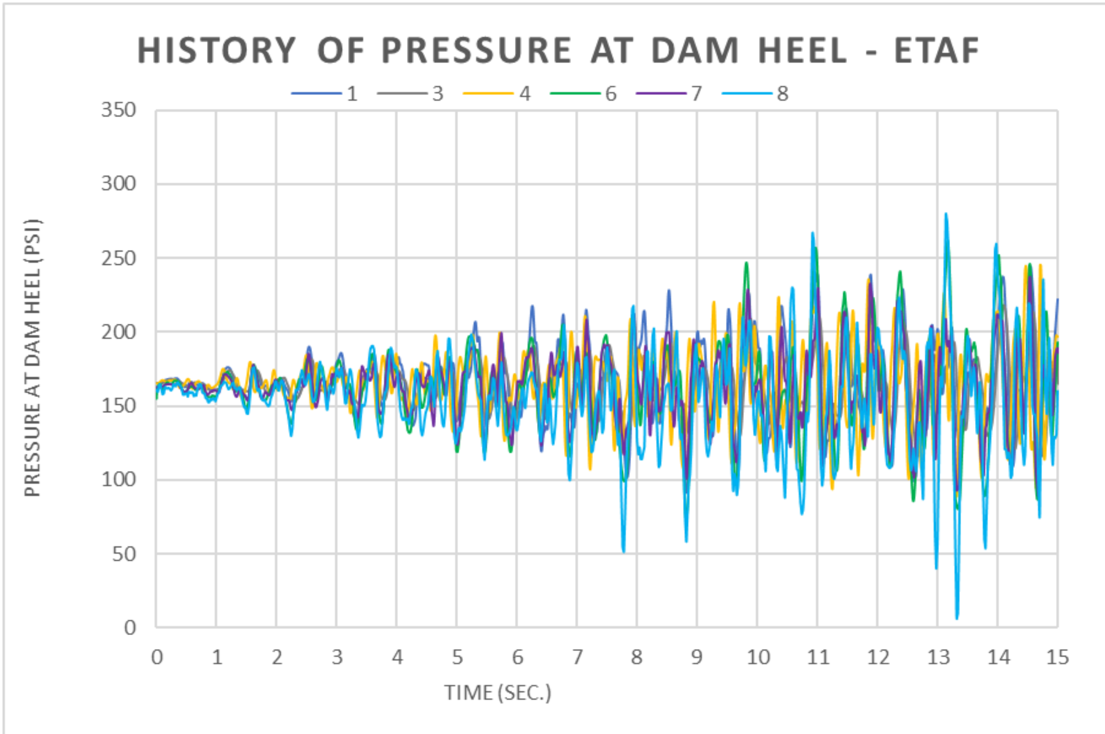
HISTORY OF PRESSURE AT DAM HEEL - ETAF
1
3
4
6
7
8
PRESSURE AT DAM HEEL (PSI)
350
300
250
200
150
100
50
0
0 1 2 3 4 5 6 7 8 9 10 11 12 13 14 15
TIME (SEC.)

(a)

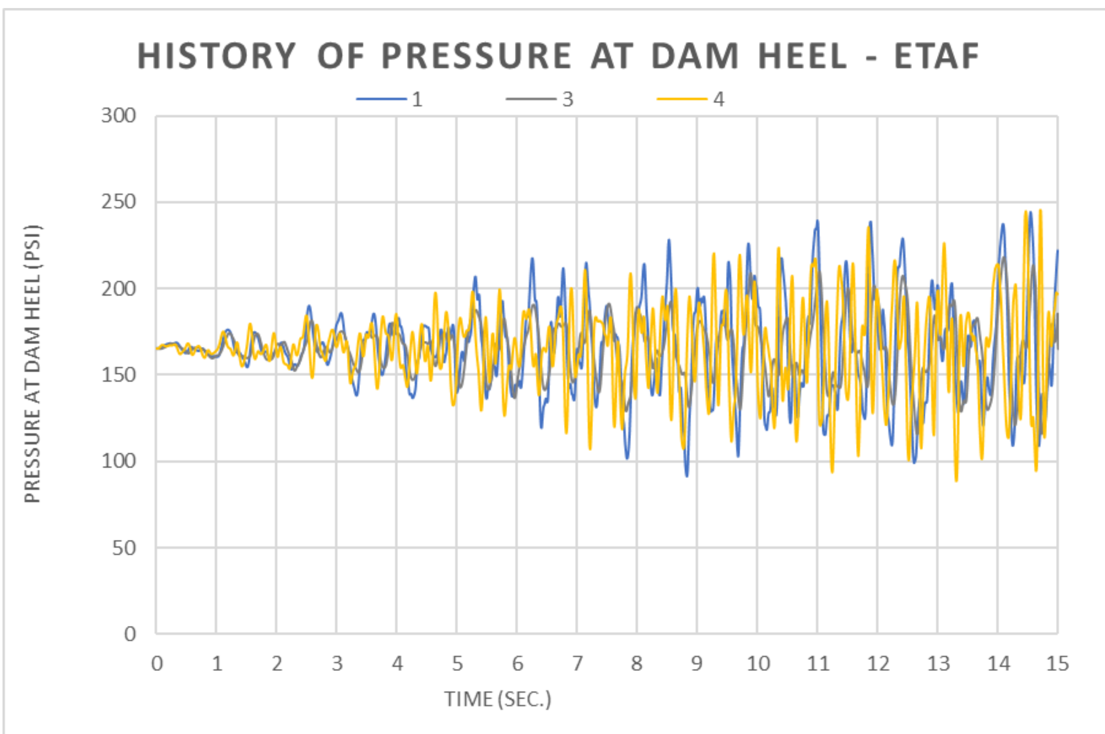
HISTORY OF PRESSURE AT DAM HEEL - ETAF
1
3
4
PRESSURE AT DAM HEEL (PSI)
300
250
200
150
100
50
0
0 1 2 3 4 5 6 7 8 9 10 11 12 13 14 15
TIME (SEC.)

(b)

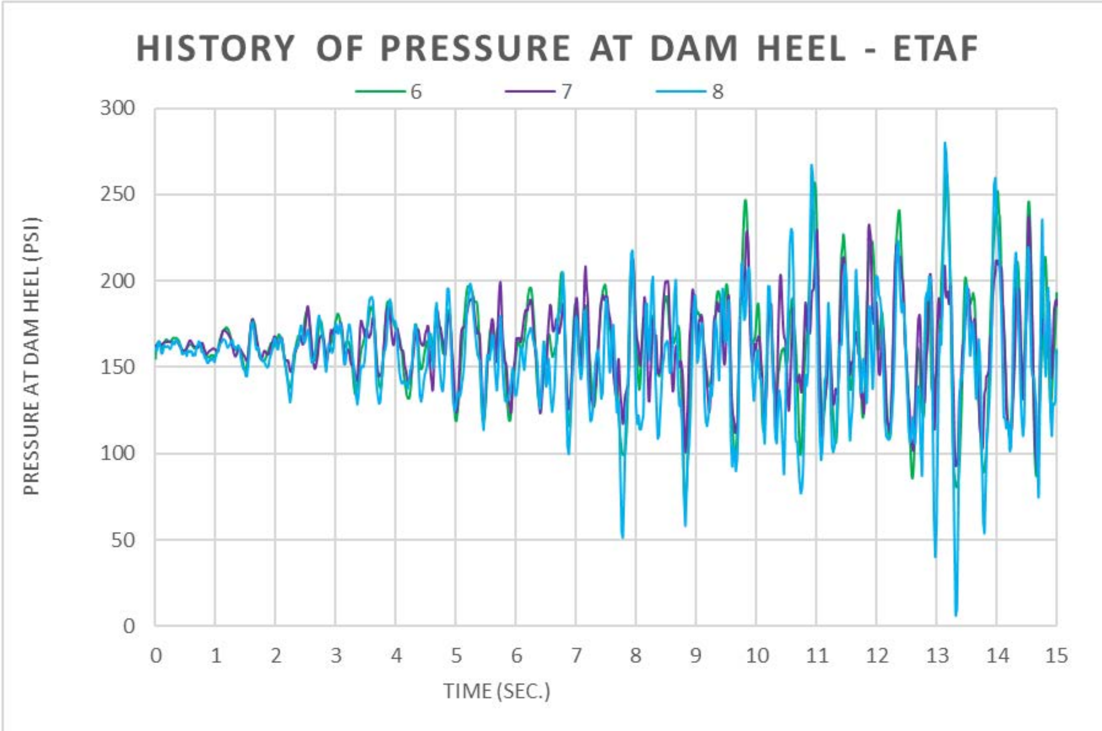

(c)

Figure 5.E.6 - ETAF Excitation - Total Pressure at the Dam Heel

Table 5.E.4 – Extreme Hydrodynamic Values for ETAF Load – Time Record 0 -50 seconds

Contributor	1	2	3	4	5	6	7	8
Max. Value	91.4	-	115.8	88.6	-	73.5	89.1	6.3
Min. Value	244.4	-	218.2	245.5	-	262.0	237.4	279.9
Variations	153.0		102.4	156.9		188.5	148.3	273.7

The maximum and minimum hydrodynamic pressure at the dam heel are shown in Table 5.E.4.

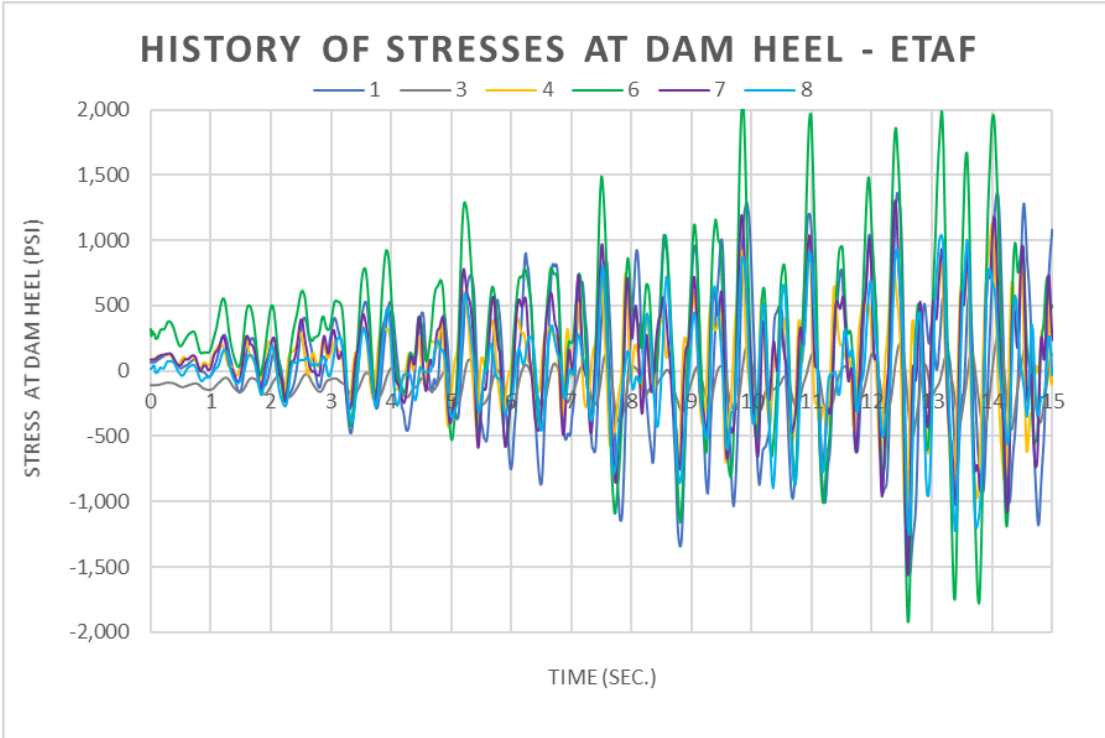
HISTORY OF STRESSES AT DAM HEEL - ETAF
1
3
4
6
7
8
2,000
1,500
1,000
500
0
-500
-1,000
-1,500
-2,000
STRESS AT DAM HEEL (PSI)
0
1
2
3
4
5
6
7
8
9
10
11
12
13
14
15
TIME (SEC.)

(a)

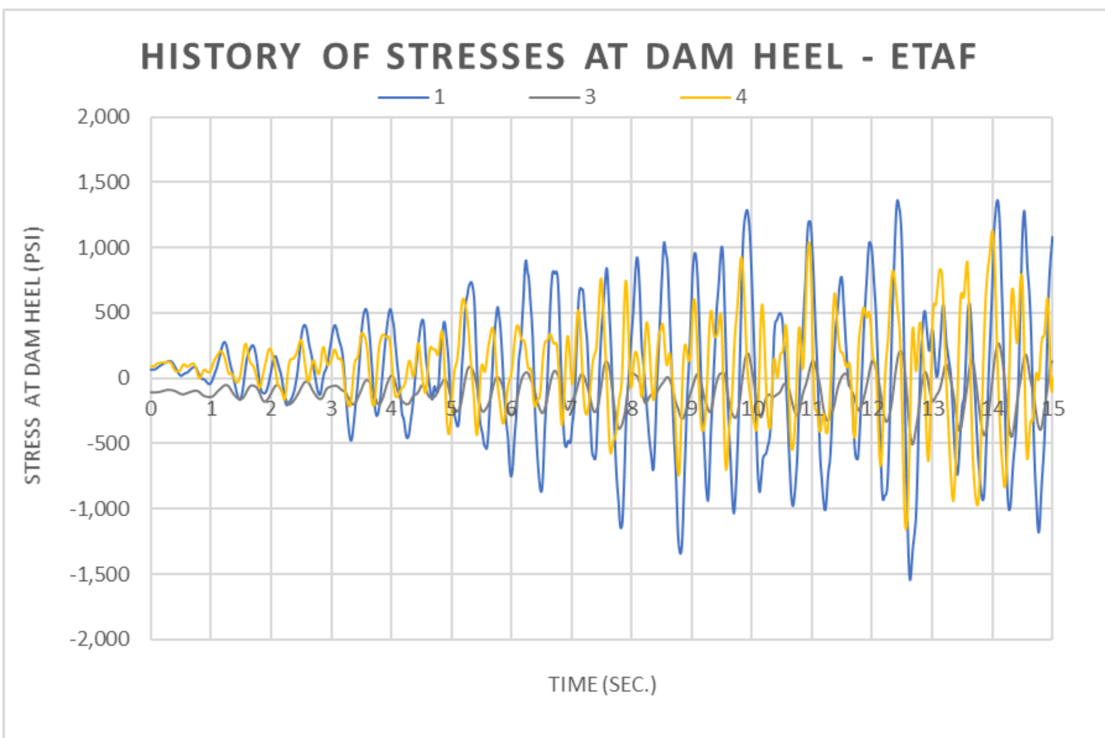
HISTORY OF STRESSES AT DAM HEEL - ETAF
1
3
4
2,000
1,500
1,000
500
0
-500
-1,000
-1,500
-2,000
STRESS AT DAM HEEL (PSI)
0
1
2
3
4
5
6
7
8
9
10
11
12
13
14
15
TIME (SEC.)

(b)

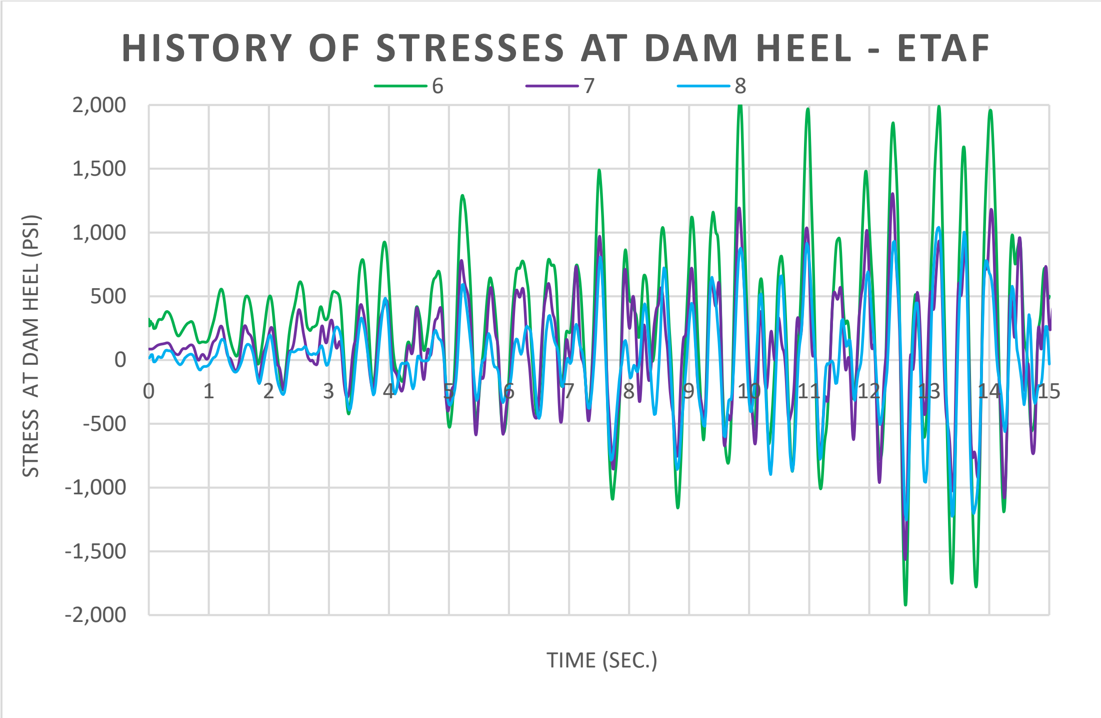

(c)

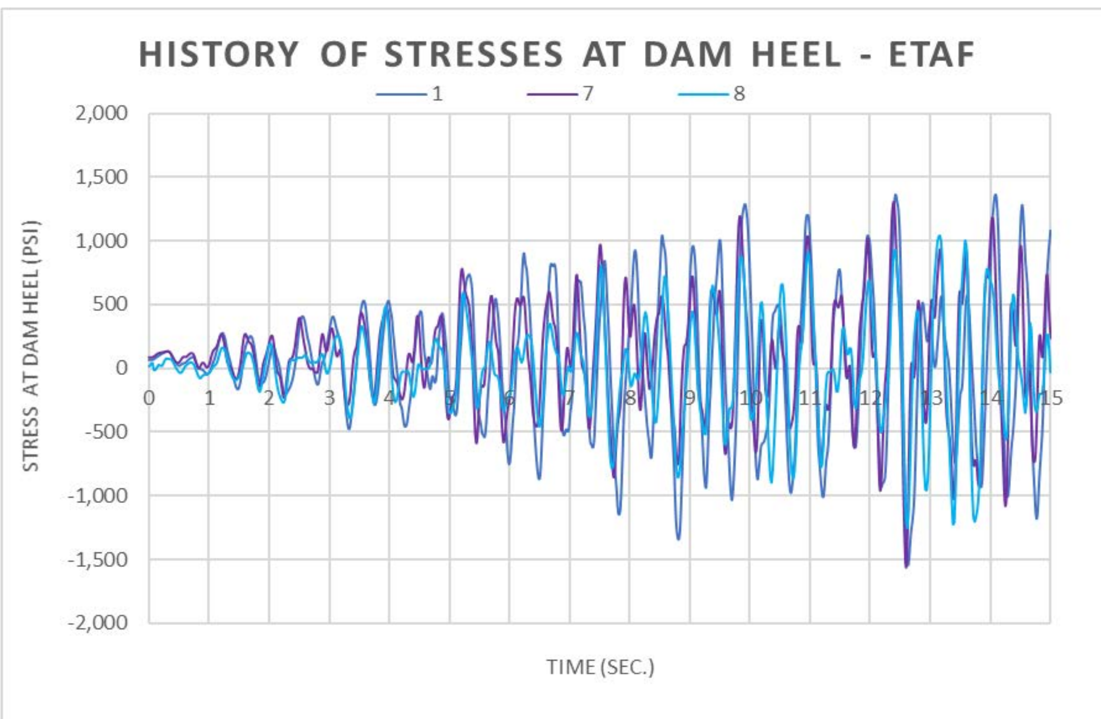

(d)

Figure 5.E.7 - ETAF Excitation – Vertical Stresses at the Dam Heel

Table 5.E.5 – Extreme Stress Values for ETAF Load [lb/in^2] – Time Record 0 -50 seconds

Contributor	1	2	3	4	5	6	7	8
Min. Value	-1,544	-	-507	-1,156	-	-1,920	-1,563	-1,254
Max. Value	1,363	-	267	1131	-	2,050	1,306	1,040
Variations	2,907	-	774	2,287	-	3,970	2,869	2,294

The maximum and minimum vertical stresses at the dam heel are shown in Table 5.E.5.

6. CONCLUSIONS

The following conclusions are made based on the results obtained from the case studies and presented within this summary report.

Static Analysis

Variations in relative displacements (between the crest and the heel of the dam) for static loads appear to be small (about 0.04 inches), however, they are in a range of about 10 percent of the total displacement. Since the geometry of the FE model, static loads and material properties used by all Contributors were the same in the linear analysis, smaller differences in the results were expected. The primary reason for these differences could be variations in FE mesh size and element type selected by the Contributors.

Natural Frequencies

- It appears that the fundamental frequency of a dam-foundation system (without reservoir) could be determined with relatively good accuracy, similar to the accuracy level obtained in an analysis for static load.
- Larger differences, especially for higher natural frequencies, are observed for the submitted results when the reservoir is included in the model. These differences could be attributed to: reporting results by the Contributors for various modes; using different computation techniques (modal analysis, Hybrid Frequency Time Domain (HFTD), and various sizes and types of FE elements).
- Good agreement in the computed fundamental frequency is observed between some Contributors for the dam-foundation system in a range of:
    - 2.46-2.56 Hz for flexible foundation (Case D),
    - 2.87-2.91 Hz for stiff foundation (Case E), and
    - 3.16-3.26 Hz for a rigid foundation (Case C).

  As can be seen, the fundamental frequency of the dam increases with the stiffness of the foundation.
- For the dam-foundation-reservoir system, good agreement is noted between a few Contributors where the fundamental frequency was in a range of:
    - 2.02-2.08 Hz for flexible foundation (Case D),
    - 2.42 – 2.44 Hz for stiff foundation (Case E), and
    - 2.54 – 2.69 Hz for rigid foundation (Case C).

  Similar to the previous observation, the fundamental frequency increases with the increase of the foundation stiffness when the reservoir is considered.
- In general, the fundamental frequency of the dam-foundation system (without reservoir) is higher when compared the corresponding frequency when the reservoir is included in the model.

Hydrodynamic Pressure at the Dam Heel

- Good agreement in the maximum hydrodynamic pressure at the dam heel, in a range between 20.8 – 22.9 lb/in^2, was found between four Contributors with a flexible foundation (Case D) for the Taft earthquake. However, hydrodynamic pressure results for a stiff foundation (Case E) resulted in a much wider range between 14.3 to 43.4 lb/in^2 with a majority of results in a range between 22.8 to 35 lb/in^2. It appears that the stiff foundation, with the elastic modulus three times the value of concrete, results in more scattered maximum pressure at the dam heel when compared the results from the case with the flexible foundation with the same elastic modulus of the concrete.

Hydrodynamic Pressure at the Dam Face

- Significant variations in the hydrodynamic pressure distributions along the face of the dam were observed for all three defined dam excitations. The primary reason for these differences is attributed to the type of numerical methods and parameters selected by the Contributors for use in time analysis, as well as the size and type of FE elements used in the analysis.
- Additionally, for the Harmonic Load case, the period of the harmonic excitation, determined individually by each Contributors, was based on the computed fundamental frequency of the dam-reservoir system. Since the computed fundamental frequency varied among Contributors, the differences in hydrodynamic pressure distributions may have been a result of the frequency differences.

Stresses in Concrete at Dam Heel

- Various FE meshing techniques were used by the Contributors and, it appears, that it is the primary reason of differences observed in vertical stresses at the dam heel for the static and dynamic loads.
- The “stress at the dam heel”, is a term commonly used in the engineering practice, but does not have a clear meaning in the FE analysis. Computed local stress concentrations at the dam heel are reliant on the type and size of the FE mesh selected in analysis.

Damping

Damping is one of the most critical parameter in the transient analysis of civil structures. Damping is defined as the energy of the vibrating system dissipated by various mechanisms, including internal and external material friction, plasticity, viscosity, hydrodynamic interaction, radiation, etc. More than one damping mechanism could be present at the same time. For the linear analysis performed in the workshop, only a few of the listed mechanisms apply. For instance, Rayleigh damping was precisely defined in the formulation, however damping may have been the factor influencing the obtained results due to the application variance in the analysis conducted by various software.

Deconvolution

Deconvolution is a procedure which allows development of the earthquake excitation at the base of the foundation block from the recorded ground motion. The existing procedures of deconvolution are not effective for all types of earthquake records including high-frequency and low-frequency ground motions. The deconvolution process chosen by the Contributors could be another source of the differences between results. Considering the complexity of the deconvolution process, it would be beneficial to develop a separate investigation program evaluating the accuracy of the procedure.

General Conclusions

The outcome of the workshop demonstrated that even for simple model geometry of a gravity dam and precisely defined model parameters, a large variance among the results may be obtained in a linear transient analysis. It appears that the numerical analysis of the dam-reservoir-foundation system for seismic loads does not lead to a unique solution, but rather depends on several factors including selection of the time integration method and the parameters defined in the analysts. With this in mind, the results of the FE analysis should not be seen as “the exact solutions of engineering problem” but rather as an approximation of such solutions. In response, the analysis procedure needs to be extended through an accuracy assessment of the solution (error estimations) when the results of the FE analysis of concrete dams for seismic loads are reported.

The following is a list of the primary uncertainties identified during the workshop exercise for the linear transient analysis of a concrete dams-foundation-reservoir system:

- Deconvolution,
- Far field boundary conditions,
- Time integration method (implicit vs explicit), parameters of the method, size time step, accuracy of the convergence (convergence error criteria),
- Size and type of FE elements,
- Damping (both the damping type and its critical parameters),
- Fluid-structure interaction – method describing the interaction.

7. REFERENCES

1. Rea D., Liaw C.Y., Chopra A. K., - Dynamic Properties of Pine Flat Dam, Report No. UCB/EERC-72/7, December 1972
2. Chopra A. K., Chakrabarti P., Gupta S., - Earthquake Response of Concrete Gravity Dams Including Hydrodynamic and Foundation Interaction Effects, Report No. UCB/EERC-80/01, January 1980
3. Fenves G., Chopra A. K., - Simplified Analysis for Earthquake Resistance Design of Concrete Gravity Dams, Report No. UCB/EERC-85/10, June 1986
4. Chavez J. W., Fenves G. L., - Earthquake Analysis and Response of Concrete Gravity Dams Including Base Sliding, Report No. UCB/EERC-93/07, December 1993
5. Chavez J. W., Fenves G. L., - EAGD_SLIDE: A Computer Program for the Earthquake Analysis of Concrete Gravity Dams Including Base Sliding, Report No. UCB/SEMM-1994/02, March 1994
6. Fenves G., Chopra A. K., - EADG-84: A Computer Program for Earthquake

8. SUMMARY OF THE WORKSHOP DISCUSSIONS

A summary of the discussion and questions raised during the workshop discussion are provided in this section:

1. If the FE analyse results provided by the Contributors are the same, are they correct or wrong? Are the differences important?
2. Selection of the boundary conditions in the model appropriate to each application. What kind and where to apply?
3. Damping: How to apply it? Pick a frequency to measure damping?
4. Seismic loads: free-field seismic input loads, their location, outcrop reference being more appropriate.
5. The Contributors agreed that the “massless foundation” model should not be used in the transient analysis of the dam-reservoir-foundation system.
6. The workshop outcome will be captured in an initial report developed by the Workshop Problem Formulators. This report together with the summary of the USSD 2016 and 2017 workshop discussion on the subject will be used as a source for developing a USSD White Paper in 2019.

9. SUGGESTIONS FOR FURTHER CONSIDERATIONS

9.1. Suggestion Submitted by Workshop Participants

The following topics were suggested by the Contributors for further investigations based on their findings.

Contributor 1

- The investigation regarding the effects of the horizontal sizes of the foundation could be further carried on taking into account the seismic signal, both for the foundation only model and for the complete dam-reservoir-foundation model.
- Evaluate the effects of modelling the reservoir and the foundation as connected or non-connected.
- Comparison of the traditional and widespread *massless foundation* approach and those of the *seismic wave propagation* approach would be quite significant.
- Outcome from the workshop could represent a good basis for the possible formulation of one of the Themes on concrete dams to be proposed in the frame of the 15th ICOLD Benchmark Workshop that is held in Milan, Italy on September 11, 2019.

Contributor 2

- Several substantial unresolved issues exist when it comes to nonlinear modeling of concrete dams and how to interpret the output from these analyses. This has become increasingly important as regulators tend to move away from a “binary” safety evaluation methodology and towards more performance-based assessment methodologies. Thus, there is a need for more research on the nonlinear behavior and nonlinear modeling of concrete dams.

Contributor 3

- Where the dam/base interface is likely to open, a non-linear (contact) surface should be incorporated to allow cracking, sliding and uplift pressures. This is particularly important for performance-based design of dams.
- Natural frequencies are also affected by base or lift joints cracking. Main frequencies would become more challenging to compute, as linear methods would not be appropriate. A frequency sweep analysis is usually performed on these cases.
- Another very common subject is the consideration of flexible features like gates on spillway, which would affect the fluid-structure interaction, on top of the geometry complexity. Posttensioned structures are also prone of relative displacements and joint opening.

- Structural fragility is very important for budget management and retrofit planning. The calculation of vulnerability requires the proper simulation of failure modes. We have used more advanced non-linear features for this purpose, like the modeling of lift joints, concrete cracking (plastic damage of concrete), material uncertainty analyses, and other techniques like response surface analysis and Monte Carlo simulations all together with the FEA approach.

Contributor 4

- Recommended an analysis for a foundation block with a baseline corrected excitation (modified Case B).
- Perform comparison analysis of the dam models with simplified loads (pulse or harmonic) for specified model parameters including size of the model, material properties, etc. to evaluate numerical aspects of the used analysis methods.
- Overview and evaluation the approach used in deconvolution of the seismic loads for the FE analysis of the dam-reservoir-foundation system.
- Validation of the FE models with laboratory test results – Reclamation is currently performing a shake test to determine a hydrodynamic interaction between a 4-ft by 4-ft structure and water.
- A hybrid frequency-time domain analysis should be implemented in the seismic simulations of the dam-reservoir-foundation system.

Contributor 5

- An earthquake often induces large deformation that leads to cracks in the concrete faces of the dam. Future study could consider fracture of gravity dam and its influence on dam performance.
- Additional study should involve an interface between dam and foundation, which can facilitate the potential sliding and overturning mechanism of gravity dam.
- Hybrid numerical method could be used to study the fluid-dam interaction problems. For instance, the particle-based method could be used to simulate fluid phase response, while mesh-based finite element method can be applied to dam and foundation structure. The performance of this hybrid approach should be benchmarked with analytical solutions and experimental results in the literature.

Contributor 6

- Modeling failure along a surface in the current model, be it at the concrete-rock interface or through the dam itself, is a logical extension of the current workshop. Contributors would be given the location of one (or more) failure planes, and a set of properties along that plane (tensile and shear strength, some measure of the surface roughness). Of interest would be: how initial fracture is modelled; how and what friction properties are chosen; modelling of uplift within the failure plane; and differences in FEM approaches to modelling sliding.

- As an extension of case B in the current workshop, we suggest a wave propagation exercise that attempts to account for the real topography around a dam. Participants would be given free-field ground motions, the size of an input box around the dam (which would constitute the boundaries of a typical FE model of a dam), and the local topography. The purpose of this problem would be to understand the effect of topography on the free-field motion, and to discuss best practices for obtaining the spatial variation of free-field at the boundaries of the input box.
- In the current workshop a single block of a concrete gravity dam was modelled, making it essentially a 2D analysis. In reality, adjacent blocks will have an impact on the movement of the block, particularly if there are shear keys at vertical contraction joints. We envision a workshop where participants are instructed to model a dam with three blocks, defined shear keys, a rigid foundation, and rigid abutments on either side which restrain the edges of the other two blocks. The effect of the shear keys would therefore be completely isolated, and it would be up to the participants to model the keys however they want. Different modeling approaches would be compared with respect to both the opening-closing and non-linear shear slip behavior of the contraction joints. This is a subject on which there is not much available literature, and a workshop on the topic would be a good way to start discussion on a topic which likely has a major effect on the response of concrete gravity dams.

Contributor 7

- The current deconvolution methodology utilizes the assumption of the elastic foundation model: (i.e. foundation domain is homogenous, no separation). In reality, most foundations are complex with existing faults and cracks. Important future work should address how these complexities affect the propagation of ground motions through these foundations.

Contributor 8

- The LS-DYNA soil-structure interactions approach to seismic shaking is useful, but at present, it only works on flat surfaces. Ultimately, it would be very useful for the industry to develop a set of best-practices for dam-water-foundation seismic analysis that includes a robust fluid modeling approach and is capable of capturing soil-structure interactions, as well as topography effects. To that end, the two most important considerations for future workshops are comparing fluid modeling approaches and comparing methods of seismic input.

9.2. Suggestions Provided during Workshop Discussion

The following are the suggestions were made by the workshop participants during the discussion:

1. Amplification of acceleration at the crest of the dam – this information would be a vital parameter in the future investigations of concrete dams.
2. Provide comparison between the workshop results with analysis performed by A. Chopra in [1].
3. Define terminology that could be used in the FE analysis of concrete dams to describe the commonly used terms in engineering practice such as “stress at the dam heel”.
4. Variation of the analysis results at the given time steps in the future investigations could be a universal measure used in the comparison of the results.
5. Difference in stresses at the dam heel were influenced by the size and type of FE elements, number of integration points, location at which the stress is reported. These differences for static solutions could be amplified in dynamic analysis.
6. Forces, not the stresses, are the key measures used in the design of concrete dams. Focus on stress analysis could lead to wrong results of the design and such analysis should be carefully evaluated (observations provided by G. Lund).
7. Perform evaluation of modal analysis to identify the importance natural modes of the structure. Evaluate contribution of higher frequencies in a model response to the seismic excitations.
8. For a total pressure (static + hydrodynamic) a pressure envelope was suggested that might be more appropriate rather than providing the max value.
9. In the analysis, some Contributors applied the atmospheric pressure. Should it be considered in the FE analysis?
10. It was suggested that the workshop results that significantly deviate from the results provided by other Contributors are excluded from the comparison.
11. Interpretations of the results from the advanced analyses
    a. Knowing what the results are telling and how interpret them in engineering practice
    b. Provide best practice for those less experienced
    c. No unique solution – necessary to define uncertainty
12. What ground motions can the dam take? Suggested to formulate a benchmark analysis of the laboratory tests conducted at the Bureau of Reclamation.
13. Damping in the FE analysis should be addressed in more detail.
14. Investigate the size of the FE mesh and how it effects the analysis results.
15. Consider verification of the analysis results with test data from in the Pine Flat study [1].

APPENDIX A

Workshop Agenda

8:00 AM **Welcome**

Jerzy Salamon - Concrete Dam Committee Chairman and Lelio Mejia - Earthquake Committee Chairman

8:05 AM **Introduction**

(Moderator: Hillery Venturini – Workshop Organizing Committee Leader)

- Introduction to the workshop
    - General discussion from 2017 USSD Workshop
    - Purpose for 2018 USSD Workshop
- Overview of problem formulation
    - Case studies
    - Description of additional topics investigated by participants
- Introduction of participants and submission information

8:30 AM **Presentation of Workshop Results**

(Moderators: Hillery Venturini and Jerzy Salamon)

- Summary of Results
    - Findings
    - Trends & Areas of Uncertainty
    - Open Discussion

9:00 AM **Berkeley Pine Flat Analysis Results**

(Presenter: Larry Nuss)

- Overview of prior Berkeley studies of Pine Flat Dam
- Discussion

9:45 AM **Break**

10:00 AM **Presentations by Participants**

(Moderators: Hillery Venturini and Yusof Ghanaat)

- Investigation Results on Focus Subject (3 participants)
    - 10 min presentation
    - 5 min discussion
- Open Discussion

11:00 PM **Break**

11:15 PM **Presentations by Participants (continued)**
(Moderators: David Queen and Vik Iso-Ahola)

- Investigation Results on Focus Subject (3 participants)
    - 10 min presentation
    - 5 min discussion
- Open Discussion

12:15 AM **Lunch (provided by USSD)**

1:15 PM **Presentations by Participants (continued)**
(Moderators: David Queen and Mohammad Amin Hariri)

- Investigation Results on Focus Subject (2 participants)
    - 10 min presentation
    - 5 min discussion
- Open Discussion
-

2:00 PM **Break**

2:15 PM **Discussion and Questions**
Moderators: Jerzy Salamon and Larry Nuss

3:15 PM **Summary and Conclusions**
Moderators: David Queen and Yusof Ghanaat

3:45 PM **Workshop Closeout**
Moderators: Jerzy Salamon and Lelio Mejia

4:00 PM Adjourn

ATTACHMENT B – PAPERS SUBMITTED BY CONTRIBUTORS

List of Submitted Papers by Contributors

1. Faggiani, Giorgia and Piero Masarati. “Summary Paper for Workshop Analysis Results on Evaluation of Numerical Models and Input Parameters in the Analysis of Concrete Dam, USSD 2018 Annual Conference, Miami”. March 2018.
2. Loekke, Arnkjell. “Summary Paper for Workshop Analysis Results on Evaluation of Numerical Models and Input Parameters in the Analysis of Concrete Dam, USSD 2018 Annual Conference, Miami”. Norwegian University of Science and Technology and University of California Berkeley. March 2018.
3. Quiroz, Juan, Nathan Grossman, Rich Barrie, and Nedda Djavid. “Summary Paper for Workshop Analysis Results on Evaluation of Numerical Models and Input Parameters in the Analysis of Concrete Dam, USSD 2018 Annual Conference, Miami”. Stantec. Chicago, Illinois. March 2018
4. Salamon Jerzy., Partovi Maz. - “Summary Paper for Workshop Analysis Results on Evaluation of Numerical Models and Input Parameters in the Analysis of Concrete Dams”, USSD 2018 Annual Conference, Miami
5. Yuan, Yixing. “Summary Paper for Workshop Analysis Results on Evaluation of Numerical Models and Input Parameters in the Analysis of Concrete Dam, USSD 2018 Annual Conference, Miami”. GZA GeoEnvironmental Inc. Norwood, Massachusetts, March 2018.
6. Bergman, Brent, Osmar Penner, Mina Shahbazi, and Jeff Yathon. “Summary Paper for Workshop Analysis Results on Evaluation of Numerical Models and Input Parameters in the Analysis of Concrete Dam, USSD 2018 Annual Conference, Miami”. BCHydro. Burnaby, British Columbia. March 2018.
7. Koltuniuk, Roman, Lan T. Nguyen, and Shohreh Hamedian. “Summary Paper for Workshop Analysis Results on Evaluation of Numerical Models and Input Parameters in the Analysis of Concrete Dam, USSD 2018 Annual Conference, Miami”. Bureau of Reclamation. Denver, Colorado. March 2018.
8. Ghanaat, Yusof and Zachary Harper. “Summary Paper for Workshop Analysis Results on Evaluation of Numerical Models and Input Parameters in the Analysis of Concrete Dam, USSD 2018 Annual Conference, Miami”. Quest Structures, Inc. Orinda, California. March 2018.

PARTICIPANT INFORMATION

Organization	RSE SpA
Authors	Giorgia Faggiani, Piero Masarati
Software	INDIA (in-house code) for modal analyses. Abaqus for time history analyses

Cases Analysed

Case	Combination						
A	A-1						
B	B-1V	B-1H	B-2V	B-2H	B-3V	B-3H	
C	C-1(a)	C-2(a)		C-2(b)	C-2(c)		
D	D-1(a)	D-2(a)	D-1(b)	D-2(b)	D-2(c)		
E	E-1(a)	E-2(a)	E-1(b)	E-2(b)	E-2(c)		

1. Method and Approach

The various Case Studies are addressed by means of the Finite Element Method, using a 3D model, realised using the provided geometry. With the only exception of Case B, the model includes the 50-foot-wide dam monolith 16 and the relevant portions of foundation and of reservoir (complete model). The mesh, showed in Figure 1, is made of linear elements (4 within the width): structural elements (1076 for the dam and 9360 for the foundation, for a total of 13930 nodes) and acoustic elements (6732 for the reservoir, for a total of 8840 nodes). In Case B (foundation only) the mesh for model B-1 is the same used in the complete model (9360 elements and 12390 nodes), the mesh for model B-2 consists of 50000 elements and 65730 nodes, the mesh for model B-3 (selected as intermediate between B-1 and B-2, with length I-F = 7300 feet) consists of 29680 elements and 39060 nodes. The different parts of the mesh (dam, foundation and reservoir) are quite uniform, with element size ranging from 10 and 20 feet.

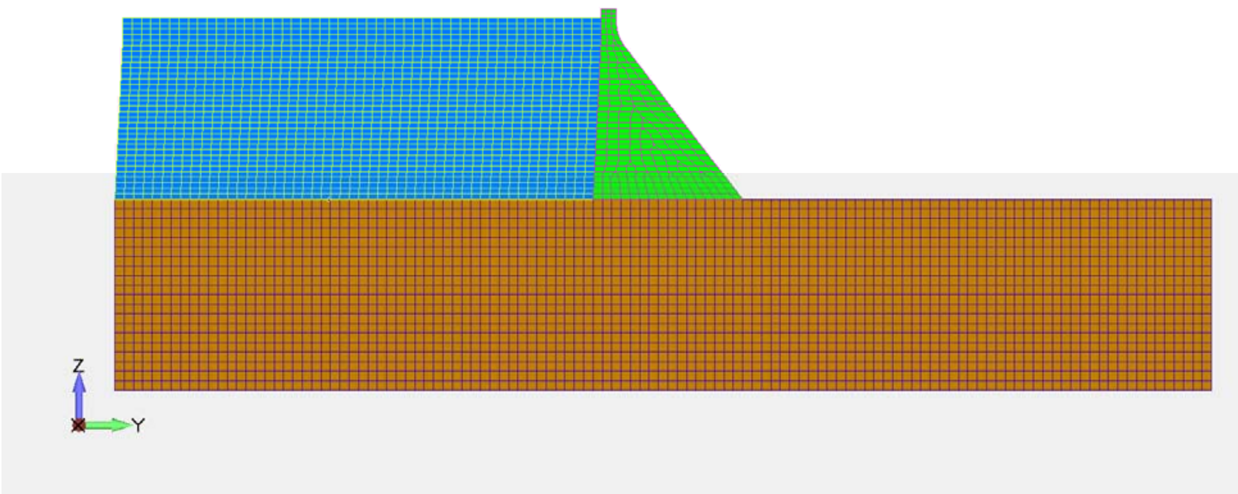

Figure 1 – FEM model of the monolith, the foundation and the reservoir

The fluid domain is obtained by extruding the upstream face of the dam mesh for a length about 2.5 times the total height of the dam, reaching the upstream boundary of the foundation. The dynamic interaction between the dam and the reservoir is achieved through the classic structural-acoustic coupling on the upstream face of the dam, where the normal component of the dam acceleration is related to the normal gradient of the water hydrodynamic pressure [1]. No dynamic interaction is considered between the foundation and the reservoir. The upstream truncation of the reservoir is provided with non-reflecting acoustic condition. No seismic excitation is applied either to the bottom or to the upstream truncation of the reservoir.

The time integration implicit method HHT [2] is adopted, with $\alpha=-0.05$ *and* $\Delta t = 0.005$ s. The convergence criteria are based on the evaluation of the nodal unbalanced forces: because of the linearity of the simulated physical problem, they are not actually used.

The only considered static loads are the weight of the dam and the weight of water for the NRWL (the weight of the foundation is not included in the analyses). The weight of water is applied as hydrostatic pressure on the upstream face of the dam and on the surface of the foundation. The boundary conditions for the static analyses consist in restraining the normal components of the displacement vector on the four vertical faces of the foundation as well as on its bottom face. Qualitatively similar boundary conditions are considered for the dynamic time history analyses with rigid foundation (Case C), as the same normal components, in this case of the acceleration vector, are assigned according either to the Taft Earthquake time history, simultaneously in upstream/downstream and vertical directions, or to the ETAF ground motion, in upstream/downstream direction only (the cross-canyon normal component is restrained in both cases, the vertical normal component is restrained in the case of the ETAF ground motion).

The dynamic time history analyses with flexible foundation (Case B, Case D and Case E), which are actually wave propagation problems in unbounded domain, require suitable "artificial boundary conditions", as an artificial boundary arises from the truncation of the unbounded foundation. Such conditions, often referred to as "absorbing boundaries", are designed so that the outgoing waves can correctly cross the external borders of the truncated foundation [3][4]. In addition, an appropriate technique is needed to calculate "effective earthquake forces" from the seismic excitation as the earthquake motion cannot be assigned directly at the model truncations: in fact this would render any absorbing boundary ineffective [4]. The viscous-spring artificial boundaries (VSAB) are adopted, making reference to the formulation and examples of application reported in [3][5][6][7] and using spring and dashpot elements available in Abaqus [8]. The effective earthquake forces are computed following the procedure detailed in [6][7], based on the theoretical solution of the elastic wave problem in a half-space: in particular, vertically propagating body waves are considered, both P-waves (vertical displacements) and S-waves (horizontal displacements). Although the effective earthquake forces should be computed and applied both on the bottom and on the side boundaries of the foundation, the choice of ignoring the forces on the side boundaries is adopted, following a pragmatic suggestion of the US Bureau of Reclamation [4][9]: as a general rule, when the effective earthquake forces are only applied on the bottom of foundation, its horizontal sizes should be properly increased.

2. RESULTS

The following sections report the main findings of static and time history simulations.

2.1. Case A

The static analyses for normal reservoir water level (NRWL) have been performed with the two sets of material properties for foundation (A-1(I) and A-1(II)): they provide results which appear reasonable and congruent.

Both total and relative displacements are rather small. The horizontal relative displacement between the top and the base of the dam does not depend on the stiffness of the foundation rock: it is therefore entirely due to the dam deformability, without any contribution from its base rotation.

Vertical stress at dam/foundation interface (Figure 2)is everywhere compressive in case of the foundation with "Properties I" (more flexible), while the stiffer foundation ("Properties II") involves slight tensile stress at dam heel: in both cases, vertical stress is quite uniform, with the only exception of the extreme upstream and downstream zones of the interface.

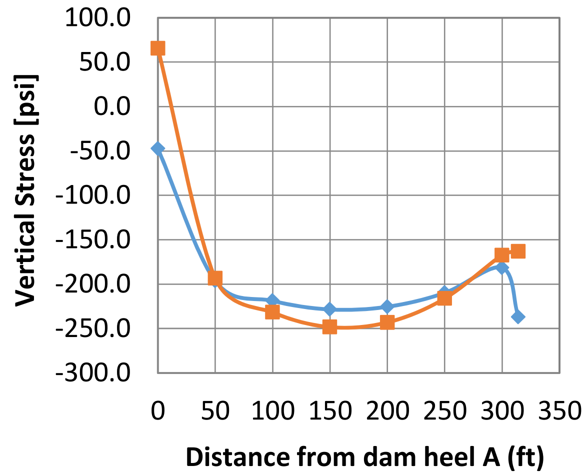

Figure 2 – Vertical stress at dam/foundation interface

2.2. Case B

The effect of foundation horizontal extent has been investigated with the two provided models (B-1 and B-2) and an intermediate one (B-3 detailed in § 1). Considering that the viscous damping is very small (1%), the double of the time pulse load itself can be used as a good approximation of the reference solution. The horizontal and vertical response time histories at ground surface are reported in Figure 3, Figure 4 Figure 5 for cases B-1, B-2 and B-3 respectively. In general, the longer the model, the better the numerical solution. For a given model, the results worsen approaching its extremes. Better results arise from the vertical pulse (P wave) than from the horizontal one (S wave), especially with the shorter model: the horizontal S wave case appears to be more sensitive to the lateral extension of the foundation.

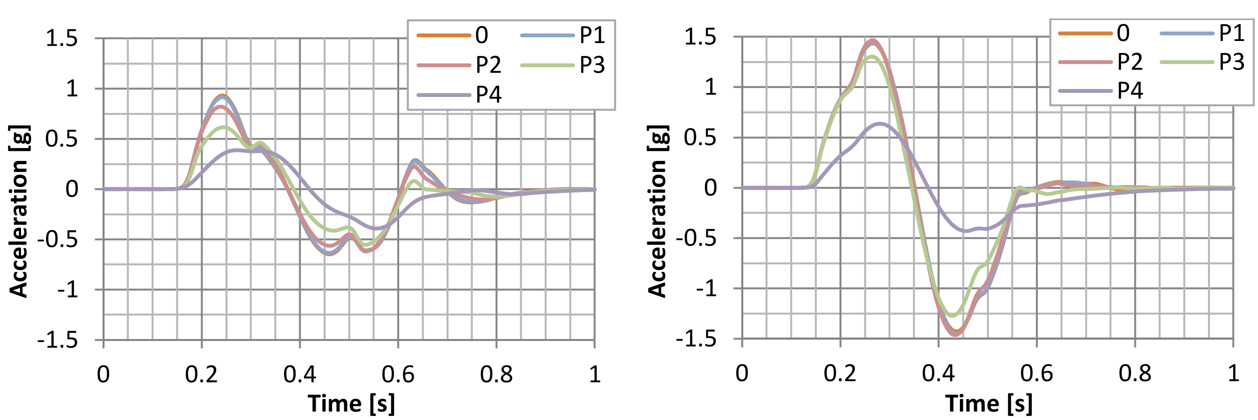

(a) (b)

Figure 3 – Case B-1: horizontal (a) and vertical (b) response time histories at ground surface

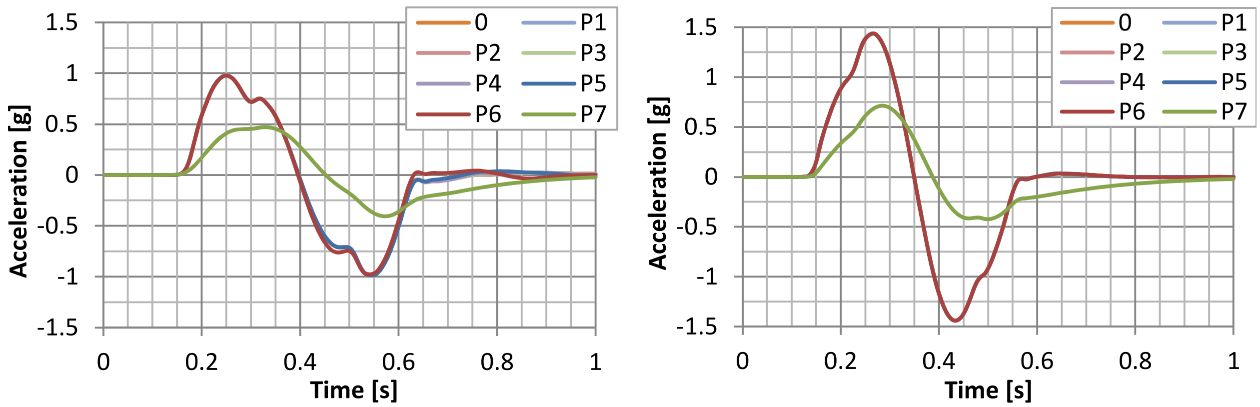

(a) (b)

Figure 4 – Case B-2: horizontal (a) and vertical (b) response time histories at ground surface

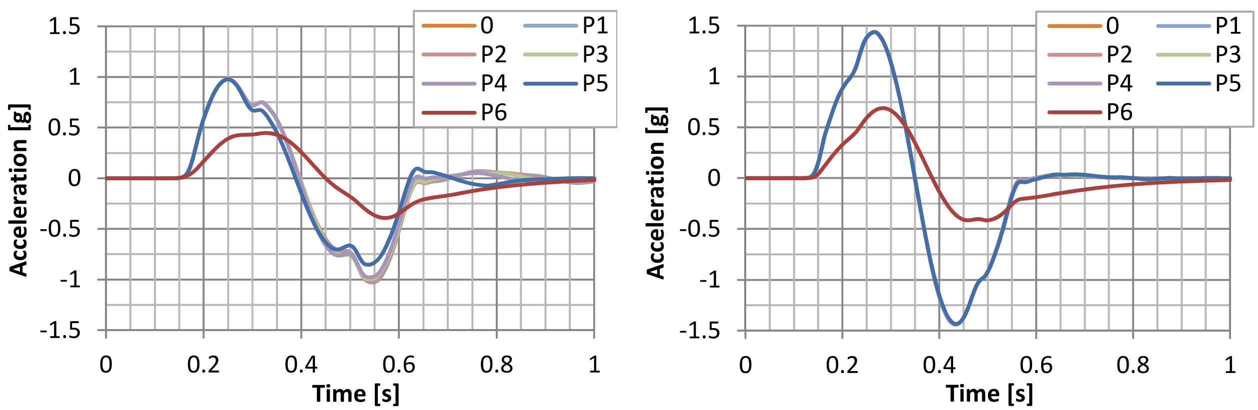

(a) (b)

Figure 5 – Case B-3: horizontal (a) and vertical (b) response time histories at ground surface

2.3. Case C

The rigid foundation has been modelled increasing rock elastic modulus by a factor 1.E+3 and using a massless foundation. Modal analyses have been performed both for empty (C-1(a)) and full (C-2(a)) reservoir. Time history analyses have been performed only for full reservoir, both with Taft Earthquake time history (C-2(b)) and ETAF time signal (C-2(c)).

The reservoir induces a remarkable decrease of the natural frequencies (about 50%), with the only exception of the first frequency (-20%); the second and third mode shape at the upstream face of the dam, quite irregular in case of empty reservoir, become as regular as the first one in case of full reservoir.

The maximum increase of water pressure caused by Taft Earthquake at dam heel results about 30% of hydrostatic pressure, the one caused by ETAF results about 45% of hydrostatic pressure. In both time history analyses the trend of water pressure at the upstream dam face reminds the Westergaard's one, which concerns the hydrodynamic part of pressure.

As only natural frequencies and mode shapes are requested for the case without the reservoir (C-1), no other consideration can be proposed about the effects of the reservoir on the behaviour of the concrete dam founded on a rigid foundation.

2.4. Case D

Modal analyses have been performed both for empty (D-1(a)) and full (D-2(a)) reservoir. Time history analyses have been performed only with Taft Earthquake (D-1(b)) for empty reservoir, both with Taft Earthquake time history (D-2(b)) and ETAF time signal (D-2(c)) for full reservoir.

The reservoir induces (Table 1) a moderate decrease of the natural frequencies (between 10% and 20%); moreover it is worth noting that even the frequencies for empty reservoir (D-1(a)) are less than the frequencies for full reservoir with rigid foundation (C-2(a)). The first, second and third mode shape at the upstream face of the dam are all quite regular both for empty and full reservoir.

Table 1– Results of modal analyses for cases D-1 and D-2: natural frequencies

	CASE D-1	CASE D-2
MODE	NATURAL FREQUENCY [HZ]	
1	1.98	1.78
2	2.71	2.44
3	4.12	3.17
4	4.98	3.92
5	5.28	4.13
6	5.78	4.95

The maximum increase of water pressure caused by Taft Earthquake at dam heel results about 10% of hydrostatic pressure. Vertical stress at dam/foundation interface is everywhere compressive in the case of empty reservoir, while the reservoir involves tensile stress at dam heel: in both cases, vertical stress is quite uniform, with the only exception of the extreme upstream zone of the interface (Figure 6).

Before summarizing the results obtained with the ETAF time signal, it is useful to consider the following peculiarities of the provided ETAF propagation behaviour, reminding mainly the request to apply it as a free field ground motion at the base of the foundation (not at its surface). The study of the upward propagation of the provided ETAF through the foundation of Case D ("Properties I") has shown that a very amplified ground motion arrives at the surface of the foundation, where it reaches the value of about 5 g at the end of the time history (the provided ETAF time signal does not exceed 0.4 g). This ground motion is mainly characterized by a unique frequency of about 4 Hz (with a small contribution at about 8 Hz) and appears to have essentially lost its original property of linearly growing with time (its most general trend is still to grow up with time, but as a result of subsequent increase and decrease intervals). The described peculiarities imply that the ground motion affecting the dam is very different from that of Case C (§ 2.3), in which the foundation does not allow any modification of the signal applied at its base. Pressure and vertical stress time histories (Figure 7 and Figure 8) at dam heel follow (both in trend and frequency) ETAF acceleration time signal evaluated at the surface of the foundation: furthermore the observed high acceleration at the top of the foundation involves high pressure and stress. The maximum increase of water pressure caused by ETAF signal results about 220% of hydrostatic pressure; the trend of water pressure at the upstream dam face reminds the Westergaard's one. Vertical stress at dam/foundation interface is tensile from dam heel up to about 100 ft: the value at the extreme upstream zone is one order of magnitude higher than in the case with Taft Earthquake.

Figure 6 shows the maximum pressure at dam face and the maximum vertical stress at dam/foundation interface also for the case D-2(c).

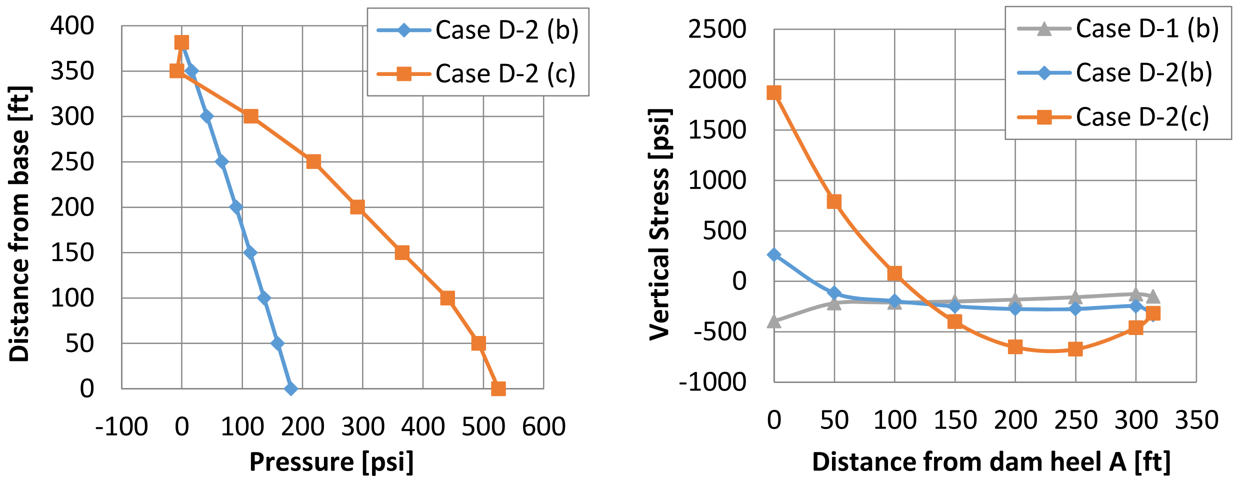

(a) (b)

Figure 6 – Maximum pressure at dam face (a) and maximum vertical stress at dam/foundation interface (b)

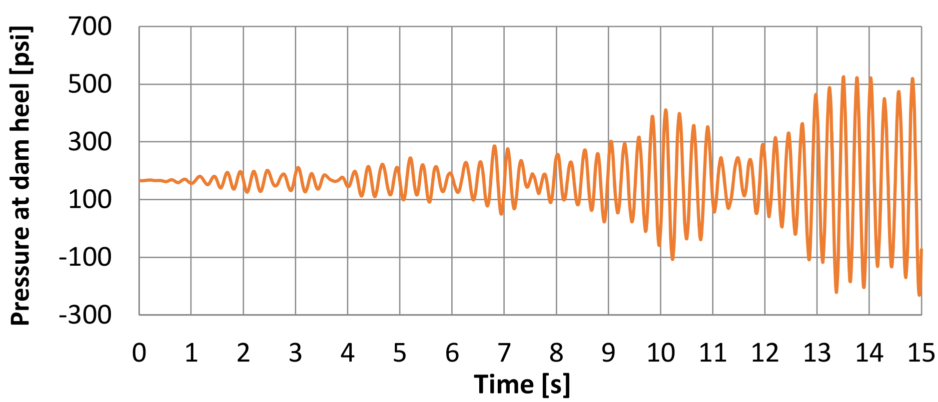

Figure 7 – Case D-2 (c): time history of pressure at dam heel

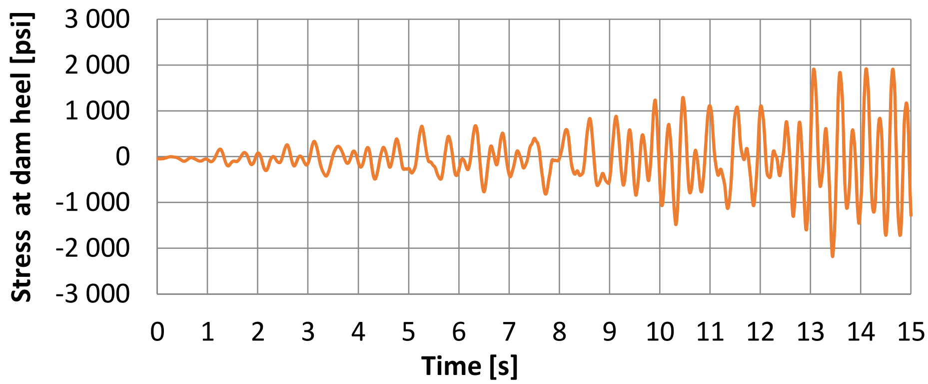

Figure 8 – Case D-2 (c): time history of vertical stress at dam heel

2.5. Case E

Modal analyses have been performed both for empty (E-1(a)) and full (E-2(a)) reservoir. Time history analyses have been performed only with Taft Earthquake (E-1(b)) for empty reservoir, both with Taft Earthquake time history (E-2(b)) and ETAF time signal (E-2(c)) for full reservoir.

The reservoir induces a significant decrease of the natural frequencies (about 35%), with the exception of the first and second frequencies (-20%); the second and third mode shapes at the upstream face of the dam, which are already rather regular in case of empty reservoir, become as regular as the first one in case of full reservoir. The modal analysis results are therefore intermediate between those of Case D (§ 2.4) and Case C (§ 2.3), in agreement with the differences among the elastic properties of the foundation.

The maximum increase of water pressure caused by Taft Earthquake at dam heel results about 15% of hydrostatic pressure; the trend of water pressure at the upstream dam face reminds the Westergaard's one. As for the previous Case D, in the case of empty reservoir vertical stress at dam/foundation interface is everywhere compressive and the stiffer foundation does not influence the trend and the values of the stress. In the case of full reservoir qualitative trend of stress is similar to that observed in the Case D but tensile stress at dam heel is more than double.

As for the previous Case D, the study of the upward propagation of the provided ETAF through the foundation of Case E ("Properties II") has shown that a very amplified ground motion arrives at the surface of the foundation, where it reaches the value of about 5 g at the end of the time history (the provided ETAF time signal does not exceed 0.4 g). This ground motion is mainly characterized by a unique frequency of about 6 Hz (with a small contribution at about 12 Hz) and appears to have essentially lost its original property of linearly growing with time (its most general trend is still to grow up with time, but as a result of subsequent increase and decrease intervals). Also in this case the ground motion affecting the dam is very different from that of Case C, in which the foundation does not allow any modification to the signal applied at its base. Pressure and vertical stress time histories at dam heel follow (both in trend and frequency) ETAF acceleration time signal evaluated at the surface of the foundation: furthermore the observed high acceleration at the top of the foundation involves high pressure and stress. The maximum increase of water pressure caused by ETAF signal results about 120% of hydrostatic pressure; the trend of water pressure at the upstream dam face reminds the Westergaard's one. Also in this case, vertical stress at dam/foundation interface is tensile from dam heel up to about 100 ft, but double in size: the value at the extreme upstream zone is one order of magnitude higher than in the case with Taft Earthquake.

3. ANALYSIS LESSONS LEARNED

Among the more interesting peculiarities highlighted by the performed analyses, the following ones are surely worth mentioning.

The wave propagation analyses (Case B) have confirmed the importance of the horizontal sizes of the foundation. In particular, at least for the adopted approach, model B-1 appears too short to correctly reproduce the propagation of the horizontal time pulse load, while model B-3 (selected as intermediate between B-1 and B-2 and three times longer than model B-1) is surely adequate, probably even a bit long, considering the recommendation suggested by Løkke [10]. The ETAF analyses with flexible foundation (Cases D-2(c) and E-2(c)) have shown that the signal can result much higher at the surface of the foundation than at its base: amplification factor of about 10 has been evaluated.

4. SUGGESTED FUTURE WORK

It is believed that the proposed case study deserves further investigations, which could be more profitably identified and formulated after comparing the contributions provided by the participants. Some initial possible suggestions are reported below.

The investigation regarding the effects of the horizontal sizes of the foundation (Case B) could be further carried on taking into account the seismic signal, both for the foundation only model and for the complete dam-reservoir-foundation model.

It could be interesting to evaluate the effects of modelling the dynamic interaction between the foundation and the reservoir.

Moreover, the comparison between the results of the traditional and widespread *massless foundation* approach and those of the *seismic wave propagation* approach would be quite significant.

Finally, these aspects and those that will outcome from the workshop could represent a good basis for the possible formulation of one of the Themes on concrete dams to be proposed in the frame of the 15th ICOLD Benchmark Workshop on Numerical Analysis of Dams that is likely to be held in Italy in Fall 2019. During the next ICOLD Congress in Vienna final decisions about date and venue will be defined.

5. REFERENCES

[1] Zienkiewicz O.C. (1977). The Finite Element Method, 3rd Edition, McGraw-Hill.

[2] H.M. Hilber, T.J.R. Hughes, R.L. Taylor (1977). Improved numerical dissipation for time integration algorithms in structural dynamics. *Earthquake Engineering and Structural Dynamics*, 5, 283-292.

[3] J. Liu, Y. Du, X. Du, Z. Wang, J. Wu (2006). 3D viscous-spring artificial boundary in time domain. *Earthquake Engineering and Engineering Vibration*, 5, 93-102.

[4] A. Løkke, A.K. Chopra (2017). Direct finite element method for nonlinear analysis of semi-unbounded dam–water–foundation rock systems. *Earthquake Engineering and Structural Dynamics*, 46, 1267-1285.

[5] C. Zhang, J. Pan (2009). Influence of seismic input mechanisms and radiation damping on arch dam response. *Soil Dynamics and Earthquake Engineering*, 29, 1282-1293.

[6] D. Chen, C. Du, J. Yuan, Y. Hong (2012). An investigation into the Influence of Damping on the Earthquake Response Analysis of a High Arch Dam. *Journal of Earthquake Engineering*, 16, 329-349.

[7] Y.S. Liu, D.H. Chen (2013). Earthquake Response Analysis of a Gravity Dam Considering the Radiation Damping of Infinite Foundation. *APCOM & ISCM*.

[8] Dassault Systemes Simulia (2017). Abaqus 2017.

[9] US Bureau of Reclamation (2013). State-of-practice for the Nonlinear Analysis of Concrete Dams 2013.

[10] A. Løkke (2017). A researcher's perspective on modelling unbounded domains for earthquake analysis of dams. Presentation in 2nd workshop of the «Dams & Earthquakes» European Working Group of ICOLD Hosted by ITCOLD in Roma, Feb 6-7 2017.

PARTICIPANT INFORMATION

Organization	Norwegian University of Science and Technology / Univ. of California, Berkeley
Authors	Arnkjell Loekke
Software	ABAQUS (2D model)

Cases Analysed

Case	Combination						
A	A-1						
B	B-1V	B-1H	B-2V	B-2H			
C	C-1(a)	C-2(a)		C-2(b)	C-2(c)		C-2(d)
D	D-1(a)	D-2(a)	D-1(b)	D-2(b)	D-2(c)		
E							

1. METHOD AND APPROACH

This paper describes analyses of Pine Flat Dam for the workshop on "Evaluation of numerical models and input parameters in the analysis of concrete dams" during the 38th annual USSD conference and exhibition annual conference in Miami April 30th – May 4th 2018.

The analyses presented herein are performed using the finite element code Abaqus. For all the dynamic analyses, the direct finite element method is utilized; a method that was recently presented by Løkke and Chopra for nonlinear earthquake analysis of 2D and 3D dam-water-foundation rock interacting systems [1,2]. The direct FE method uses viscous-damper absorbing boundaries (dashpots) to model the semi-unbounded extend of the foundation rock and fluid domains, and specifies the seismic input as effective earthquake forces directly at these boundaries. The procedure considers all the factors important in the earthquake response of dams: dam-water interaction including water compressibility and wave absorption at the reservoir boundaries; dam-foundation rock interaction including mass, stiffness, and material damping in the rock; radiation damping due to the semi-unbounded sizes of the foundation and fluid domains; spatial variation of the ground motions around the dam–canyon interface; and possible nonlinear behavior in the dam and adjacent parts of the foundation-rock and fluid domains. Furthermore, because the direct FE method only makes use of features that are standard in FE analyses, it can be implemented with any commercial software without modification of the source code. For the subsequent analyses, the direct FE method was implemented with the commercial FE code Abaqus using only a few simple pre-processing scripts in Matlab.

A two-dimensional, plane-stress FE model of unit width is analyzed (Figure 1). The assumption of plane-stress, while strictly speaking not appropriate for the foundation rock, is dictated by the expected behavior of "individual vibration" of dam monoliths during intense ground motion. The finite element mesh consists of 1625 quadrilateral solid elements for the dam, 1020 quadrilateral solid elements for the foundation rock, and 925 quadrilateral compressible acoustic fluid elements for the water in the reservoir. A tie constraint is applied at the dam-water and water-rock interfaces to couple accelerations with hydrodynamic pressures. The dam is assumed to be fully tied to the foundation at the dam-foundation interface. Damping is modeled using Rayleigh damping as suggested by the workshop organizers (also see comment on damping in Section 3).

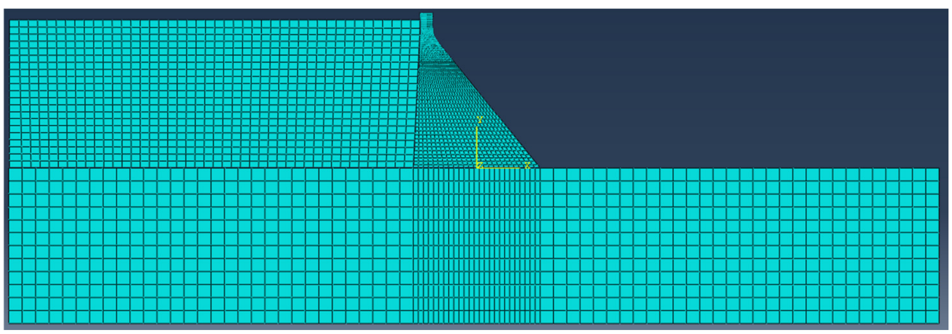

Figure 1: Two dimensional finite element mesh.

For the dynamic analyses, viscous dampers (dashpots) are applied at two locations: (1) at the bottom and side boundaries of the foundation to model its semi-unbounded geometry, and (2) at the upstream fluid boundary to model its essentially unbounded length. Since these viscous dampers do not have any static stiffness, a static analysis is first performed with fixed foundation boundaries, and the reaction forces at the boundaries recorded. These forces are subsequently applied to the dynamic model with viscous damper boundaries to ensure static equilibrium.

The time histories for case D (Taft, ETAF, harmonic) are deconvolved using a 1D deconvolution analysis to provide the motion at the bottom foundation boundary; a separate 1D wave propagation analysis is then performed to obtain the spatially varying motions along the vertical side boundaries. Finally, these motions are converted to effective earthquake forces and applied to the boundaries; the complete procedure is described in refs. [1,2]. This way, the seismic input is "exact" to within the assumptions made regarding the wave field, i.e., the specified free-field motion will be exactly reproduced at the foundation surface in absence of the dam or water (see case B results).

For the time-integration, the implicit dynamic HHT-alpha algorithm is used.

2. RESULTS

This section will only provide a brief overview of the results. The reader is referred to the accompanying analysis results spreadsheet for detailed results.

For the static analysis with self-weight of the dam and hydrostatic pressures, a noticeable stress concentration is observed at the heel of the dam, both for foundation properties I and II (most significant for properties II). It was found that this is due to the tied interface assumption; from the author's experience, allowing for even a minimum amount of slip at the interface will alleviate these stresses (this was not done for the benchmark results).

From the modal analyses results shown in Table 1, the lengthening of the fundamental period due to dam-water and water-rock interaction can be identified by comparing the natural periods for the four different cases. The computed vibration properties agrees well with values obtained using the simplified formulas proposed by Fenves and Chopra [3].

Table 1: Fundamental vibration properties

Analysis case	**Fundamental vibration period (sec)**	
	Abaqus	Simplified formulas [3]
C1 - Dam alone	0.32	0.31
C2 - Dam-water system	0.39	0.39
D1 - Dam-foundation system	0.41	0.37
D2 - Dam-water foundation system	0.50	0.46

The results for case B-1a, analysis of the foundation domain alone for horizontal excitation, are shown in Figure 2a. For this analysis, the excitation with a peak acceleration value of 0.5g was assumed as an *upwards propagating seismic wave* at the bottom foundation boundary. Thus, a peak acceleration value of 1.0g should theoretically be observed at the surface of the foundation domain. From the results in Figure 2a, two interesting observations can be made: (1) the peak acceleration value is almost identical to the theoretical value of 1g (9.81 m/s^2), and (2) the response is identical at every node at the foundation surface. For comparison, results obtained when only applying forces at the bottom boundary, but ignoring forces at the side boundaries, are shown in Figure 2b. Clearly, these results are unsatisfactory.

These results highlight an important feature of the direct FE method: when effective earthquake forces are applied both at the bottom and side boundaries of the foundation, the results will be "exact" to within FE discretization errors for this simple flat box system. This applies to a foundation model of *any* width. Thus, there is no need to use an unreasonably wide foundation domain or to implement an iterative deconvolution analysis to obtain accurate results.

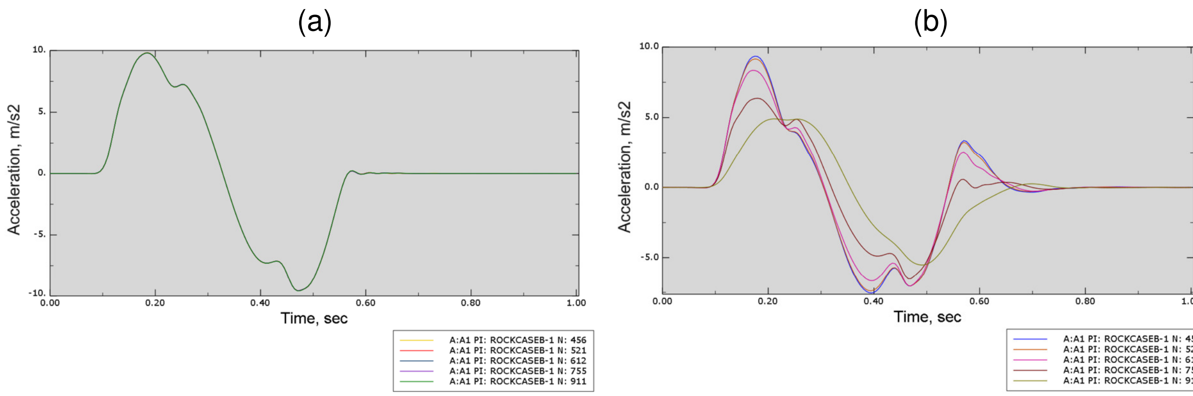

Figure 2: Acceleration response for analysis case B-1a, sampled at five nodes over the length of the foundation surface: (a) direct FE method with forces at bottom and side boundaries, (b) forces applied at bottom boundary, but ignored at side boundaries.

3. ANALYSIS LESSONS LEARNED

Several lessons were learned during the preparation of these results. Here, three lessons are highlighted:

1. Eigenvalue analysis for dam-water-foundation rock system

It was found problematic to extract the natural frequencies and mode shapes for the combined model with the dam, foundation with mass, and acoustic fluid elements. Many non-structural modes (reservoir modes / foundation modes) contributed to the output, and it was difficult to identify the relevant structural modes. To overcome this issue, a massless foundation model was used for the eigenvalue analysis of the dam-foundation and dam-water-foundation systems, and modes with little or no mass participation were eliminated from the output. While a massless model should not be used for the dynamic analyses, it can be useful for eigenvalue analyses as it is known to predict the natural frequencies of the system reasonably well. For example, the fundamental period of the dam-foundation system predicted using the massless foundation model is 0.41 sec, this compares to 0.42 sec when using a foundation model with mass. For higher modes the discrepancies tends to be somewhat larger.

2. Forces should be applied to the bottom AND side boundaries of the foundation

The results in Figure 2b demonstrate the deficiencies of using a model which ignores the effective earthquake forces on the side boundaries of the foundation domain. The large errors occurs because such a model is not able to reproduce the assumed wave-field in the system. There are procedures readily available for including the earthquake forces at the side boundaries with minimal computational effort (see e.g. [1,2]); these should be used for earthquake analysis of 2D and 3D dam-water-foundation systems to avoid introducing unneccesary errors in the results.

3. Damping in dam-water-foundation rock systems

A separate analysis using the half-power bandwidth method applied to the resonance curve revealed that specifying 5% viscous damping in the dam and 5% viscous damping in the rock, which corresponds to the Rayleigh damping factors of 0.95 and 0.002 given in the workshop materials, leads to an overall damping in the first vibration mode of the dam-water-foundation system of approximately 12%. This is much higher than the damping values of 2-4% that was measured at Pine Flat Dam during forced vibration tests in the 1970s [4].

To illustrate the influence of damping on the results, case D2 (the complete dam-water-foundation system) was re-analyzed using new damping values: 1% in the dam and 1% in the rock. The results are shown in Table 2. Even with these much lower values for material damping, the overall damping in the system is still as high as 7.9%. This highlights the considerable contribution from radiation damping in the foundation domain to the total damping in the 2D model. Reducing the damping values leads to a noticeable increase in the peak crest acceleration (+16%) and in the peak stresses at the heel and neck (+25% and +26%).

Table 2: Results for case D with two different damping values

Damping in dam, rock	5%, 5%	1%, 1%	Difference
Overall damping in system	12.0%	7.9%	
Peak crest acceleration (g)	1.08	1.25	+16%
Max. vertical stress heel (psi)	399	500	+25%
Max. principal stress neck (psi)	261	328	+26%

As a general "rule", the analyst should try to achieve overall damping in the numerical model that is consistent with damping values measured at dam sites. Comparison of recorded responses with computed response at several concrete dams during earthquakes have shown that damping values on the order of 1-2% for the dam and 1-4% for the rock gives numerical results that are in good agreement with the recorded response (see e.g. [5,6]). Consequently, the practice of "blindly" specifying 5% viscous damping for the dam concrete, and a similar value for the foundation rock, should be abandoned because it is likely to lead to excessive damping in the overall dam-water-foundation system, and thus, underestimate the response of the dam.

4. SUGGESTED FUTURE WORK

The analysis methods and numerical models used for earthquake analysis of concrete dams must be validated against observed motions and performance of actual dams subjected to earthquakes. Such analyses are required to broaden our understanding of the dynamic behavior of these systems, and give confidence in the output from the analysis models.

This workshop has only focused on the linear modeling of concrete dams, which is – at least in this author's view – a relatively well advanced field. In contrast, there are several substantial unresolved issues when it comes to nonlinear modeling of concrete dams and how to interpret the output from these analyses. This has becoming increasingly important as regulators tend to move away from a "binary" safety evaluation methodology and towards more performance based assessment methodologies. Thus, there is a need for more research on the nonlinear behavior and nonlinear modeling of concrete dams.

5. REFERENCES

1. Løkke A, Chopra AK. Direct finite element method for nonlinear analysis of semi-unbounded dam-water-foundation rock systems. *Earthquake Engineering & Structural Dynamics* 2017; **46**(8): 1267–1285. DOI: 10.1002/eqe.2855.
2. Løkke A, Chopra AK. Direct finite element method for nonlinear earthquake analysis of 3-dimensional semi-unbounded dam-water-foundation rock systems. *Earthquake Engineering & Structural Dynamics* 2018. DOI: 10.1002/eqe.3019.
3. Fenves G, Chopra AK. Simplified earthquake analysis of concrete gravity dams. *Journal of Structural Engineering* 1987; **113**(8): 1688–1708. DOI: 10.1061/(ASCE)0733-9445(1987)113:8(1688).
4. Rea D, Liaw CY, Chopra AK. Mathematical models for the dynamic analysis of concrete gravity dams. *Earthquake Engineering & Structural Dynamics* 1974; **3**(3): 249–258. DOI: 10.1002/eqe.4290030304.
5. Chopra AK, Wang JT. Earthquake response of arch dams to spatially varying ground motion. *Earthquake Engineering & Structural Dynamics* 2009; **39**(8): 887–906. DOI: 10.1002/eqe.974.
6. Robbe E, Kashiwayanagi M, Yamane Y. Seismic analyses of concrete dam, comparison between finite-element analyses and seismic records. *Proc. for 16th World Conference on Earthquake Engineering*, Santiago, Chile: 2017.

PARTICIPANT INFORMATION

Organization	STANTEC
Authors	JUAN E. QUIROZ
	NATHAN GROSSMANN
	RICH BARRIE
	NEDDA DJAVID
Software	ABAQUS

Cases Analysed

Case	Combination					
A	A-1					
B	B-1V	B-1H	B-2V	B-2H		
C	C-1(a)	C-2(a)	C-1(b)	C-2(b)	C-2(c)	-	C-2(d)
D	D-1(a)	D-2(a)	D-1(b)	D-2(b)	D-2(c)		
E	E-1(a)	E-2(a)	E-1(b)	E-2(b)	E-2(c)		

1. METHOD AND APPROACH

All analyses have been carried out by the Finite Element Method (FEM) using the ABAQUS software. The models were kept consistent all across in terms of size, mesh, element types, constraints, loading, boundary conditions, etc. The reservoir was included using acoustic elements with a constitutive behavior assumed to be inviscid and compressible, so that the bulk modulus relates the dynamic pressure in the medium to the volumetric strain. The pressure degree of freedom accounts for the dynamic pressure wave, while hydrostatic pressures were directly applied to the face of the dam and foundation. The dynamic cases were carried out using an implicit coupled acoustic-structural direct integration analysis approach. For simulating properly a seismic wave propagation it is required to consider mass of the foundation, to deconvolve the target motion down to the base of the model (Figure 1-a), and to include non-reflective boundaries (Figure 1-b), or Absorbing Boundary Conditions (ABC). These ABC allow radiation damping to be considered in the analysis. Deconvolutions were also performed using FEM in ABAQUS in the time-domain. The ABC are implemented on the analysis by means of special coded elements, which incorporate two main behaviours: 1) a classical viscous component to absorb the radiating waves, and 2) a representation of the free-field column that propagates the waves from the base to the surface and provides input to the sides of the model. The resulting elements, in this case 2D, relate the two degrees of freedom (d.o.f.) horizontal and vertical on the free-field column side to the corresponding two d.o.f. on the foundation domain side. This relationship is composed by dampers and springs, and includes off-diagonal terms, which entails an unsymmetric matrix storage for the solution. For instance, the vertical d.o.f. of the free-field column has an effect on the horizontal d.o.f of the foundation domain, this is the case of a p-wave being propagated. Damping coefficients do not need to be calibrated, like other approaches. These coefficients are simply part of the foundation properties using classical elasticity.

a) b) c)

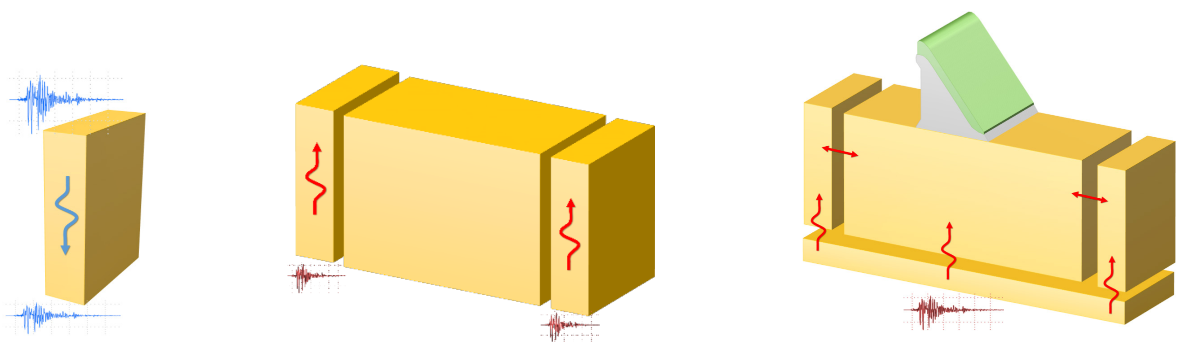

Figure 1 – a) Deconvolution to Model Base, b) Free-Field Wave Propagation, c) Soil-Structure Interaction

	Description
FE Model	2D Model
Interfaces	No contact, Tie constraints bewteen Water/Dam/Foundation
Mesh	Linear plain strain elements for Concrete and Rock, acoustic elements for Water: Approx. mesh size Dam = 15ft → 400 Foundation = 30ft → 1200 Water = 30ft → 500 nodes
Time analysis	Implicit direct-intergation, coupled acoustic-stress Maximum running time = 1000sec (TAFT earthquake)
Boundary condtions	Absorbing Boundary Conditions. Simulate far-field motion outside the domain, considers off-diagonal terms for relationship between vertical and horizontal d.o.f. between far field and domain, uses unsymmetric matrix storage.
Reservoir Boundary	An acoustic non-reflective impedance at the infinite side of the reservoir is included to simulate the infinite reservoir.
Other	No sediment or impedance is considered at the reservoir/foundation interface (reservoir bottom absorption)

2. RESULTS

Since the motion is deconvolved to the base of the model (400ft deep), the recovered motion should match the target free-field at the assumed rock outcrop, in this case at the surface. The motion is deconvolved using FEM in ABAQUS on the time-domain. For verification purposes, a comparison of the TAFT motion with the recovered motion after deconvolution and convolution is presented on Figure 2 for the horizontal component, on Figure 4 for the vertical component, as well as the responses. There is a slight time shift due to the wave travel time through the rock with respect to the beginning of load application. Since s-waves and p-waves velocities are different, the time shift for each component is different. The response comparison for the rock property set I is presented on Figure 6, and for set II on Figure 7.

Rock properties set I

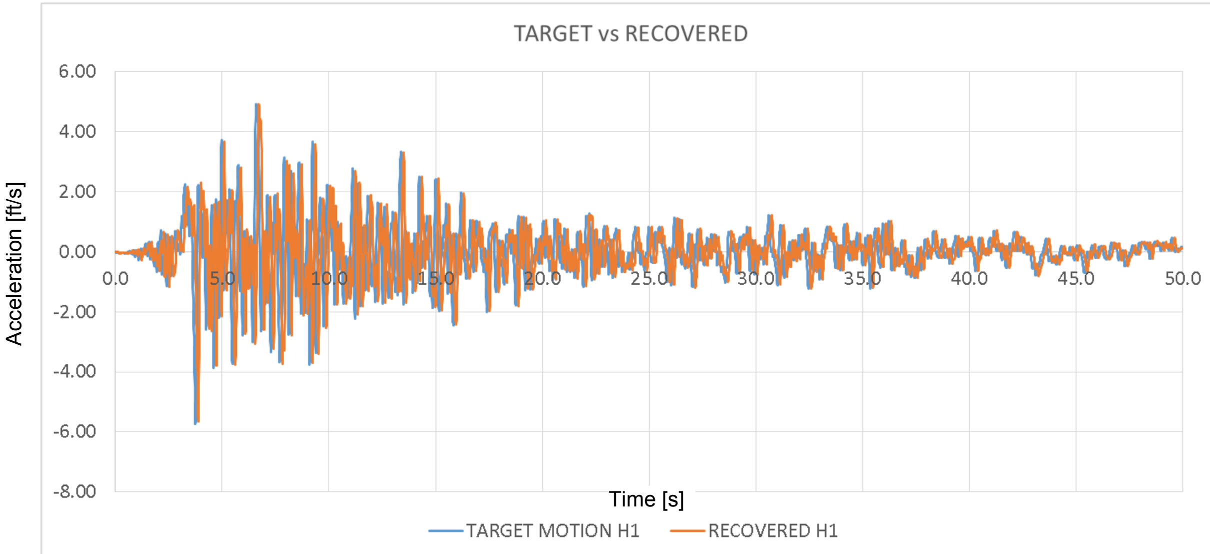

Figure 2 – Deconvolution – Target vs Recovered Horizontal Component

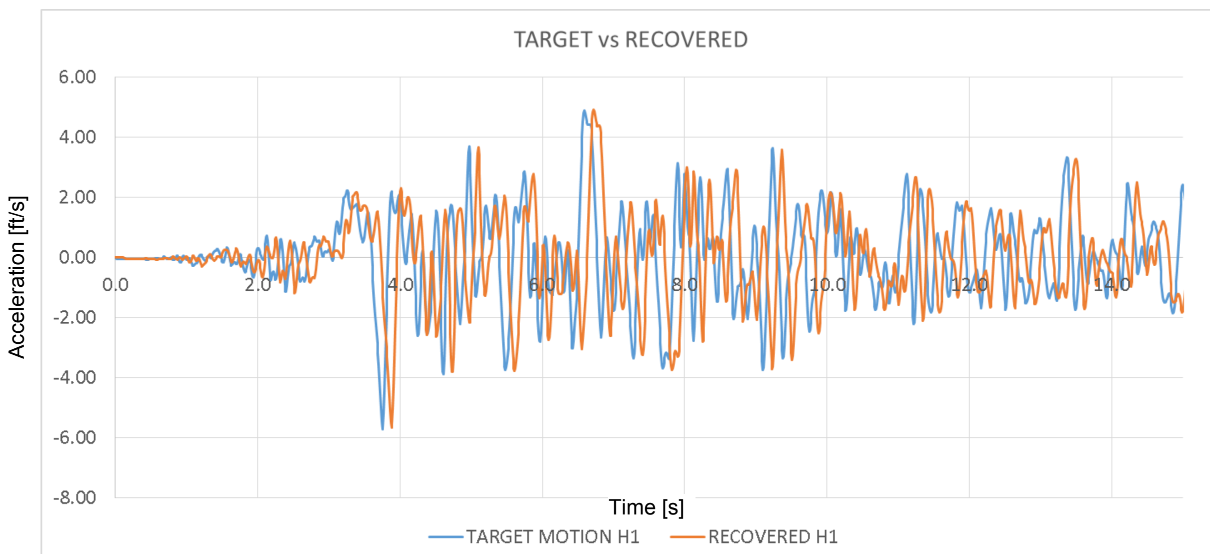

Figure 3 – Deconvolution – Target vs Recovered Horizontal Component - Closeup

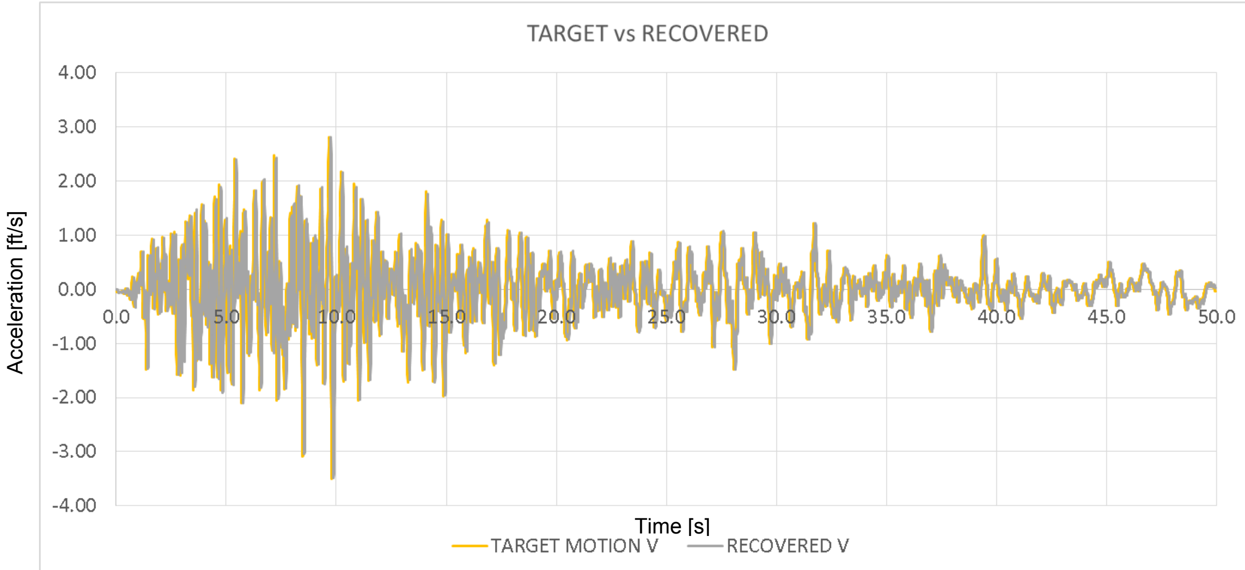

Figure 4 – Deconvolution – Target vs Recovered Vertical Component

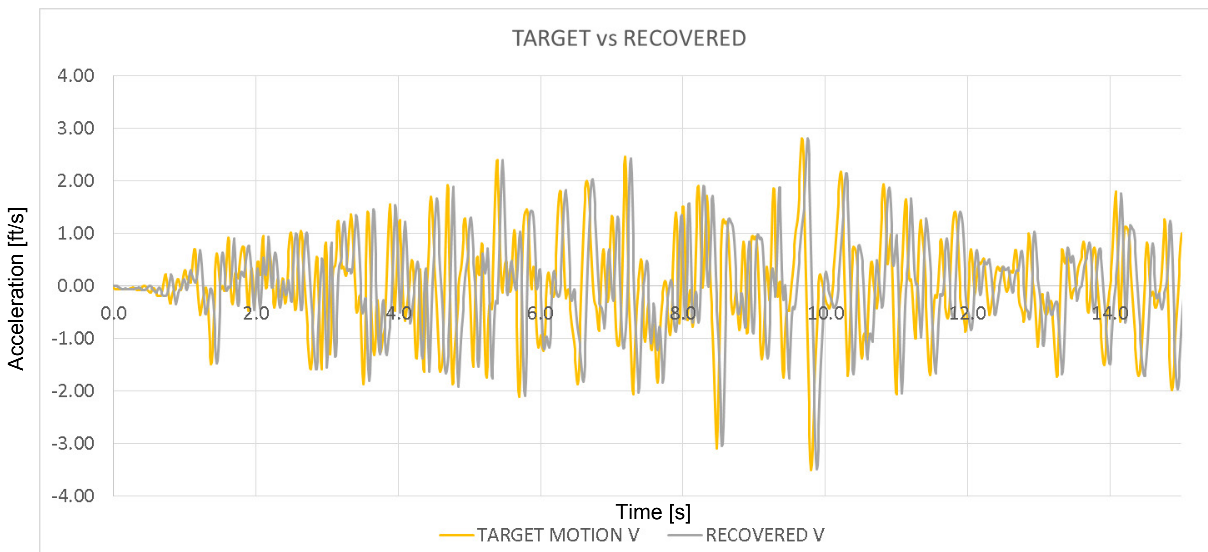

Figure 5 – Deconvolution – Target vs Recovered Vertical Component - Closeup

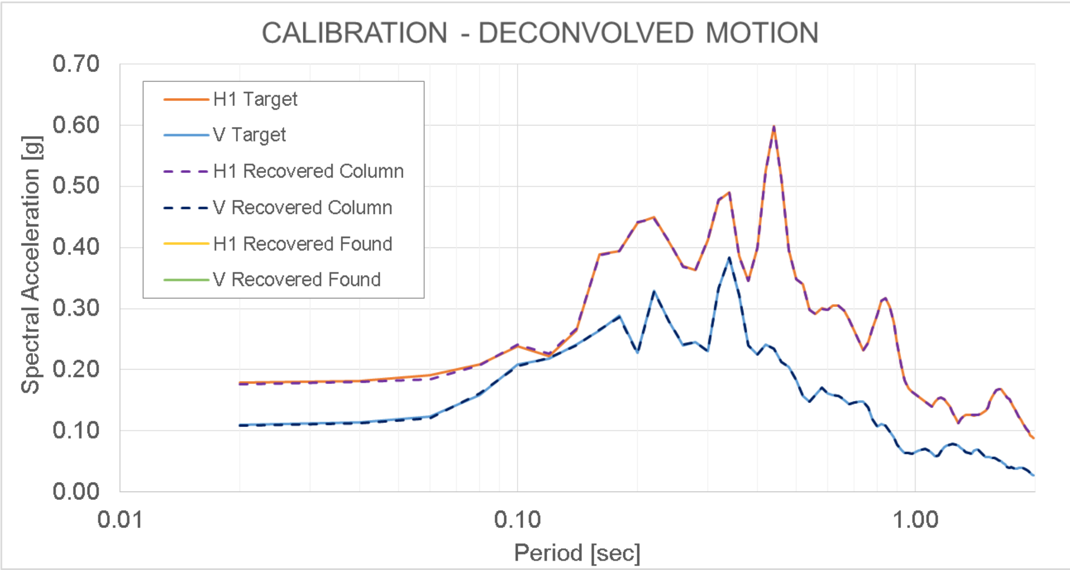

Figure 6 – Deconvolution – Target vs Recovered Responses – Prop Set I

Likewise, for the rock properties set II, Figure 7:

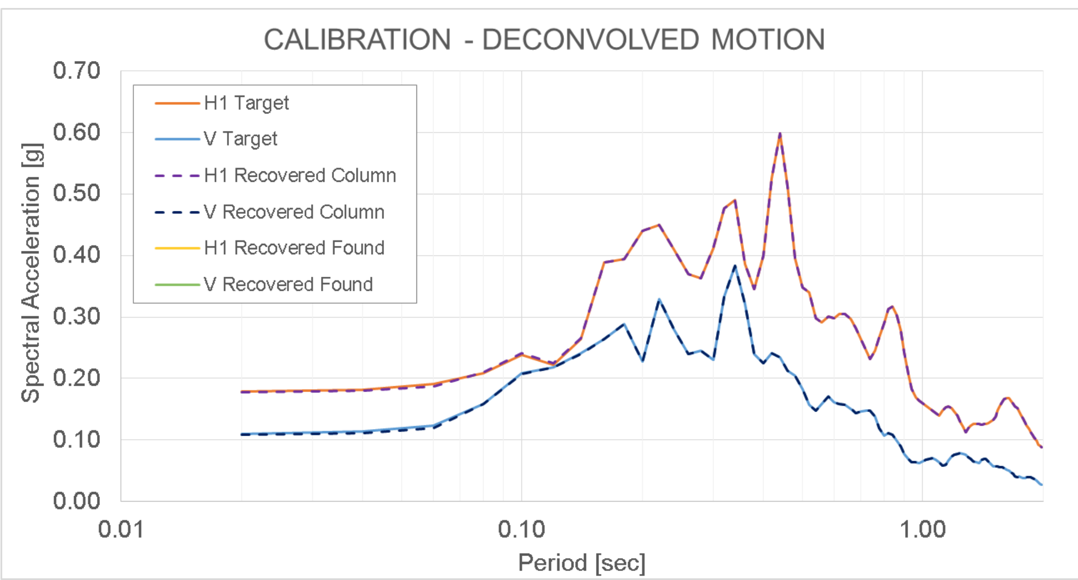

Figure 7 – Deconvolution – Target vs Recovered Responses – Prop Set II

Consider a simple test where a wave is prescribed at the bottom of the free-field column. On this example a wave is tracked as it propagates to the top, then reflects at the free surface back to the bottom, and tracked down to the base of the model. The wave should eventually radiate out of the domain without any reflection. Figure 8 shows the free-field column deformed shape on the left, while the wave is traveling to the top at time step t=0.64sec, also marked as a vertical line of the right hand side plots for reference. This figure also shows two graphs for the horizontal deformation time-history being tracked at the base and at the surface. This shows an inside wave applied at the base of the model with a non-reflective or ABC. It is noted on Figure 8 that the wave is originated at the base (lower graph time range 0 to 0.25sec), and it reaches the top surface at around 1sec (upper graph), then the wave is reflected and exits the domain at about 1.75sec. The wave is absorbed without being trapped within the domain as it can be seem on these graphs.

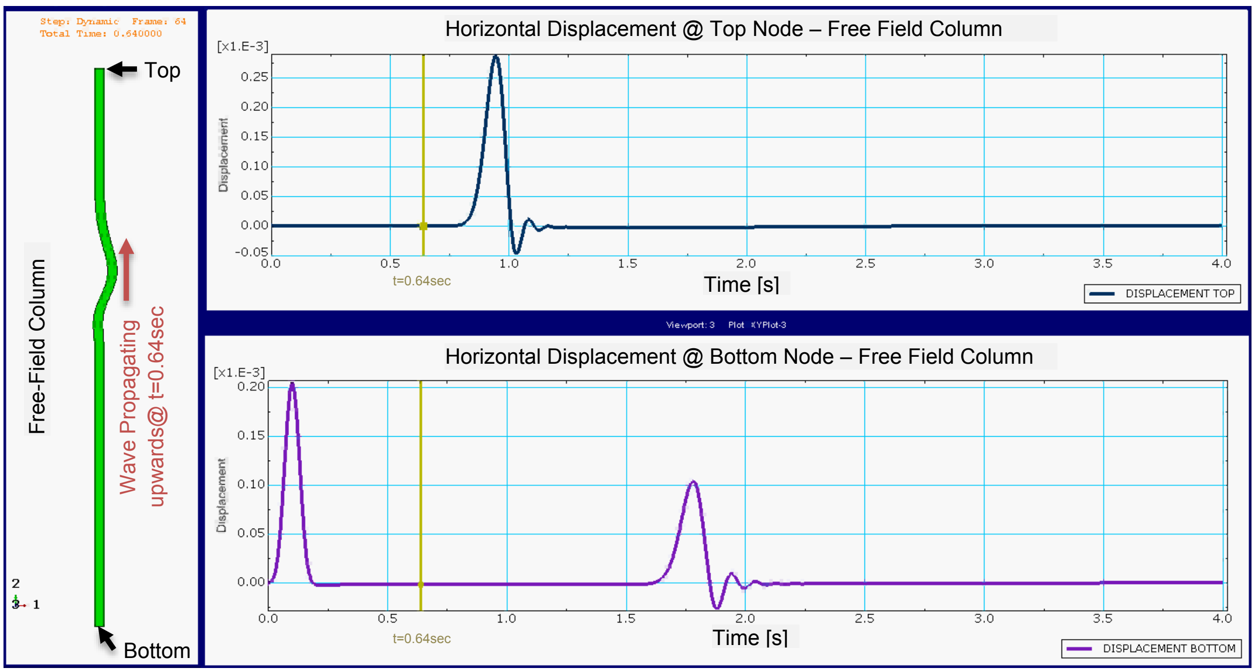

Figure 8 – Wave Propoagation Example

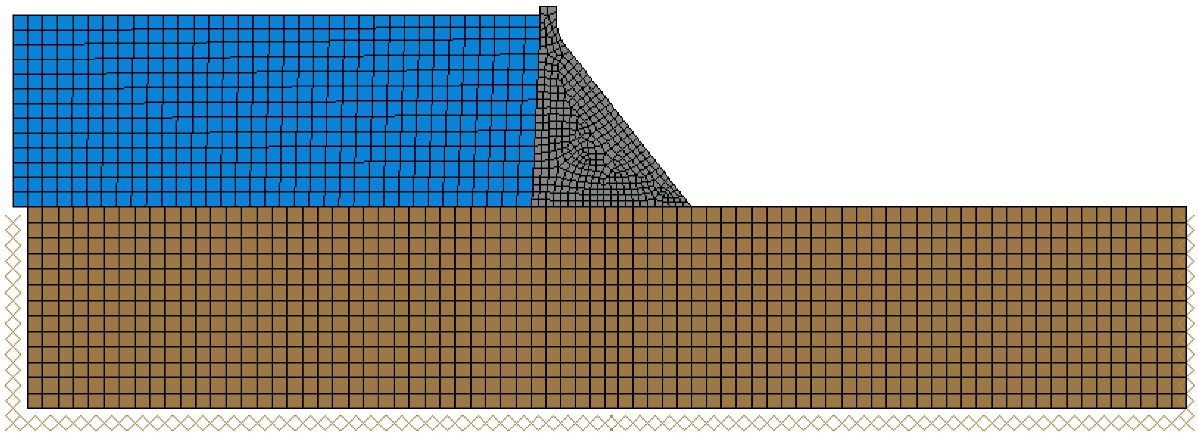

Figure 9 – Overall Model Mesh

Other runs were made to compare the results using linear stress elements to model the water, some results were comparable, but some wave reflection was noted. An acoustic non-reflective impedance at the infinite side of the reservoir is included to simulate the infinite reservoir.

As expected, frequencies increase with foundation stiffness and decrease with the presence of the reservoir vs empty. Hydrodynamic pressure also decreases with foundation flexibility.

Foundation Heel Vertical Stress Comparisson (added masses per traditional Westergaard vs Acoustic elements) is presented on Figure 10 and Figure 11, and wall displacements onFigure 12 and Figure 13.

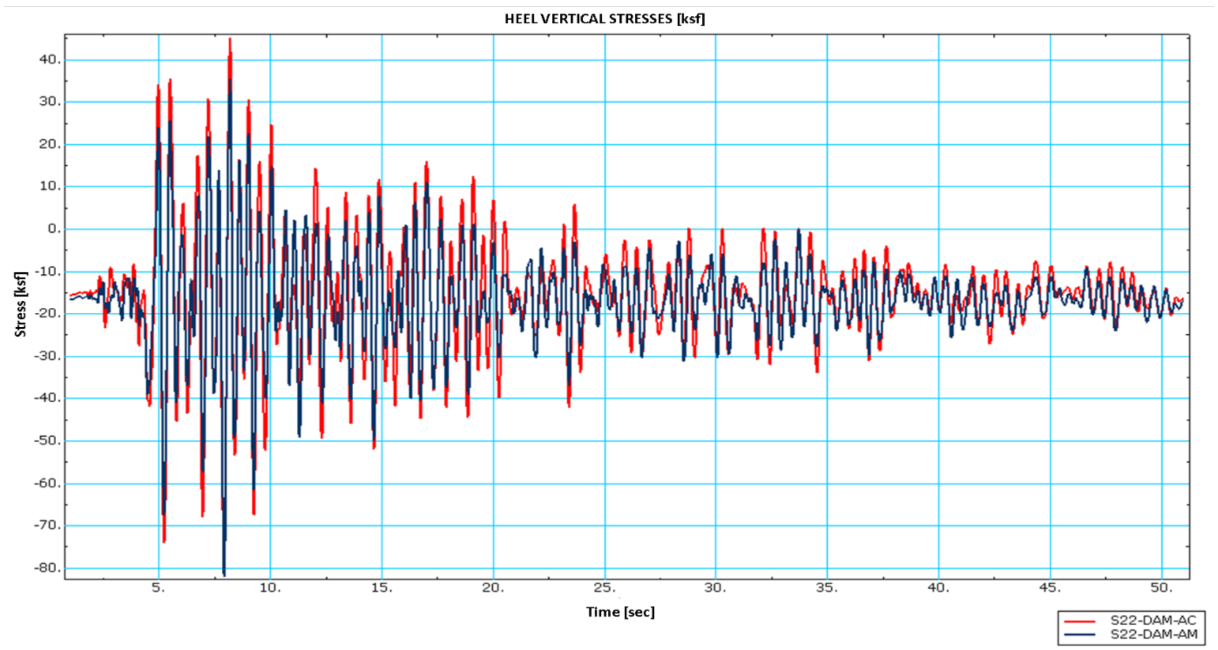

Figure 10 – Vertical Stresses – Added Masses vs Acoustic Elements

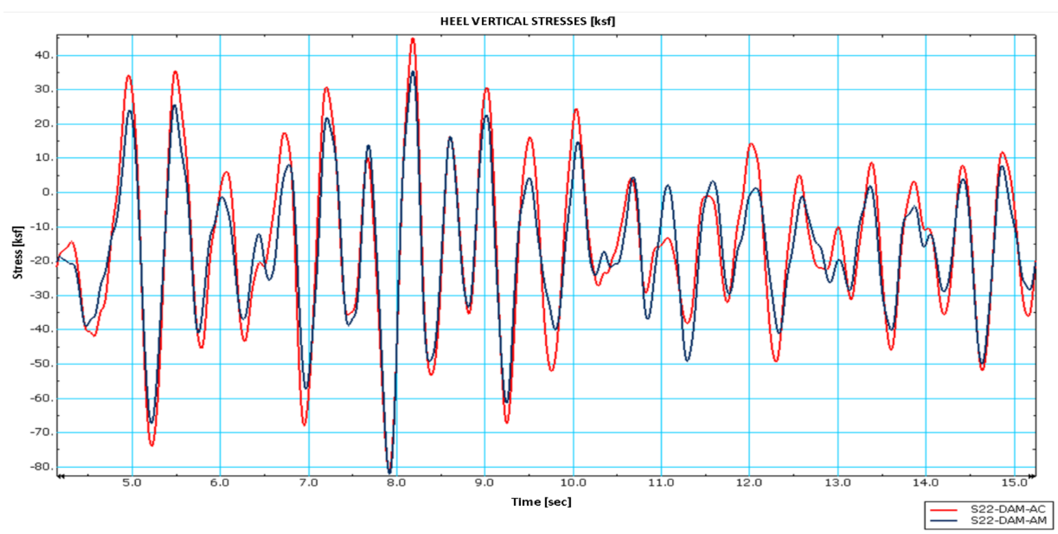

Figure 11 – Vertical Stresses – Added Masses vs Acoustic Elements – Closeup

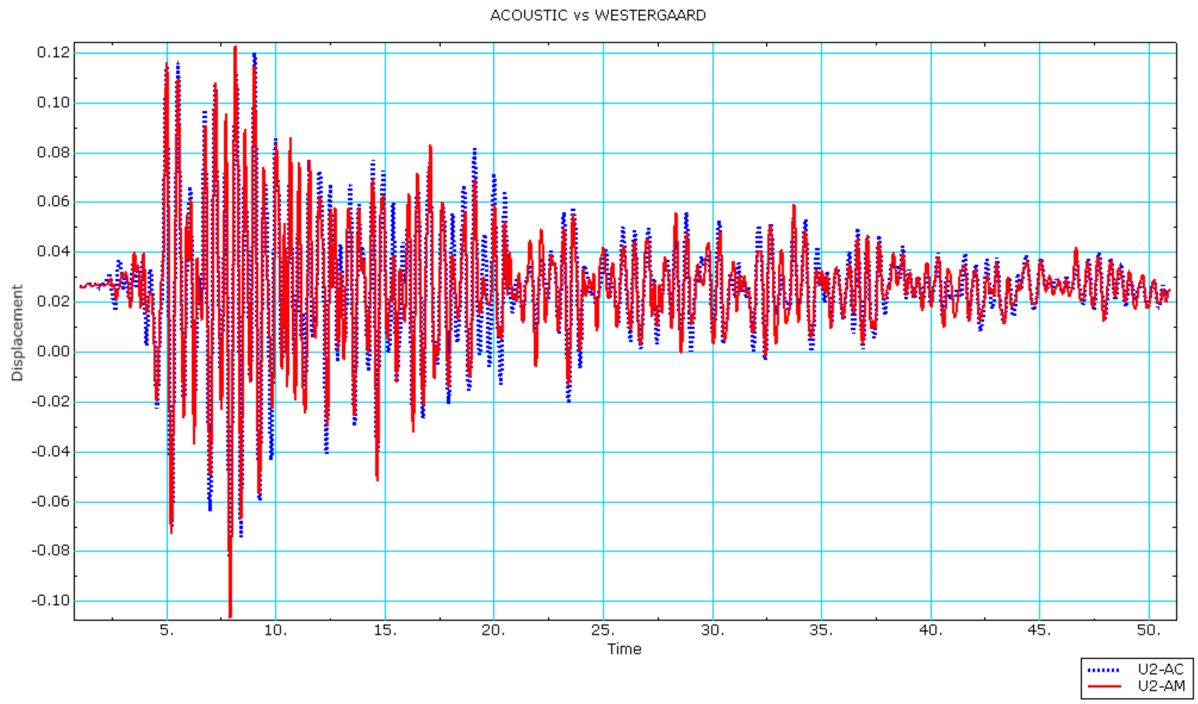

Figure 12 – Horizontal Displacement (C-A) – Added Masses vs Acoustic Elements

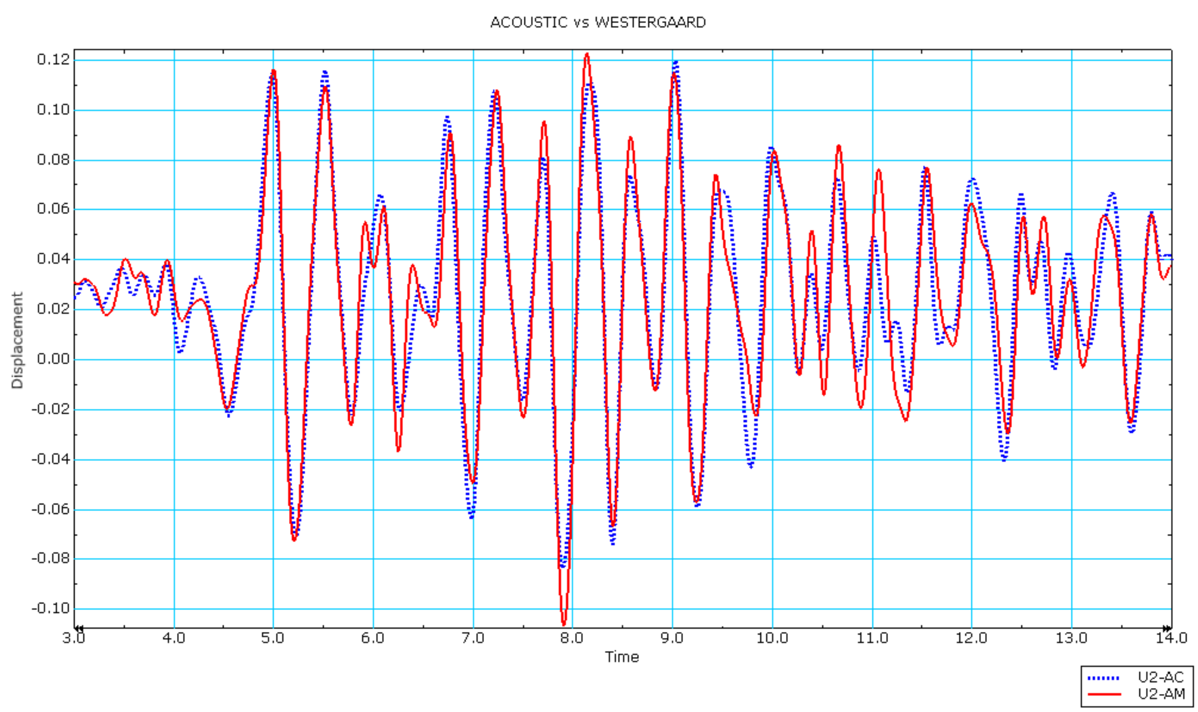

Figure 13 – Horizontal Displacement (C-A) – Added Masses vs Acoustic Elements - Closeup

3. ANALYSIS LESSONS LEARNED

Acoustic water modeling was also compared against Westergaard added masses for case D. Hydrodynamic pressures exhibit parabolic shapes, similar to Westergaard added masses, but some differences are noted. Foundation vertical stresses are similar between Westergaard added masses vs Acoustic elements. Frequency content is similar, but peak compression stresses are slightly higher for added masses, while tensile stresses are close (when dam is pushed downstream). Pine Flat dam is a typical dam configuration and Westergaard added masses resulted in acceptable results. However, more complex project conditions would show greater differences, for instance inclined faces, piers, valley shape, sediments, etc. Also, second and third mode frequencies affect the reponse. Boundary conditions are found to be very important drivers of the solution. Acoustic elements in ABAQUS are very effective for modeling water, including compressibility, and have the capability of considering impedance or admittance. They are also easier to setup, from the user perspective, as compared to even the simple added mass approach. The workshop input data was not sufficient to assess an impedance amount and was not considered at the reservoir bottom (sediments). The reservoir was considered as part of a frequency analysis to determine main modes, where symmetric boundary conditions for the foundation were included in liu of fixed boundaries.

4. SUGGESTED FUTURE WORK

A few topics for discussion are suggested:

- Where dam/base interface is likely to open, a non-linear (contact) should be incorporated to allow cracking, sliding and uplift pressures. This is particularly important for performance-based design of dams.
- Initial frequency analyses are carried out assuming no cracks and linear elastic material properties. On special cases an existing crack, damage area, or a joint may be left unconnected to obtain the correspondent system stiffness. Frequencies are affected by base or lift joints cracking, for example. Main frequencies would become more challenging to compute, as linear methods would not be appropriated. A frequency sweep analysis is usually performed on these cases.
- Another very common subject is the consideration of flexible features like gates on spillways, that would affect the fluid-structure interaction, on top of the geometry complexity. Postensioned structures are also prone of relative displacements and joint opening.
- Structural fragility is very important for budget management and retrofit planning. The calculation of vulnerability requires the proper simulation of failure modes. We have used more advanced non-linear features for this purpose, like the modeling of lift joints, concrete cracking (plastic damage of concrete), material uncertainty analyses, and other techinques like response surface analyses and Monte Carlo simulations all together with the FEA approach.

PARTICIPANT INFORMATION

Organization	Reclamation & Diana FEA
Authors	Jerzy Salamon – Bureau of Reclamation Maziar Partovi – Diana FEA
Software	DIANA

Cases Analysed

Case	Combination						
A	A-1						
B	-	-	-	-	-	-	-
C	C-1(a)	C-2(a)	C-1(b)	C-2(b)	C-2(c)	C-1(d)	C-2(d)
D	D-1(a)	D-2(a)	D-1(b)	D-2(b)	D-2(c)		
E	E-1(a)	E-2(a)	E-1(b)	E-2(b)	E-2(c)		

1. Method and Approach

This paper summarizes an analysis of the case study for Pine Flat Dam, prepared for the USSD workshop on "Evaluation of numerical models and input parameters in the analysis of concrete dams", Miami, May 4th, 2018. The analysis results presented herein were obtained using DIANA FEA commercial software [1].

Assuming symmetry, a 25-ft wide dam finite element model, one half of the actual width of a single dam monolith, with corresponding width of the foundation and the reservoir was developed (Figure 1). The analysis was carried out using a coupled acoustic-structural approach using implicit integration method.

In the dynamic analysis, a 25-ft wide by 2300-ft long and 400-ft deep mass foundation block was considered. Far-field viscous damper absorbing boundaries, Lysmer-Kuhlemeyer formulation, were applied at the u/s, d/s and bottom face of the foundation block.

The reservoir was modeled by acoustic elements considering incompressible the fluid. The pressure in the fluid elements accounts for the hydro-dynamic effects only, while hydrostatic pressures were directly applied at the faces where the reservoirs contacts the dam and foundation. The pressure equal to zero was defined at the upstream and upper surface of the reservoir model.

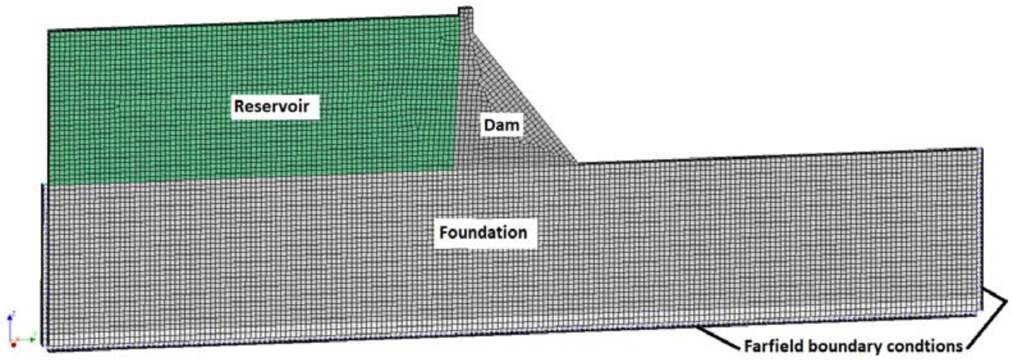

Figure 1 – Model of the dam-reservoir-foundation system with the far field boundary conditions

Table 1. Summary of the analysis model.

	Description
FE Model	Model type: 25-ft wide model assuming symmetry of the dam monolith, foundation and the reservoir 2D surface models for far-field boundary elements
Materials	Dam & foundation: linear elastic Reservoir: incompressible fluid
Mesh	Mesh type: solid fully integrated 8-node solid elements Mesh size: 12.5 ft
Interface	Dam/reservoir: interface for coupled acoustic-structural elements. Tie constraints between foundation & dam
Time analysis	Time integration method: Implicit – Newton-Raphson interative Time steps: 0.01 seconds Convergence criteria: force norm
Boundary condtions	Foundation: far-field boundary condtions at u/s, d/s, bottom faces using Lysmer-Kuhlemeyer formulation Dam: symmetry boundary condtions at the center of the monolith and free opposite face

2. RESULTS

Natural Frequencies of the Model

The ratio of the natural frequency of the reservoir to the natural frequency of the dam is the key parameter determining the effect of the reservoir compressibility in the reservoir-dam interaction during an earthquake. The first natural frequency of the reservoir can be determined by the equation:

$$f_r = \frac{c_w}{4\,h} \qquad \text{(Eq.1)}$$

For a reservoir with the depths of 381.5 feet, the fundamental frequency of the reservoir, determined from Eq. 1, is 3.09 Hz.

Table 2. Computed eigenfrequencies [Hz] for FE models.

Reservoir	Foundation	1st	2nd	3rd
Empty reservoir	rigid (C-1)	3.16	6.39	8.75
Empty reservoir	flexible (D-1)	2.48	4.16	4.48
Empty reservoir	stiff (E-1)	2.91	5.58	6.94
Compressible reservoir	rigid (C-2)	2.67	5.57	8.62
Compressible reservoir	flexible (D-2)	2.06	3.98	4.81
Compressible reservoir	stiff (E-2)	2.43	5.02	6.90

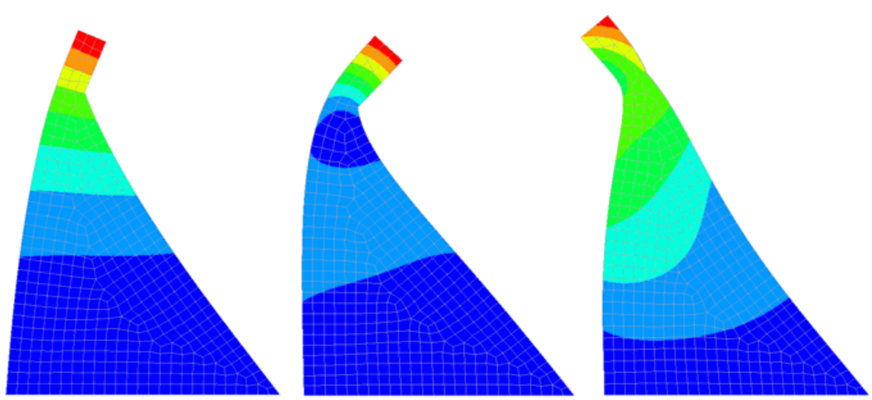

Figure 2 – Modal shapes corresponding to the lowest three natural frequencies for Case C2

In general, it could be concluded from Table 2 that the natural frequencies of the dam-foundation-reservoir system are lower when compared with the system that does not include the presence of the reservoir.

The results show that the eigenfrequencies of the system vary significantly with the type of the dam-reservoir-foundation model considered in the analysis. The highest natural frequencies are obtained for the dam model on rigid foundation without the presence of the reservoir. Flexibility of the foundation is a significant factor influencing the natural frequency of the dam-reservoir-foundation system.

In general, the fundamental frequency of the reservoir is higher 115.7, 150.0, and 127.2 percent than the fundamental frequencies of the dam-reservoir-foundation system defined for Case C-2, D-2, E-2, respectively.

Case D

The Taft Lincoln School Tunnel (TAFT) history record was provided for Case Study D as free field ground motions at the surface of the foundation, in a form of a baseline correlated acceleration time history record. The ground motions were then deconvoluted to determine the acceleration time history that can be applied at the base of the foundation. The deconvolved acceleration record was then converted to the stress time history record that was applied at 30 feet above the bottom face of the foundation. For ETAF seismic load, the provided in the formulation acceleration time history record was applied at the same location.

Case D vs Case E

Higher natural frequencies are determined for the model with stiffer foundation (higher elastic modulus) for both cases, with and without presence of the reservoir.

3. ANALYSIS LESSONS LEARNED

Evaluation of Westergaard Formulation

The classical model of a rigid dam placed on a rigid foundation (Westergaard's formulation [2]) is evaluated in this section. Water pressure distributions at the face of the rigid dam with an incompressible fluid (modified Case C-2), obtained by both the approximate and the exact Westergaard's solutions [5], are compared with the FE analysis results.

Figure 3 (left) is showing an excitation of the Case C model for rigid and flexible dam models. On the right accelerations are shown at the heel and the crest of the dam. The magnification of the acceleration is estimated to be 3.9 times.

Figure 4 compares distribution of the approximate Westergaard formula with the hydrodynamic pressure obtained for a rigid (left) and a flexible (right) dam at 2.67, 3.09, 1.0 Hz with. Both, the Westergaard's solution is in relatively good agreement with the FE analysis results for a rigid type dam but significant differences are observed for the flexible dam model.

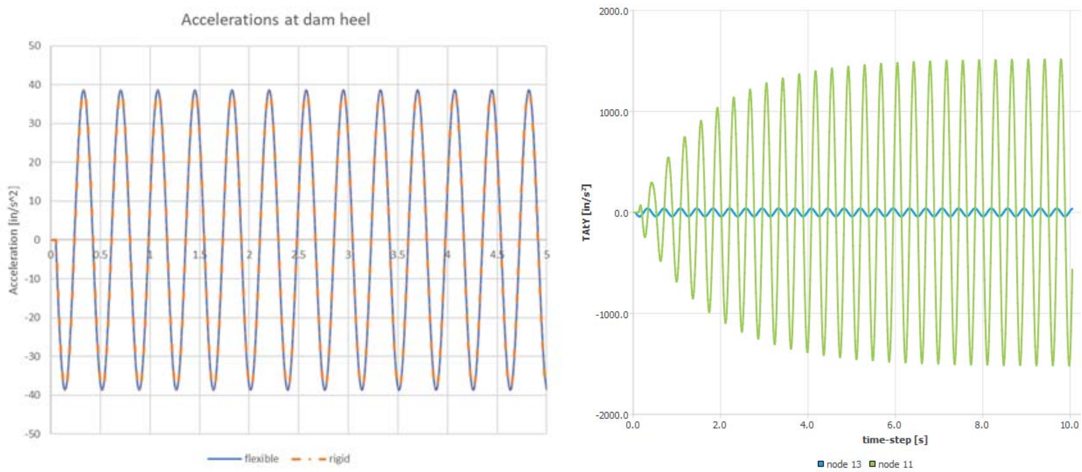

Figure 3 – Left - accelerations at the heel (node 13) for a rigid and flexible dam model; Right accelerations at the heel and the crest (node 11) for a flexible dam model.

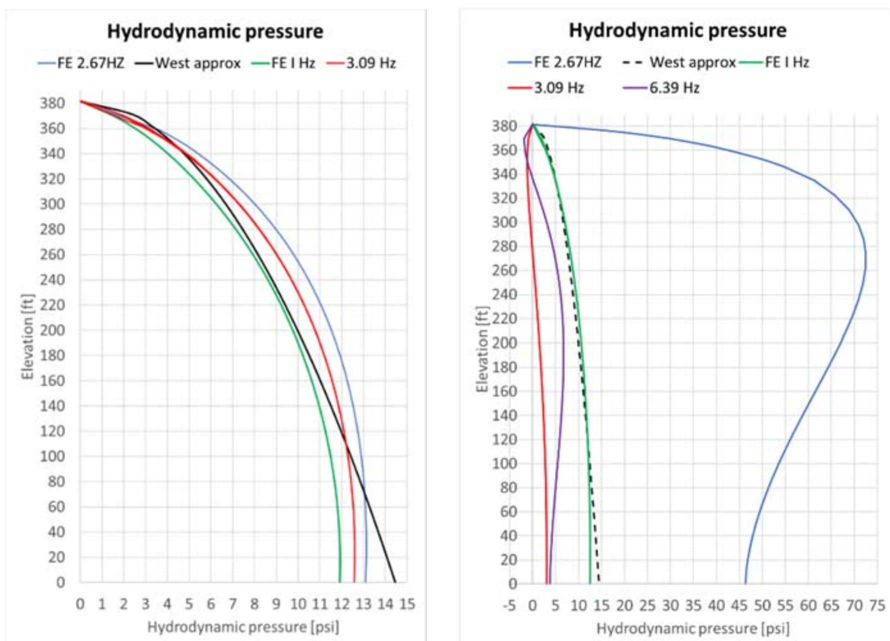

Figure 4 – Westergaard approximate solution compared with the FE analysis results for Case C at 0.1g acceleration amplitude: left - rigid dam excited at 1.0, 2.67 and 3.09 Hz; right - flexible dam excited at 1.0, 2.67, 3.09, and 6.39 Hz.

The “added mass” may provide relatively good results only for “rigid” type dams with vertical upstream face.

The above analysis results support the statement [3] that the Westergaard added mass approach only roughly estimates the mass of water interacting with the dam during an earthquake. The error is particularly large when the excitation frequency is similar to the first natural frequency of the system.

It appears that the "added mass" approach should not be implemented in the advanced time-history analysis, and that it only be used in a preliminary estimation of seismically induced hydrodynamic loads on dams.

Stresses at the Heel of the Dam

A stress concentration is observed at the dam heel. The actual computed stress at the heel may significantly vary with the mesh size used in the FE analysis and the reported location in the element use to determine such stresses (Gauss points, element nodes, or center of the element). The stress at the dam heel may not be the best measure for comparison of the analysis results provided by the case study participants.

4. Suggested Future Work

The following topics for further investigations are suggested:

- An analysis for a foundation block with a baseline correction of the pulse load, modified Case B.
- Perform comparison analysis of the dam models with simplified loads (pulse or harmonic) for specified model parameters including size of the model, material properties, etc. to evaluate numerical aspects of the used analysis methods.
- Overview and evaluation approaches used in deconvolution of the seismic loads used in the FE analysis of the dam-reservoir-foundation system.
- Validation of the FE models with laboratory test results – Reclamation is currently performing a shake test to determine a hydrodynamic interaction between a 4-ft by 4-ft structure and water.
- A hybrid frequency-time domain analysis should be implemented in the seismic simulations of the dam-reservoir-foundation system.

References

[1] Manie J. (Ed.), DIANA User's Manual, Delft 2017

[2] Westergaard H. M., Water Pressures on Dams during Earthquakes, ASCE Transactions, November 1931

[3] Salamon J., Manie J. – Numerical Assessment of Hydrodynamic Loads Induced during Seismic interaction between Reservoir and Concrete Dam, USSD, Anaheim 2017

PARTICIPANT INFORMATION

Organization	GZA GeoEnvironmental Inc.
Authors	Yixing Yuan
Software	Plaxis 3D with Dynamic Module

Cases Analysed

Case	Combination						
A	A-1						
B	B-1V	B-1H	B-2V	B-2H			
C	C-1(a)	C-2(a)					
D	D-1(a)						
E	E-1(a)						

1. METHOD AND APPROACH

Plaxis 3D 2017 was used to conduct finite element (FE) analyses of the Pine Flat Dam under the static and dynamic loading. This FE software is widely used for three-dimensional (3D) soil-structure interaction, while its Dynamic module allows the evaluation of ground response under earthquake loading. However, the application of Plaxis in modeling the interaction of concrete dam-reservoir-foundation is rare in the literature. This paper presents an attempt of using Plaxis in the analyses of Pine Flat Dam and lessons learned from this exercise.

The model represents the tallest monolith of Pine Flat Dam, with a height of 400 feet and width of 50 feet. The geometry could be simplified as a 2D model. However, as explained in Chopra et al. (1980), plane stress condition is more suitable for describing the monolith behavior, whereas the rock foundation corresponds to plane strain conditions. Therefore, 3D model is created with plane stress and strain conditions on dam monolith and rock foundation, respectively.

The FE mesh is generated with 10-noded tetrahedral elements. Meshes created for current study do not include the interface between dam and foundation. In dynamic analyses, the averaged element size is set generally less than $\lambda/8$, where λ is the minimum wavelength of interest (Kuhlmeyer & Lysmer, 1973). Far-field non-reflection boundaries were used on lateral sides and the base of rock foundation to mimic infinite elastic plane. The dynamic load is applied directly at the base of the foundation or at the base of the dam and reservoir for the case with rigid foundation. Both dam and foundation use Rayleigh damping with coefficients α =0.95 and β=0.002, leading to averaged damping of 5 percent for the frequency between 2Hz and 6Hz. This range of frequency is of interest, as it is generally consistent with the 1st and 2nd natural frequency for the considered combination between dam, reservoir and foundation system.

Plaxis 3D does not provide a built-in function for modal analysis. An alternative approach was used to evaluate the natural frequency and modal shape for the model, which entails free vibration and forced vibration analyses. In free vibration analysis, dam system was allowed to vibrate after a removal of a concentrated force at the dam crest, and the natural frequencies can be estimated from the acceleration history in frequency domain. Then a harmonic excitation at a specific natural frequency was applied horizontally at the model base to evaluate the corresponding modal shape.

Current version of Plaxis 3D cannot directly model dynamic effect of the water pressure on the upstream face of dam during earthquake. A numerical trick is incorporated, which models the water with continuum solid elements during the dynamic analyses. This “reservoir” element uses typical unit weight of water, a Poisson’s ratio close to 0.5, a bulk modulus based on compression wave velocity, and very low shear resistance to emulate the fluid-like behavior. Although this approach allows an approximated representation of hydrodynamic effect, it requires the “reservoir” element to be constantly at plastic failure state, leading to significant computation time and difficulties for the analysis to converge.

2. RESULTS

In the static analysis Case A-1, the settlement and deflection of the dam depend on the assumption of boundary condition along dam axis. Assuming plane stress and plane strain conditions for dam and foundation, respectively, produced consistent results when compared to the values obtained by other participants.

The lateral boundary influence of rock foundation was studied in Cases B-1 and B-2. Upon a pulse excitation at the base, the acceleration response calculated on the surface appeared consistent with the input signal at central locations (e.g., P1, P2 in Case B-1), but discrepancies were observed when moving to the far field boundary (e.g., P3 and P4), and difference is more pronounced in the case of vertical excitation. In case of B-2, extending the far field boundary reduced effectively the boundary effects, where the difference was only observed at P7.

In Cases C-1 and C-2, the 1st natural frequency evaluated for dam monolith itself and dam-reservoir system were 3.183 and 2.539Hz, respectively, which generally agree with the reported values, 3.154 and 2.518 Hz by Chopra et al. (1980).

The 1st natural frequency for Cases C-2 and D-1 were 2.539 and 2.881Hz, respectively, lower than 3.183Hz for dam monolith. This comparison indicates that both hydrodynamic effect and foundation interaction reduces the 1st natural frequency. The 1st natural frequency for Cases D-1 and E-1 were 2.881 and 3.125Hz, respectively. These results suggest that more flexible foundation leads to a lower 1st natural frequency.

Due to the difficulties in modeling the “reservoir” element in Plaxis 3D, the analyses for Case C-2, D-2 and E-2 that comprises dam-reservoir-foundation interaction failed to produce reasonable hydrodynamic pressure on upstream face. Further study is needed for a reliable approach to model the reservoir behavior.

Detailed analysis results are presented in the companion spreadsheet.

3. ANALYSIS LESSONS LEARNED

Modeling dynamic responses of dam-reservoir-foundation interaction with the popular FE software, Plaxis 3D, faces several challenges. The following lessons were learned:

1) Plaxis 3D does not provide a convenient function for modal analysis (unlike the built-in procedure in Abaqus and Ansys). A workaround could be possible by performing free vibration and force vibration analyses to investigate the natural frequency and modal shape of Dam. However, this requires extensive post-process efforts, and higher frequency modes were very difficult to obtain in free vibration analysis.
2) The greatest challenge for using Plaxis 3D in the current study is the model of hydrodynamic effect during earthquake analysis. The current version of Plaxis 3D neglects the hydrodynamic effect of water pressure, i.e., the reservoir remains hydrostatic throughout earthquake. A numerical trick is invoked to model the water as continuum solid elements with very low shear strength. However, this approach led to numerous difficulties and eventually failed to reach convergence.
3) Mesh size still needs to be iteratively examined and adjusted for dynamic analyses to provide good convergence and acceptable computation time. One-eighth of the minimum wavelength is often used to guide averaged element size (Kuhlmeyer & Lysmer, 1973).
4) The option of manually choosing a constant time step size is often preferred to facilitate debugging and post-processing process.

This study suggests there are great needs for expanding and improving the capability of Plaxis 3D in modeling dam-reservoir-foundation interaction under dynamic loading.

4. SUGGESTED FUTURE WORK

Future work could focus on some of the following aspects:

1) Earthquake loading often induces large deformation that leads to cracks in the concrete faces of the dam. Future study could consider fracturing of gravity dam and its influence on dam performance.
2) Additional study should involve an interface between dam and foundation, which can facilitate the potential sliding and overturning mechanism of gravity dam.

3) A hybrid numerical method could be used to study the fluid-dam interaction problems. For instance, the particle-based method could be used to simulate fluid phase response, while mesh-based finite element method can be applied to the dam and foundation structure. The performance of this hybrid approach should be benchmarked with analytical solutions and experimental results in the literature.

Reference

Kuhlmeyer, R.L, Lysmer, J. (1973). “Finite Element Method Accuracy for Wave Propagation Problems”, Journal of the Soil Mechanics and Foundation Division, vol.99 n.5, pp.421-427

Chopra, A.K., Chakrabarti, P. and Gupta, S. (1980). “Earthquake Response of Concrete Gravity Dams Including HydroDynamic and Foundation Interaction Effects” Report No. UCB/EERC-80/01

PARTICIPANT INFORMATION

Organization	BC Hydro
Authors	Brent Bergman Osmar Penner Mina Shahbazi Jeff Yathon
Software	LS-DYNA

Cases Analysed

Case	Combination					
A	A-1					
B	B-1V	B-1H	B-2V	B-2H	B-3V	B-3H
C	C-1(a)	C-2(a)		C-2(b)		
D	D-1(a)	D-2(a)	D-1(b)	D-2(b)	D-2(c)	
E	E-1(a)	E-2(a)	E-1(b)	E-2(b)	E-2(c)	

1. Method and Approach

The analysis approach for the Pine Flat dam workshop model (hereafter referred to as the model) was based on work completed at BC Hydro over the past few years to improve the methodology for seimsic analysis of our concrete gravity dams. Analysis was done using LS-DYNA, as it has several important features: explicit time integration, a large library of contacts, and implementation of the effective seismic input method. An elevation overview of the model is shown in Figure 1, and a brief summary table is provided in Table 1. All aspects of the analysis approach have undergone extensive verification and validation. See Penner et al. [4] for more details.

Explicit time integration is useful for highly nonlinear problems, as convergence is guaranteed given a sufficiently small time step. This allows us to model, for example, the reservoir-dam interaction (including separation), or stick-slip sliding behaviour along failure planes.

Even in a relatively simple model such as this one, we make use of several contact formulations. Constraint-based contacts that “tie” the nodes of one surface to another are used to facilitate mesh transitions, such as the dam/foundation interface. Other contacts allow relative movement and separation between surfaces, and are used for the reservoir-dam interface.

A key feature of the analysis approach is the effective seismic input method (ESIM; [2, 3]). This method re-arranges the equations of motions such that the seismic excitation can be applied directly to an interface within the model, referred to as the “seismic input interface” (Figure 1). The seismic input is defined in terms of the total free-field motion (i.e. the motion that would have occurred in the absence of the structure) at each location on the seismic input interface. The total response of the generalized structure (which can include parts of the reservoir and foundation) and the scattered (perturbed) response of the linear foundation (which can include parts of the reservoir) are computed. The interface between the generalized structure and the linear foundation is shown in Figure 1 as the “foundation-structure interaction interface.” The linear foundation can effectively simulate an infinite domain by using an absorbing boundary—in LS-DYNA we use a perfectly-matched layer (PML, [1]).

The combination of the ESIM and PML allows us to avoid deconvolution of the free-field ground motion to some depth, since there is no need to apply input motion at the boundaries of the foundation domain. It also allows us to avoid using conventional viscous dampers. For the workshop problem, the seismic input interface can be defined close to the base of the dam (effectively at the ground surface). For stability we input the motions one element below the bottom of the dam in the model. The inaccuracies introduced by this shift in the input location will be relatively small. If the free-field motion at the ground surface is known (e.g. for the Taft record), it can be applied to the seismic input interface directly. If only the upward-propagating motion is known (e.g. for the ETAF record), then the total free-field motion must be computed in an auxiliary analysis (Section 2.3).

Because the PML can not support static loads, we must first run a static analysis where we determine the stress state in the structure and the reactions at the foundation-structure interaction interface. When we run transient analyses, static stresses and reactions are applied to the generalized structure but not to the linear foundation.

Damping was applied primarily through "frequency-range damping," a proprietary algorithm implemented in LS-DYNA which results in relatively uniform damping over a specified frequency range. For the workshop model, a range of 2 Hz to 20 Hz was used.

During previous validation work of the reservoir-dam interaction, it was found that the inclusion of atmospheric pressure more accurately represented the reservoir-dam interaction; without including it, the fluid elements would prematurely separate from the dam near the surface under seismic loading. This pressure is applied to the reservoir and the downstream side of the reservoir-dam contact within the generalized structure only (the light blue elements in Figure 1). Hydrodynamic pressures reported in this workshop have had the atmospheric pressure subtracted in order to be comparable to those of other participants.

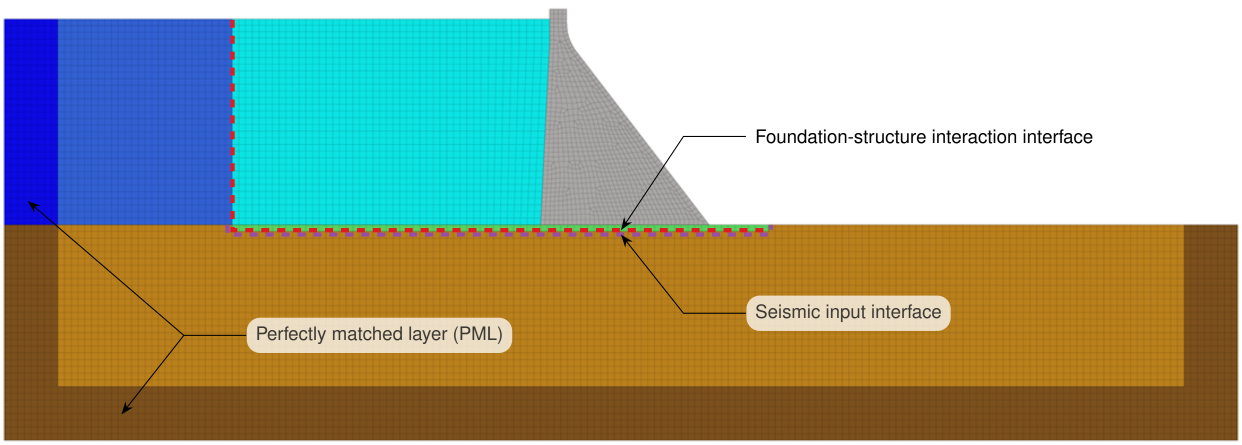

Figure 1: Elevation overview of the model, highlighting key components of the modelling approach

Table 1: Summary of key components of the FE model

	Description
FE model	3D, 50 ft wide
Mesh	Single point integration hex elements, Lagrangian fluid elements, average size within dam ≈ 8 ft and within reservoir/foundation ≈ 12.5 ft, number of nodes = 50 514
Interface	Dam/reservoir interface modelled using compression-only contacts
Time integration	Explicit integration, convergence achieved by setting time based on smallest/stiffest element (used $\Delta t = 3\times10^{-5}$ s)
Seismic input	Using the effective seismic input method
Boundary conditions	Absorbing boundaries using a perfectly matched layer

2. Results

2.1. General comments on results

Our results for Cases A, B, D, and E are consistent with the results of models of similar concrete gravity dams that we have validated and verified. Case C is not a situation we normally consider. In particular, case C2 is not a type of model we have attempted to create before, and is not an ideal implementation of the ESIM/PML approach. We are therefore less confident in our results for case C.

The vertical stresses reported at the heel of the dam were taken from the element directly at the heel, which is at a singularity in the FE model (the re-entrant corner). The stresses computed at this location are highly mesh-dependent. We reported the stresses from our model for the sake of completeness, but the exact values are physically meaningless. However, the overall profile of the stresses along the interface seems reasonable.

2.2. Frequency, mode shapes, and damping

Due to the absorbing boundaries requiring explicit integration, it is impossible for us to directly get the frequencies and mode shapes from the eigenvalues of an implicit analysis. What we have done instead is borrow from the techniques of experimental modal analysis. By calculating the frequency response function of an input at the soil-structure interface to an output node near the top of the dam, we can determine the approximate fundamental frequency. In addition, we use the half-power-bandwidth to approximate the total damping, which provides us with an estimate of the radiation damping.

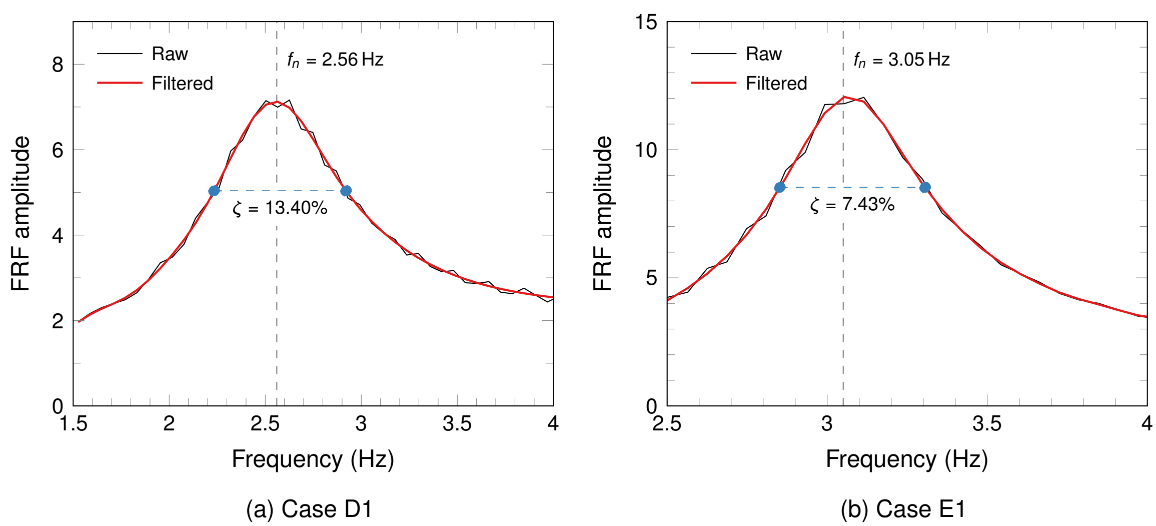

Figure 2: Frequency response functions of a node near the top of the dam due to a sine sweep input at the base for two different cases

For an input motion, we have used a sine sweep (prepended with a polynomial function for baseline correction). Two examples of the frequency response functions from cases D1 and E1 are shown in Figure 2. The actual frequency response functions contain some noise from the analysis and some jaggedness as a result of the discrete Fourier transform, so a filter is applied to the function to get a smoothed curve. Table 2 shows the calculated frequency and damping for all cases. The frequency increases with the stiffness of the foundation as expected, and is smaller when the reservoir is included in the model. Much of the damping comes from radiation damping in the foundation. The case C1 (ridid foundation) frequency of 3.36 Hz compares well to the frequency of 3.17 Hz from an eigenvalue analysis of the same model. Mode shapes were not identified.

Table 2: Frequencies and damping ratios calculated by modal identification using a sine sweep input. E_f and E_c are the elastic moduli of the foundation and dam

		No reservoir (1)		With reservoir (2)	
	Case	f_n (Hz)	ζ (%)	f_n (Hz)	ζ (%)
$E_f = E_c$	D	2.6	13.4	2.1	13.0[1]
$E_f = 3E_c$	E	3.1	7.4	2.4	8.2
$E_f = \infty$	C	3.4	5.5	2.7	6.1

[1] Damping should always increase with addition of the reservoir. The lower damping here could be due to numerical issues with curve fitting or the LS-DYNA frequency range damping algorithm.

2.3. Effect of foundation extent on the free-field motion

Using a two step methodology, we can obtain a uniform free-field acceleration response at the top of a flat foundation (without the structure), irrespective of the foundation extent. In the first step, a single column of elements with the same depth as the actual foundation is subjected to the effective forces of the incident motion. Viscous dampers are used at the base of the column to absorb the reflected wave. This model captures the variation of the upward propagating motion through the depth of foundation along with the effect of foundation damping.

The second step consists of a model of the actual foundation with the same depth but any arbitrary horizontal extent, wrapped by the seismic input interface and PML. In this model the effective seismic time history forces and the acceleration time histories obtained from the first model are input at each node along the seismic interface. The acceleration time histories at the top surface of the foundation in the second model will be exactly the same as those in the single-column model. With this method, a uniform acceleration time history response will be obtained on the top surface of foundation regardless of the extent of the foundation (see Figure 3). The pulse inputs for case B were assumed to be upward propagating shear waves.

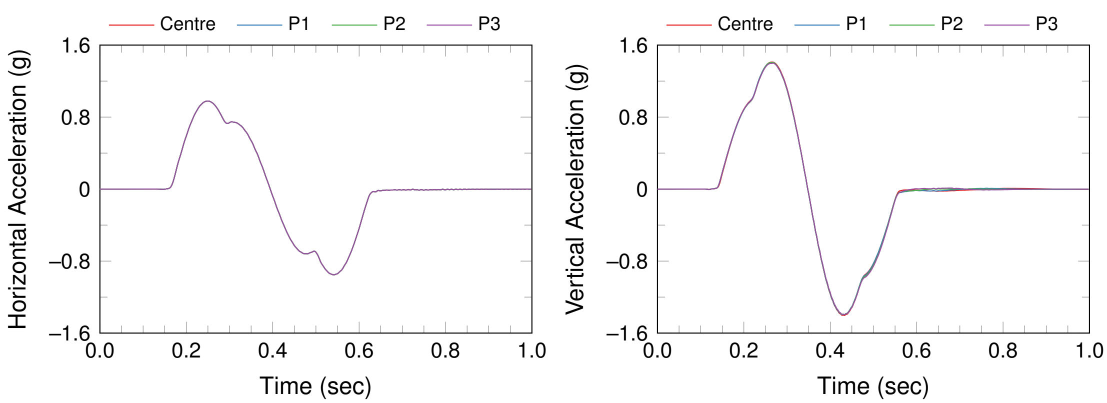

(a) Horizontal acceleration

(b) Vertical acceleration

Figure 3: Acceleration responses due to a pulse applied to the foundation for Case B1. Output points are defined in spreadsheet provided by workshop organizers

3. Analysis Lessons Learned

Although the foundation extent was fixed in the model, we were interested in investigating stress convergence with increasing foundation size. In order to do this, we constructed a simple 2D FE model of a rectangular block resting on an elastic foundation. The depth and width of the foundation were increased equally. Parameters were the extent of the foundation as a ratio of the length of the block (0.1 to 100) and the stiffness of the foundation relative to the stiffness of the block (0.1 to 10).

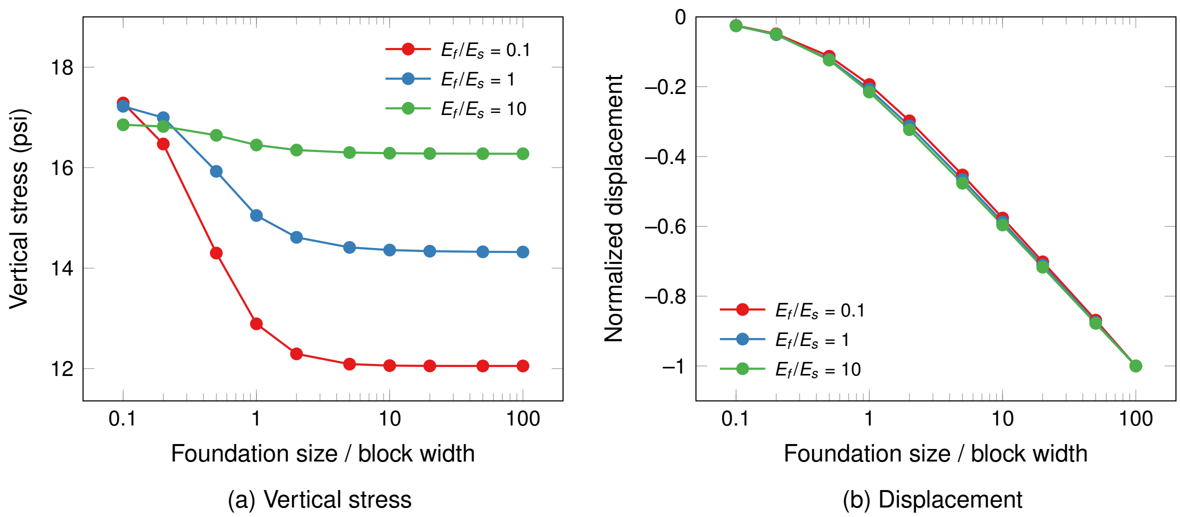

Figure 4: Stresses and displacements at the centre of the dam/foundation interface for varying foundation sizes and relative stiffnesses

Figure 4a shows the convergence of the vertical stress with increasing foundation size. The rate of convergence is similar for all stiffness ratios, and reaches a nearly constant value around a foundation size of five times the block width. However, even at foundation sizes around two to three times the block width, the error introduced is minimal.

The displacements are also shown in Figure 4b for reference. It can be seen that they do not converge with increasing foundation size. We developed a simple mathematical model which confirms that the displacements never converge in a 2D (or pseudo-2D) model—the foundation size needs to increase in both horizontal directions to achieve displacement convergence.

4. Suggested Future Work

Although there are many worthwhile topics that could be covered in future workshops, we suggest three that are of particular interest. They address topics that we are dealing with in our current work, and it would be highly beneficial to see how other groups are approaching these issues.

1. *Fracture and sliding along failure planes in a 2D model*

   Modelling fracture and sliding along a surface in the current model, be it at the concrete-rock interface or through the dam itself, is a logical extension of the current workshop. Participants would be given the location of one (or more) failure planes, and a set of properties along that plane (tensile and shear strength, some measure of the surface roughness). Of interest would be: how initial fracture is modelled; how friction properties are defined; how uplift along the failure plane is modelled; and how sliding is simulated in the selected FE code.

2. *Effect of 3D topography on input motions*

   As an extension of case B in the current workshop, we suggest a wave propagation exercise that attempts to account for the real topography around a dam. Participants would be given free-field ground motions (i.e. representing the motion at the surface of a semi-infinite flat foundation domain), the size of an input box around the dam (which would constitute the boundaries of a typical FE model of a dam), and the local topography. The purpose of this problem would be to understand the effect of topography on the free-field motion at various locations on the dam-foundation interface in the absence of the dam and reservoir, and to discuss best practices for obtaining the spatial variation of the free-field motion at the boundaries of the input box.

3. *Interaction between adjacent blocks (shear keys)*

   In the current workshop only a single block of a concrete gravity dam was modelled, making it essentially a 2D analysis (with the exception of the cross-valley restraints defined in the problem). In reality, adjacent blocks will have an impact on the response of the block, particularly if there are shear keys at vertical contraction joints. We envision a workshop where participants are instructed to model a dam with three blocks, defined shear keys, a rigid foundation, and rigid abutments on either side which restrain the edges of the outer two blocks. The effect of the shear keys would therefore be completely isolated, and it would be up to the participants to model the keys however they want. Different modelling approaches would be compared with respect to both the opening-closing and non-linear shear slip behaviour at the contraction joints. This is a subject on which there is not much available literature, and such a workshop would be a good way to start discussion on a topic which likely has a major effect on the response of concrete gravity dams.

References

[1] Basu, U. (2009). Explicit Finite Element Perfectly Matched Layer for Transient Three-Dimensional Elastic Waves. *International Journal for Numerical Methods in Engineering*, 77(2):151–176.

[2] Bielak, J. and Christiano, P. (1984). On the Effective Seismic Input for Nonlinear Soil-Structure Interaction Systems. *Earthquake Engineering & Structural Dynamics*, 12(1):107–119.

[3] Cremonini, M. G., Christiano, P., and Bielak, J. (1988). Implementation of Effective Seismic Input for Soil-Structure Interaction Systems. *Earthquake Engineering & Structural Dynamics*, 16(4):615–625.

[4] Penner, O., Bergman, B., Razavi-Darbar, S., Queen, D., and Léger, P. (2017). Nonlinear Time Domain Analysis of Ruskin Dam in LS-DYNA Including Reservoir-Foundation-Structure Interaction. In *Proceedings of the United States Society on Dams 2017 Annual Meeting and Conference*, Anaheim.

PARTICIPANT INFORMATION

Organization	Bureau of Reclamation
Authors 1	Roman Koltuniuk, P.E
Authors 2	Lan T Nguyen, Ph.D, P.E
Authors 3	Shohreh (Sherry) Hamedian, P.E
Software	LS-DYNA

Cases Analysed

Case	Combination						
A	A-1						
C	C-1(a)	C-2(a)	C-1(b)	C-2(b)	C-2(c)		
D	D-1(a)	D-2(a)	D-1(b)	D-2(b)	D-2(c)		
E	E-1(a)	E-2(a)	E-1(b)	E-2(b)	E-2(c)		
Sensitivity analysis	A-1(with no damping)						
10 Sensitivity analysis	D-1(a) (with and without damping)	D-2(a) (with and without damping)					

1. METHOD AND APPROACH

A 3D model representing a 50 foot wide of dam monolith was constructed. Boundary conditions restrained in X, Y, Z directions were assigned to the upstream, downstream, cross canyon, and the bottom of the foundation for the static run. These same constraints were assigned to the upstream and the cross canyon faces of the reservoir. All nodes on the dam face and the reservoir were merged. Both faces of the dam in the cross canyon direction were set free to replicate the effect of the monolith joints. Figure 1 shows these boundary conditions. Since an explicit analysis is to be performed, the gravity load assigned to the model was ramped from 0 seconds to 10 seconds and remained constant to 65 seconds. For the dynamic analyses, all the boundary conditions as described above were replaced with reaction forces. Non-reflective boundaries were applied on the upstream faces of the foundation and reservoir, along the bottom of the foundation and along the downstream face of the foundation.

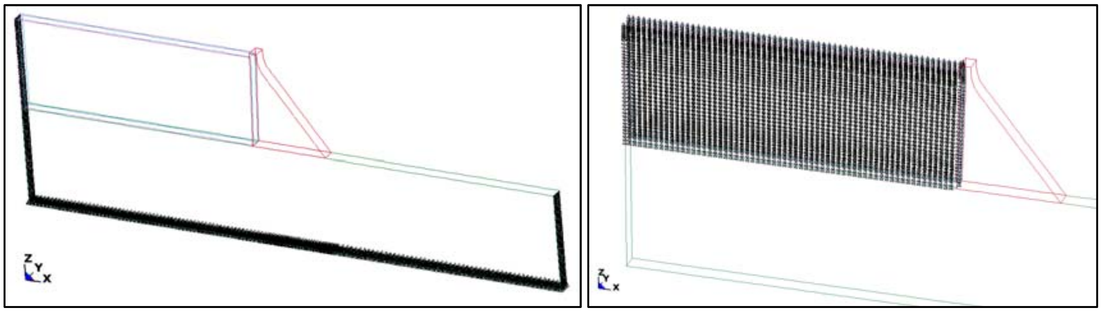

Figure 1a (left) shows boundary conditions at the foundation, Figure 1b (right) shows restrains in the cross canyon for the reservoir.

Table 1 below shows a brief description of the model.

Table 1. Model description

	Description
FE Model	3D model represents a 50 foot wide of dam monolith.
Mesh	Mesh type: quad mesh for 8 node hexahedron brick element Mesh size: approximately 108 inchx108 inch (9 feetx9 feet) for a side of a 8 node hexahedron brick element Number of nodes: 63490 nodes
Interface	Dam / reservoir interface: full connection (merged nodes)
Time analysis	Time integration method: Both Implicit and Explicit Convergence criteria on Implicit run for modal analysis case D1, displacement tolerance factor was set at 1 percent.
Boundary conditions for foundation	Far field conditions: Non-reflecting boundaries were assigned at upstream, downstream, and bottom faces of foundation
Boundary conditions for reservoir	Non-reflecting boundaries were assigned at upstream face of the reservoir

Boundary condition for dam section	Constrained displacement in the cross canyon direction at the center of the dam, along the upstream face for model stability. No boundary conditions at the cross canyon faces of the dam to replicate the free expansion at monolith construction joints.

For case D, the implicit method was performed in solving for the modal analysis requested in case D1 (dam and foundation). All twisting modes were skipped, the results are for modes in the upstream / downstream direction only. Explicit method however was used particularly for case D2, where fluid structure interaction exists. This is to bypass the limitation of solving for modal shape with using water material implemented in LS-DYNA. This method will be discussed in detailed in the result section.

2. RESULTS

2.1. Natural Frequencies

As an overall perspective on the analysis results, we observed that the natural frequencies of the dam to be higher on the rigid foundation material (results seen in Case C analysis) and lowest on the soft foundation (results seen in Case D analysis). Figure 2 illustrates this variation.

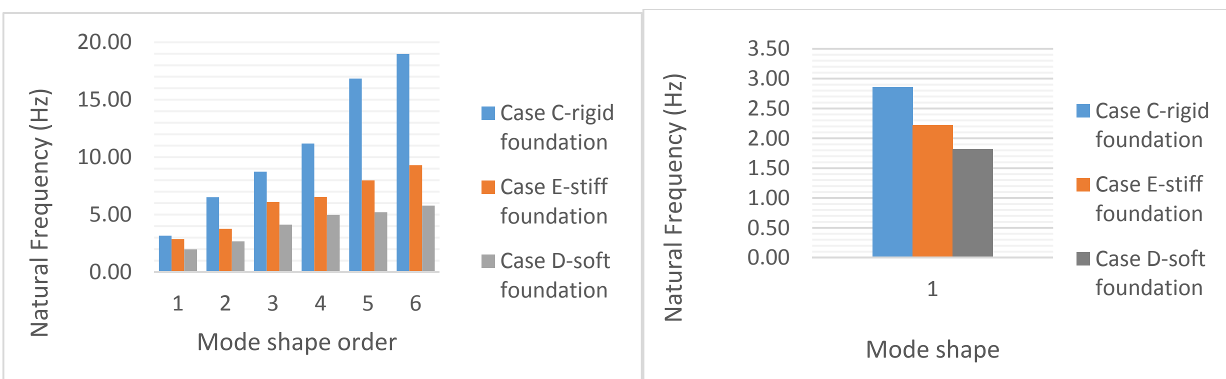

Figure 2a (left). Variation of natural frequency of dam with respect to foundation for dam and foundation models. Figure 2b (right). Variation of natural frequency of dam with respect to foundation for dam, foundation, and reservoir models.

This is as expected, since softer foundations would produce a more flexible response leading to a lower frequency.

Stiffness of foundation also has an impact on the vertical stress at the heel of the dam. From our results, it was found that the stiffer the foundation the higher the vertical stress at the heel of the dam. This observation is shown in Figure 3.

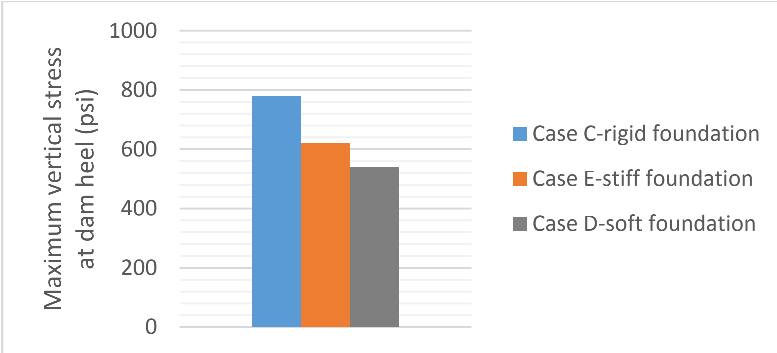

Figure 3. Vertical stress at dam heel with respect to foundation properties.

This again is as expected, since a stiffer foundation attracts more localized high stresses in a finite element model.

2.2. Deconvolution

A deconvolution analysis is performed to determine the acceleration time history that can be applied to the base (or near the base) of the foundation to reproduce the specified free-field acceleration time history. Based on the study by [1], in dealing with deconvolution, the size of the foundation should be assumed to be three times the height of the dam, which in turn, results in a relative wide and square 3D foundation model consisting of a large amount of elements. This is in effort to keep model edge effects far enough away. Seismic motions would then be applied as deconvolved orthogonal stress time histories along a horizontal layer of element faces at depth and allowed to propagate up to the ground surface. These responses are then compared with the free-field motions to see how well the model is acting. In lieu of the aforementioned 3D square foundation model, a 50 foot wide, flat-section model of the foundation only, with the same element density and spacing as the 3D model was used. Non-reflecting boundary conditions were assigned to the bottom and the up-downstream faces of this model of the foundation. Figures 4 and 5 below show examples of the free field Taft acceleration response spectra compared with the measured acceleration response spectra for the full 3D foundation model as well as with the 50 foot wide foundation model. The comparison is favorable meaning that a full foundation model can be reduced to a model of a slice through the foundation when evaluating response in the up-downstream and vertical directions.

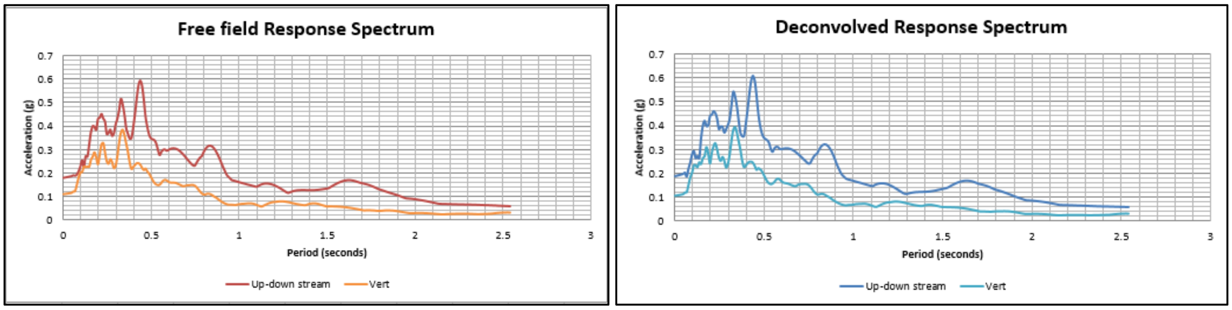

Figure 4. Free field response spectrum and deconvolved response spectrum for full 3D foundation model

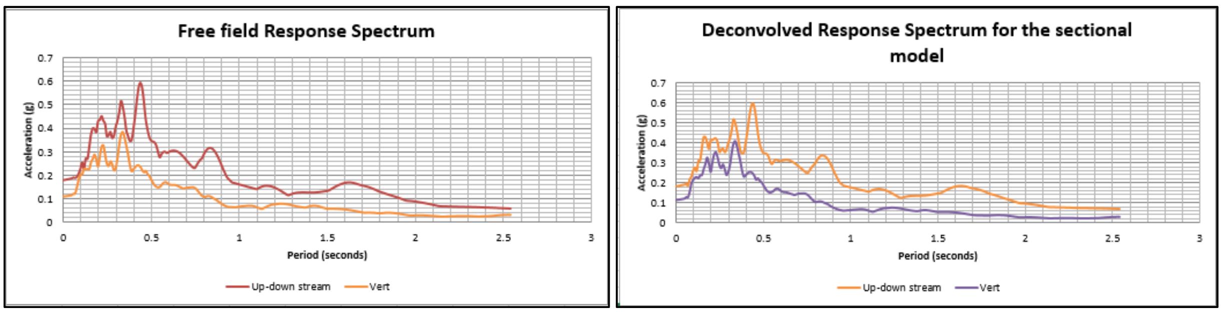

Figure 5. Free field response spectrum and deconvolved response spectrum for 50 foot section of foundation model

3. ANALYSIS LESSONS LEARNED

With the nature of the implemented “fluid-like” element type, there is no capacity of calculating the eigen values for the dam and foundation implicitly once the water is involved. In this analysis, modal shape analysis for the dam, foundation, and reservoir was performed simply by exciting the dam in the direction of the expected deformation, and measuring the frequency of the vibration of the dam. The approach could be visualized as a shown in Figure 6.

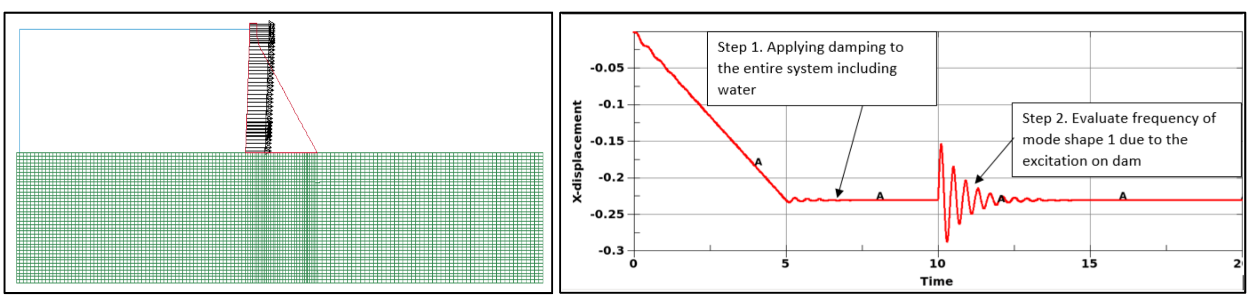

Figure 6. Sketch shows the methodology of determine frequency of the fundamental mode shape of the model.

While the first mode shape could be approximated as discussed, the second and the third could not be estimated with any certainty and therefore were omitted.

We also pursued a study of the damping experienced with this model. Essentially, the study is in accordance with finding damping using the decay of motion $ln\frac{u_i}{u_{i+1}} = \frac{2\pi\xi}{\sqrt{1-\xi^2}}$ in [3], with u_i being the amplitude of the vibration record, and ξ being the damping ratio. With this, we pursued a series of analysis to determine the damping the system experienced. Table 2 shows the results found from our analysis.

Table 2. Sensitivity analysis results for damping in the system

α value in Rayleigh damping equation	Damping in {Dam+foundation+reservoir}	Damping in {Dam+foundation}
1.5	9.3%	8.4%
1.1	8.6%	7.5%
0.75	8.4%	6.4%
0.60	7.5%	5.3%

These results show that even with a small amount of Rayleigh damping, the inclusion of water in the model increases the damping of the system. This is believed to be the result of hourglass control of the water element.

In LS-DYNA, solid, single integration point elements with a “null” material were used in modeling the reservoir. This material allows equation of states (ideal gas equation) to be considered without computing the deviatoric stresses. The material has no yield strength, no shear stiffness, and has a “fluid-like” behavior [2]. This simplification is attractive particularly for the equation of motion formulation$M\ddot{u}(t) + C\dot{u}(t) + Ku(t) = P(t)$, where the water element is “fictitiously” considered as the “solid type” and its mass contributes directly into M matrix. Beside the mathematical advantage of having a simple balance within the equation of motion, another major advantage of this element is its surfaces of deformation follow (or deform as analysis takes place) automatically. One major disadvantage of using a single integration element is that the integration point might not be able to respond to certain deformations of the element. Element energy control in this case is achieved by hourglass. However, once the energy from hourglass initiates, the damping in the element type domain increases, resulting in the observed increase in damping of the entire system. If too much hourglass control is needed, too much damping is introduced, leading overdamped results.

4. Suggested Future Work

In the authors’ perspective, the current deconvolution methodology utilizes the elastic assumption of the foundation model: (i.e, foundation domain is homogenous, no separation). In reality, most foundations are complex with existing faults and cracks. Important future work should address how these complexities effect the propagation of ground motions through these foundations.

5. REFERENCE

[1] A. Bayraktar, T. Turker, M. Akkose and S. Ates, "The effects of reservoir length on seismic performance of gravity dams to near and far fault ground motions," *Natural Hazards,* vol. 52, no. No.2, pp. 257-275, 2001.

[2] L. S. T. Corporation, LS-DYNA 971 Manual Volume II, Livermore: Livermore Software Technology Corporation, 2009.

[3] A. K. Chopra, Dynamics of Structures-Theory and Applications to Earthquake Engineering, New Delhi: Prentice-Hall of India, 2008.

PARTICIPANT INFORMATION

Organization	Quest Structures, Inc.
Authors	Yusof Ghanaat and Zachary Harper
Software	LS-DYNA

Cases Analyzed

Case	Combination						
A	A-1						
B	B-1V	B-1H	B-2V	B-2H	B-3V	B-3H	
C	C-1(a)	C-2(a)					
D	D-1(a)	D-2(a)	D-1(b)	D-2(b)	D-2(c)		
E	E-1(a)	E-2(a)	E-1(b)	E-2(b)	E-2(c)		

1. METHOD AND APPROACH

We used LS-DYNA to model and analyze Cases A, B, C, D, and E. We modeled the dam using four fully-integrated 3D elements through the monolith thickness for a total of 1,664 elements in the dam, 10,880 in the water, and 23,552 in the foundation (Figure 1). The total number of nodes were 46,335. Majority of elements were 12.5-foot cubes, with some elements having reduced length of 6.5 ft and others enlarged length of 20.5 ft on the side faces of the monolith. We used this model in Case A, and Cases C, D, and E with changes noted below.

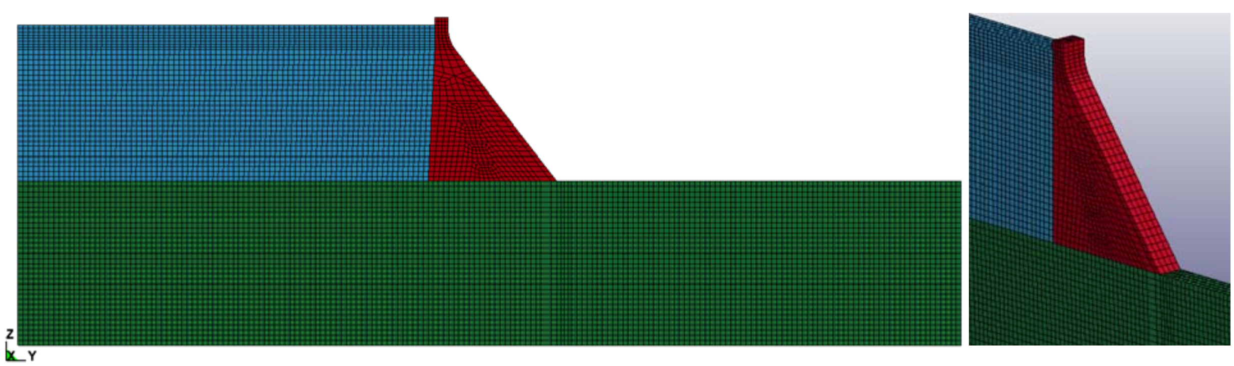

Figure 1. dam-water-foundation model for static and modal analyses

Case A-1: Linear Static Analysis

We ran the static analysis using the LS-DYNA implicit engine. We used MAT_ELASTIC water material properties with an elastic modulus of 901.58 psi and a Poisson's ratio of 0.4995. This approach combines the correct compression wave velocity of 4,720 ft/s with an assumed Poisson's ratio very close to 0.5. The model assumed fully connected nodes, with no interfaces between the dam, water, or foundation. The model boundary conditions consisted of: nodal fixity in the out-of-plane or x-direction, rollers on the bottom to restrain vertical movements and on the sides to restrain horizontal movements of the foundation.

We applied gravity loads to the dam monolith and impounded water but not the foundation rock.

Cases B-1, B-2, and B-3: Foundation Response Analysis with Pulse Input

We ran Case-B foundation response analyses using the LS-DYNA explicit engine. We employed a relatively coarse FE mesh with 25-ft-cube 8-node solid elements. The analysis cases included the specified Cases B-1 and B-2 with an intermediate Case B-3 7,300 ft in length. We applied non-reflecting boundary conditions to the bottom and sides of the models and used 1% constant damping applied to element deformation over a frequency range of 0.25 to 25 Hz. In our practice, we apply seismic tractions (or forces) to the bottom and sides of the foundation model. For this workshop, we applied seismic tractions only to the bottom to highlight the problem encountered with not applying seismic tractions to sides of the foundation model.

Modal Analysis – Cases C-1a, C-2a, D-1a, D-2a, E-1a, and E-2a

We performed modal analysis for the dam with and without water on rigid foundation (C-1a and C-2a), the dam with and without water on flexible foundation (D-1a and D-2a), and the dam with and without water on the flexible foundation with rock properties II using LS-DYNA implicit engine. For eigenvalue analysis, we changed the water material model from MAT_ELASTIC to MAT_ELASTIC_FLUID to remove sporous fluid modes caused by the non-zero shear modulus. For eigensolution, we fixed boundary nodes in space, except that we introduced rollers on the upstream side of the fluid in Case C-2.

Cases D-1b and E-1b (Empty Reservoir): Dynamic Analysis with Taft Earthquake Record

We performed dynamic analyses using the LS-DYNA explicit engine with the foundation-structure-interaction perfectly-matched-layer (PML) approach. We employed the Case A-1 finite-element mesh with water elements removed and nodal separation added between dam monolith and foundation to incorporate dam-foundation interface into the model for the application of an effective seismic input according to the PML requirements. Each case required two separate analyses: a static analysis followed by a transient analysis.

We performed the static analysis with gravity load applied to the monolith but not the foundation in a one-second ramp and fixed boundary nodes. In the transient analysis, the model included 5-element-thick PML layers added to the bottom and sides of the foundation with exterior nodes fixed in space (Figure 2). The transient analysis began with introducing an interface between the monolith and foundation for the application of the effective seismic input and proceeded with the static deformation and stress results as initial conditions and a 5% frequency-independent constant critical damping ratio over the frequency range of 0.25 to 25 Hz.

Cases D-2b, D-2c, E-2b, and E-2c (Full Reservoir): Dynamic Analysis with Taft Record

Dynamic analyses with full reservoir also employed the LS-DYNA explicit engine with the foundation-structure-interaction PML approach. In the presence of reservoir water, this approach requires two preparatory analyses – a static analysis as an initial condition, and an auxiliary analysis to capture the effect of upstream motion in the water. The finite-element mesh was identical to Case A-1, except for the PML boundary condition and the division of water into two parts: near-field (NF) water and far-field (FF) water (Figure 2). The NF water consists of all water within 330 ft of the monolith. Both the NF and FF use the same MAT_ELASTIC water properties as in Case A-1. The model included full nodal separation between NF and FF water, as well as between the foundation and the monolith/water to define the interface for scattering and transient dynamic analyses.

The application of the ETAF acceleration at the ground surface was produced by repurposing an analysis model from Case B-2. We applied the provided in-depth ETAF ground motion at the base of the foundation model without the dam and the resulting acceleration at the ground surface was recorded and used as input to the dynamic analysis PML model.

Each dynamic analysis with full reservoir required three separate static, auxiliary, and transient analyses as follows:

1) Static analysis to apply gravity loads to the monolith and impounded water to record static reactions at the foundation-structure interface and obtain initial static deformations and stresses for the subsequent transient analysis.

2) Auxiliary analysis to obtain the free-field motion associated with the impounded water. The auxiliary analysis model consisted of the FF water and foundation model with PML layers introduced around the foundation and at the upstream reach of the FF water

3) Transient analysis to compute the dynamic response of the dam with PML boundary conditions. The transient analysis started with static stress initialization and continued with dynamic transient analysis with the free-field ground accelerations and those associated with the water from the auxiliary analysis.

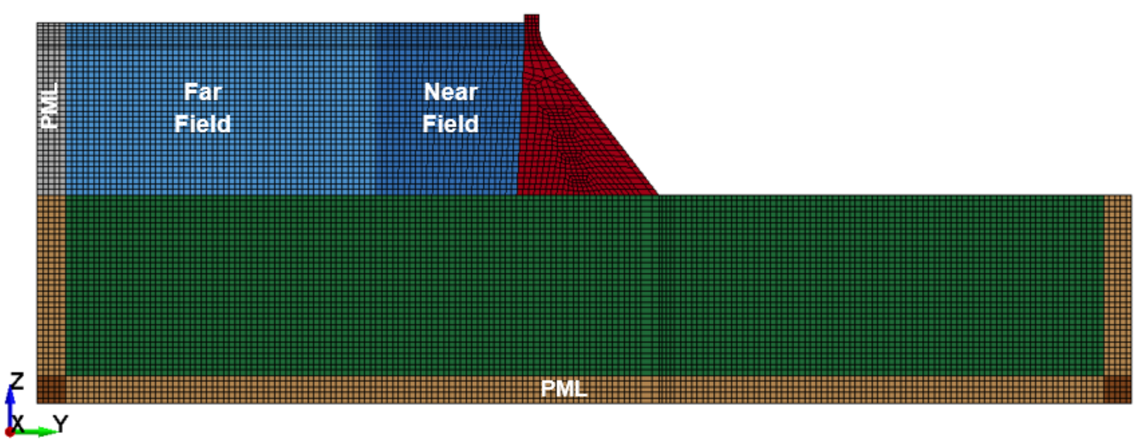

Figure 2. Dam-water-foundation SSI/PML model for dynamic analysis Cases D and E.

2. RESULTS

Case A – Static Analysis

Static deflection and stress results are as expected. The results show a net horizontal downstream crest deflection and settlement at the heel and the toe. The stress distribution at the base of the dam is nonlinear and sensitive to the foundation modulus and subject to stress concentration at the heal and toe. One interesting observation was that the stiffer foundation generated identical or slightly higher downstream relative displacement. The reason for this is demonstrated in Figure 2, which shows the more flexible foundation causes more settlement and slightly upstream rotation. The stiffer foundation increases bearing within the base and decreases at the heal and toe and particularly switches the dam heel stress from compression to tension.

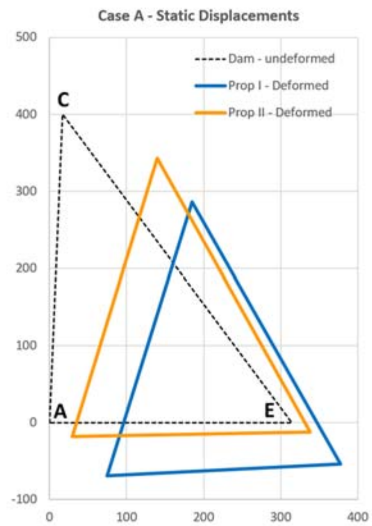

Figure 3. Dam settlement and downstream movement.

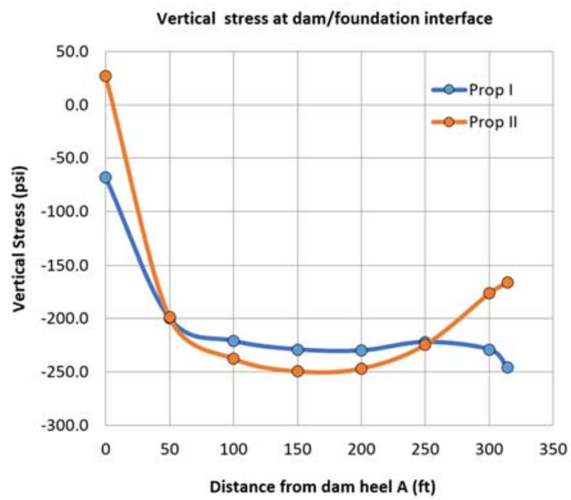

Figure 4. Stress distribution at base of dam.

Case B – Foundation Response Analysis

Case B-1 results demonstrate that a foundation model with non-reflecting boundaries and a length to depth ratio of 5.75 (L/D=5.75) is not sufficiently long to achieve a uniform acceleration profile at the ground surface. The surface accelerations along the length of the foundation vary significantly from expected values. Cases B-2 (L/D=30.75) and B-3 (L/D=18.75) are long enough to generate uniform-magnitude pulse responses along the length of the foundation (except at the outside edges). The vertical responses are similar, but their peak magnitude is greater than the expected value of 1g. The results highlighted the need for larger foundation models if seismic forces are applied to the bottom but not sides of the model (Figure 5).

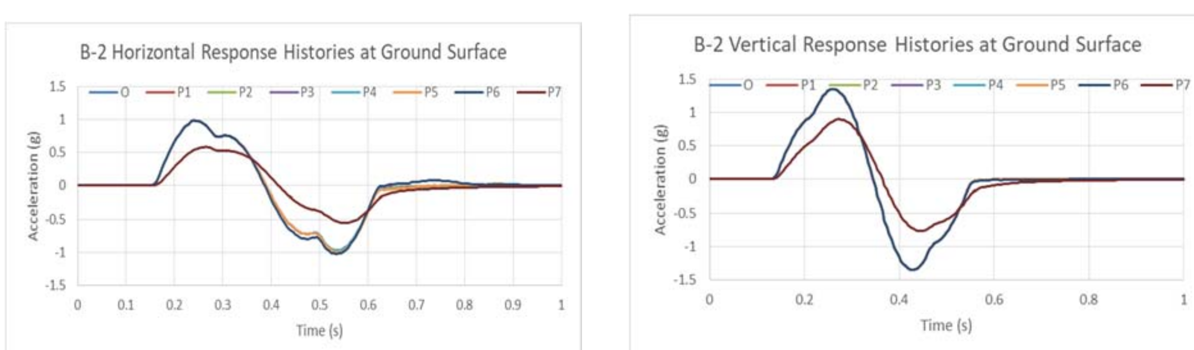

Figure 5. Horizontal and vertical pulse responses at ground surface for Case B-2.

Case C – Rigid Foundation with and without Reservoir Water

Only Case C modal analysis option was carried out for comparison with other cases (i.e., Cases C-1a and C-2a). As expected, the results show that natural frequencies of the dam on rigid foundation decrease significantly with the addition of the reservoir water. The decrease in frequency is higher for higher modes and varies from 39% for Mode-1 to as high as 75% for Mode-6. Case C-1 with empty reservoir indicates three distinct mode shapes of differing bending orders with zero deflection at the base of the dam. The addition of reservoir water in Case C-2 resulted in more single-order bending mode shapes with closely spaced natural frequencies. We believe the use of rollers on the upstream side of the fluid engaged fluid modes that artificially increased the hydrodynamic effects.

Case D – Flexible Foundation with and without Reservoir Water

Case C with rigid foundation indicated that the addition of the reservoir water decreases natural frequencies due to the added mass of the water. This behavior, however, was not observed in Case D with flexible foundation. Modes one and two frequencies for case D increase instead of decreasing with the addition of the reservoir water, and frequencies of Mode 3 and higher show relatively smaller reduction than expected. The reason for this behavior is because the interaction of the reservoir water with flexible foundation generates vibration modes that differ from those obtained from the hydrodynamic added-mass attached to the dam only. Thus, for dams on flexible foundations, the addition of reservoir water may not always reduce natural frequencies of the dam-water-foundation system.

The total pressures (hydrostatic+hydrodynamic) on the upstream face of the dam, concurrent with the time of maximum pressure at the heel, exceed hydrostatic pressures at all elevations but fall below the hydrostatic pressures near the top of the dam for ETAF record. Time histories of maximum total pressure at the heel of the dam appear reasonable and consistent with the Taft and ETAF acceleration records (Figure 6).

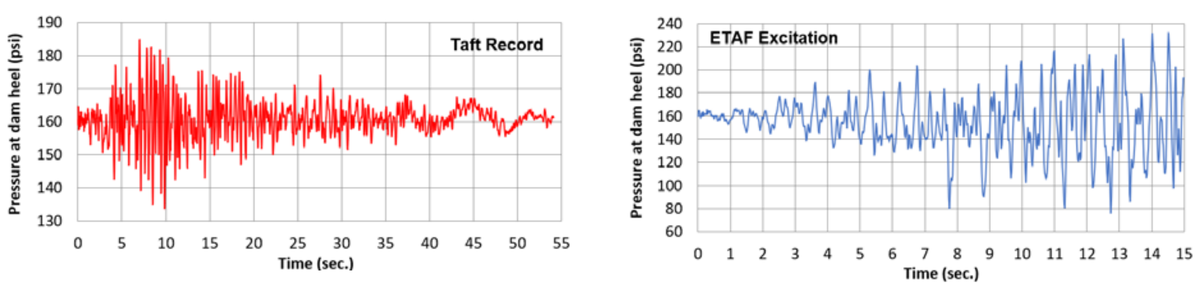

Figure 6. History of total pressure at the heel of the dam for TAFT and ETAF excitations.

All stress time histories look reasonable. As expected, the addition of water in Case D-2b significantly reduces the compressive stress and increases the tensile stress at the heel, compared to D-1b. The stress patterns under the dam all look reasonable, with extreme values at the heel, and more moderate values toward the toe. For ETAF excitation, the addition of water increases both the compressive and tensile stresses at the heel of the dam.

Case E – Same as case D with Foundation Properties II

Compared to Case D, the stiffer foundation in Case E reduces the effect of foundation and produces reduced natural frequencies for all modes with the addition of the reservoir water. The stiffer foundation slightly increased the magnitude of the observed hydrodynamic pressures, but otherwise had little effect. The stiffer foundation resulted in tensile static vertical stresses at the heel compared to Case D that showed compression but without much change in the magnitude of the oscillating dynamic stresses.

3. ANALYSIS LESSONS LEARNED

This workshop served as a test case for using the LS-DYNA SSI system to perform seismic analyses, as well as the use of PML material layers to provide far-field absorbing boundary conditions. Overall, the foundation-structure-interaction PML approach appears to work well for certain classes of problem, but it needs improvements and expanded documentation. It is difficult to validate the results and has some quirks that need a workaround.

For example, when performing a full dam-water-foundation analysis, the nodes at the corner of the dam heel (where the dam, water, and foundation all meet) began moving around in unphysical ways, presumably due to some conflict between the various forces and constraints at play in that region. While this oddly didn't affect the rest of the model in any way, it ruined the stress output in the one location that was of primary interest for this workshop. It was necessary to divide the water into "near-field" and "far-field" parts to work around this problem. The near-field water was then included together with the dam to form a greater generalized "structure" in the SSI setup to push the problem away from the heel of the dam. This modeling adjustment kept the troublesome corner nodes far from the area of interest in the model.

Another recurring problem is numerical instability in the water. The MAT_ELASTIC_FLUID employed in SSI example models distributed by LSTC frequently resulted in numerical instabilities during dynamic analyses. Eventually, the use of a MAT_ELASTIC material model instead with a Poisson's ratio of 0.4995 resolved the issue and produced a reasonable approximation of fluid water behavior with a small shear modulus.

(The exception to this is for the modal analysis, where it was necessary to model the water using MAT_ELASTIC_FLUID to obtain eigensolution. Otherwise, the presence of a small finite shear stiffness in the fluid medium will generate many low-frequency reservoir water modes that dominate the eigensolution.)

4. SUGGESTED FUTURE WORK

The LS-DYNA foundation-structure-interaction approach to the seismic analysis of dams is useful, but at present, it applies to dams built on flat ground surfaces. Ultimately, it would be very useful for the industry to develop a set of best-practices for dam-water-foundation seismic analysis that includes a robust fluid modeling approach and is capable of capturing foundation-structure interactions, as well as topography effects. To that end, the three important considerations for future workshops are to advance fluid modeling, application of seismic input approaches, with realistic radiation damping, all of which are essential to the nonlinear seismic analysis. Specifically, further investigations should be devoted to:

- Formulate benchmark problems to investigate and compare fluid modeling approaches
- Expand Case-B foundation response analysis considering various boundary conditions, seismic input for flat and canyon sites, and realistic radiation damping.
- Formulate benchmark problems to address significant nonlinear mechanisms such as contraction joint opening/closing and cracking followed by sliding and overturning

ATTACHMENT C – WORKSHOP PRESENTATIONS BY CONTRIBUTORS

2018 USSD Conference and Exhibition

Miami| Florida, 30 Apr – 04 May 2018

Workshop on Evaluation of Numerical Models and Input Parameters in the Analysis of Concrete Dams

Giorgia Faggiani, Piero Masarati

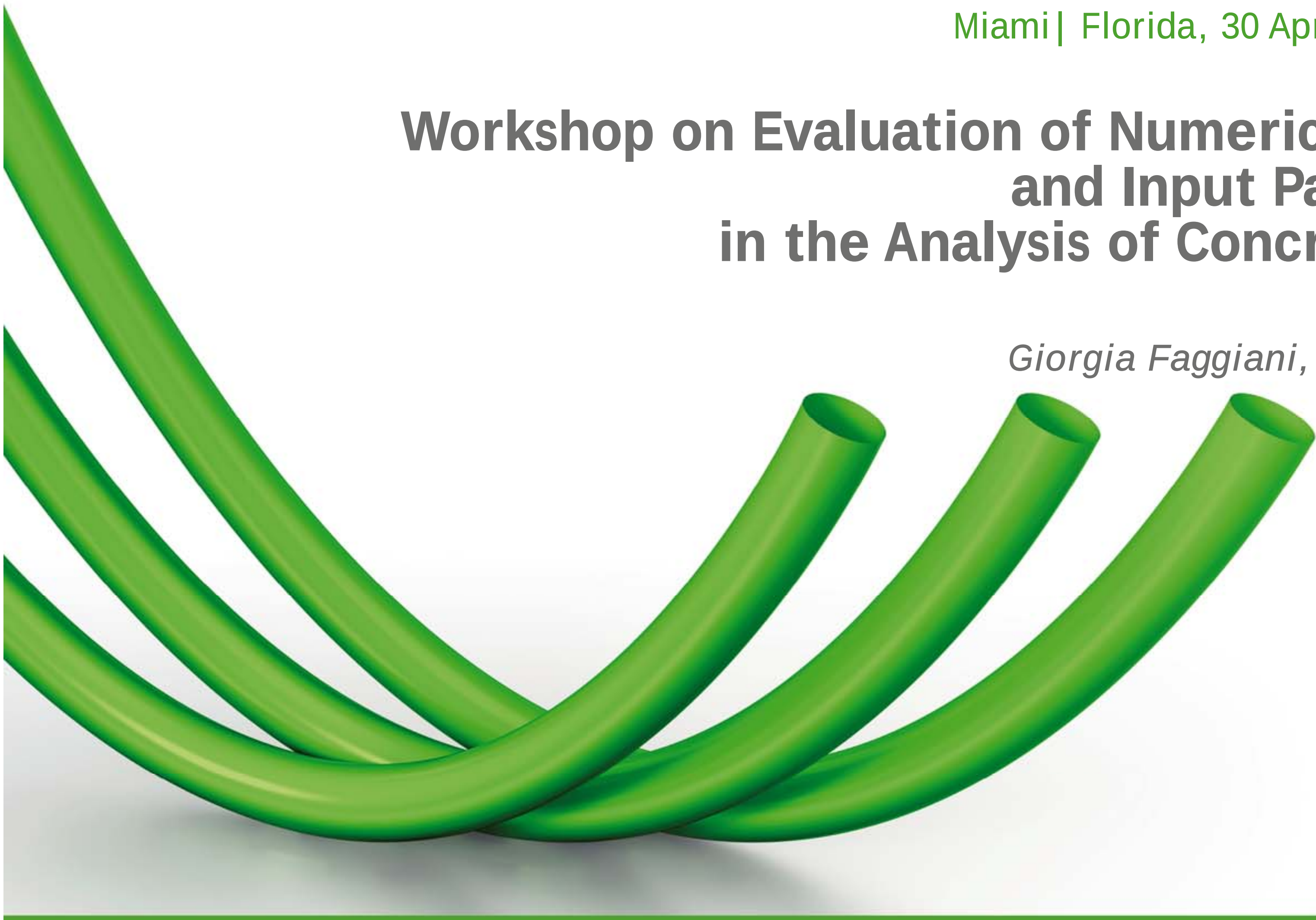

Agenda

METHODS & APPROACHES

Performed analyses

FEM and physical model

RESULTS

Main results

FINAL REMARKS

Lessons learned

Further investigations

Performed Analyses

Static analyses
Foundation properties I: A-1(I)
Foundation properties II: A-1(II)

Time-pulse analyses (foundation only)
2300 ft: B-1
12300 ft: B-2
7300 ft: B-3

Seismic analyses (rigid foundation)
Modal analysis: C-1(a) empty and C-2 (a) full reservoir
Taft Time History: C-2 (b) full reservoir
ETAF Excitation: C-2 (c) full reservoir

Seismic analyses (flexible foundation properties I)
Modal analysis: D-1(a) empty and D-2 (a) full reservoir
Taft Time History: D-1(b) empty and D-2 (b) full reservoir
ETAF Excitation: D-2 (c) full reservoir

Seismic analyses (flexible foundation properties II)
Modal analysis: E-1(a) empty and E-2 (a) full reservoir
Taft Time History: E-1(b) empty and E-2 (b) full reservoir
ETAF Excitation: E-2 (c) full reservoir

3D model

50-foot-wide dam monolith 16: 1076 solid linear elements (4 in the width)

Foundation: 9360 solid linear elements

Fluid: 6732 acoustic elements

Assumptions

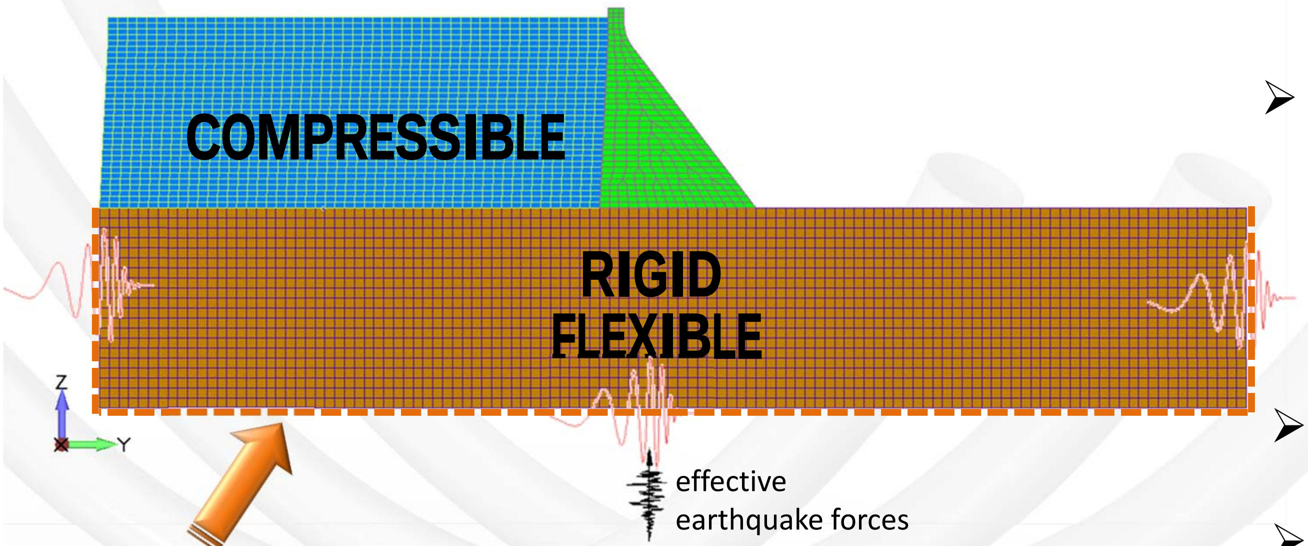

viscous spring boundaries

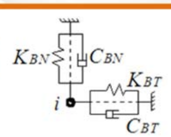

$$\begin{cases} K_{BN} = \frac{1}{1+\alpha}\frac{\lambda+2G}{r_b}, C_{BN} = \beta\rho c_p \\ K_{BT} = \frac{1}{1+\alpha}\frac{G}{r_b}, C_{BT} = \beta\rho c_s \end{cases}$$

- dam and foundation: **linear-elastic** model
- Rayleigh **damping:** **5%** at 1.5 and 6 Hz
- fluid-structure interaction: **coupled mechanical-acoustic** approach (Zienkiewicz, 1977)

dam-foundation interaction

- rigid foundation: **massless** approach (Clough, 1980)
- flexible foundation: **seismic wave propagation** approach (Chuan, 2009; Chen, 2012; Liu, 2013)

Effect of foundation extent

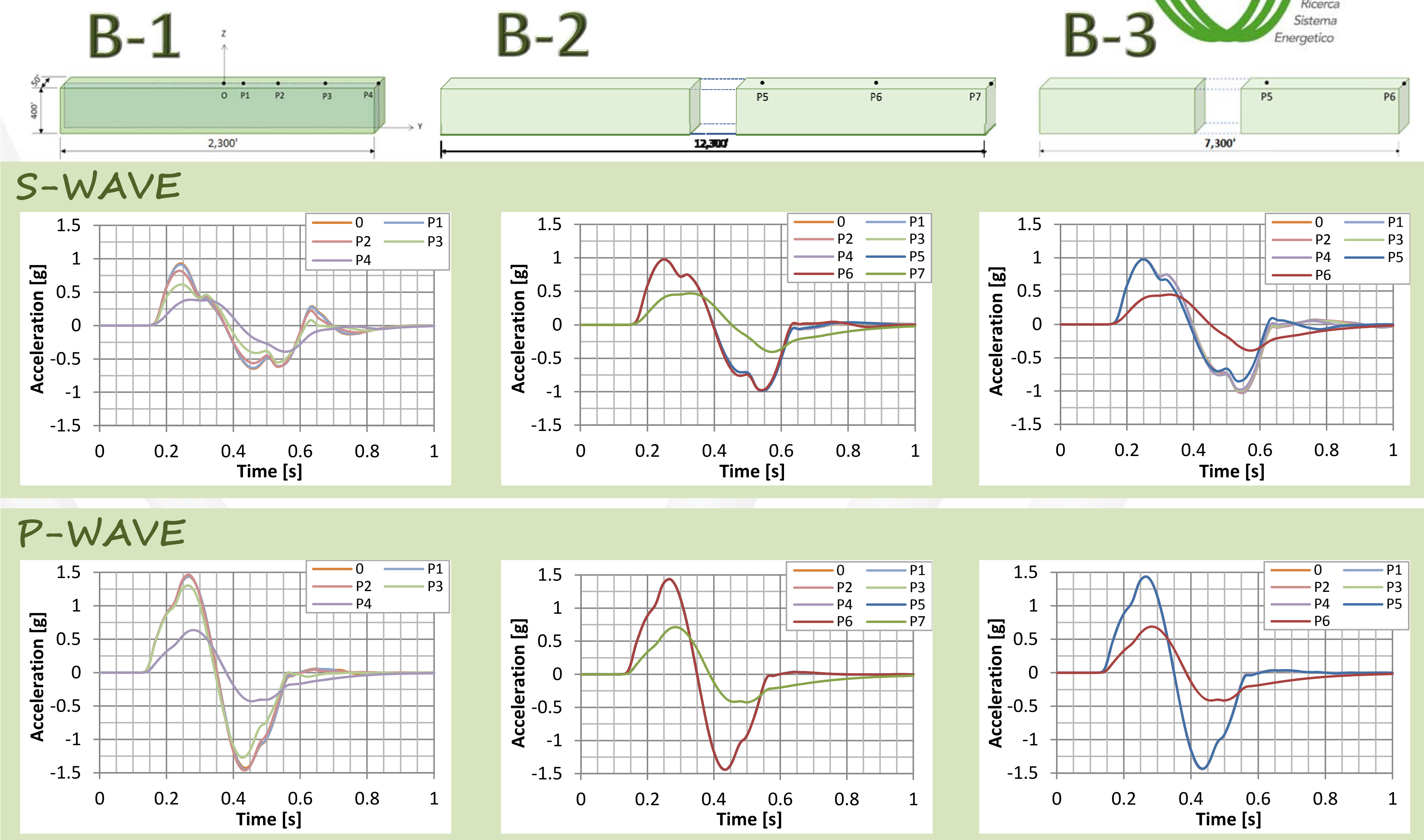

Seismic Analyses

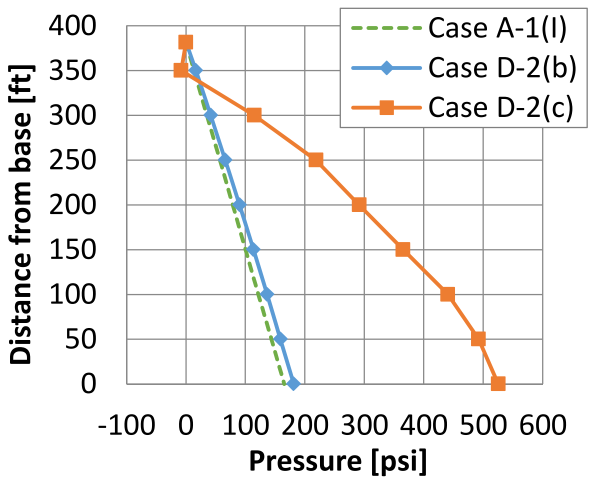

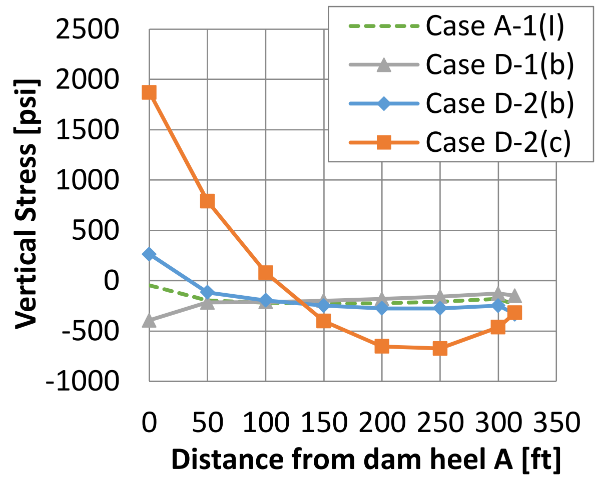

Modal Analysis

	Case D-1	Case D-2
Mode	Natural Frequency [Hz]	
1	1.98	1.78
2	2.71	2.44
3	4.12	3.17
4	4.98	3.92
5	5.28	4.13
6	5.78	4.95

Peculiarity of ETA time signal

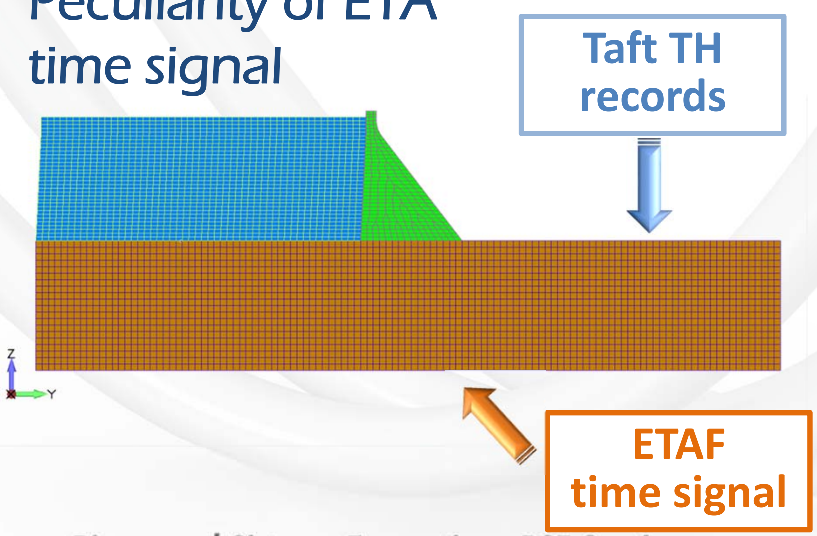

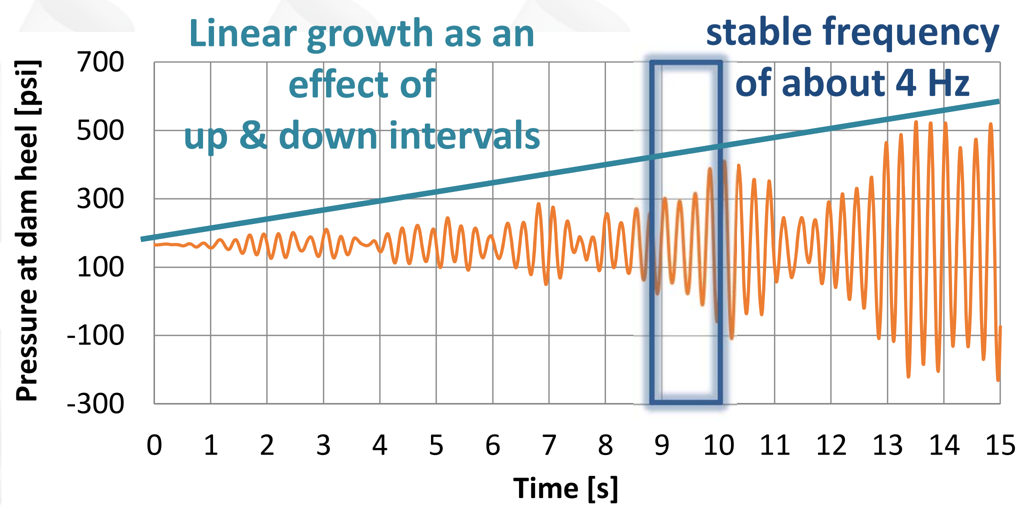

The additional **case M** (**flexible foundation, massless approach**) has been carried out to investigate the effect of advanced model on the seismic response of the dam

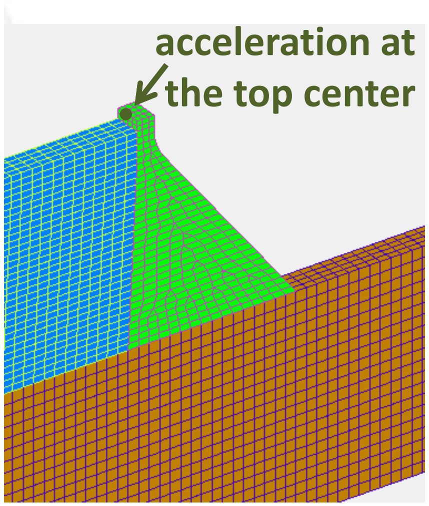

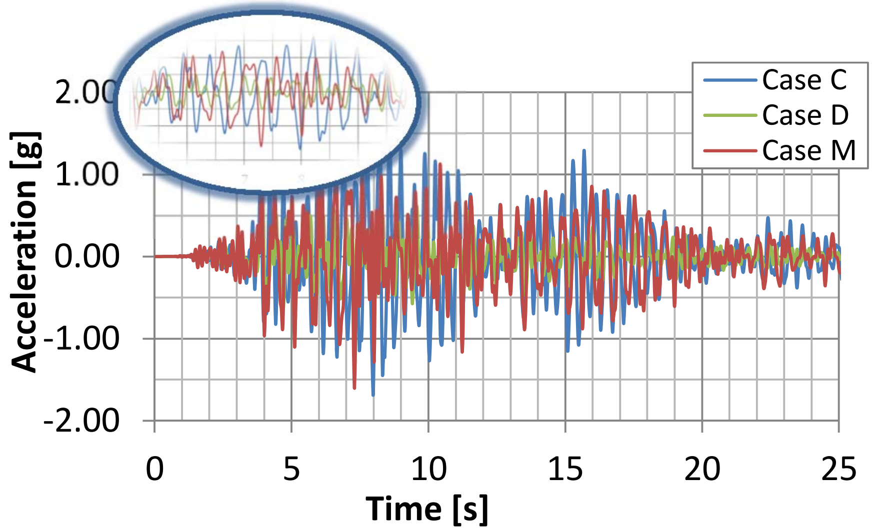

Both the **rigid** and the **flexible foundation** models with the ***massless*** approach provide acceleration values higher than the **flexible foundation model** with ***seismic wave propagation*** approach

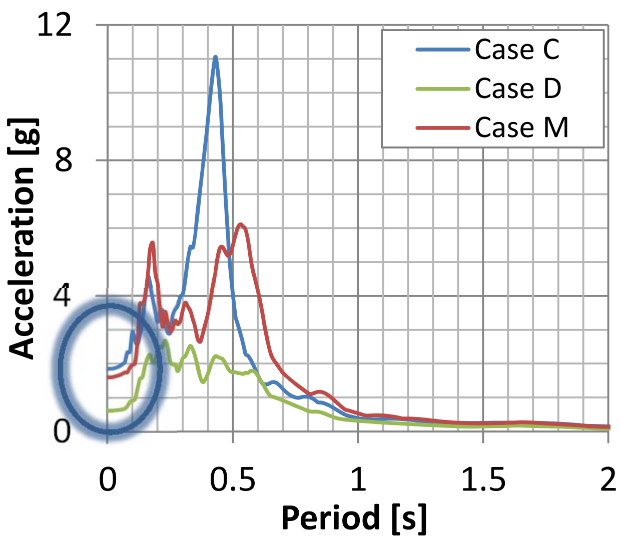

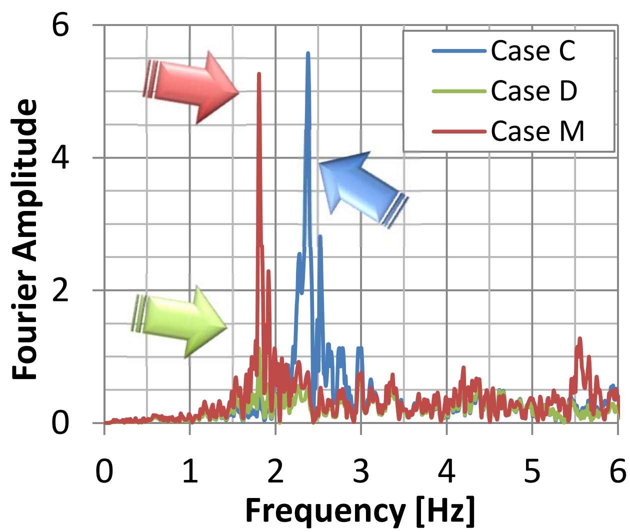

Frequencies of the resonant peaks are comparable for **flexible foundation model** with both the ***massless*** and ***seismic wave propagation*** approach

Frequency of the resonant peaks is higher in the **rigid foundation model**

Final remarks

The time-pulse propagation analyses have confirmed **the importance of the horizontal *sizes* of the foundation**: future in-depth studies regarding the effects of the horizontal sizes could take into account the propagation of the seismic signal both in the foundation only model and in the complete dam-reservoir-foundation model.

A deeper **comparison** between the results of the traditional widespread ***massless foundation*** approach and those of the ***seismic wave propagation*** approach would be quite significant.

The effects of modelling the **dynamic interaction** between the **foundation** and the **reservoir** could be evaluated.

To enhance the **reliability** of **FEM models** and the **confidence in using advanced models** for dam safety assessment, the availability of ***earthquake records on dams*** would really represent an added value.

Further investigations on Pine Flat case could be proposed in the frame of the **15th ICOLD International Benchmark Workshop On Numerical Analysis Of Dams**.

ICOLD Technical Committee A: *Computational Aspects Of Analysis And Design Of Dams*

T.O.R.: organize **Benchmark Workshops** to compare numerical models between one another and/or with reference solution, including the dissemination and publication of results

Bergamo (Italy)	1991/1992
Paris (France)	1994/2009
Madrid (Spain)	1996
Denver (USA)	1999
Salzburg (Austria)	2001
Bucarest (Romania)	2003
Wuhan (China)	2005
Saint Petersburg (Russia)	2007
Valencia (Spain)	2011
Graz (Austria)	2013
Lausanne (Switzerland)	2015
Stockholm (Sweden)	2017












15th ICOLD Benchmark Workshop (Milan, Fall 2019)

ITCOLD and **the Polytechnic University of Milan** express the intention to organize the **15th ICOLD International Benchmark Workshop on Numerical Analysis of Dams** in Milan

Possible themes

Theme A

__Static and seismic analysis__ of a gravity (Pine Flat) dam

Theme B

__Cracking of a concrete__ hollow gravity buttress (Gioveretto) dam

Theme C

Theme on __hydromechanical machinery__

Theme D

Theme on __embankment dam__

Theme E

Theme on __risk analysis__

Open Themes *on numerical safety assessment*

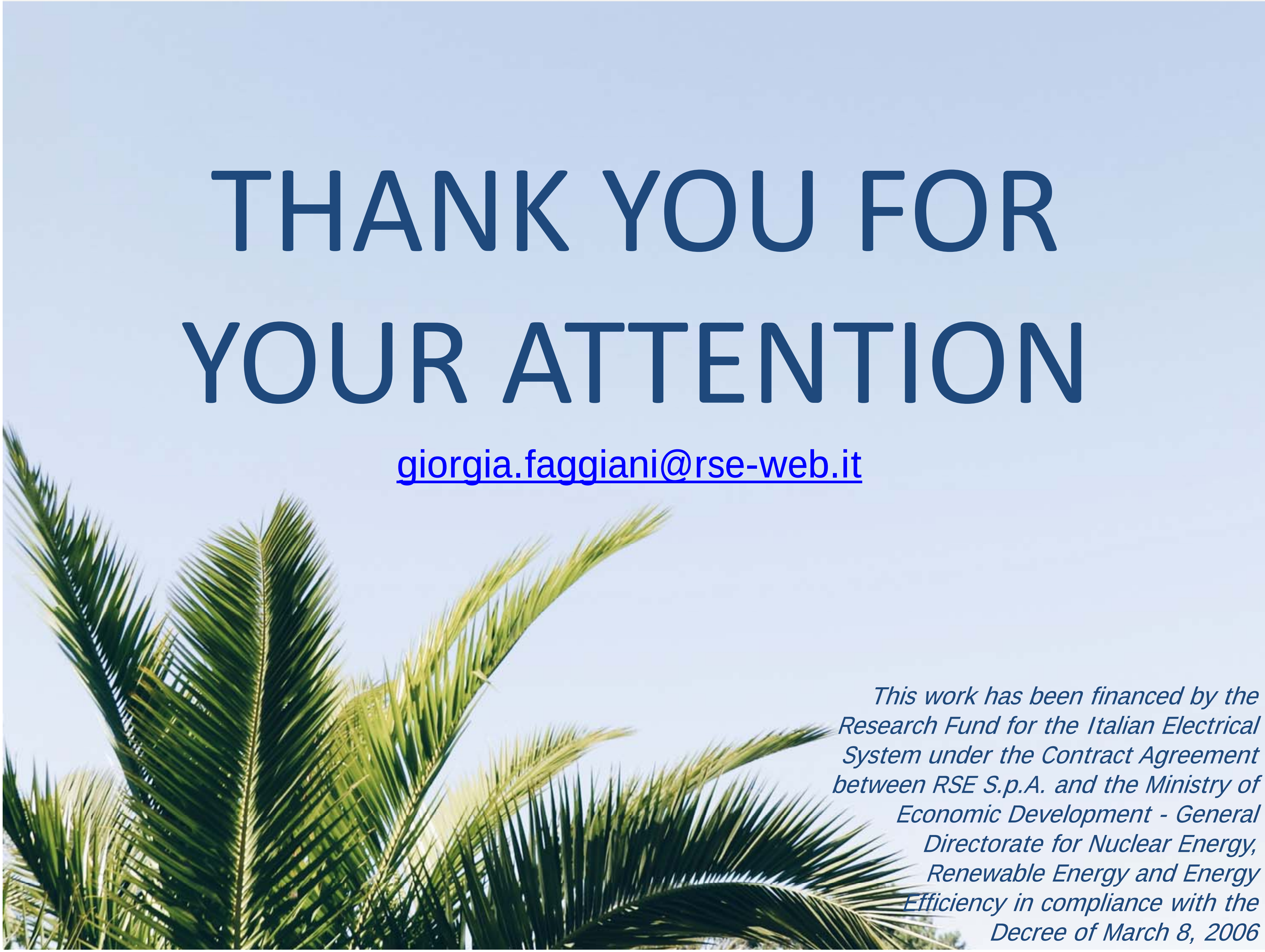

THANK YOU FOR YOUR ATTENTION

giorgia.faggiani@rse-web.it

This work has been financed by the Research Fund for the Italian Electrical System under the Contract Agreement between RSE S.p.A. and the Ministry of Economic Development - General Directorate for Nuclear Energy, Renewable Energy and Energy Efficiency in compliance with the Decree of March 8, 2006

Comparison of Case C, Case D and Case E

Seismic Analyses Pressure

Seismic Analyses Vertical Stress

Taft TH records

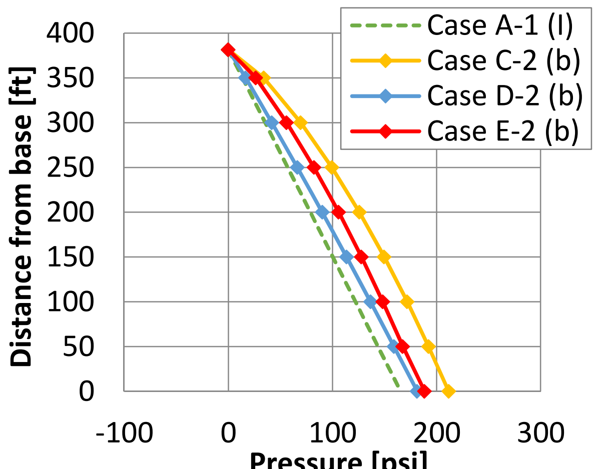

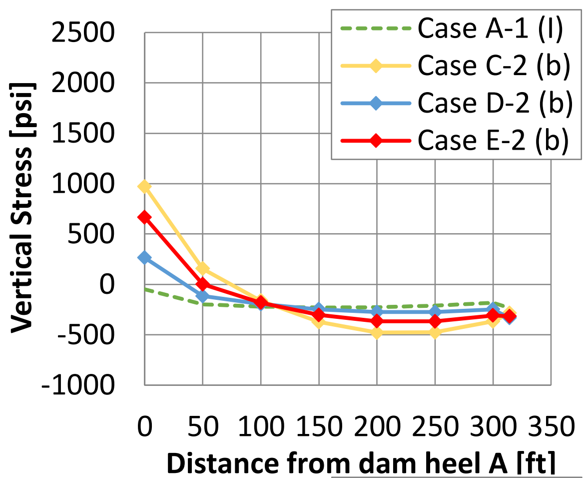

ETAF time signal

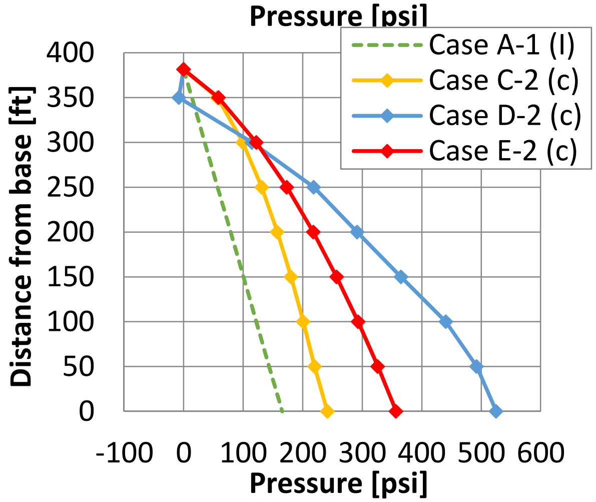

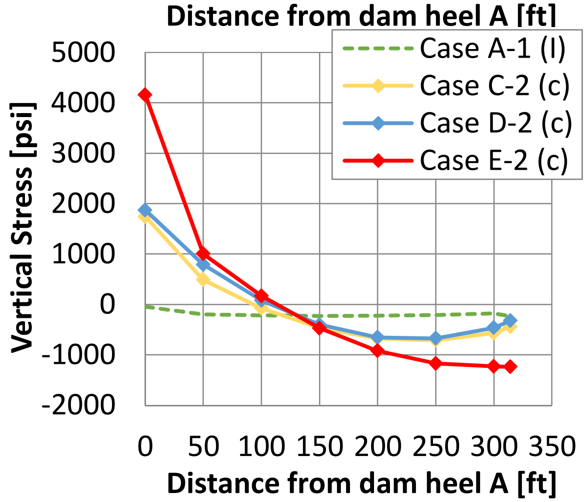

Modal Analysis

Empty reservoir

	Case C-1	Case D-1	Case E-1
Mode	Natural Frequency [Hz]		
1	3.20	1.98	2.89
2	6.65	2.71	3.76
3	8.75	4.12	6.23
4	11.46	4.98	6.52
5	17.36	5.28	8.00
6	19.12	5.78	9.31

Full reservoir

	Case C-2	Case D-2	Case E-2
Mode	Natural Frequency [Hz]		
1	2.57	1.78	2.33
2	3.20	2.44	3.18
3	3.96	3.17	3.68
4	5.46	3.92	4.01
5	6.48	4.13	5.41
6	7.83	4.95	6.24

Case D – ETAF time signal at the base of the foundation

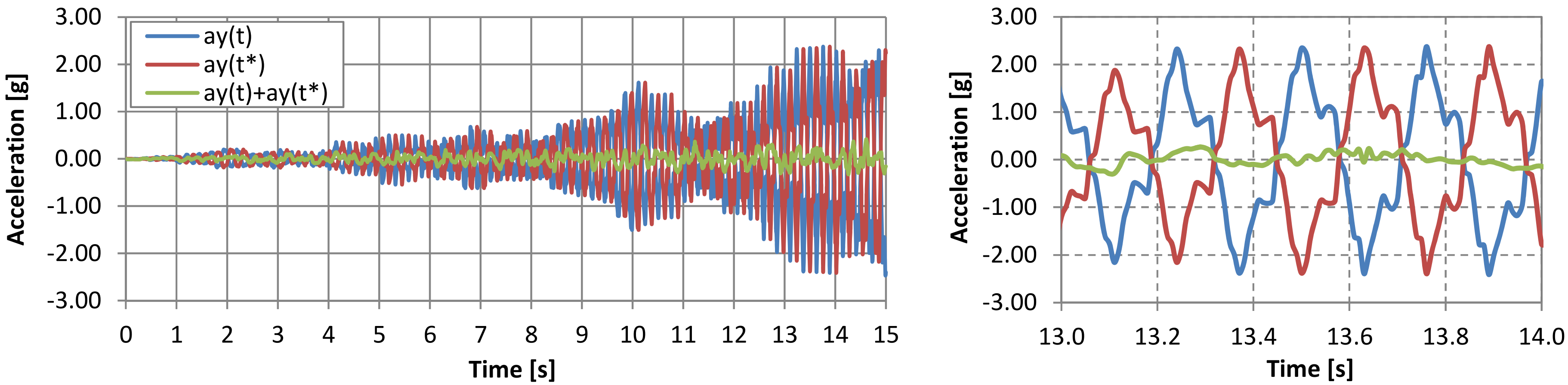

Case E – ETAF time signal at the base of the foundation

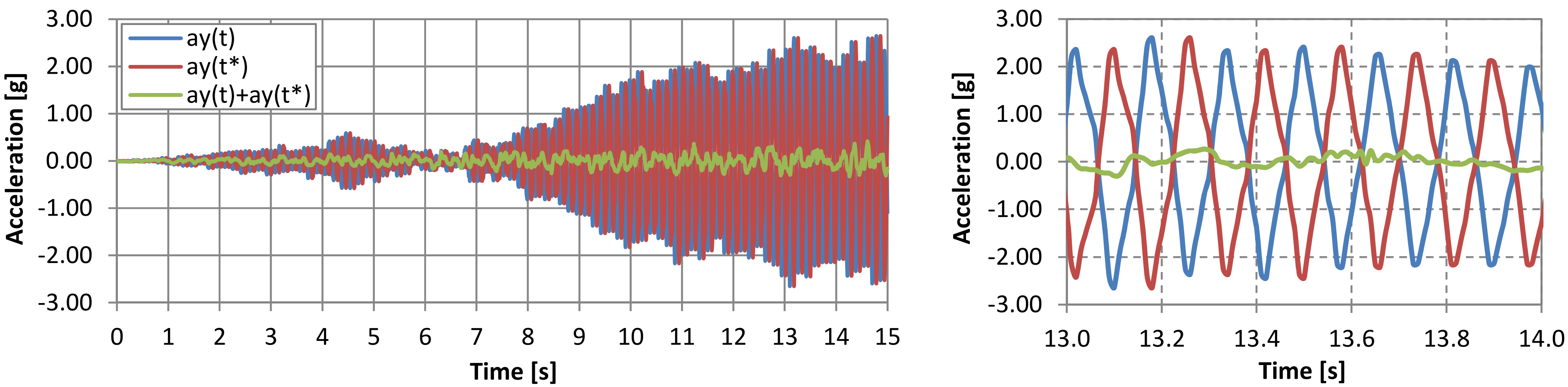

DRAFT – Not for distribution

Evaluation of Numerical Models and Input Parameters in the Analysis of Concrete Dams

Arnkjell Løkke,

PhD student
Norwegian Univ. of Science and Technology (NTNU) and
University of California, Berkeley

A 2D ABAQUS model was used for the analyses

Basic model features

- Solid elements for dam and foundation (with Rayleigh damping)
- Acoustic fluid elements for water in reservoir

The direct FE method (Løkke & Chopra, 2017) implemented for dynamic analyses

- Viscous damper absorbing boundaries at: (1) upstream reservoir boundary, (2) bottom and sides of foundation
- Seismic input applied as effective earthquake forces to bottom *and sides* of foundation domain

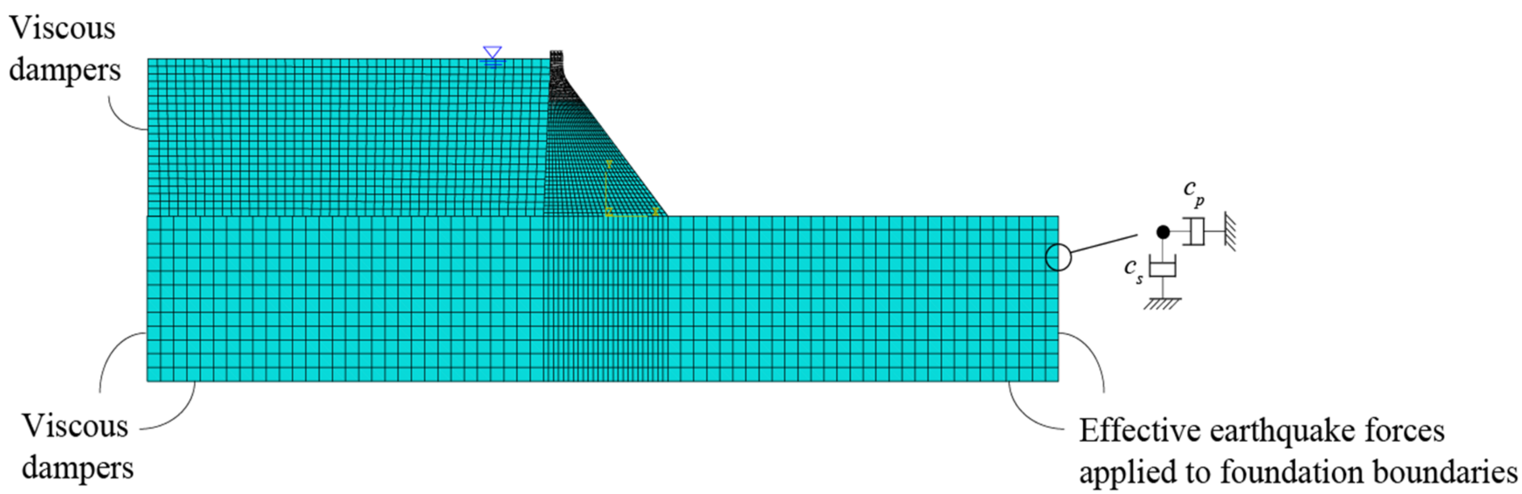

DRAFT – Not for distribution

This presentation addresses two modeling issues

1. Specifying seismic input to the numerical model

2. Calibration of damping values

The full set of analysis results will not be presented (can be found in the workshop proceedings)

This presentation addresses two modeling issues

1. Specifying seismic input to the numerical model

2. Calibration of damping values

The full set of analysis results will not be presented (can be found in the workshop proceedings)

DRAFT – Not for distribution

The direct FE method uses a three-step process to apply the seismic input

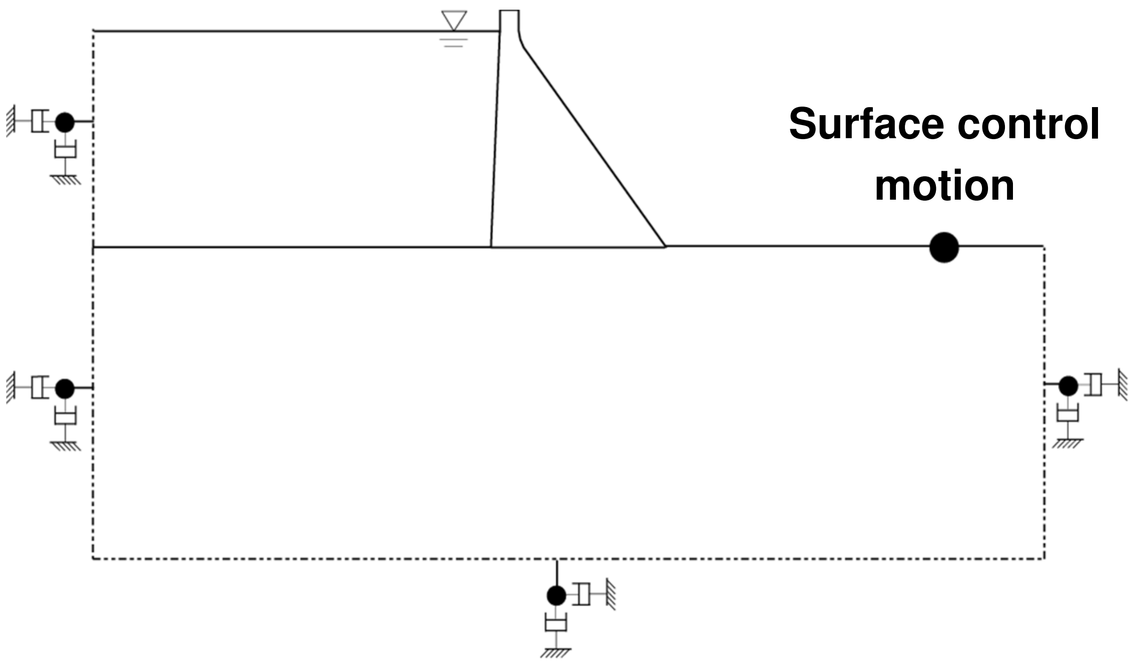

DRAFT – Not for distribution

The direct FE method uses a three-step process to apply the seismic input

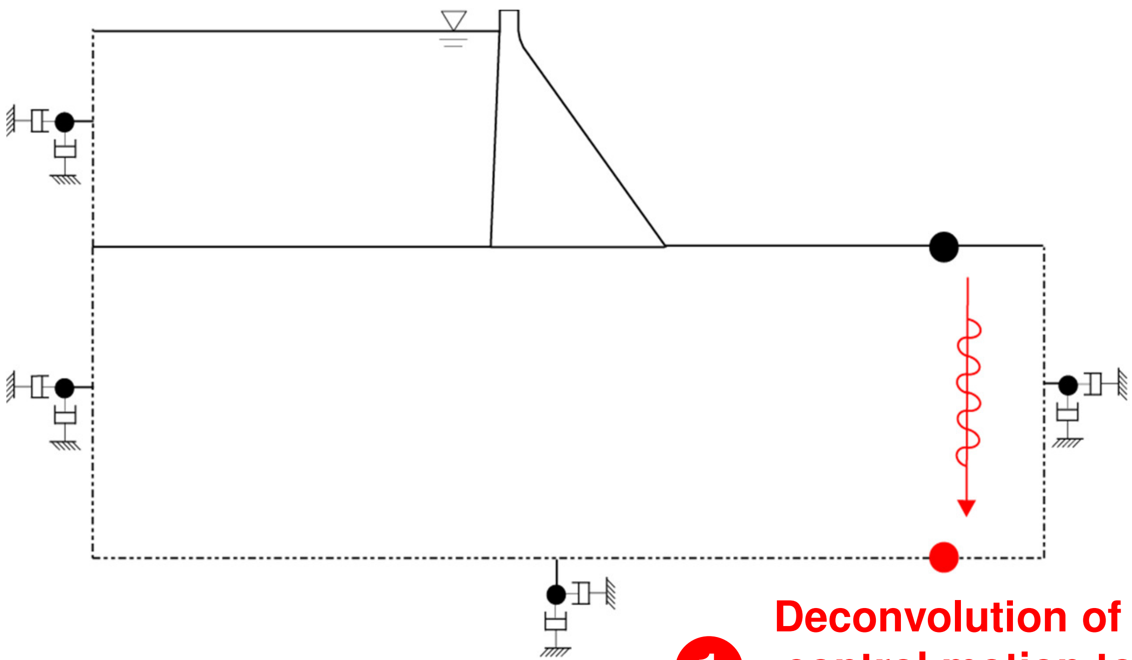

1 Deconvolution of surface control motion to obtain forces at bottom boundary

DRAFT – Not for distribution

The direct FE method uses a three-step process to apply the seismic input

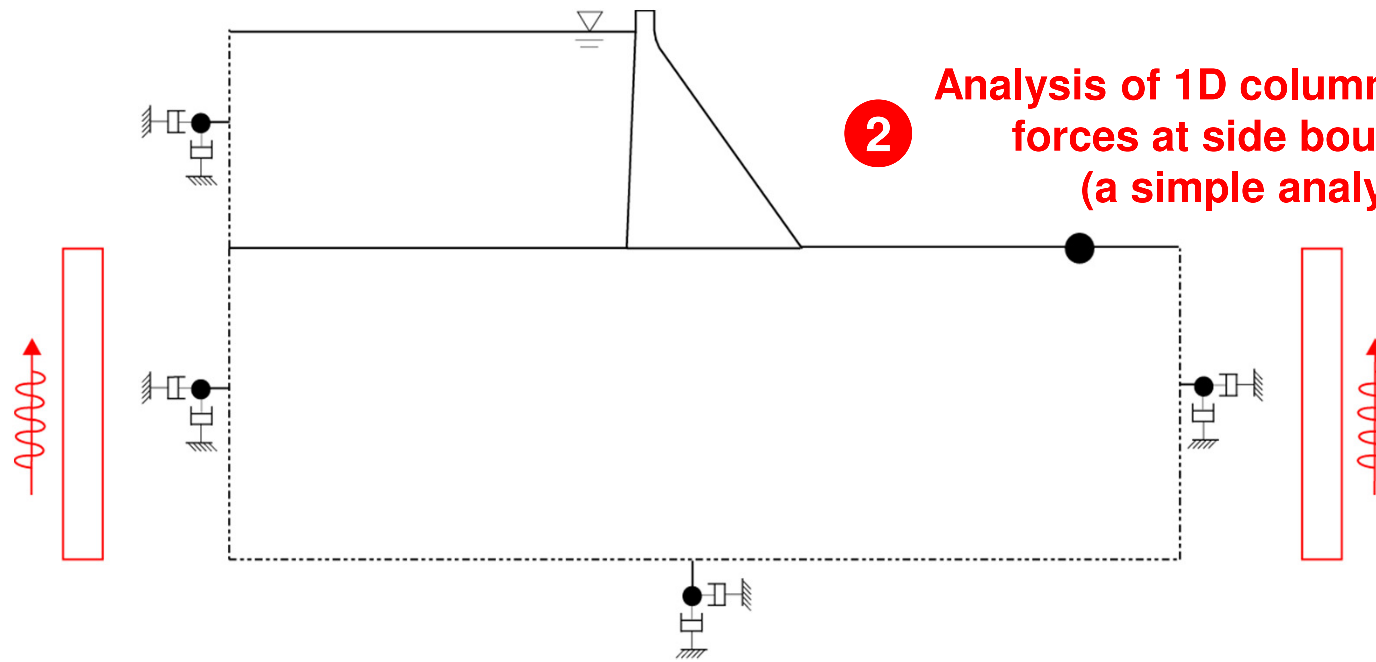

2 Analysis of 1D columns to obtain forces at side boundaries (a simple analysis)

DRAFT – Not for distribution

The direct FE method uses a three-step process to apply the seismic input

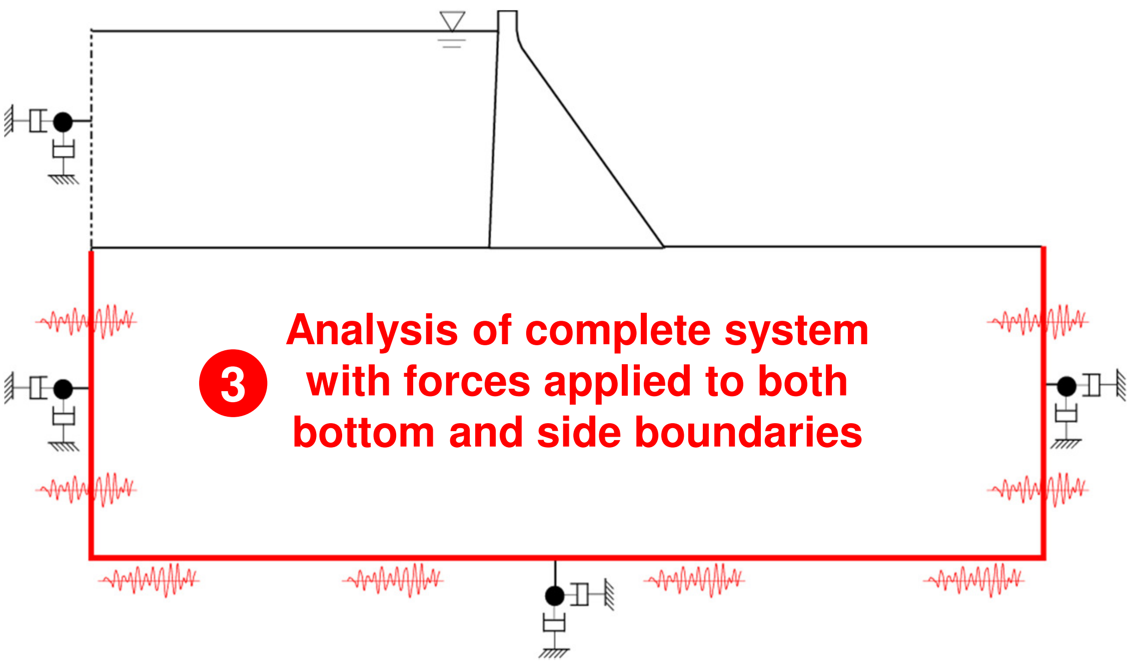

DRAFT – Not for distribution

The direct FE method uses a three-step process to apply the seismic input

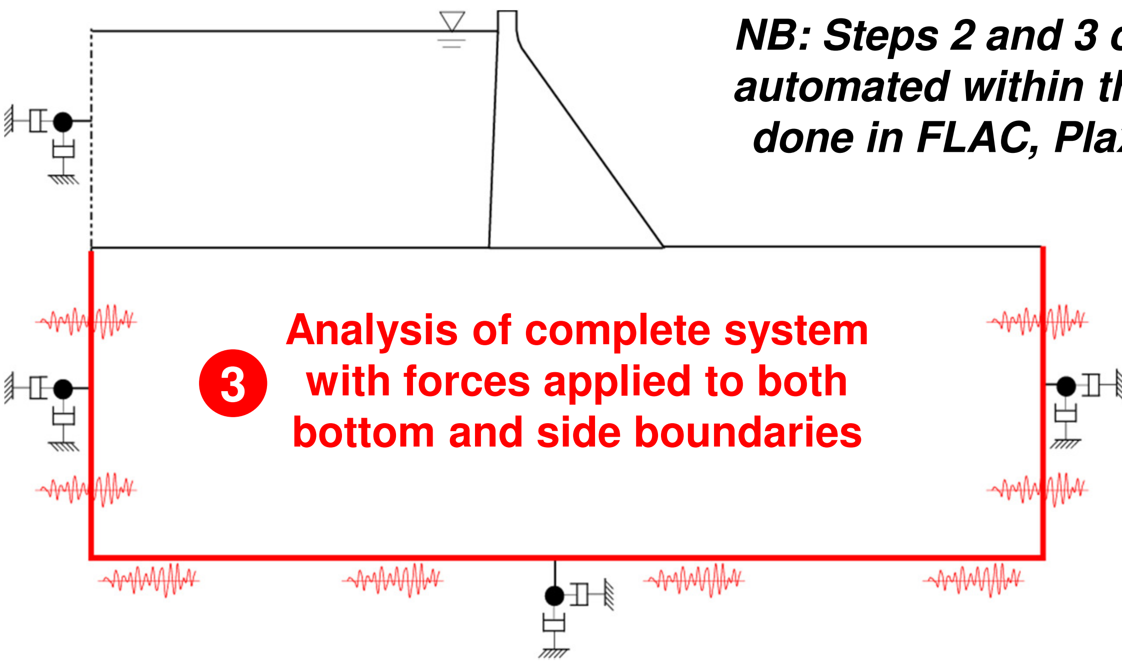

NB: Steps 2 and 3 can easily be automated within the FE code, as is done in FLAC, Plaxis, Code_Aster

DRAFT – Not for distribution

In dam engineering practice, forces on the side boundaries are often ignored

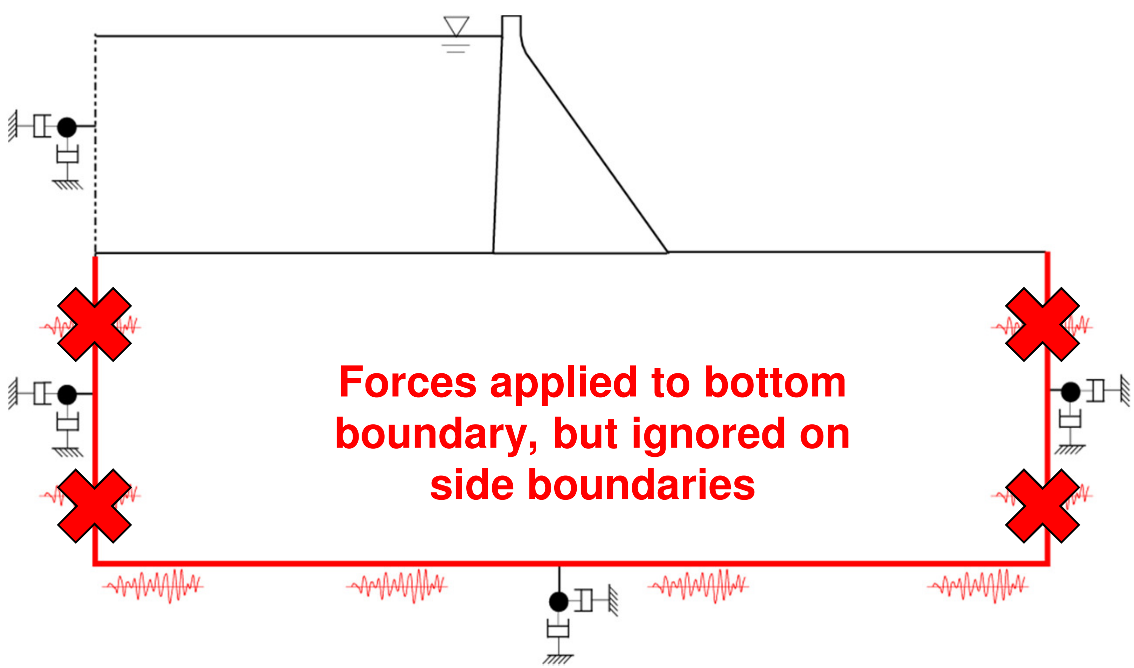

Attractive because it avoids special treatment of side boundaries, but can result in significant error

DRAFT – Not for distribution

Results for flat foundation box

Case B in workshop

Surface motion sampled at five locations

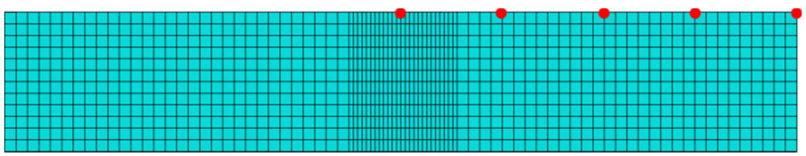

With forces on side boundaries

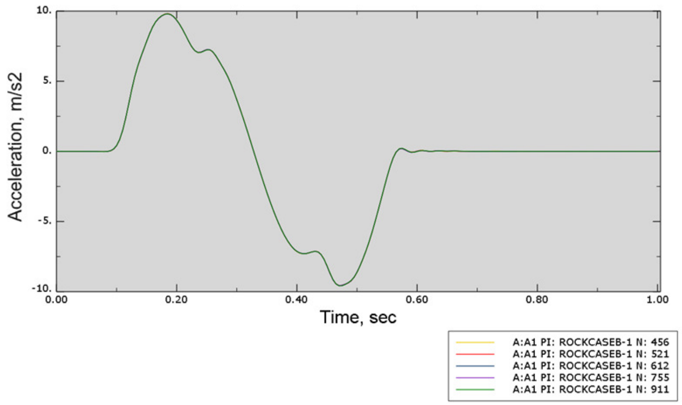

Without forces on side boundaries

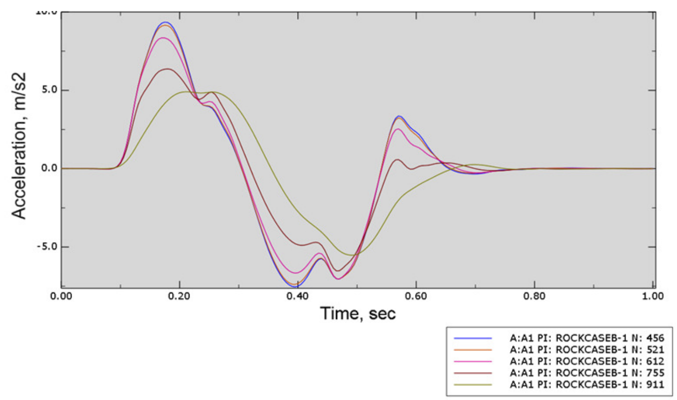

Observations:

- When including forces on side boundaries, the response is “exact” at all nodes
- When ignoring forces on the side boundaries, significant error arises, and varies over the width of the foundation

DRAFT – Not for distribution

Results for dam response confirms observations

Case D1 in workshop

Pine Flat Dam: frequency response function

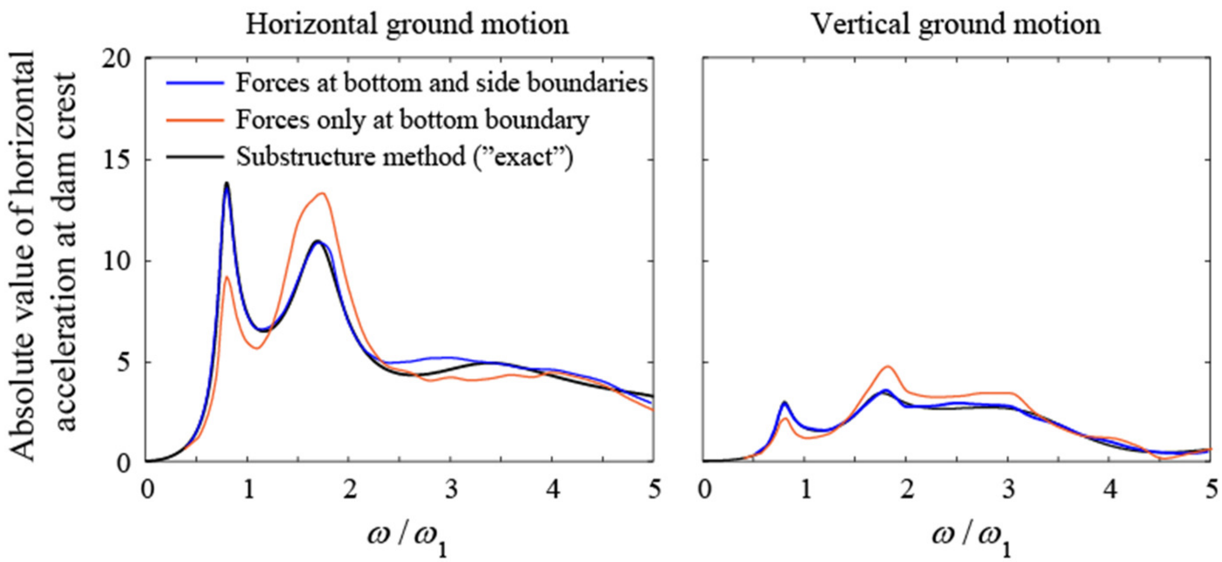

- **Significant error when ignoring forces on side boundaries**
- **It is possible to improve results by (a) iterative frequency scaling of input motion or (b) using a very wide foundation model…**
- **… but why ignore forces on side boundaries in the first place when they can be included with minimal effort?**

DRAFT – Not for distribution

Agenda

1. Specifying seismic input to the numerical model

2. Calibration of damping values

DRAFT – Not for distribution

The selection of damping values has significant influence on the dam response

Example from case D2 in workshop

- Model 1: 5% material damping in dam and 5% in rock (workshop parameters)
- Model 2: 1% material damping in dam and 1% in rock
- All other parameters remain unchanged

Changing the damping leads to noticeable changes in the dam response:

- Peak crest acceleration increases by 16%
- Max. vertical stress at heel increases by 25%
- Max. principal stress at neck increases by 26%

Which result (if any) is the most realistic one?

DRAFT – Not for distribution

Material damping is only one part of the total damping in the system

Three mechanisms for (linear) damping in the numerical model:

- Material damping in dam and rock
- Radiation damping in the semi-unbounded domains (fluid and foundation)
- Dissipation of hydrodynamic pressure waves at reservoir bottom

DRAFT – Not for distribution

Material damping is only one part of the total damping in the system

Three mechanisms for (linear) damping in the numerical model:

- Material damping in dam and rock
- Radiation damping in the semi-unbounded domains (fluid and foundation)
- Dissipation of hydrodynamic pressure waves at reservoir bottom

Using half-power bandwidth method, the total damping in the 2D model was found to be

- 12% when using 5% material damping
- 8% when using 1% material damping

DRAFT – Not for distribution

Material damping is only one part of the total damping in the system

Three mechanisms for (linear) damping in the numerical model:

- Material damping in dam and rock
- Radiation damping in the semi-unbounded domains (fluid and foundation)
- Dissipation of hydrodynamic pressure waves at reservoir bottom

Using half-power bandwidth method, the total damping in the 2D model was found to be

- 12% when using 5% material damping
- 8% when using 1% material damping

High overall damping stems from large contribution from radiation damping

- Very prominent for 2D gravity dam models
- Much less prominent for 3D models

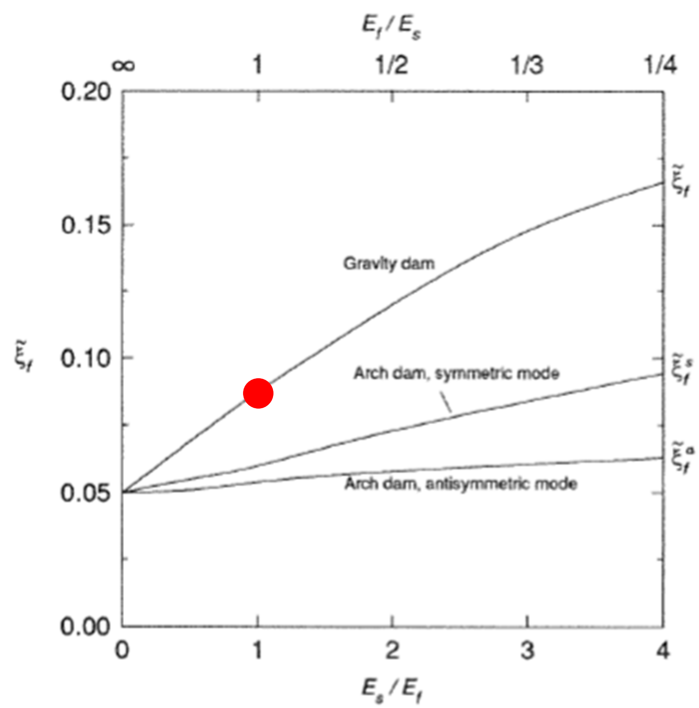

From Han and Chopra (1996)

DRAFT – Not for distribution

Damping measured at 32 concrete dams suggests a maximum of 5% total damping in the system

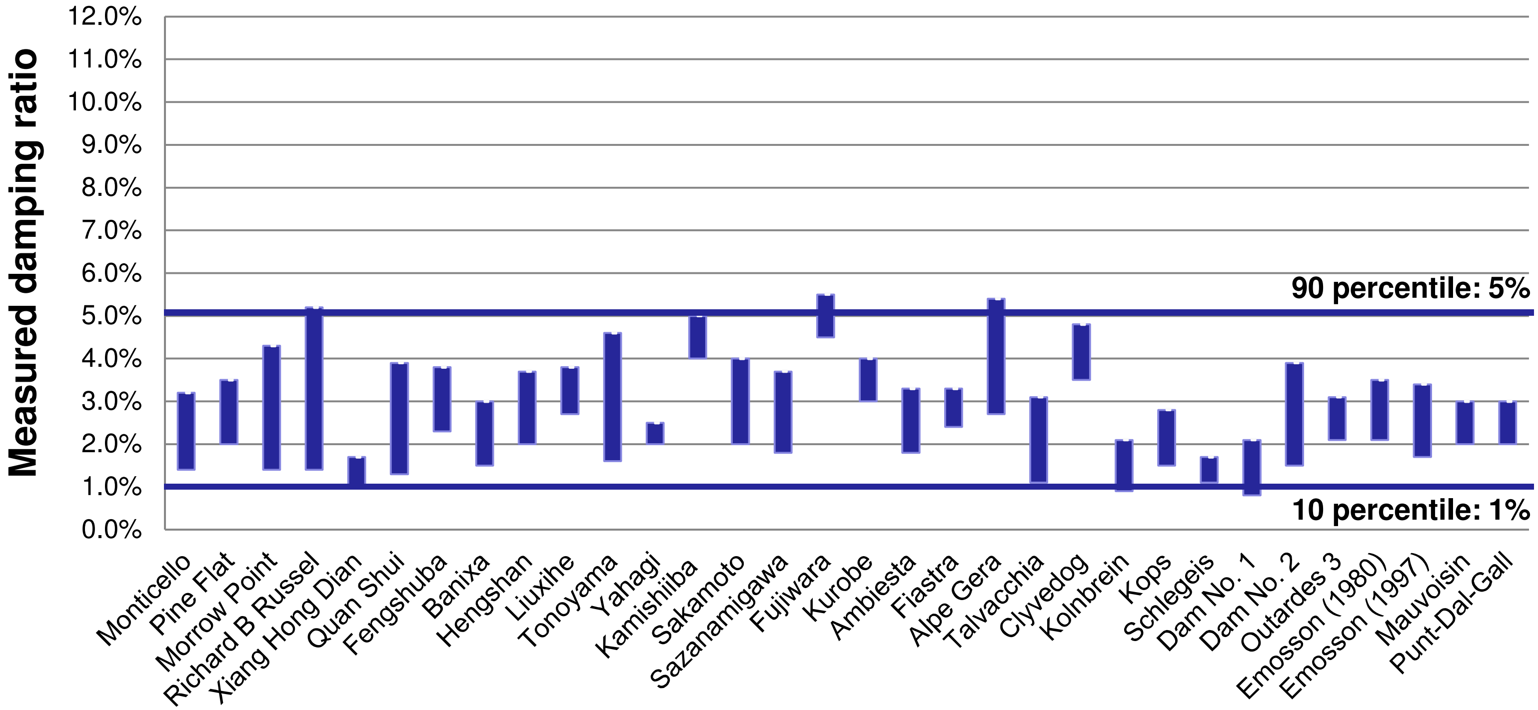

- Obtained by forced vibration tests and ambient vibration measurements
- Results reflect the *total* damping in the dam-water-foundation system

Damping measured at 32 concrete dams suggests a maximum of 5% total damping in the system

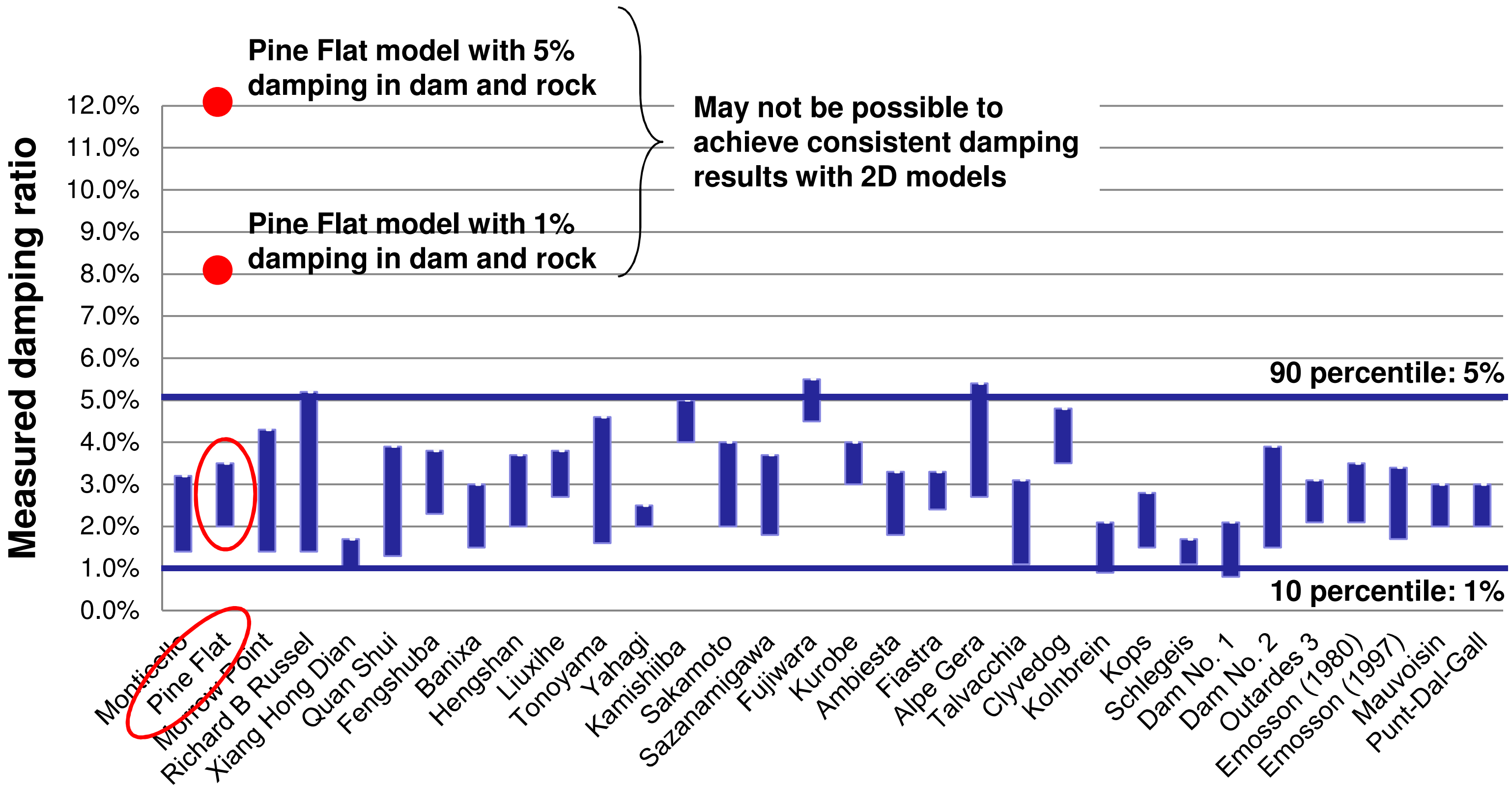

- Obtained by forced vibration tests and ambient vibration measurements
- Results reflect the *total* damping in the dam-water-foundation system

Final remarks

Available data suggests limiting damping to no more than 5% *total* damping in dam-water-foundation systems (unless there is data to justify higher damping)

- Damping in the range of 1-2% for the dam and 1-4% for the rock are likely to satisfy this condition for 3D models, may be difficult for 2D models
- In contrast, “blindly” specifying 5% damping in the dam and rock is likely to significantly overestimate the total damping in the system

Because damping cannot be specified with confidence, these parameters should always be varied to test the sensitivity of the dam response to the selected values

DRAFT – Not for distribution

Questions?

DRAFT – Not for distribution

Thank you for your attention!

Arnkjell Løkke
Department of Structural Engineering
NTNU

Contact:
E-mail: *arnkjell.lokke@ntnu.no*
Phone: *+47 48 04 88 43*

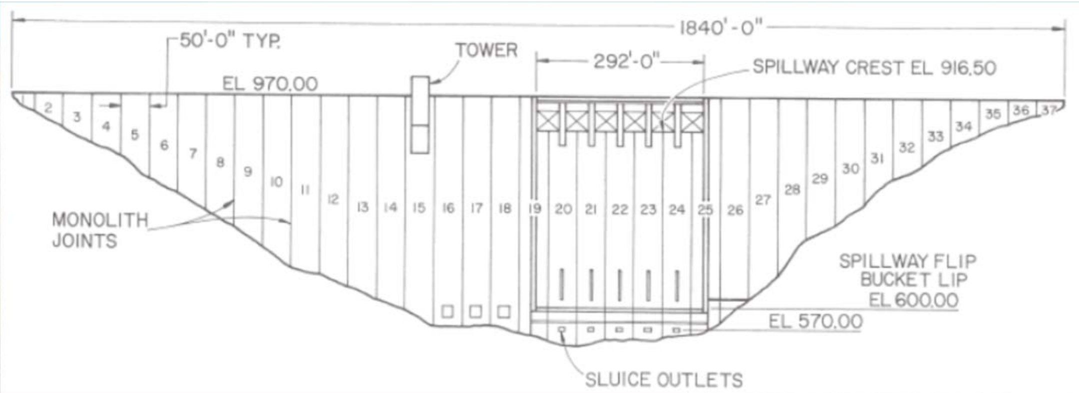

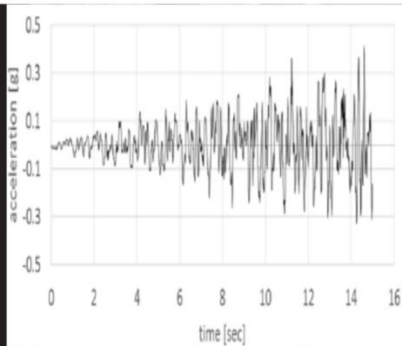

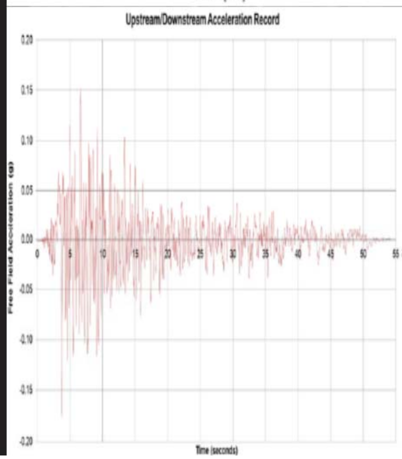

Stantec

RESULTS & DISCUSSION
JUAN E. QUIROZ, Ph.D., P.E.

USSD WORKSHOP

Evaluation of Numerical Models and Input Parameters in the Analysis of Concrete Dams

ANALYSIS METHOD

METHOD & APPROACH

- ABAQUS software
  - Consistent model
  - Mesh
  - Boundaries
  - Size
  - Loads

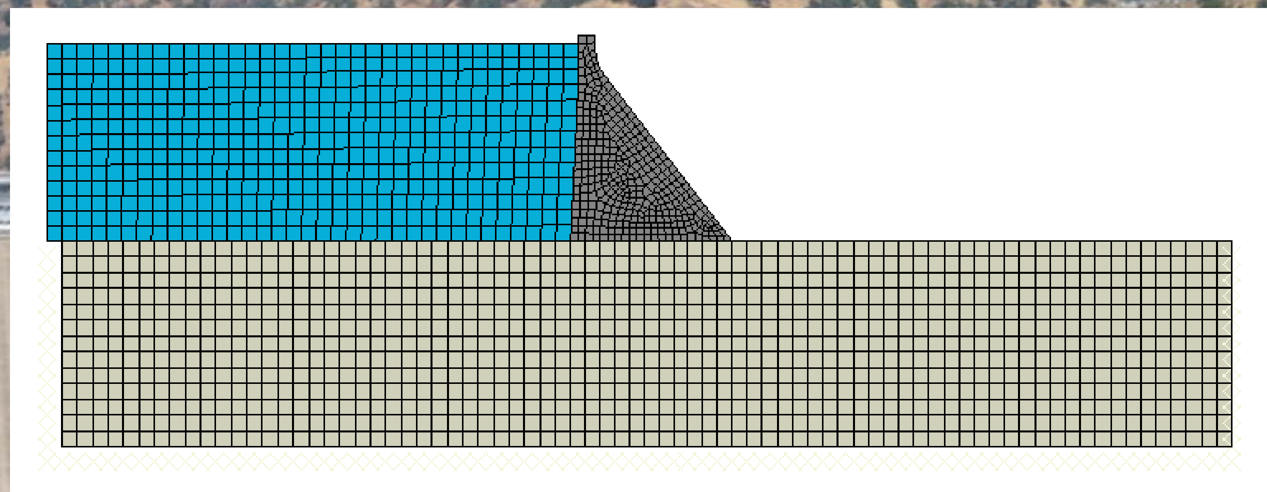

- Implicit coupled acoustic-structural direct integration analysis approach

RESERVOIR

- Reservoir → acoustic elements
  - Inviscid.
  - Compressible.
  - Bulk modulus relates the dynamic pressure in the medium to the volumetric strain.
  - Efficient 1 d.o.f. for pressure waves
  - Impedance boundary conditions representing absorbing surfaces or radiation to an infinite exterior.

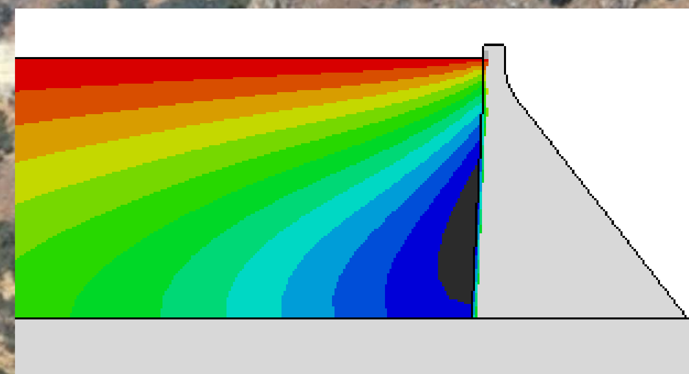

DAMPING

Rayleigh Coefficients

To adjust to two given frequencies [Hz]:

$w1 := 2$ $w2 := 6$ $\xi 2 := 5\%$

$$\alpha_o := \frac{2 \cdot \xi 2 \cdot w1 \cdot w2}{w1 + w2} \cdot 2 \cdot \pi \qquad \alpha_o = 0.9425$$

$$\beta_o := \frac{2 \cdot \xi 2}{w1 + w2} \cdot \frac{1}{2 \cdot \pi} \qquad \beta_o = 0.002$$

$$\xi(\alpha, \beta, w) := \frac{\alpha}{2 \cdot w \cdot 2 \cdot \pi} + \frac{\beta \cdot w \cdot 2 \cdot \pi}{2}$$

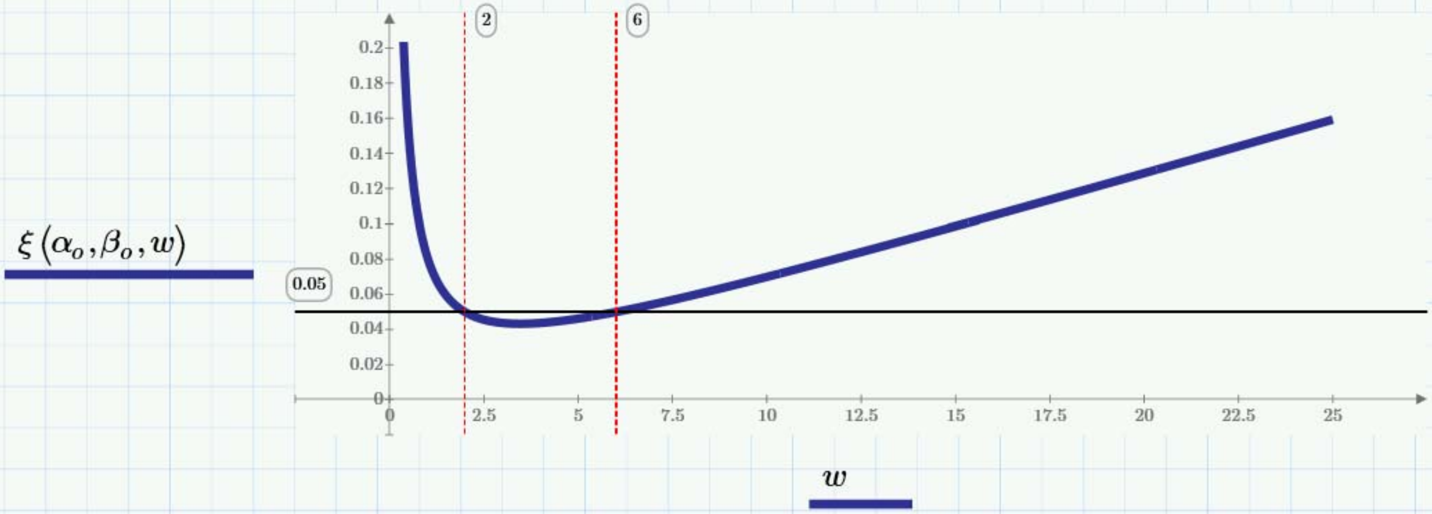

SOIL-STRUCTURE INTERACTION

- Seismic wave propagation requirements:
  - Foundation with mass
  - Motion Deconvolution
  - Radiation Damping

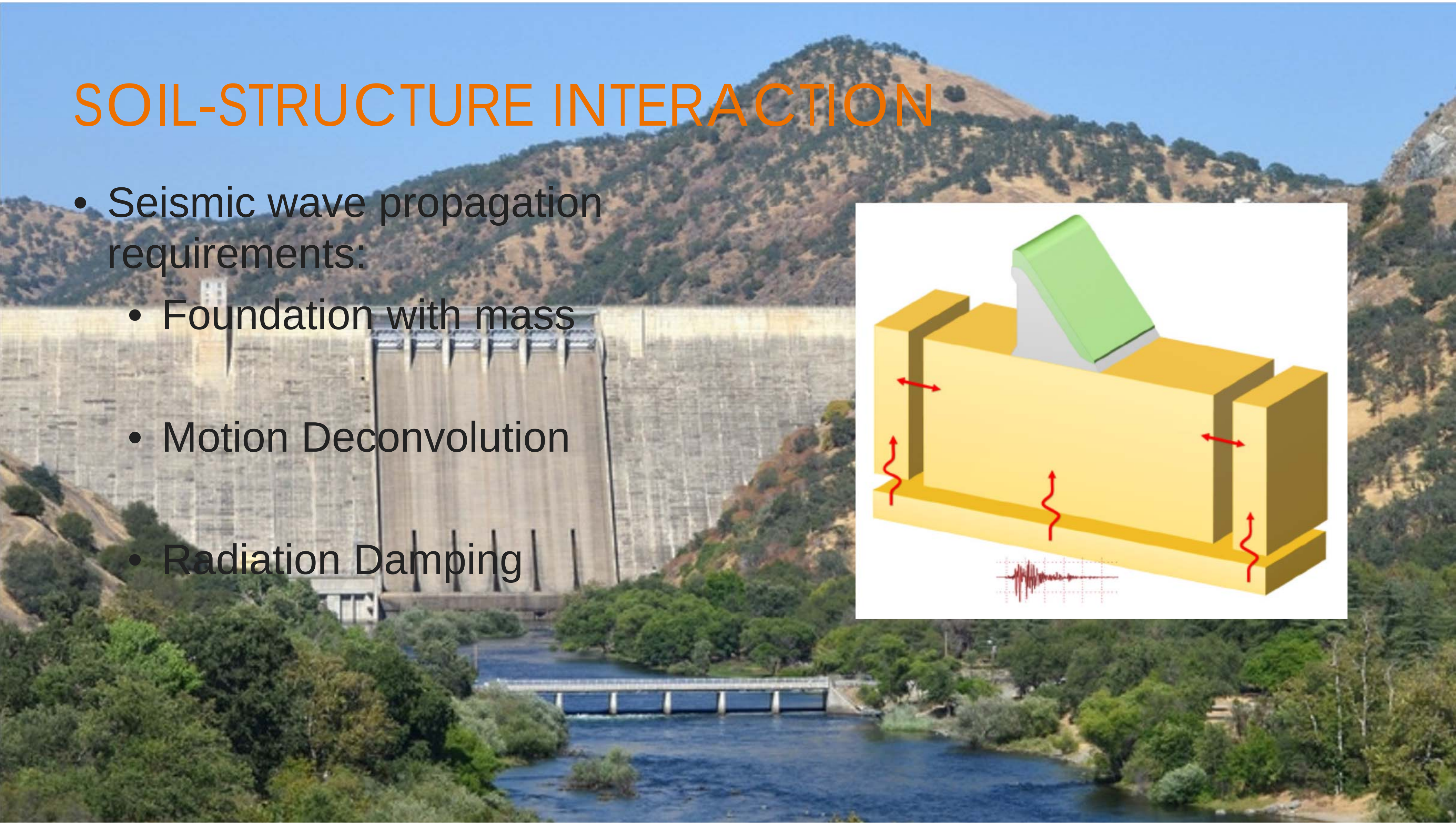

SOIL-STRUCTURE INTERACTION

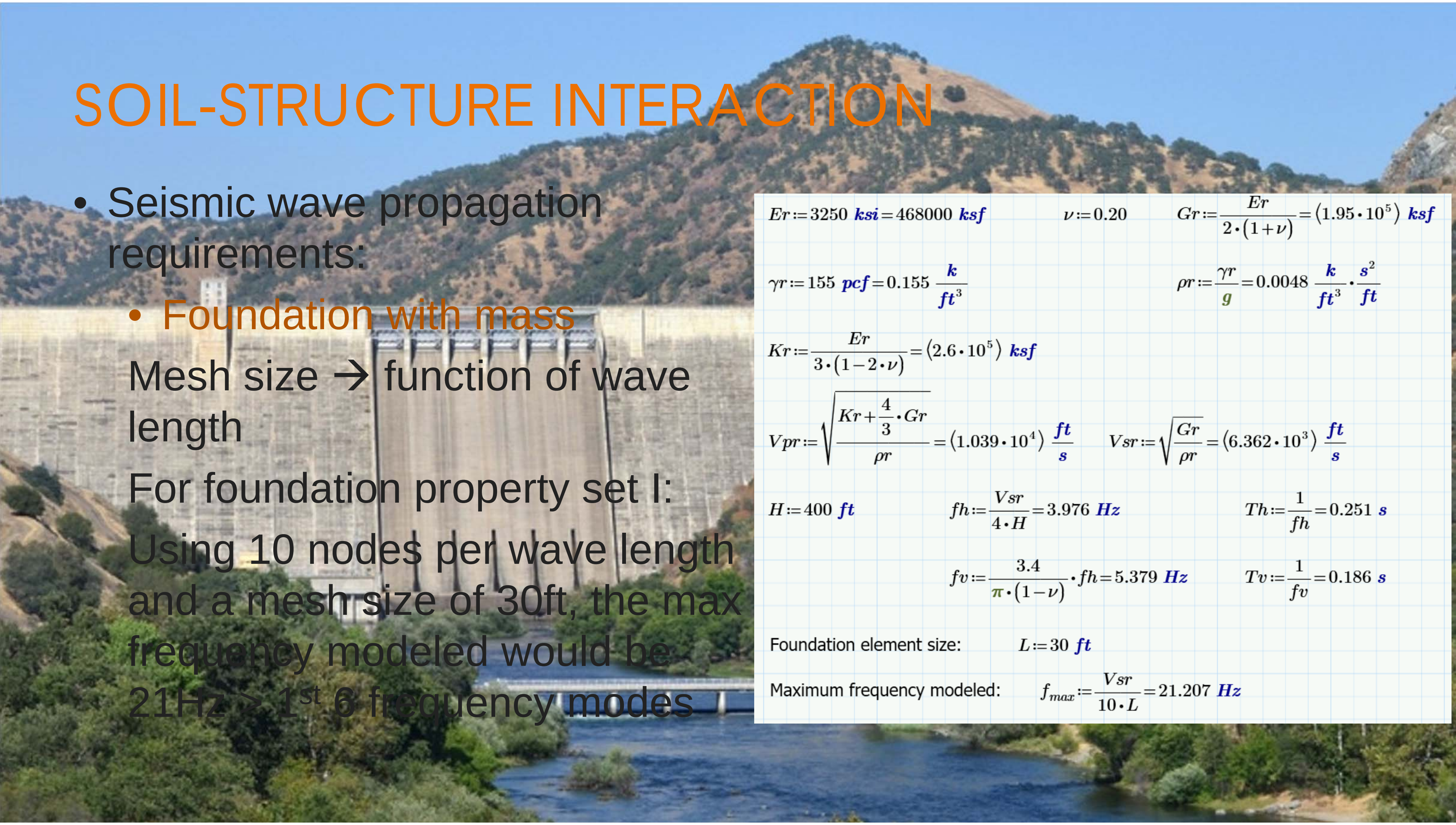

- Seismic wave propagation requirements:
  - Foundation with mass

  Mesh size → function of wave length

  For foundation property set I:

  Using 10 nodes per wave length and a mesh size of 30ft, the max frequency modeled would be 21Hz > 1st 6 frequency modes

$$Er := 3250\ ksi = 468000\ ksf \qquad \nu := 0.20 \qquad Gr := \frac{Er}{2\cdot(1+\nu)} = (1.95\cdot 10^5)\ ksf$$

$$\gamma r := 155\ pcf = 0.155\ \frac{k}{ft^3} \qquad \rho r := \frac{\gamma r}{g} = 0.0048\ \frac{k}{ft^3}\cdot\frac{s^2}{ft}$$

$$Kr := \frac{Er}{3\cdot(1-2\cdot\nu)} = (2.6\cdot 10^5)\ ksf$$

$$Vpr := \sqrt{\frac{Kr + \frac{4}{3}\cdot Gr}{\rho r}} = (1.039\cdot 10^4)\ \frac{ft}{s} \qquad Vsr := \sqrt{\frac{Gr}{\rho r}} = (6.362\cdot 10^3)\ \frac{ft}{s}$$

$$H := 400\ ft \qquad fh := \frac{Vsr}{4\cdot H} = 3.976\ Hz \qquad Th := \frac{1}{fh} = 0.251\ s$$

$$fv := \frac{3.4}{\pi\cdot(1-\nu)}\cdot fh = 5.379\ Hz \qquad Tv := \frac{1}{fv} = 0.186\ s$$

Foundation element size: $L := 30\ ft$

Maximum frequency modeled: $f_{max} := \frac{Vsr}{10\cdot L} = 21.207\ Hz$

SOIL-STRUCTURE INTERACTION

- Seismic wave propagation requirements:
  - Motion Deconvolution

Can be done on frequency domain or time domain

Performed using FEA time-domain

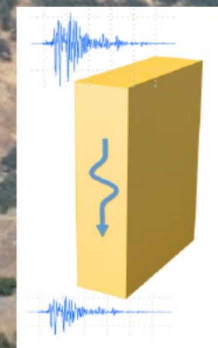

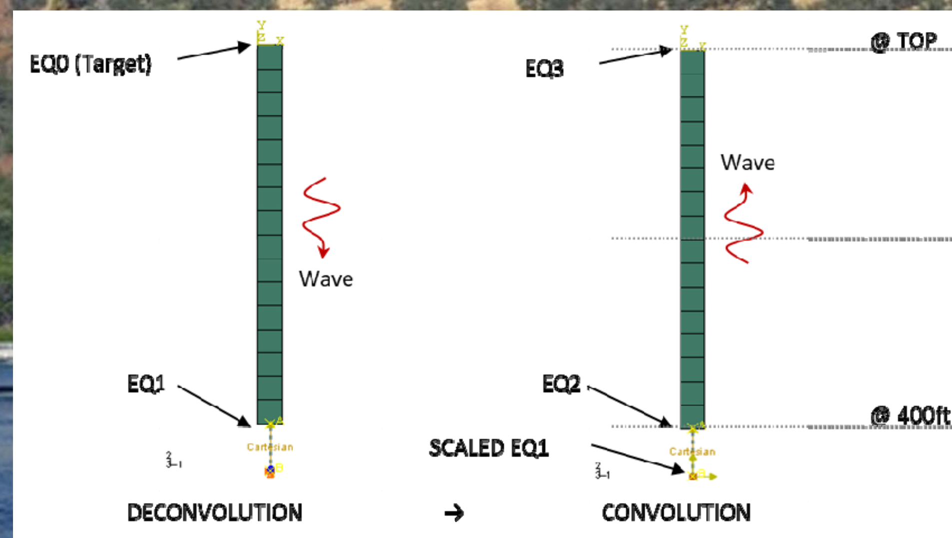

SOIL-STRUCTURE INTERACTION

- Seismic wave propagation requirements:
  - Motion Deconvolution

Recovered motion should match the target free-field at the surface

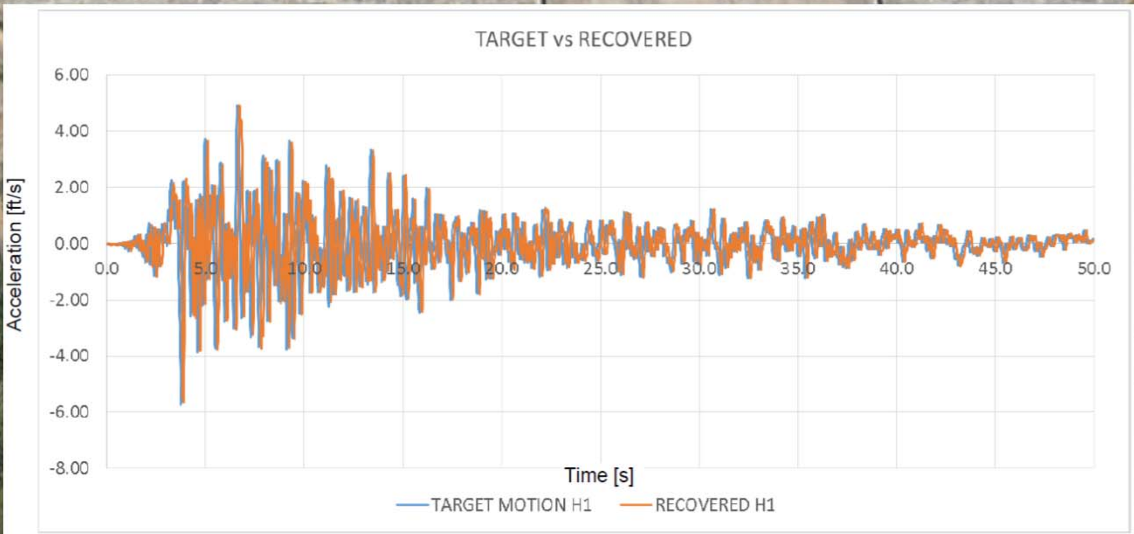

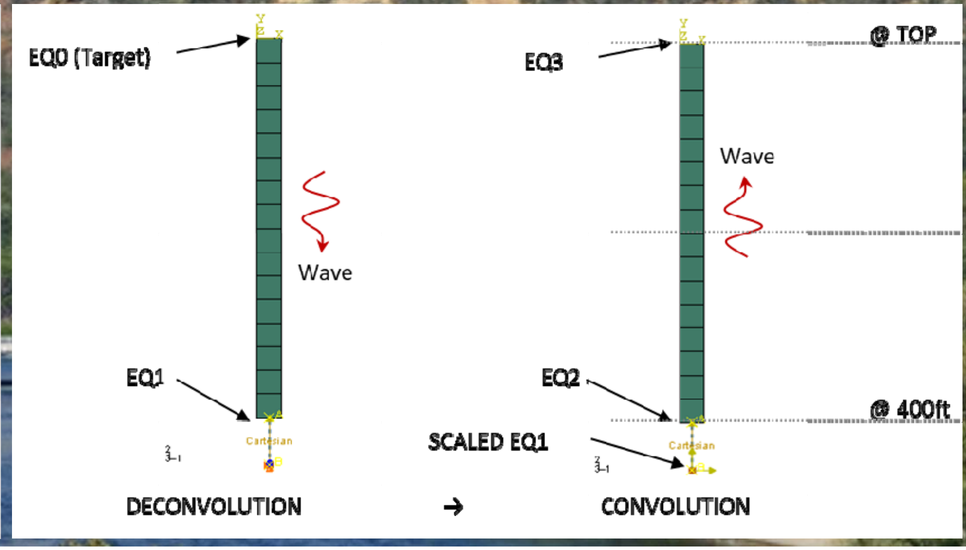

SOIL-STRUCTURE INTERACTION

- Seismic wave propagation requirements:
  - Motion Deconvolution

Recovered motion should match the target free-field at the surface

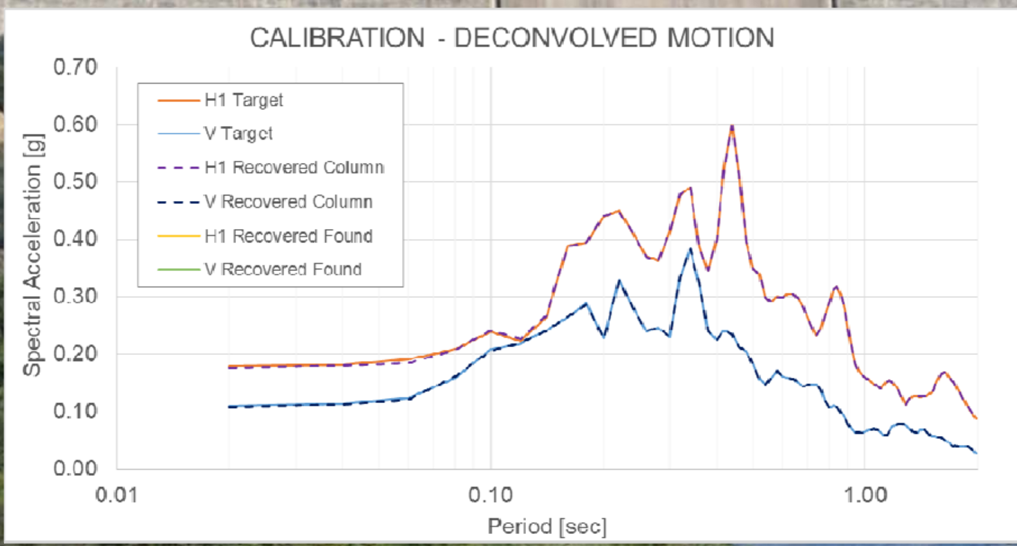

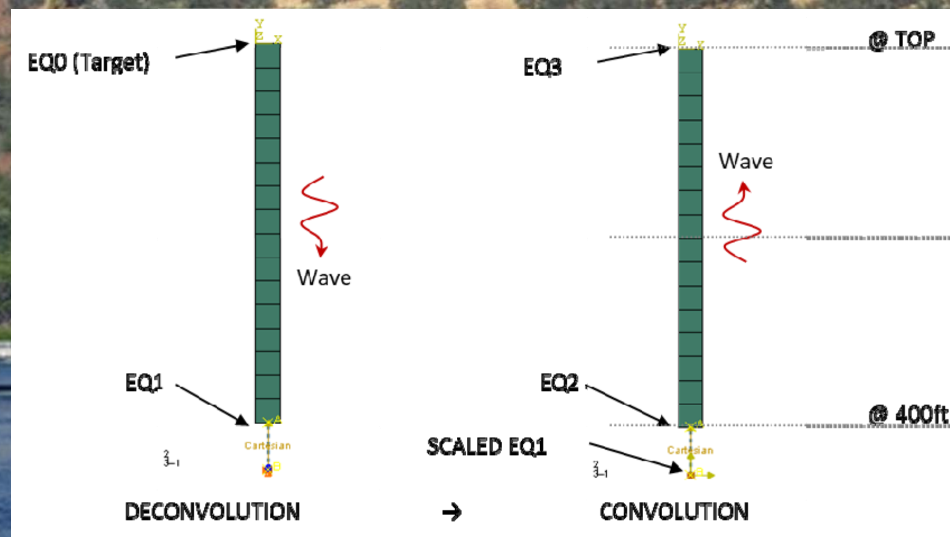

SOIL-STRUCTURE INTERACTION

- Seismic wave propagation requirements:
  - Radiation Damping

  Absorbing Boundary Conditions (ABC)

  Special coded elements 2 behaviors:

  1) Classical viscous component to absorb the radiating waves
  2) Representation of free-field column that propagates the waves from the base to the surface and provides input to the sides of the model.

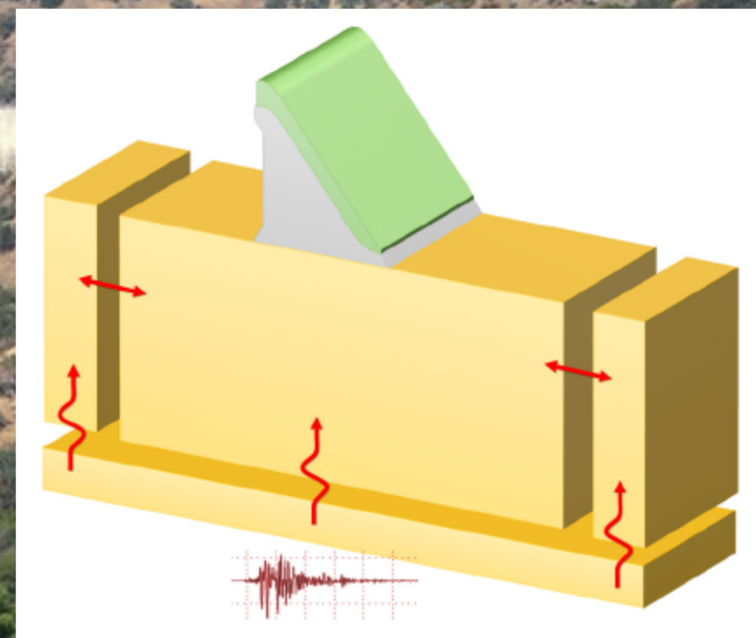

SOIL-STRUCTURE INTERACTION

Absorbing Boundary Conditions (ABC):

Unsymmetric dampers & springs

Off-diagonal terms → unsymmetric matrix storage

Example: P-wave being propagated vertical d.o.f. of the free-field column has an effect on the horizontal d.o.f of the foundation domain

- No need to calibrate any coefficients or include spurious constants as it follows classical elasticity.

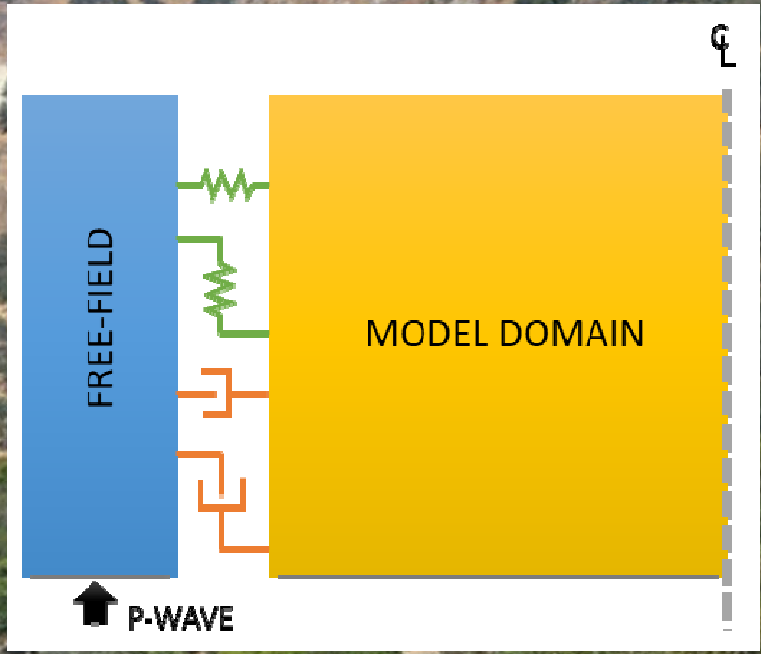

SOIL-STRUCTURE INTERACTION

Wave propagation example

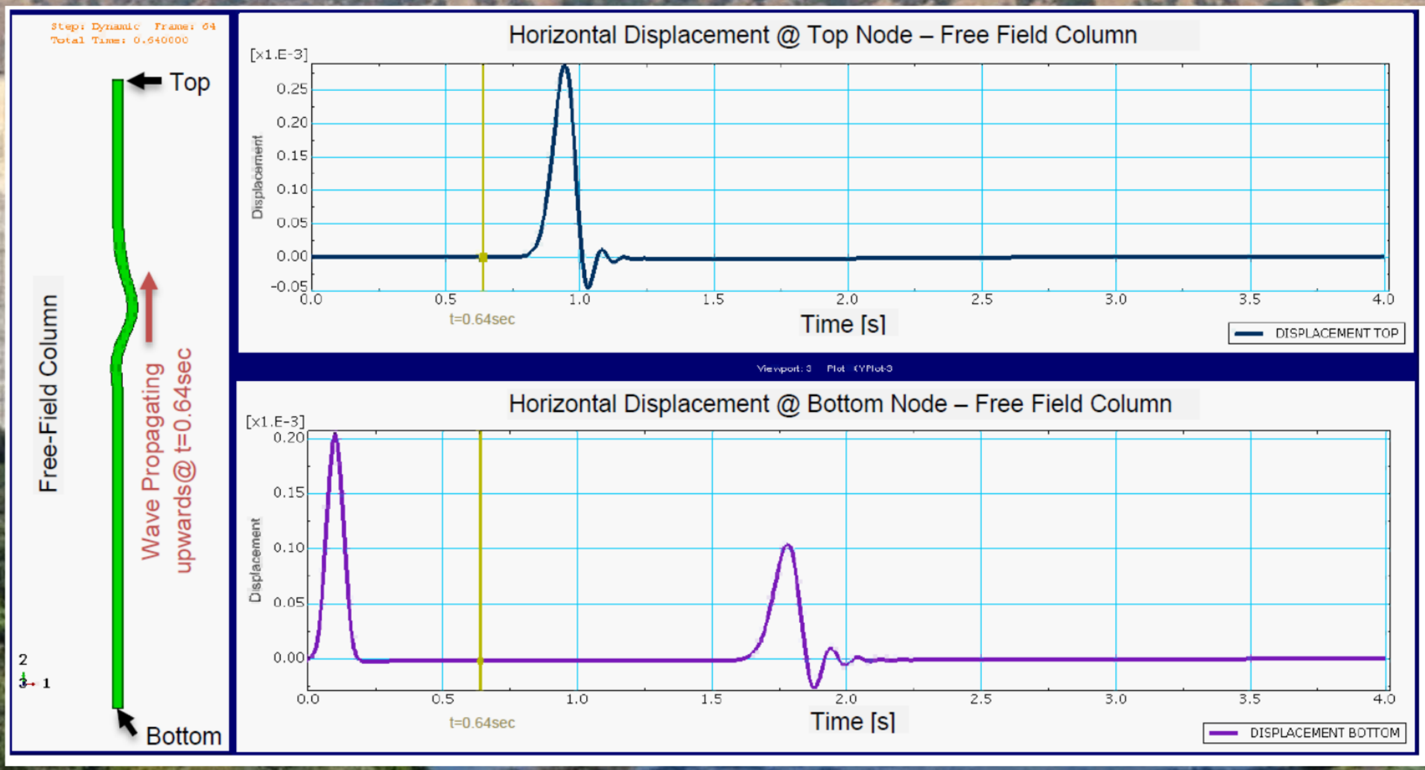

SOIL-STRUCTURE INTERACTION

Wave propagation example

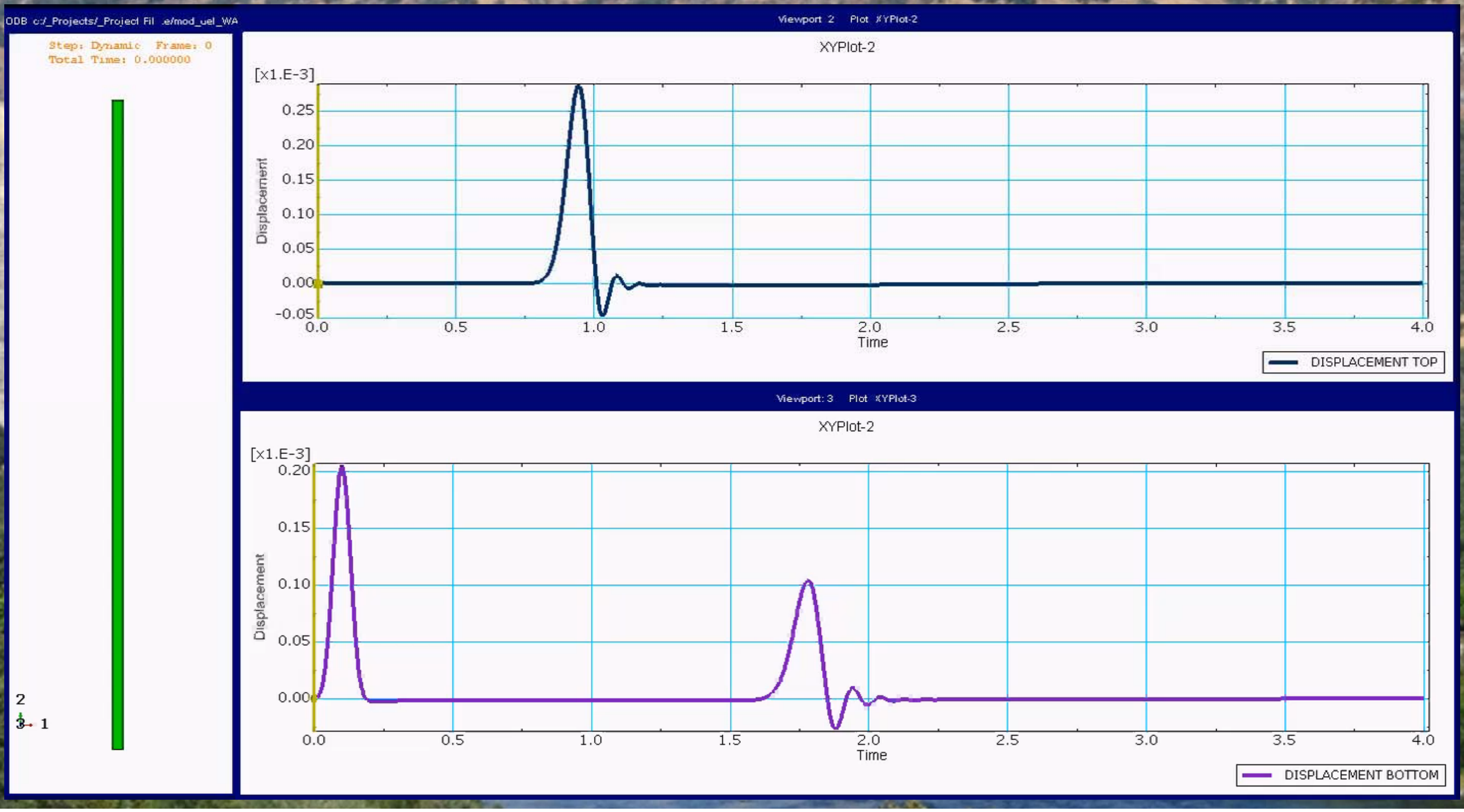

SOIL-STRUCTURE INTERACTION

Wave propagation example

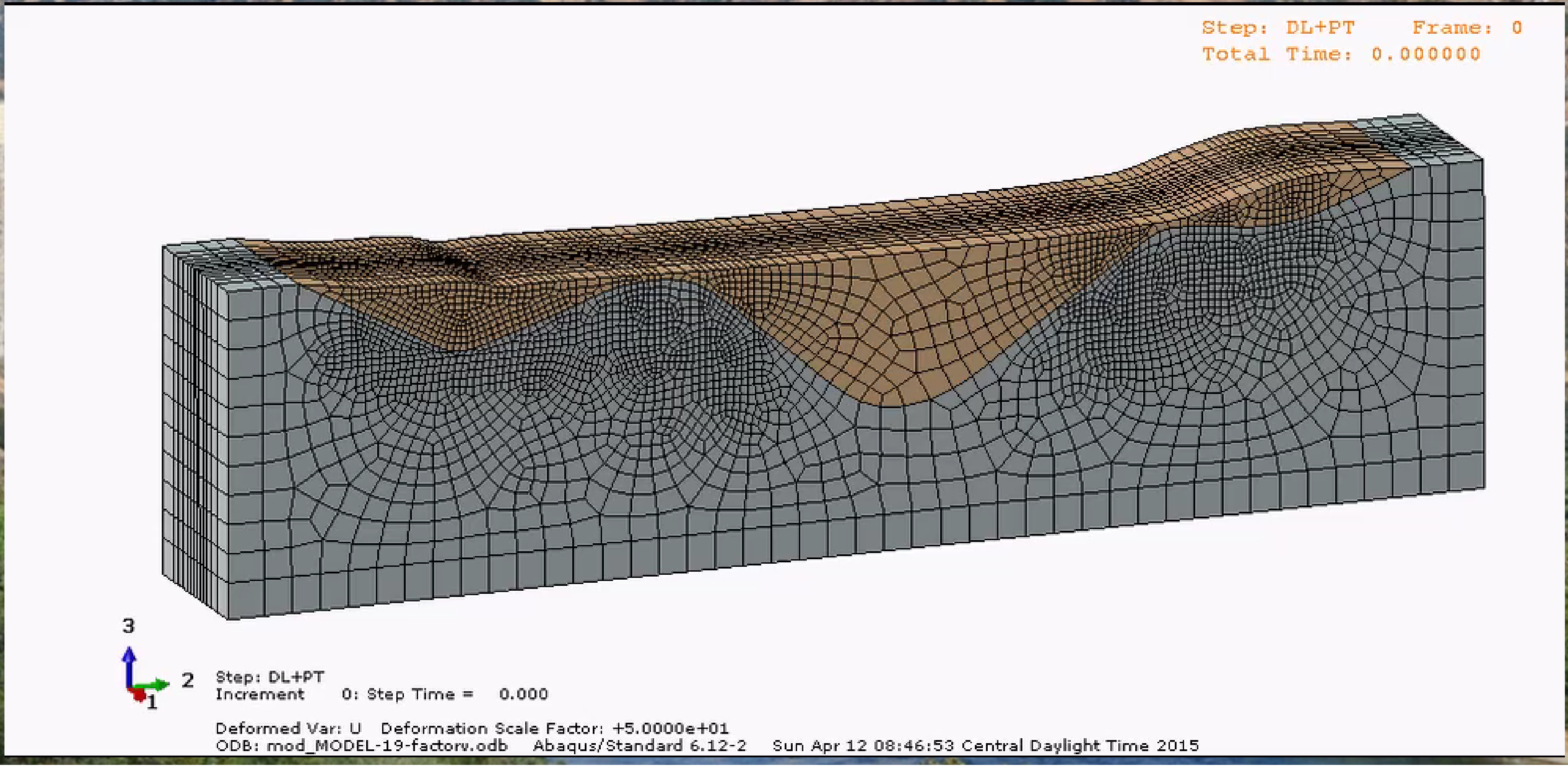

SOIL-STRUCTURE INTERACTION

Wave propagation example (Monticello)

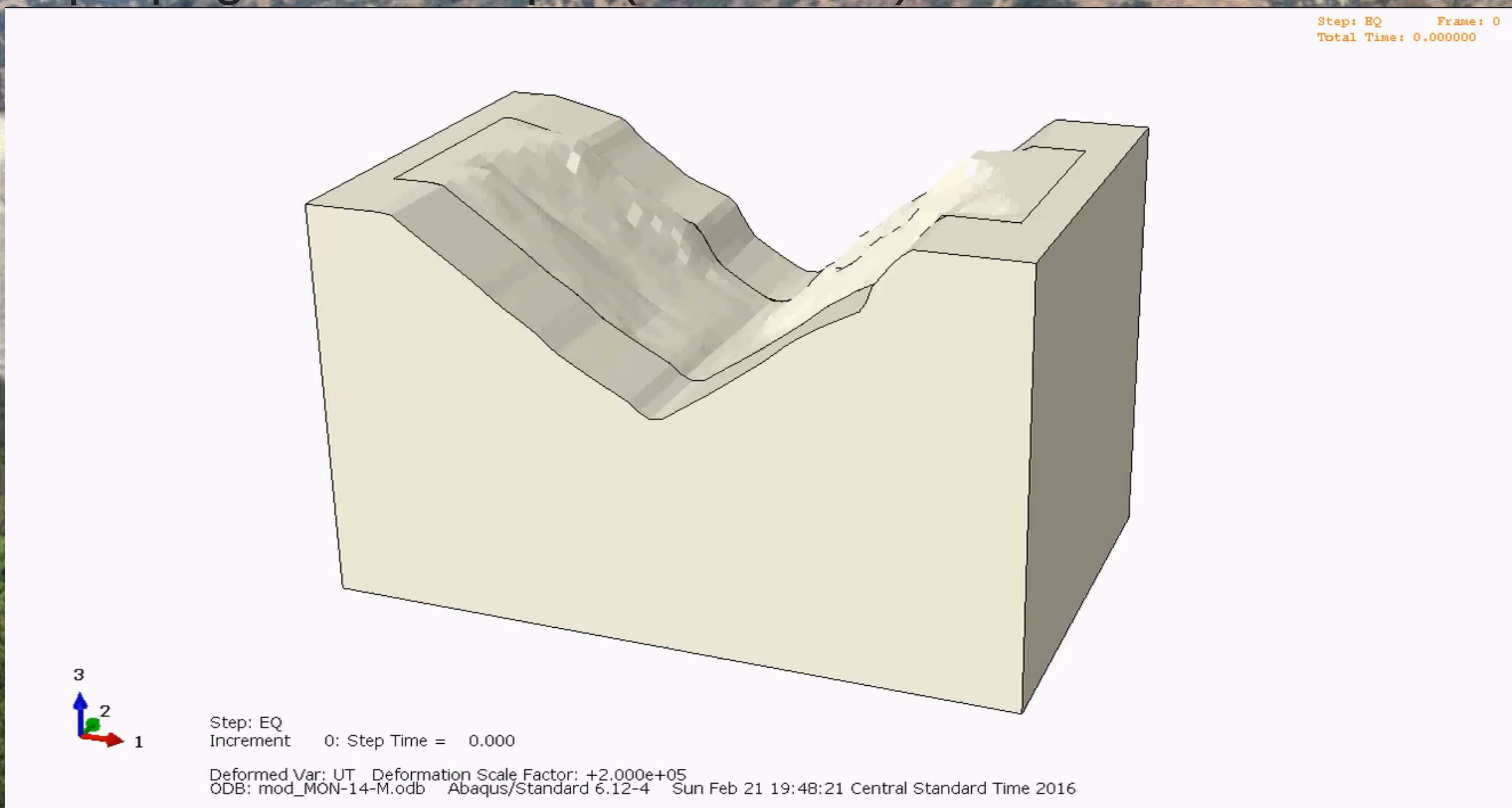

ANALYSIS RESULTS

CASES ANALYZED

Case	Combination						
A	A-1						
B	B-1V	B-1H	B-2V	B-2H			
C	C-1(a)	C-2(a)	C-1(b)	C-2(b)	C-2(c)	-	C-2(d)
D	D-1(a)	D-2(a)	D-1(b)	D-2(b)	D-2(c)		
E	E-1(a)	E-2(a)	E-1(b)	E-2(b)	E-2(c)		

FE MODEL

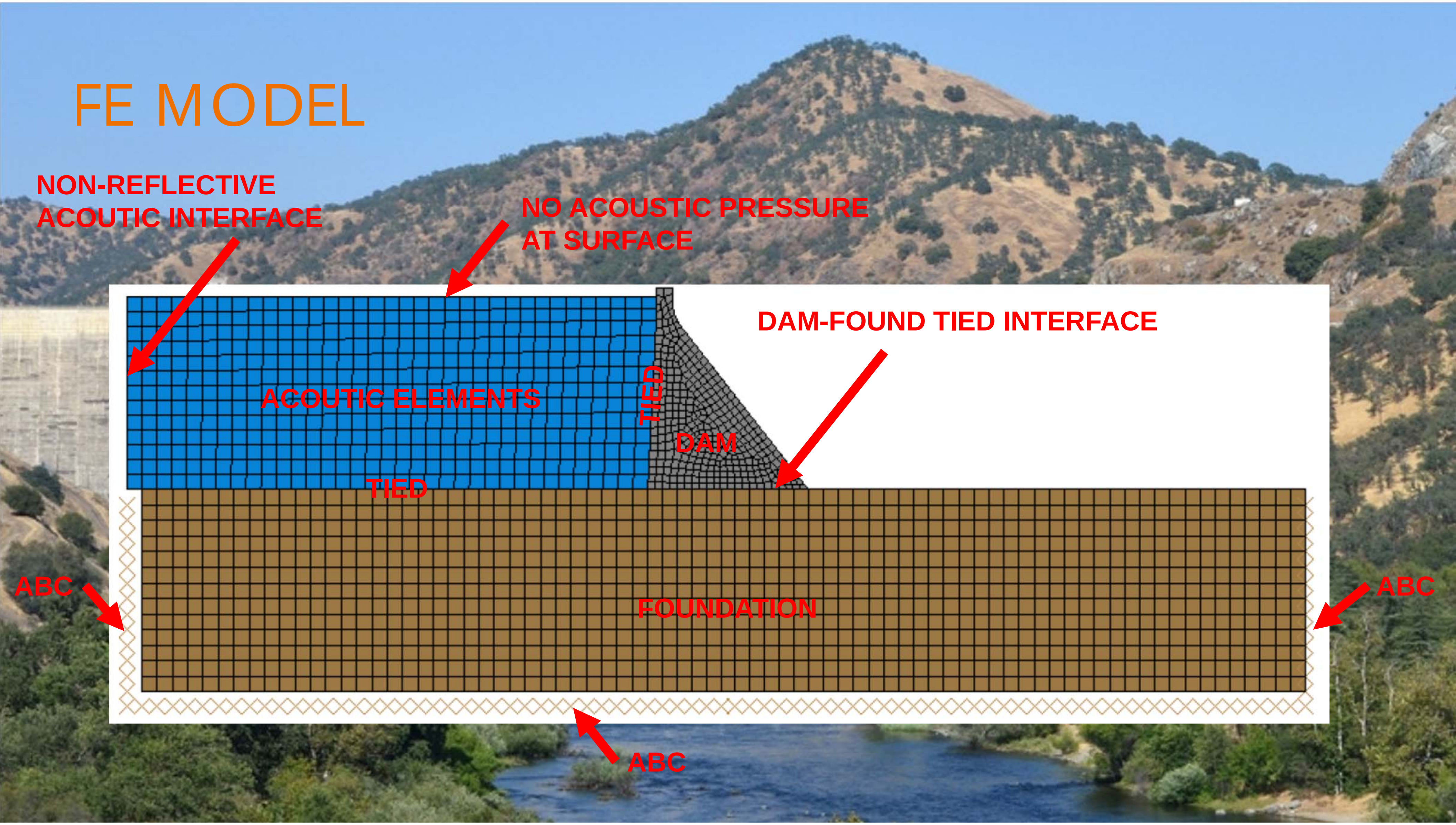

NON-REFLECTIVE
ACOUTIC INTERFACE
NO ACOUSTIC PRESSURE
AT SURFACE
DAM-FOUND TIED INTERFACE
ACOUTIC ELEMENTS
TIED
DAM
TIED
ABC
FOUNDATION
ABC
ABC

FOUNDATION ONLY ANALYSIS – CASE B

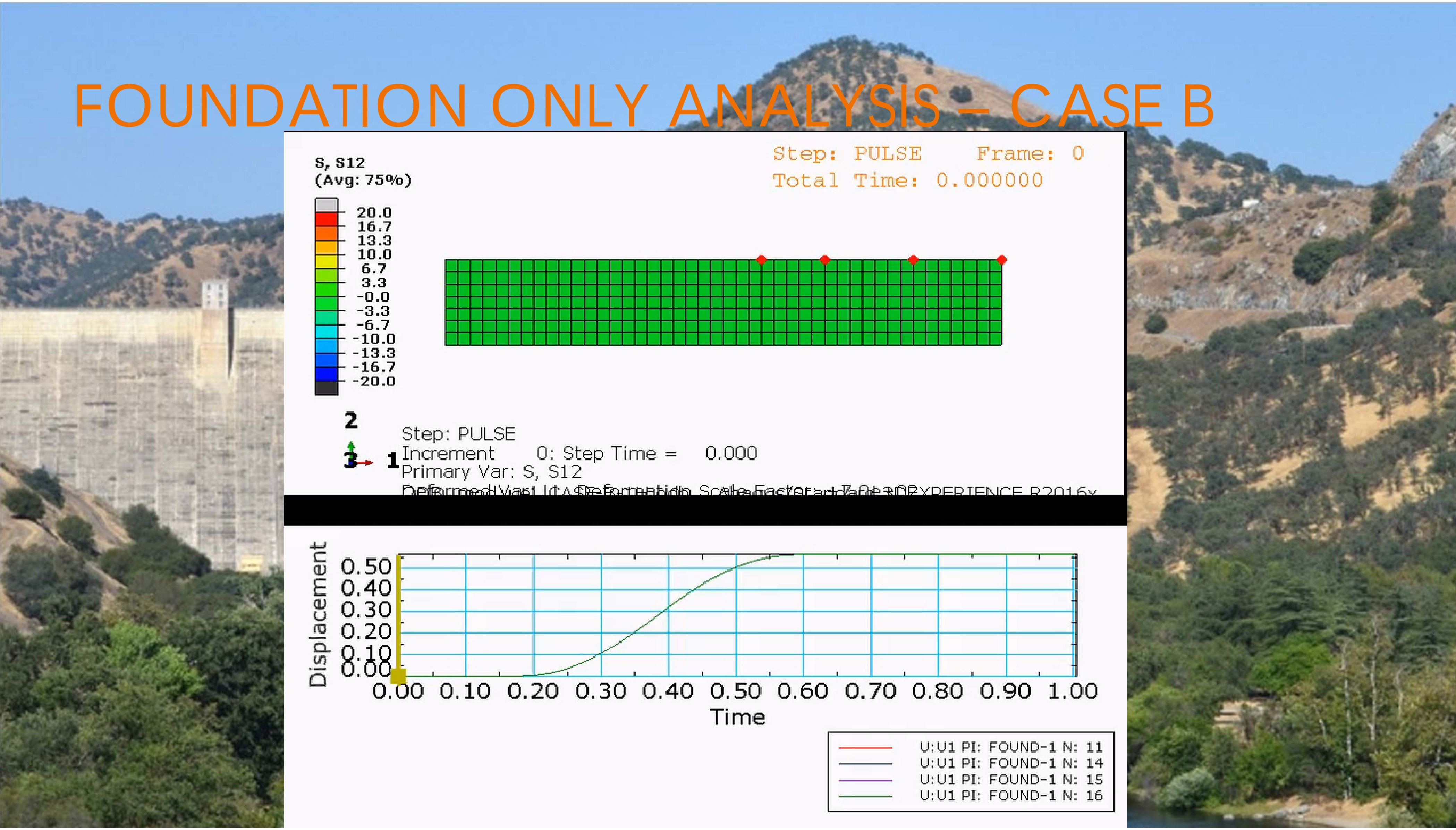

FREQUECY CASE D2

- MODE 1 = 2.1Hz
- FOUND MODE = 3.7Hz

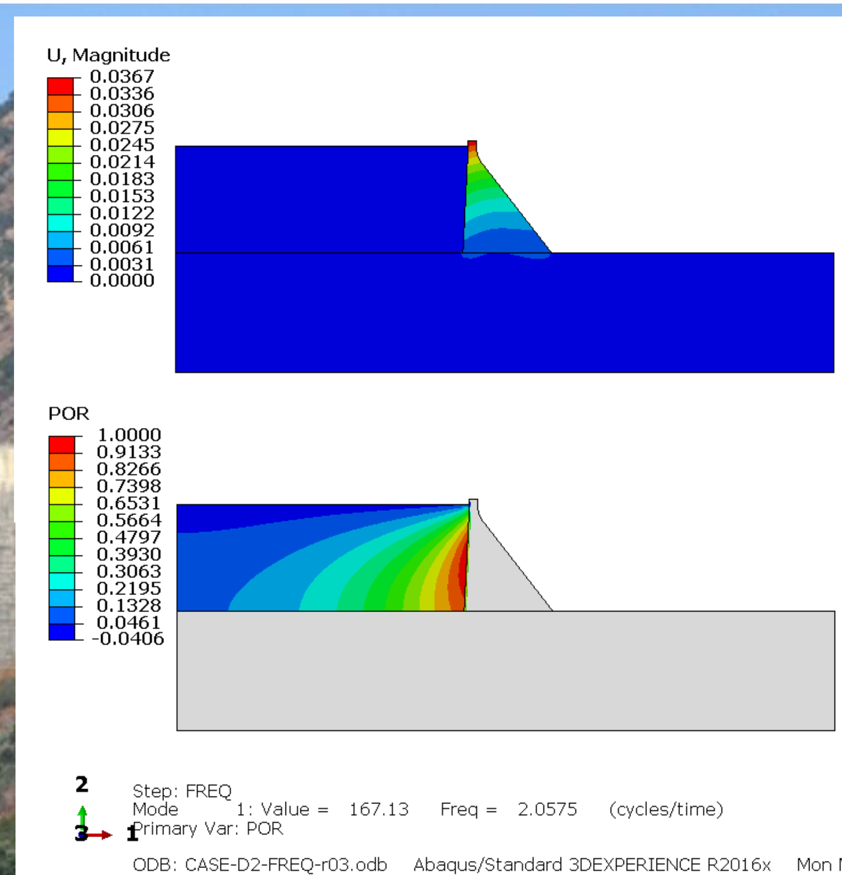

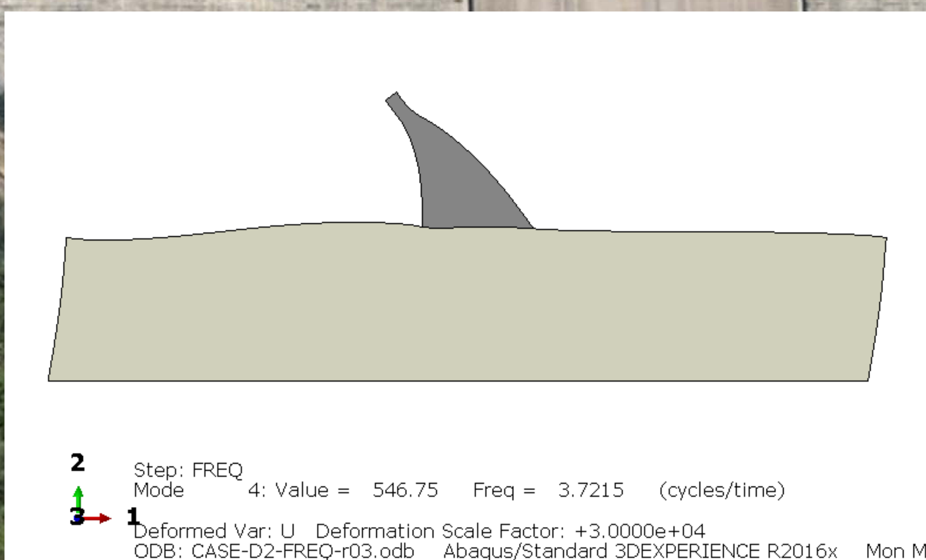

DYNAMIC ANALYSIS

Note absolute motion & relative velocity (ABC)

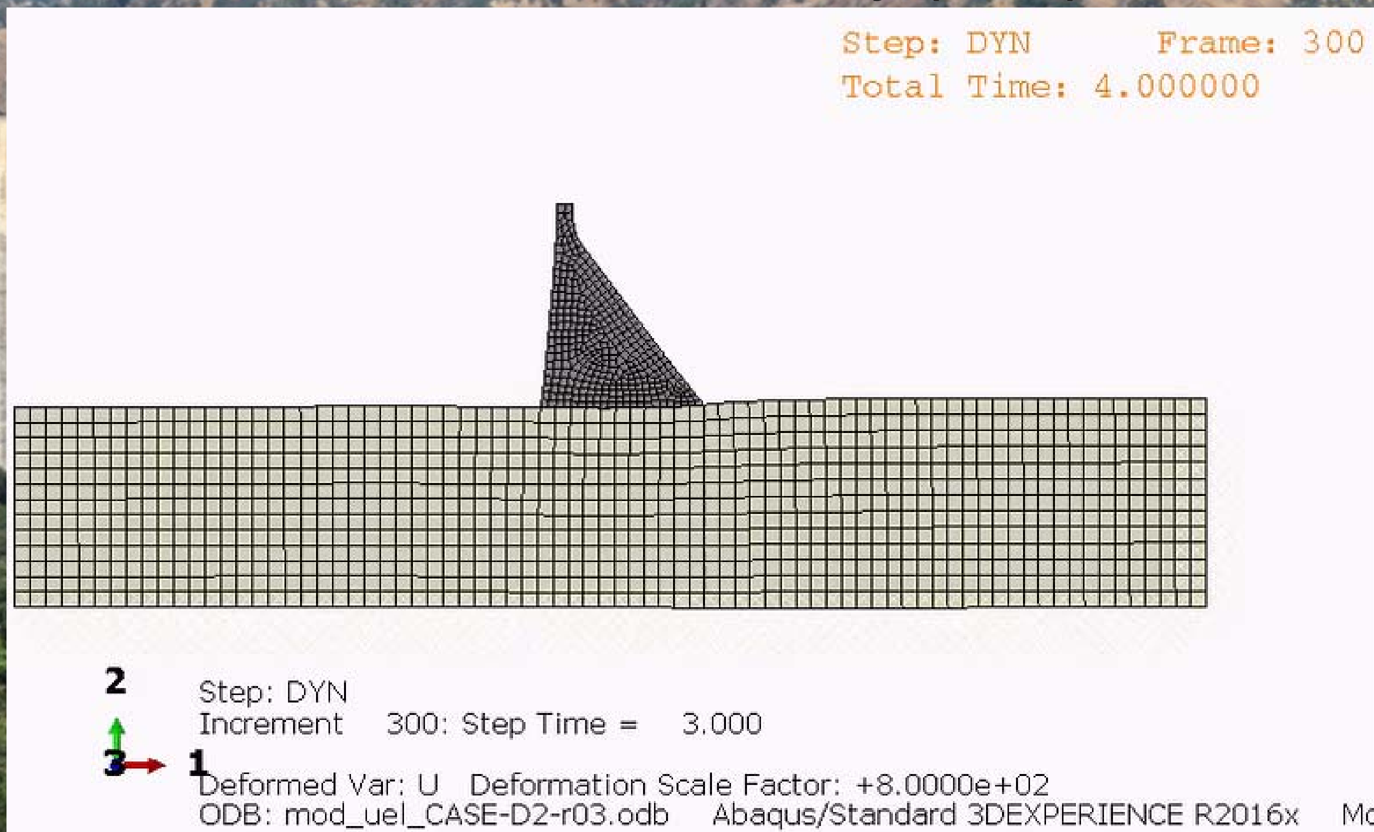

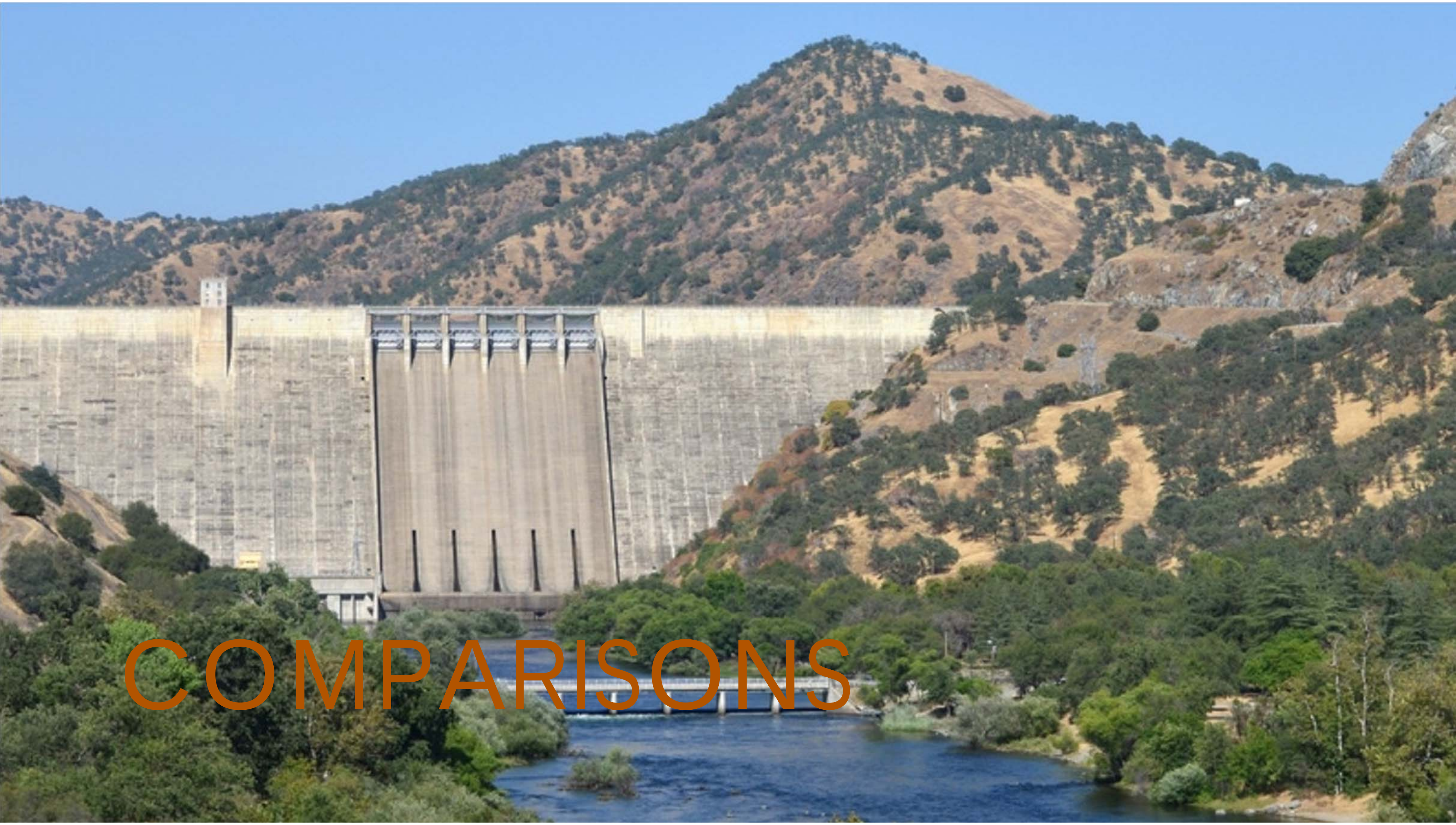
COMPARISONS

ACOUSTIC vs ADDED MASSES

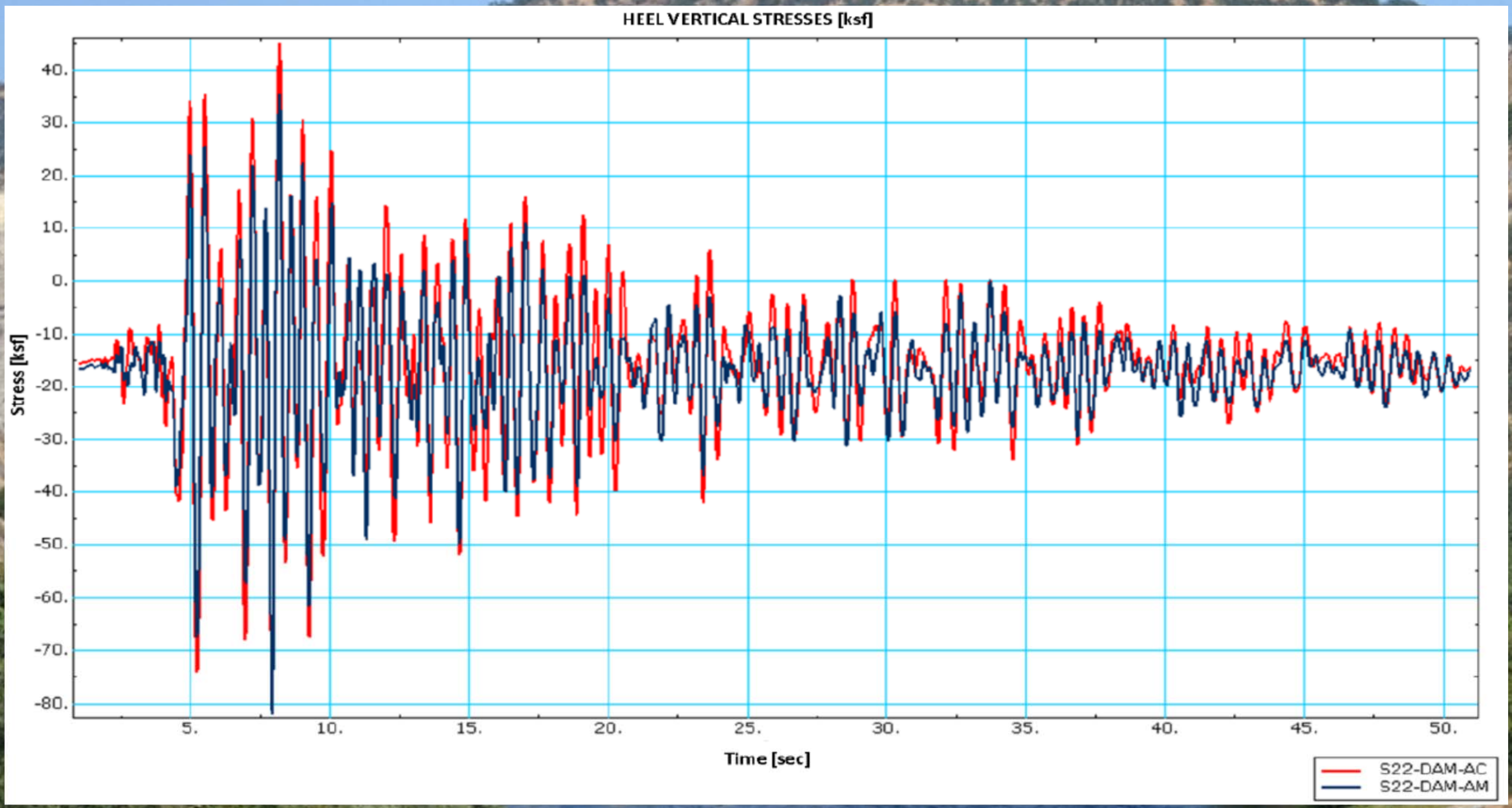

ACOUSTIC vs ADDED MASSES

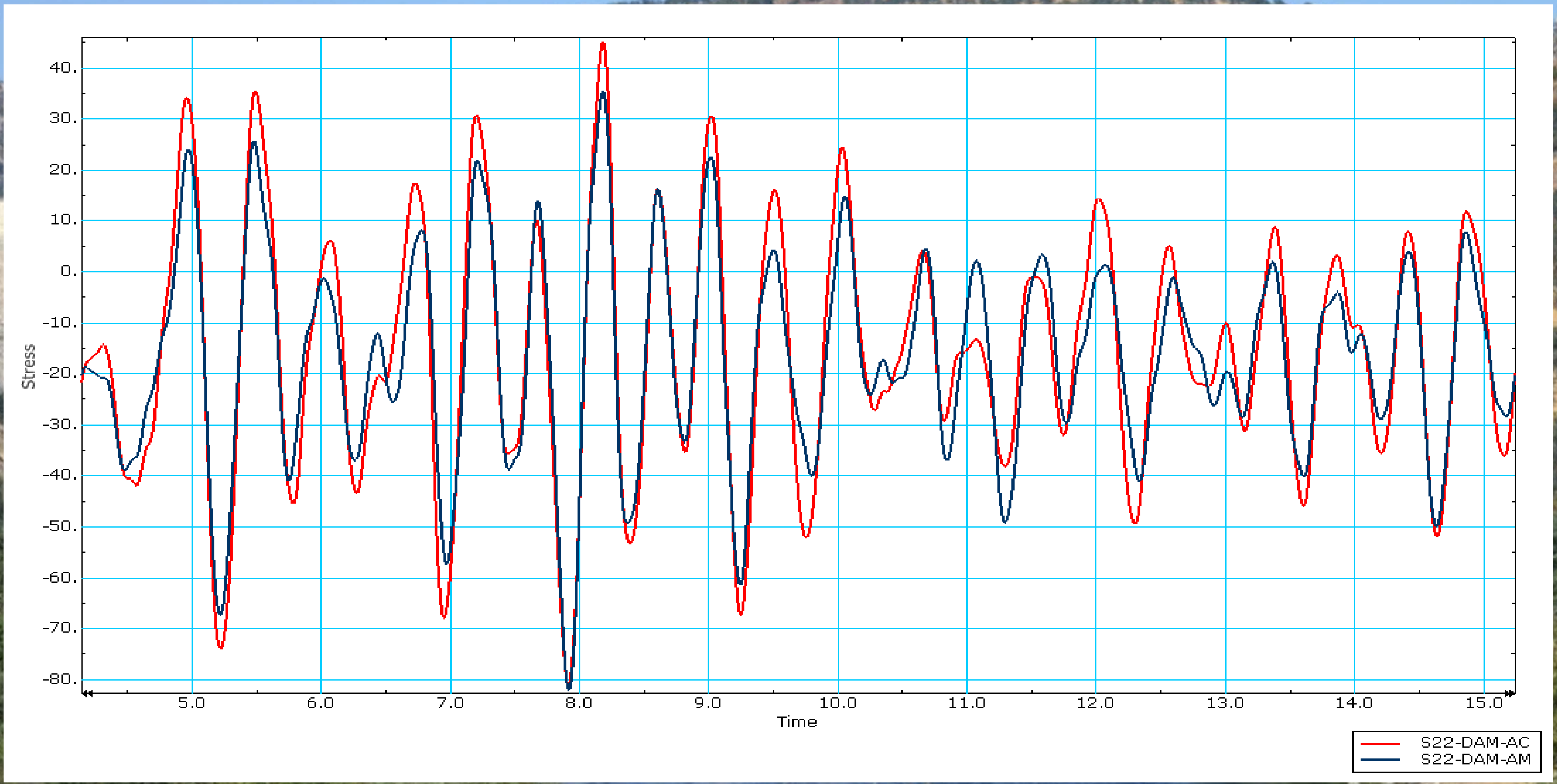

FOUNDATION SIZE → REDUCED TO HALF

- If ABC are robust → very efficient to reduce foundation size

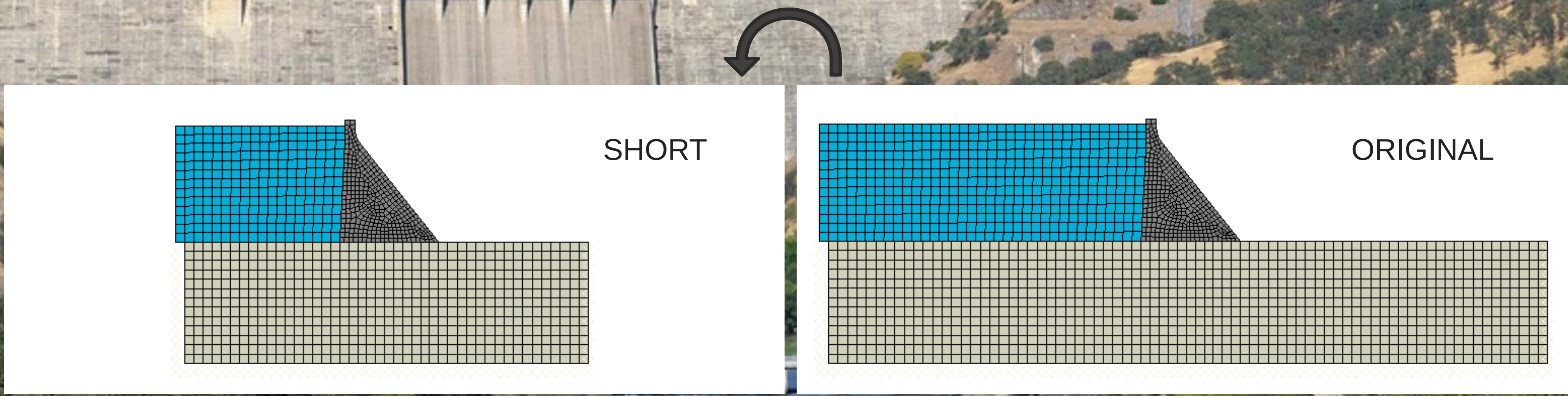

FOUNDATION SIZE → REDUCED TO HALF

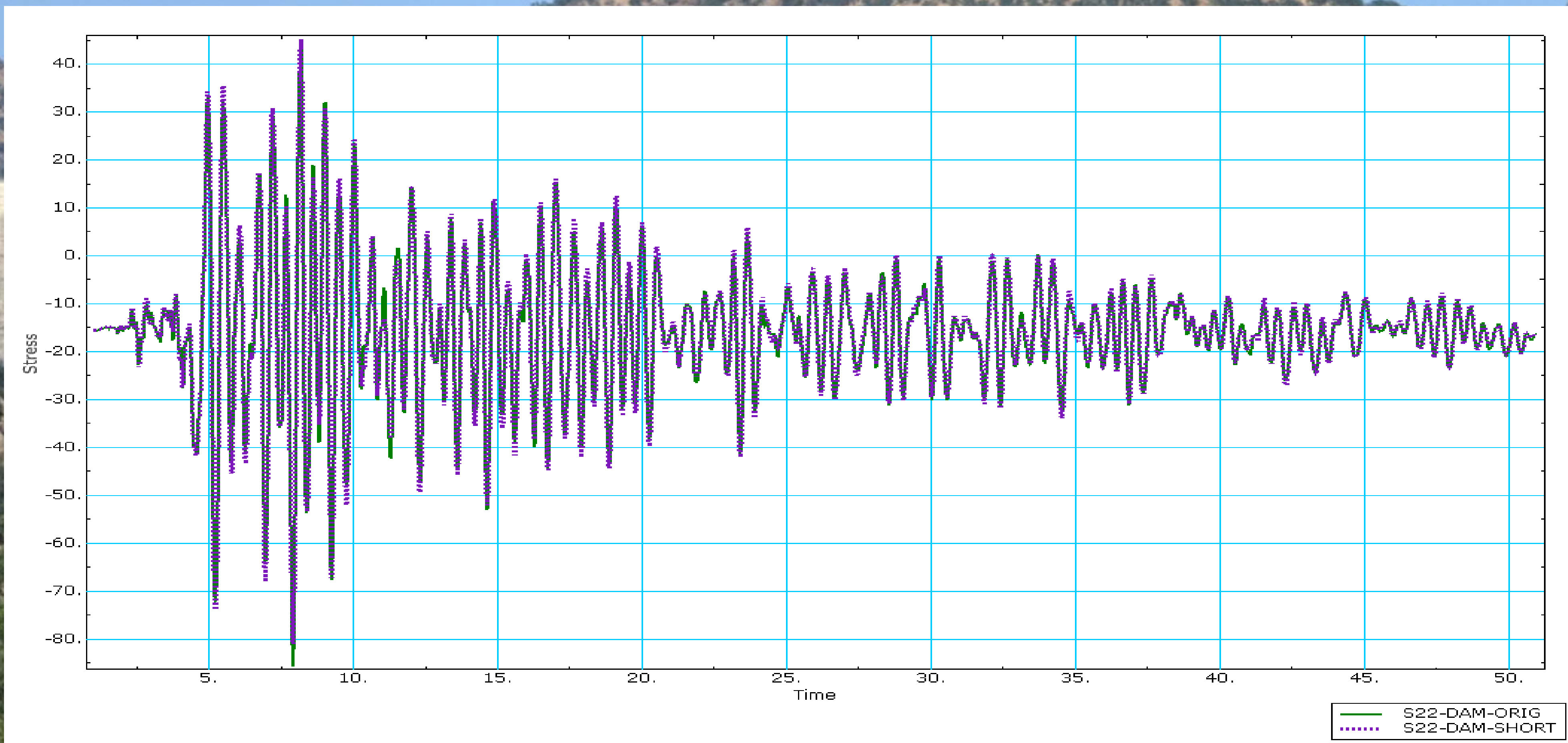

FOUNDATION SIZE → REDUCED TO HALF

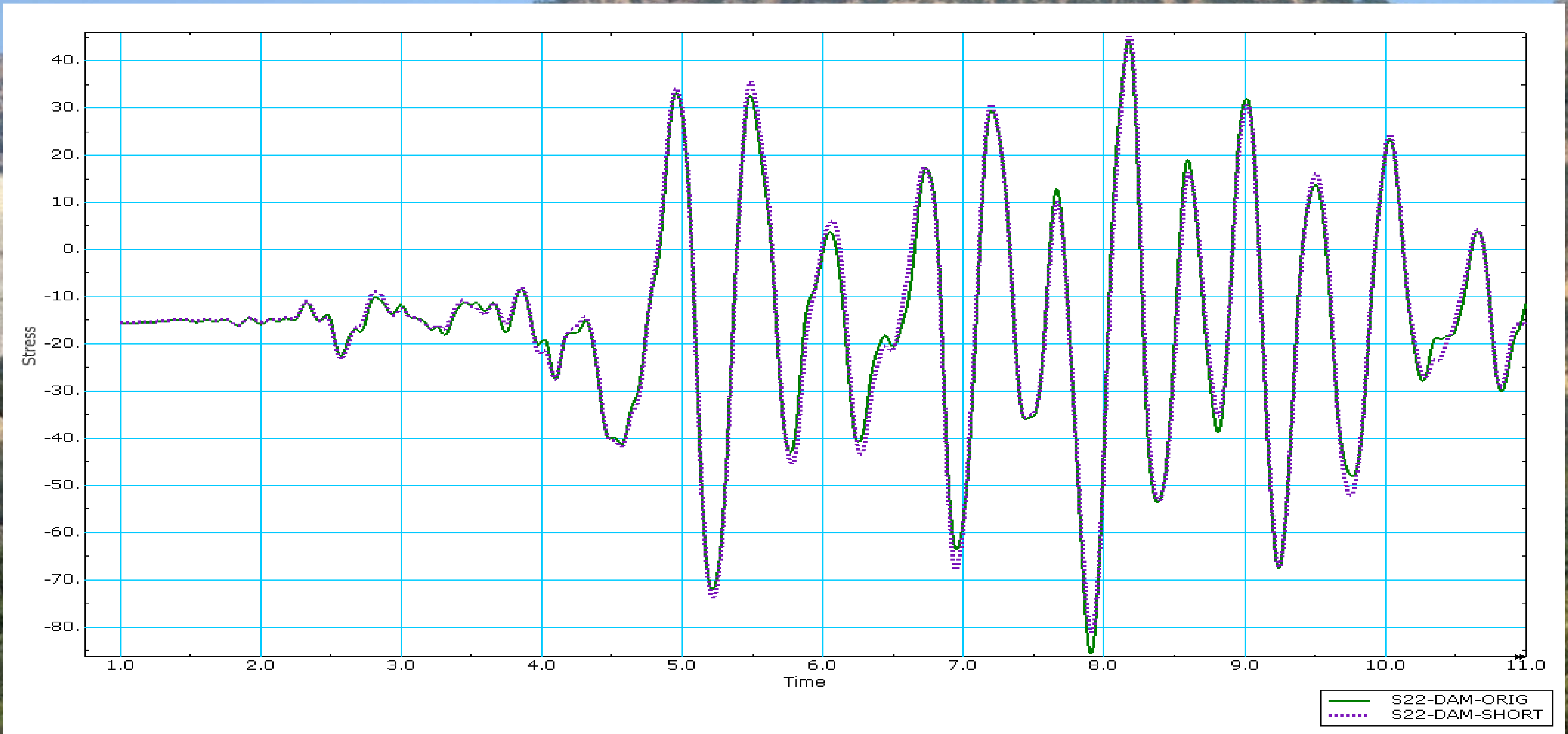

FOUNDATION SIZE → REDUCED TO HALF

Maximum stress time step

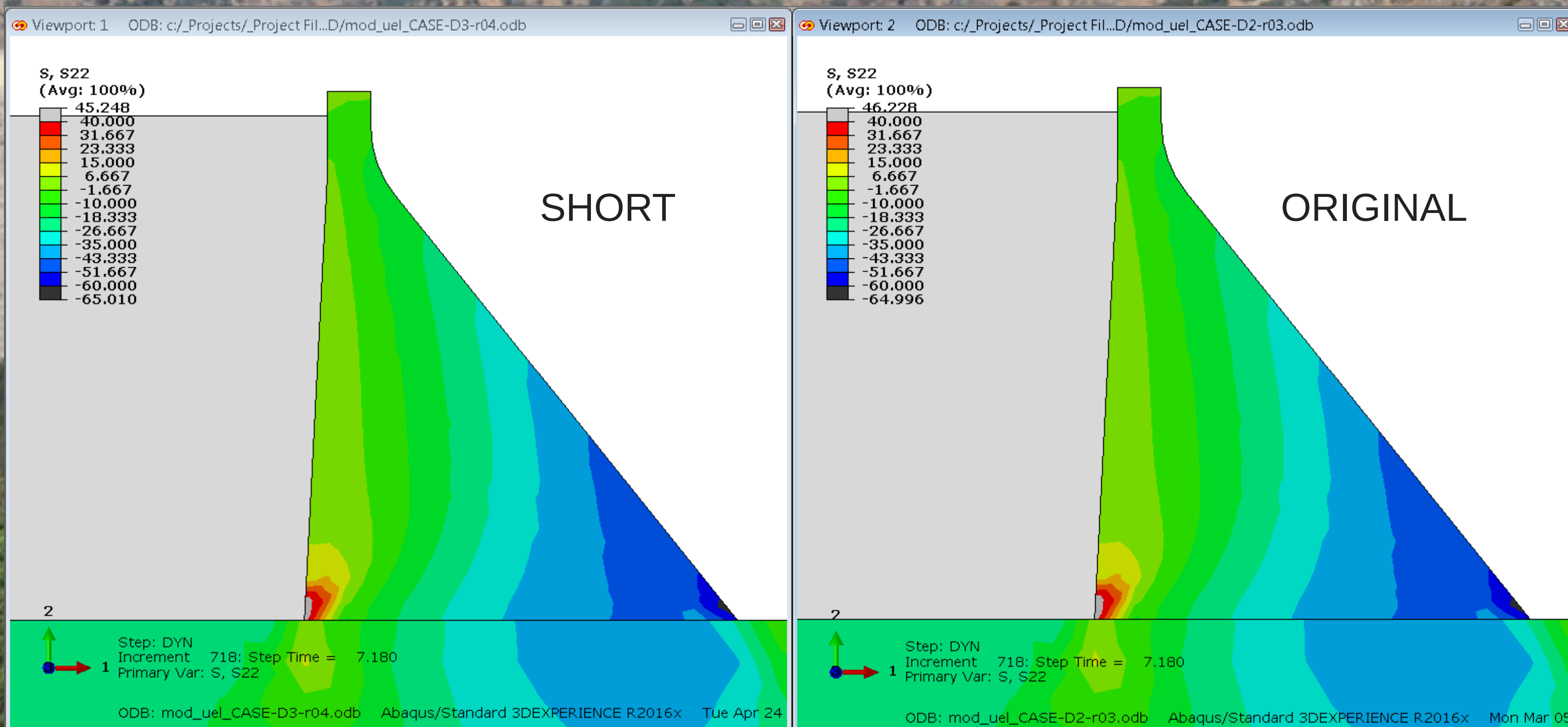

FOUNDATION SIZE → REDUCED TO HALF

Maximum hydrodynamic pressure time step

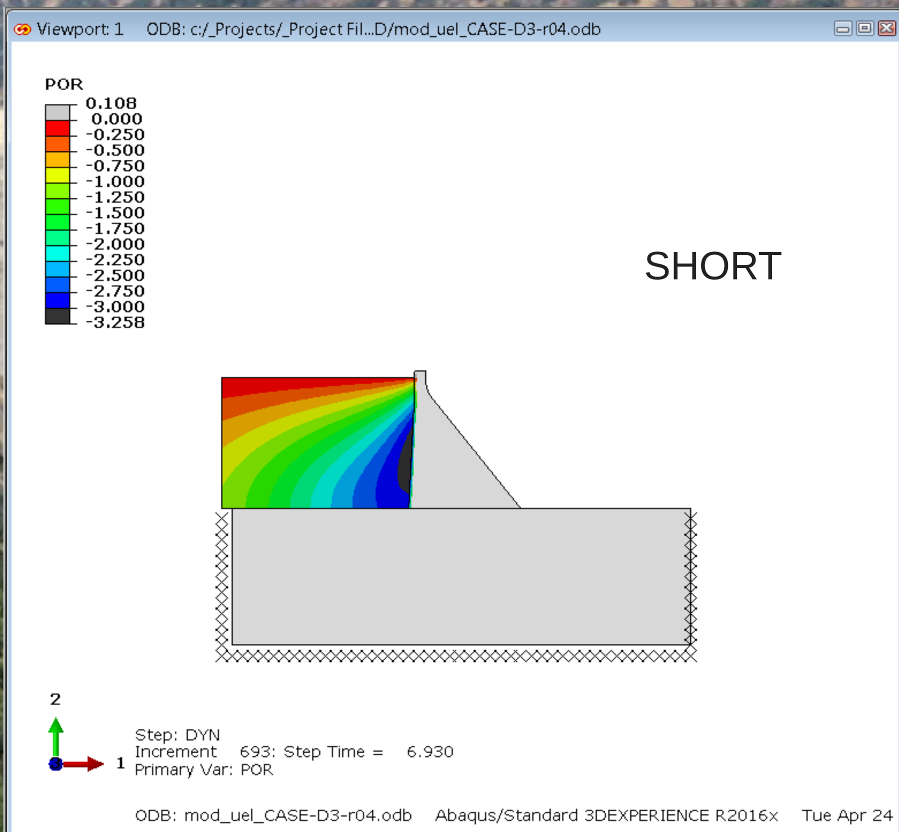

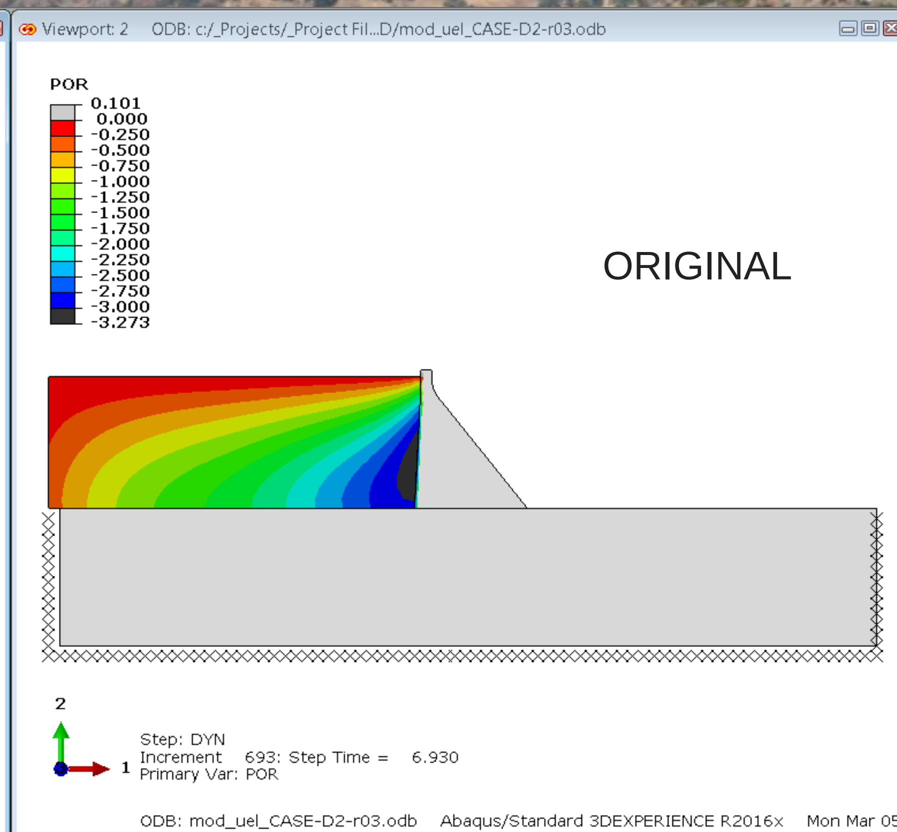

FINER FOUNDATION & WATER MESH

- 30ft vs 15ft element size

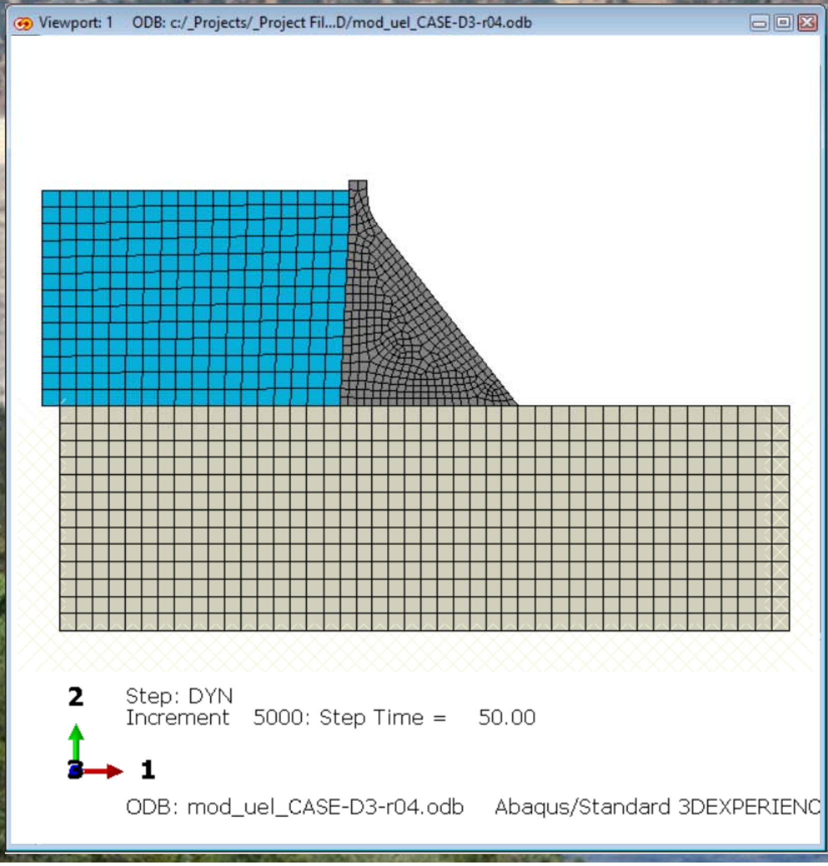

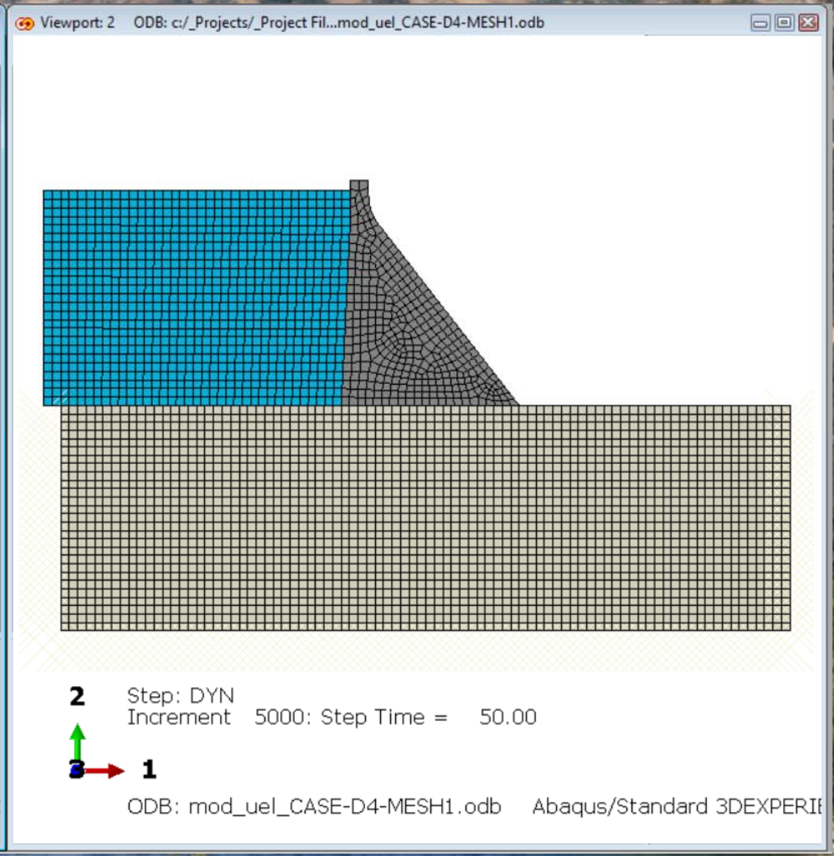

FINER FOUNDATION & WATER MESH

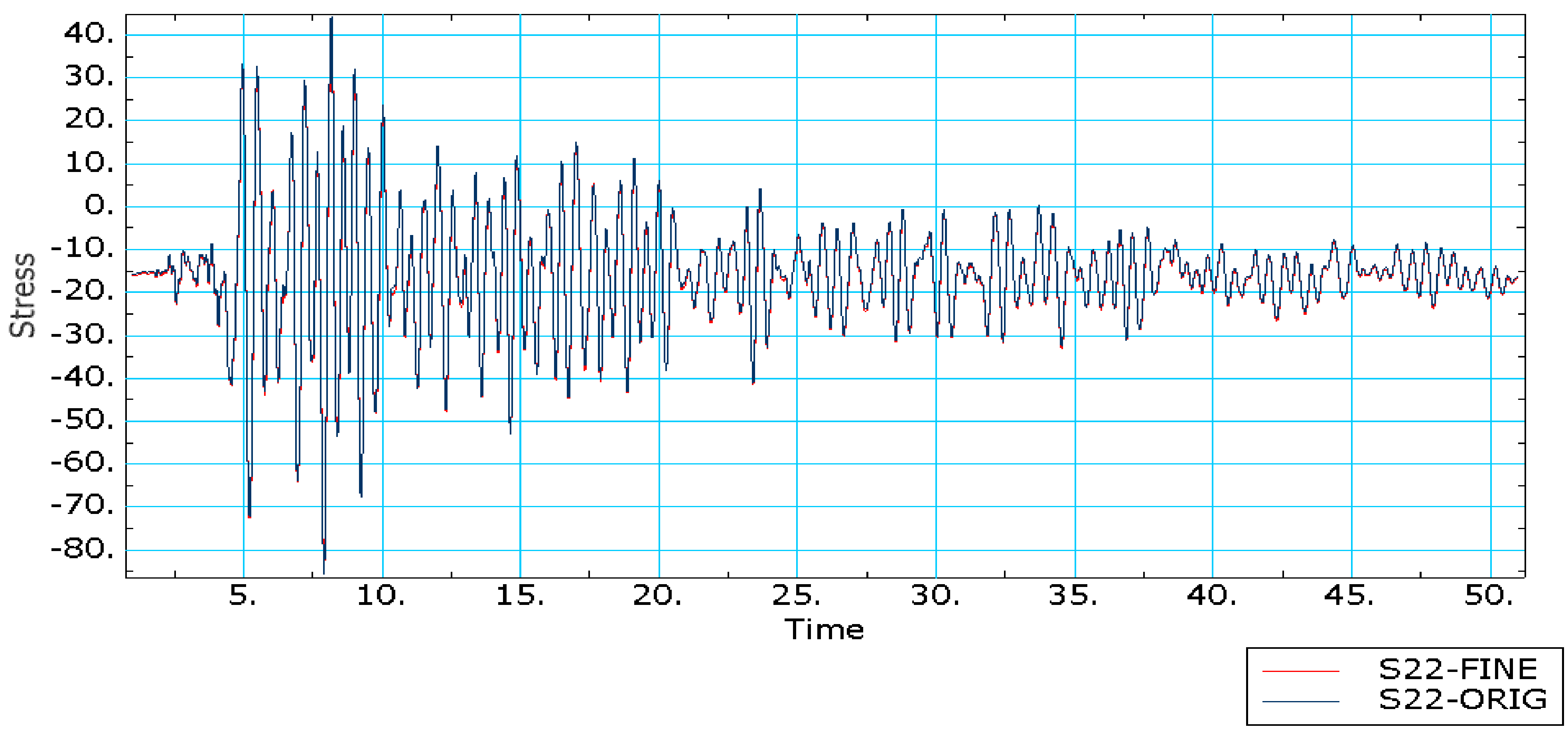

FINER FOUNDATION & WATER MESH

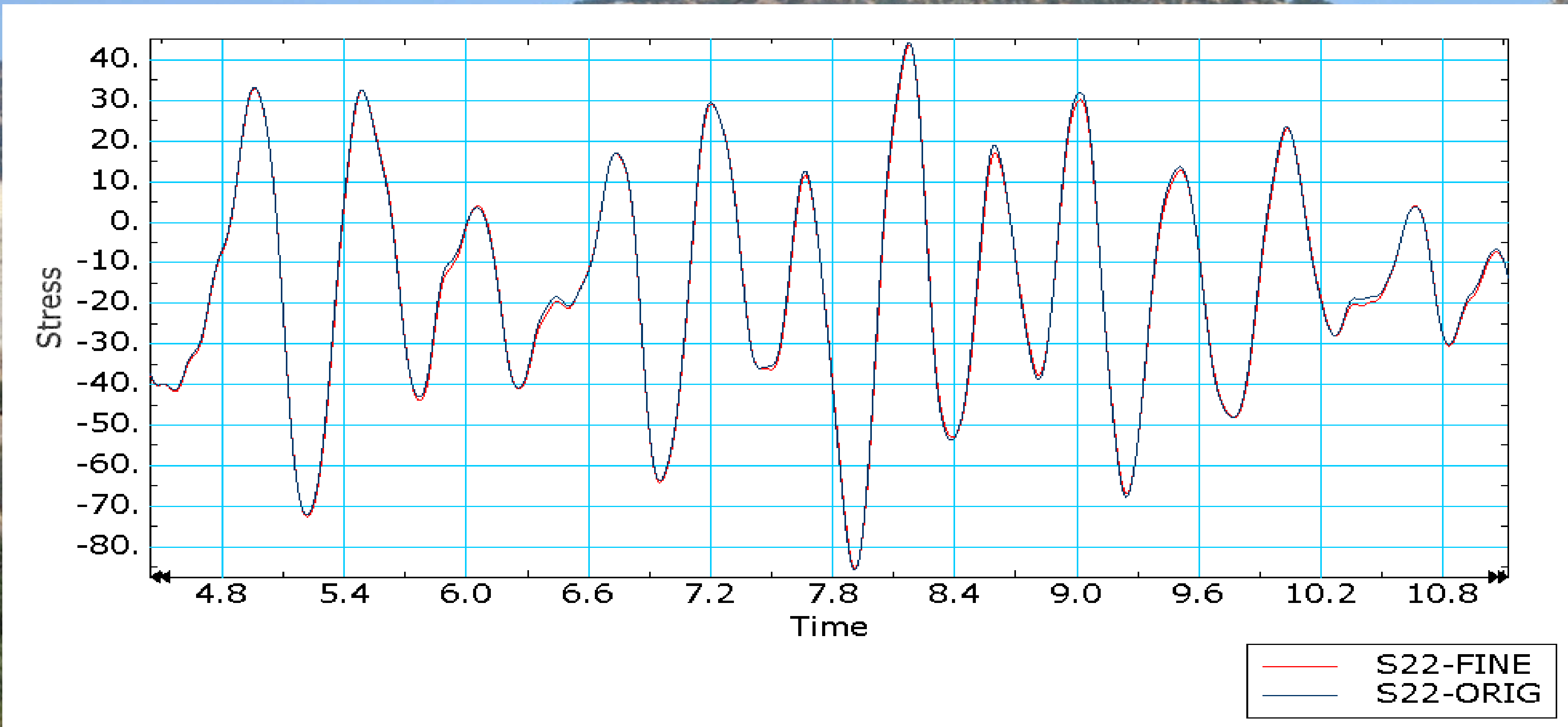

COARSER FOUNDATION & WATER MESH

- 30ft vs 50ft element size

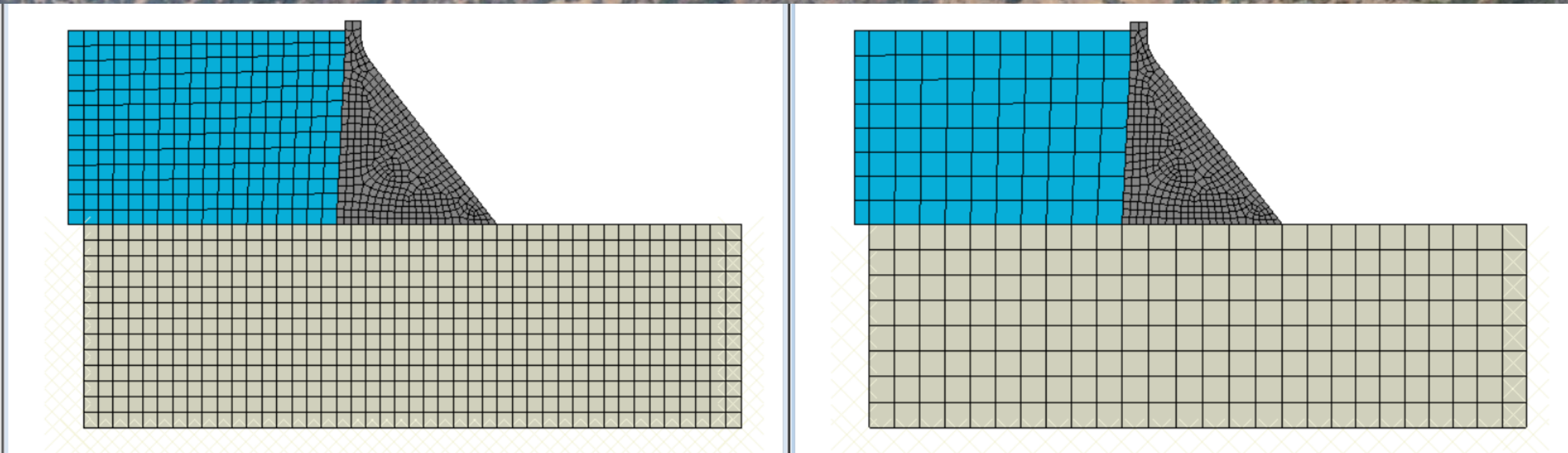

COARSER FOUNDATION & WATER MESH

- 30ft vs 50ft element size

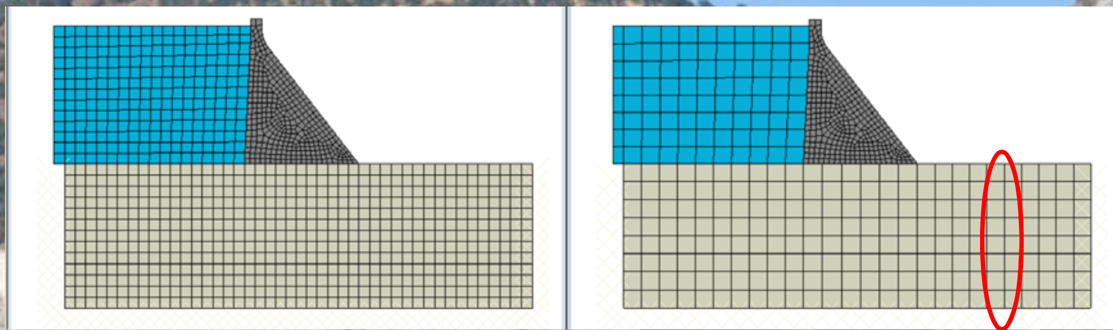

ONLY 1 WAVE LENGTH

$Er := 3250\ ksi = 468000\ ksf$ $\quad \nu := 0.20$ $\quad Gr := \dfrac{Er}{2 \cdot (1+\nu)} = (1.95 \cdot 10^5)\ ksf$

$\gamma r := 155\ pcf = 0.155\ \dfrac{k}{ft^3}$ $\quad \rho r := \dfrac{\gamma r}{g} = 0.0048\ \dfrac{k}{ft^3} \cdot \dfrac{s^2}{ft}$

$Kr := \dfrac{Er}{3 \cdot (1 - 2 \cdot \nu)} = (2.6 \cdot 10^5)\ ksf$

$Vpr := \sqrt{\dfrac{Kr + \dfrac{4}{3} \cdot Gr}{\rho r}} = (1.039 \cdot 10^4)\ \dfrac{ft}{s}$ $\quad Vsr := \sqrt{\dfrac{Gr}{\rho r}} = (6.362 \cdot 10^3)\ \dfrac{ft}{s}$

$H := 400\ ft$ $\quad fh := \dfrac{Vsr}{4 \cdot H} = 3.976\ Hz$ $\quad Th := \dfrac{1}{fh} = 0.251\ s$

$fv := \dfrac{3.4}{\pi \cdot (1-\nu)} \cdot fh = 5.379\ Hz$ $\quad Tv := \dfrac{1}{fv} = 0.186\ s$

Foundation element size: $L := 30\ ft$

Maximum frequency modeled: $f_{max} := \dfrac{Vsr}{10 \cdot L} = 21.207\ Hz$

$Er := 3250\ ksi = 468000\ ksf$ $\quad \nu := 0.20$ $\quad Gr := \dfrac{Er}{2 \cdot (1+\nu)} = (1.95 \cdot 10^5)\ ksf$

$\gamma r := 155\ pcf = 0.155\ \dfrac{k}{ft^3}$ $\quad \rho r := \dfrac{\gamma r}{g} = 0.0048\ \dfrac{k}{ft^3} \cdot \dfrac{s^2}{ft}$

$Kr := \dfrac{Er}{3 \cdot (1 - 2 \cdot \nu)} = (2.6 \cdot 10^5)\ ksf$

$Vpr := \sqrt{\dfrac{Kr + \dfrac{4}{3} \cdot Gr}{\rho r}} = (1.039 \cdot 10^4)\ \dfrac{ft}{s}$ $\quad Vsr := \sqrt{\dfrac{Gr}{\rho r}} = (6.362 \cdot 10^3)\ \dfrac{ft}{s}$

$H := 400\ ft$ $\quad fh := \dfrac{Vsr}{4 \cdot H} = 3.976\ Hz$ $\quad Th := \dfrac{1}{fh} = 0.251\ s$

$fv := \dfrac{3.4}{\pi \cdot (1-\nu)} \cdot fh = 5.379\ Hz$ $\quad Tv := \dfrac{1}{fv} = 0.186\ s$

Foundation element size: $L := 50\ ft$

Maximum frequency modeled: $f_{max} := \dfrac{Vsr}{10 \cdot L} = 12.724\ Hz$

HALF

COARSER FOUNDATION & WATER MESH

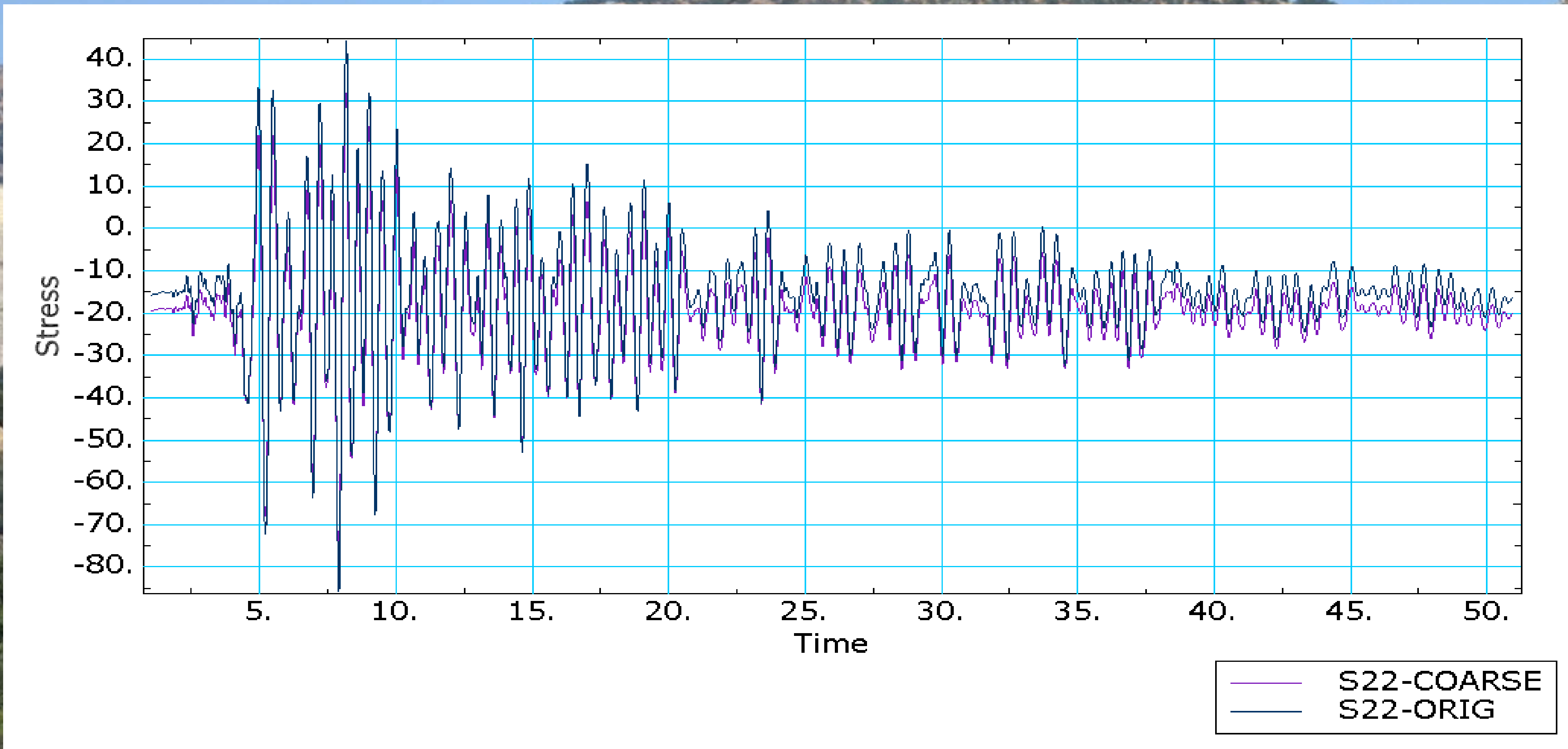

COARSER FOUNDATION & WATER MESH

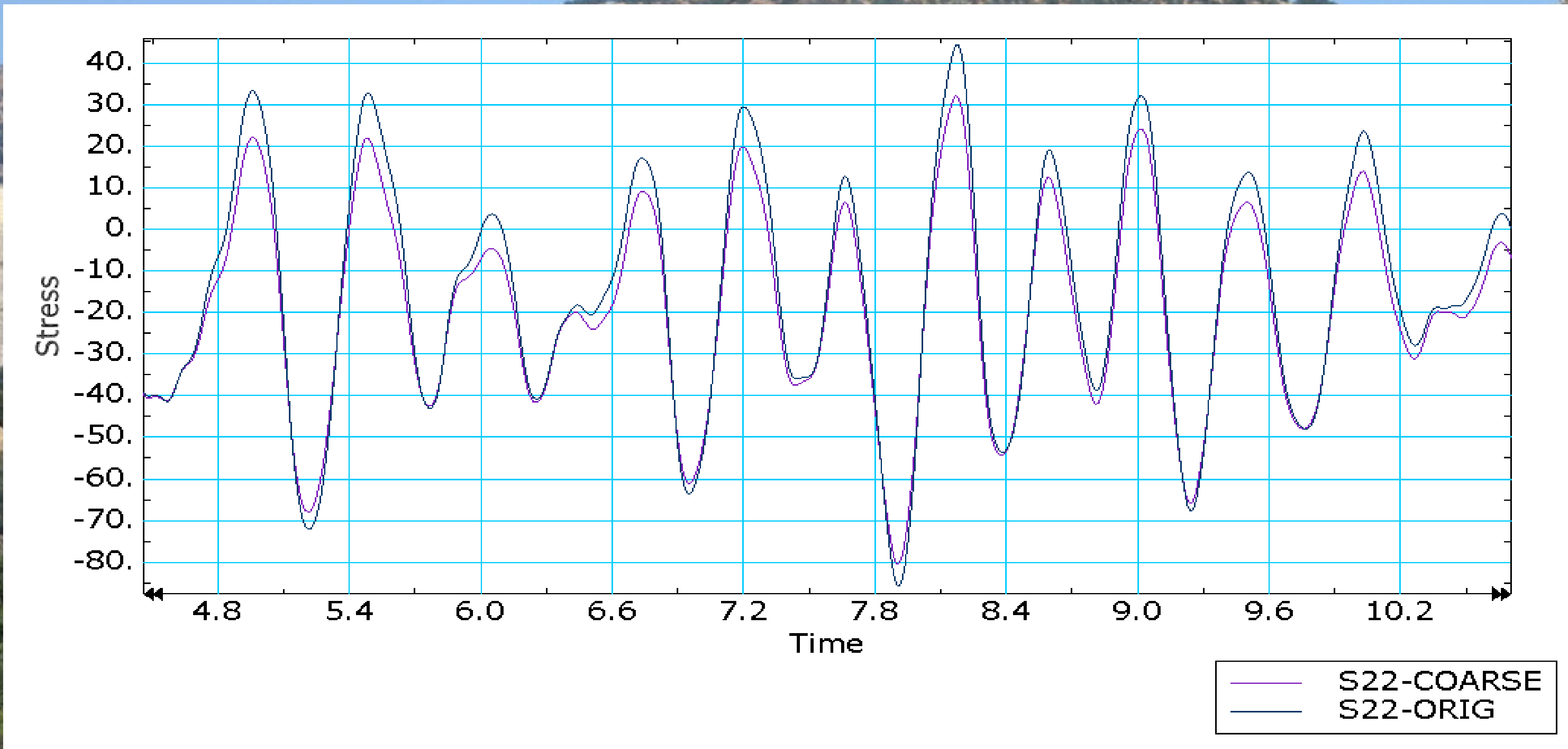


FUTURE WORKSHOPS

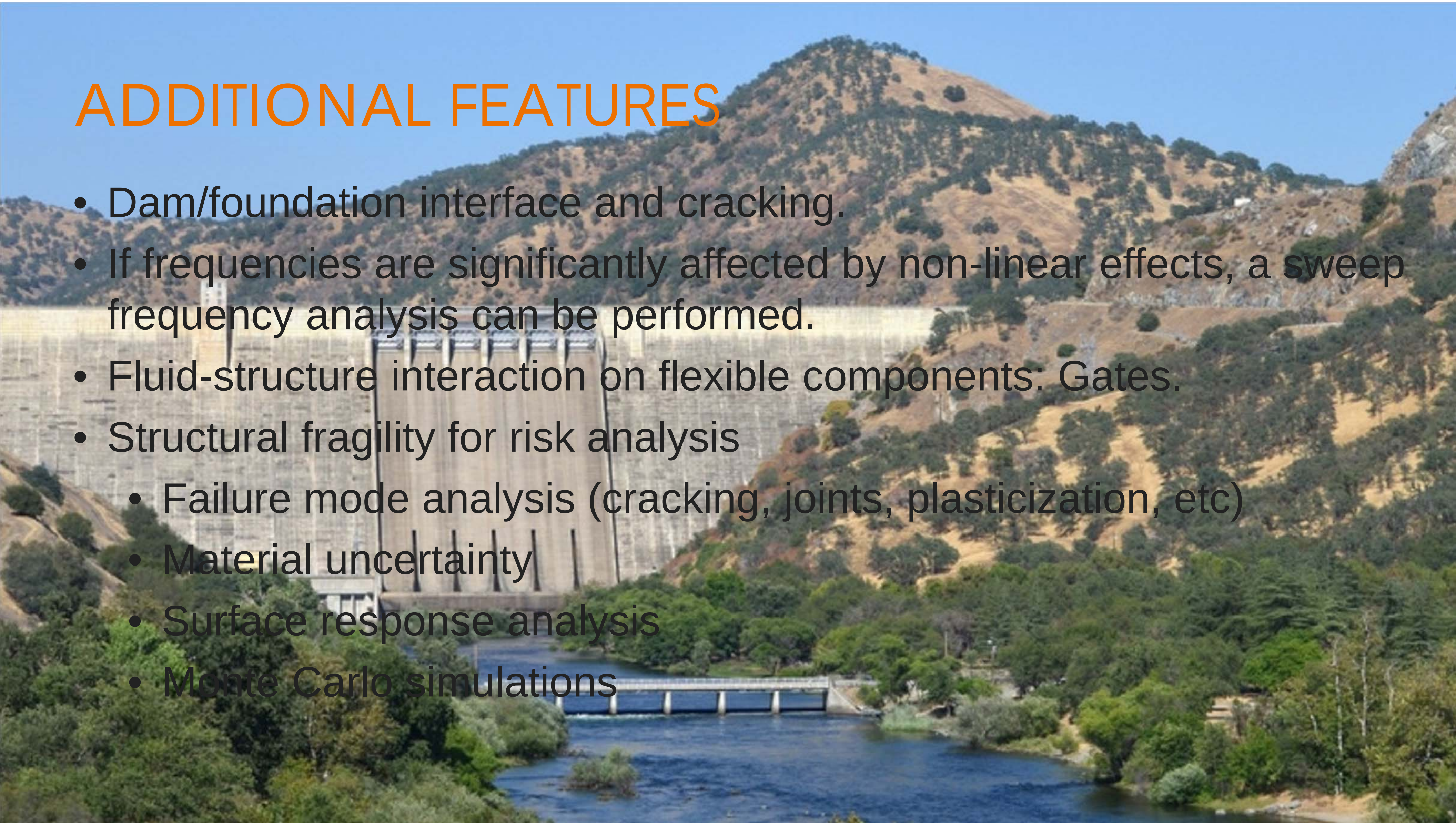

ADDITIONAL FEATURES

- Dam/foundation interface and cracking.
- If frequencies are significantly affected by non-linear effects, a sweep frequency analysis can be performed.
- Fluid-structure interaction on flexible components: Gates.
- Structural fragility for risk analysis
  - Failure mode analysis (cracking, joints, plasticization, etc)
  - Material uncertainty
  - Surface response analysis
  - Monte Carlo simulations


Step: Step-1   Frame: 0
Total Time: 0.000000
THANKS

USSD Conference

Workshop on

EVALUATION OF NUMERICAL MODELS AND INPUT PARAMETERS IN THE ANALYSIS OF CONCRETE DAMS

May 3, 2018

Jerzy Salamon, Ph.D., P.E. - Bureau of Reclamation

Maziar Partovi, Ph.D. – Diana FEA

DIANA FEA a TNO Company

RECLAMATION

Outline

- Overview of coupled acoustic-structural formulation for dam-reservoir interaction
- Case study for a rigid vs flexible dam
- Case study for a compressible vs in-compressible fluid
- Summary

Acoustic Fluid Approach

Coupling of Acoustic Fluid and Structural Elements

Structural domain Ω_S

$$M_S\ddot{u} + C_S\dot{u} + K_S u + f_I = f_S^{ext}$$

Fluid domain Ω_F

$$\nabla^2 p = \frac{1}{c^2}\ddot{p}$$

$$\boldsymbol{P\ wave\ veliciy\ c = \sqrt{\frac{K}{\rho}}}$$

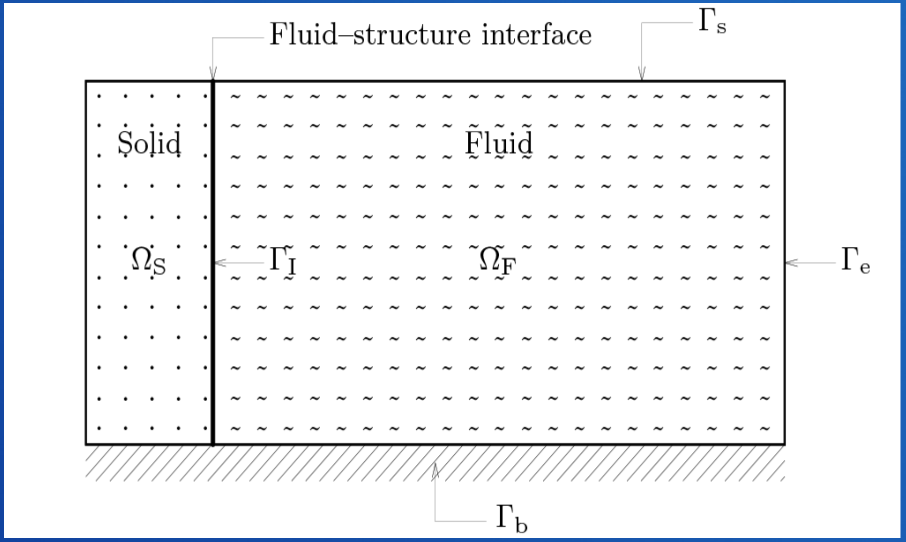

Fluid-structure interface

$$\sigma\, n_S = p\, n_F$$

Coupled system of equations for fluid-structure interaction

$$\begin{bmatrix} M_S & 0 \\ \rho_F R & M_F \end{bmatrix} \begin{Bmatrix} \ddot{u} \\ \ddot{p} \end{Bmatrix} + \begin{bmatrix} C_S & 0 \\ 0 & 0 \end{bmatrix} \begin{Bmatrix} \dot{u} \\ \dot{p} \end{Bmatrix} + \begin{bmatrix} K_S & -R^T \\ 0 & K_F \end{bmatrix} \begin{Bmatrix} u \\ p \end{Bmatrix} = \begin{Bmatrix} f_S^{ext} \\ 0 \end{Bmatrix}$$

DIANA FEA a TNO Company

RECLAMATION

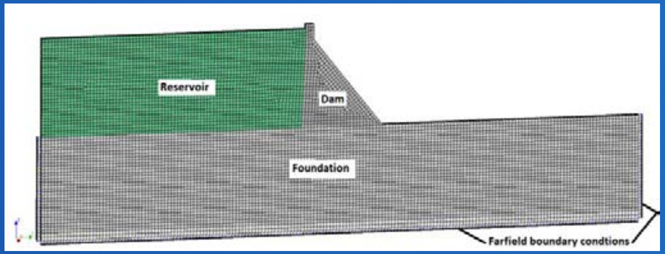

Natural Frequencies

Natural frequencies of the system

- Natural frequency of the dam & the foundation
- Natural frequency of the reservoir – first natural frequency:
  - for h = 381.5 feet
  - and Cw = 4715 ft/s
  - fr = 3.09 Hz

$$f_r = \frac{c_w}{4\,h}$$

- Natural frequency of the dam-foundation-reservoir system is a combination

In-compressible Reservoir

Natural Frequencies for in-compressible fluid

- Natural frequencies of the dam-foundation-reservoir system are lower when compared with the system that does not include the presence of the reservoir

- Eigenfrequencies vary significantly with the type of the dam-reservoir-foundation model

Reservoir	Foundation	1st	2nd	3rd
Empty reservoir	rigid (C-1)	3.16	6.39	8.75
Empty reservoir	flexible (D-1)	2.48	4.16	4.48
Empty reservoir	stiff (E-1)	2.91	5.58	6.94
In-compressible reservoir	rigid (C-2)	2.67	5.57	8.62
In-compressible reservoir	flexible (D-2)	2.06	3.98	4.81
In-compressible reservoir	stiff (E-2)	2.43	5.02	6.90

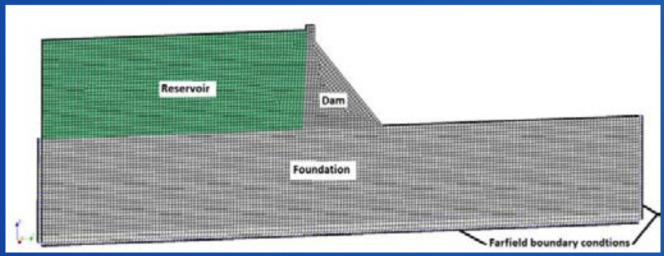

DIANA FEA a TNO Company

RECLAMATION

Case C – right vs flexible dam

Harmonic acceleration in horizontal direction of 0.1 g applied at the base of a rigid dam

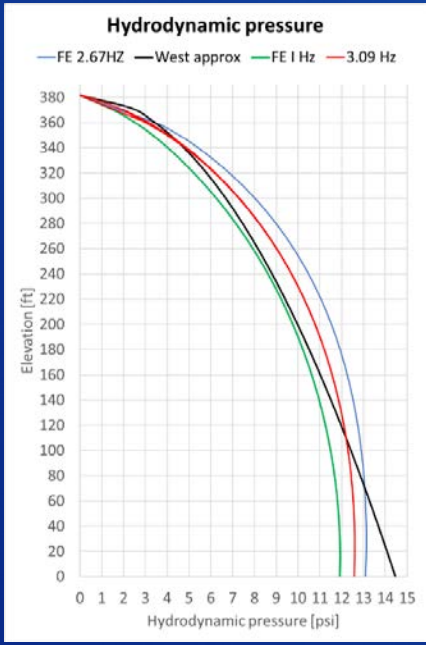

left - **rigid** dam excited at 1.0, 2.67 and 3.09 Hz

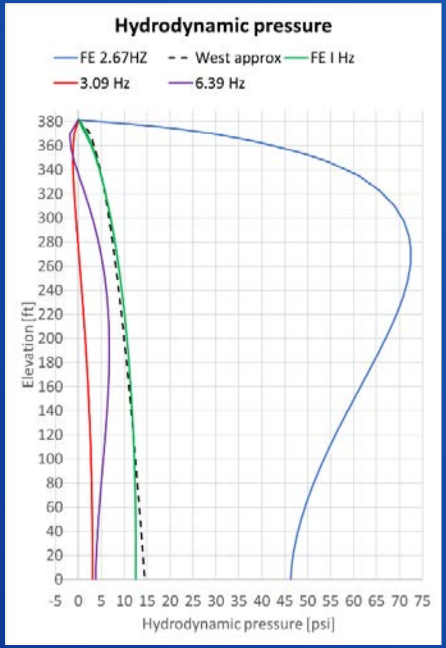

right - **flexible** dam excited at 1.0, 2.67, 3.09, and 6.39 Hz

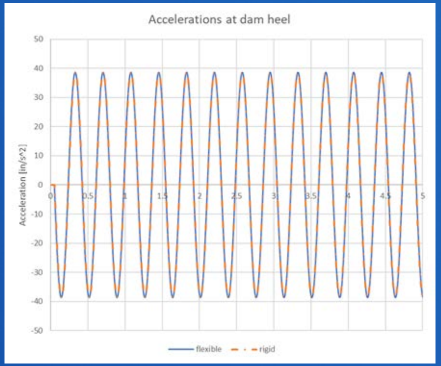

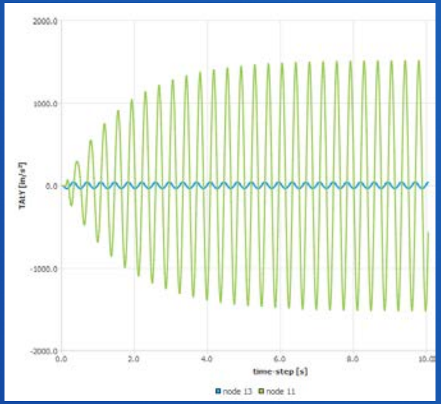

DIANA FEA

RECLAMATION

Case C – right vs flexible dam

Observations:

- The “added mass” may provide relatively good results only for “rigid” type dams with vertical upstream face

- The Westergaard added mass approach only roughly estimates the mass of water interacting with the dam during an earthquake. The error is particularly large when the excitation frequency is similar to the first natural frequency of the system

DIANA FEA a TNO Company
RECLAMATION

Compressible vs in-compressible fluid

Eigenfrequency

- **In-compressible fluid:**
  Standard modal analysis

- **Compressible fluid:**
  Hybrid Frequency-Time Domain (HFTD) analysis

I will present the mode shapes and eigenfrequencies for the compressible fluid case and try to compare them with the corresponding incompressible ones

Compressible vs in-compressible fluid

Case D – far field boundary conditions <u>removed</u>

Compressible fluid (direct frequency response analysis with upstream down-stream load as trigger; investigated 0.05-8.00 Hz in steps of 0.05 Hz)

Spikes at:

Compressible vs In-compressible

Compressible	In-compressible
– 1.8 Hz	1.81 Hz
– 2.45 Hz	2.453 Hz
– 3.5 Hz	4.13 Hz
– 4.55 Hz	4.69 Hz
– 5.3 Hz	4.97 Hz
– 5.8 Hz	5.78 Hz
– 6.35 Hz	6.32 Hz

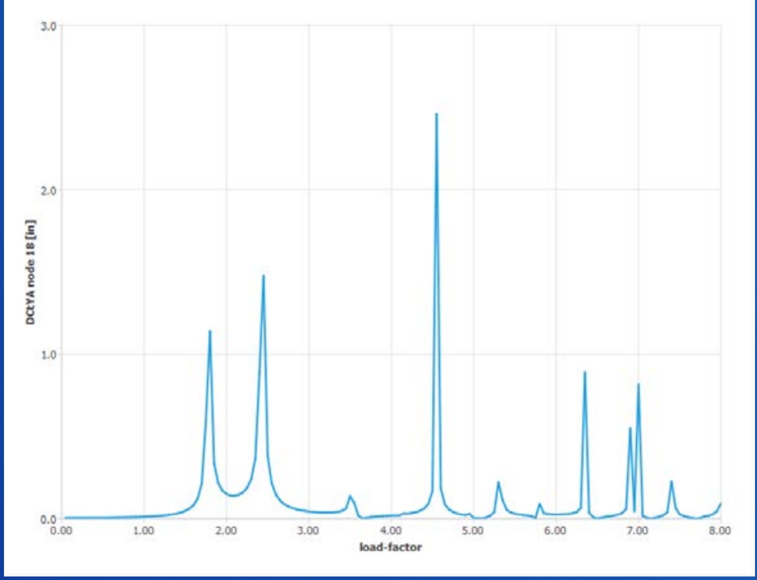

DIANA FEA a TNO Company

RECLAMATION

Compressible vs in-compressible fluid

Compressible fluid vs In-compressible fluid

f_{c1} = 1.80 Hz

f_1 = 1.81 Hz

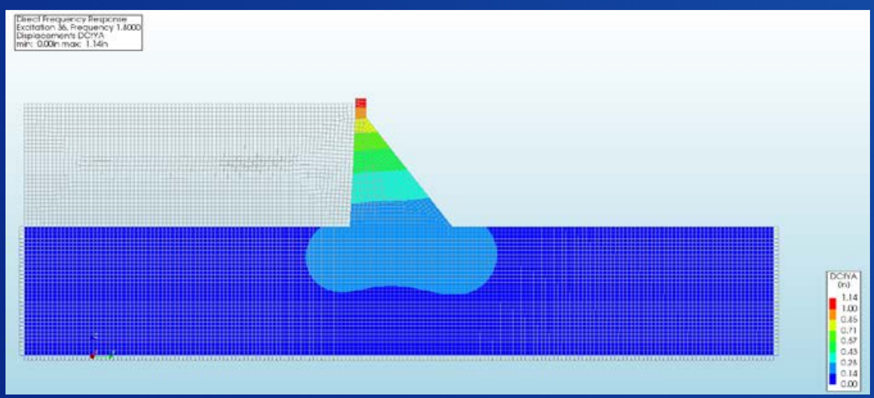

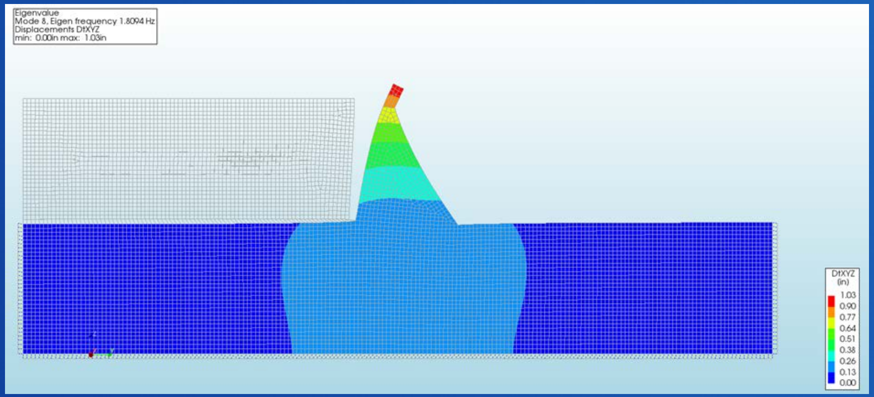

DIANA FEA a TNO Company RECLAMATION

Compressible vs in-compressible fluid

Compressible fluid vs In-compressible fluid

f_{c2} = 2.45 Hz

f_2 = 2.45 Hz

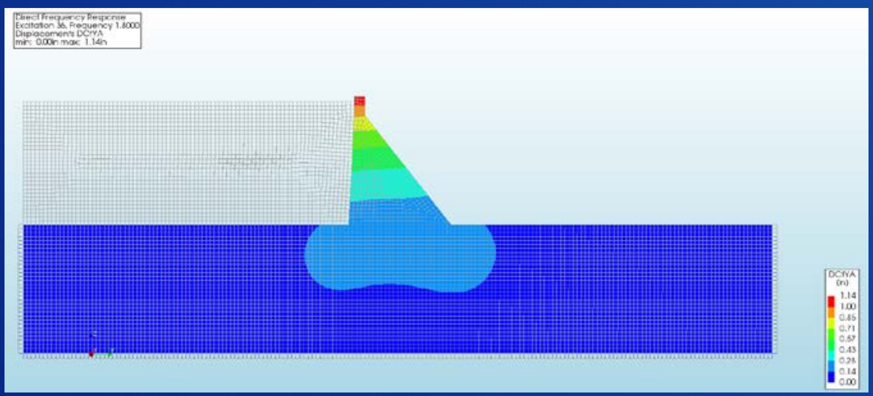

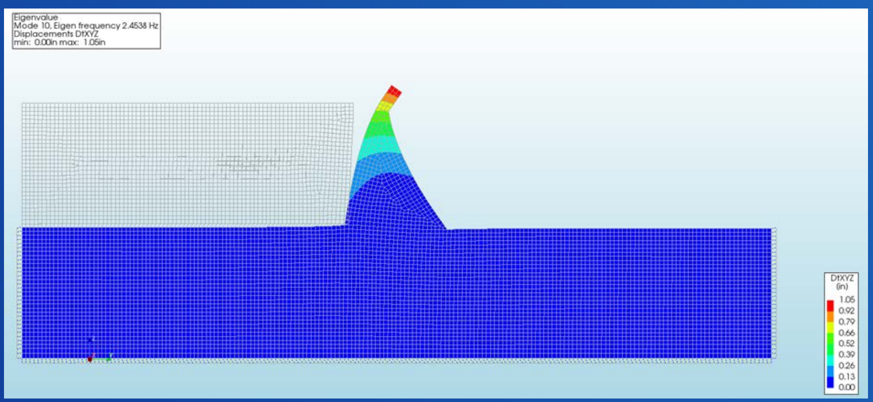

DIANA FEA a TNO Company

RECLAMATION

Compressible vs in-compressible fluid

Compressible fluid vs In-compressible fluid

f_{c3} = 3.55 Hz

f_3 = 4.13 Hz

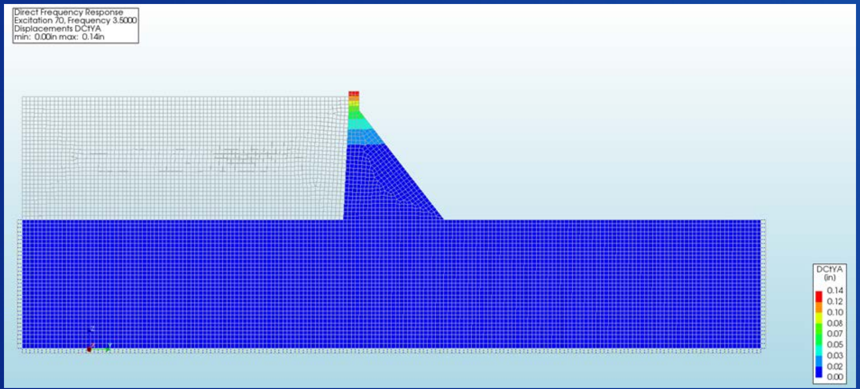

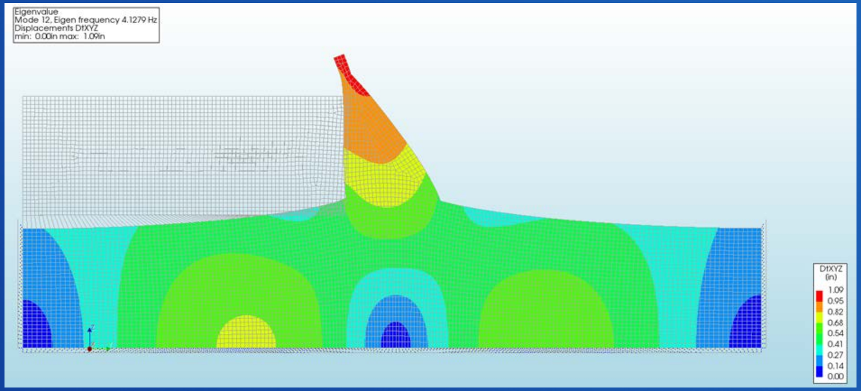

DIANA FEA a TNO Company

RECLAMATION

Compressible vs in-compressible fluid

Observations:

- **It is much more complicated to find the eigenfrequencies for compressible fluid**

- **Eigenfrequencies for compressible fluid appear more as ranges where the phase angle is changing and some sharp spikes where the response is definitely amplified.**

- **Therefore, it is difficult to define "THE" eigenfrequencies of the model with compressibility.**

Compressible vs in-compressible fluid

Case D for
ETAF signal
Total Pressure:

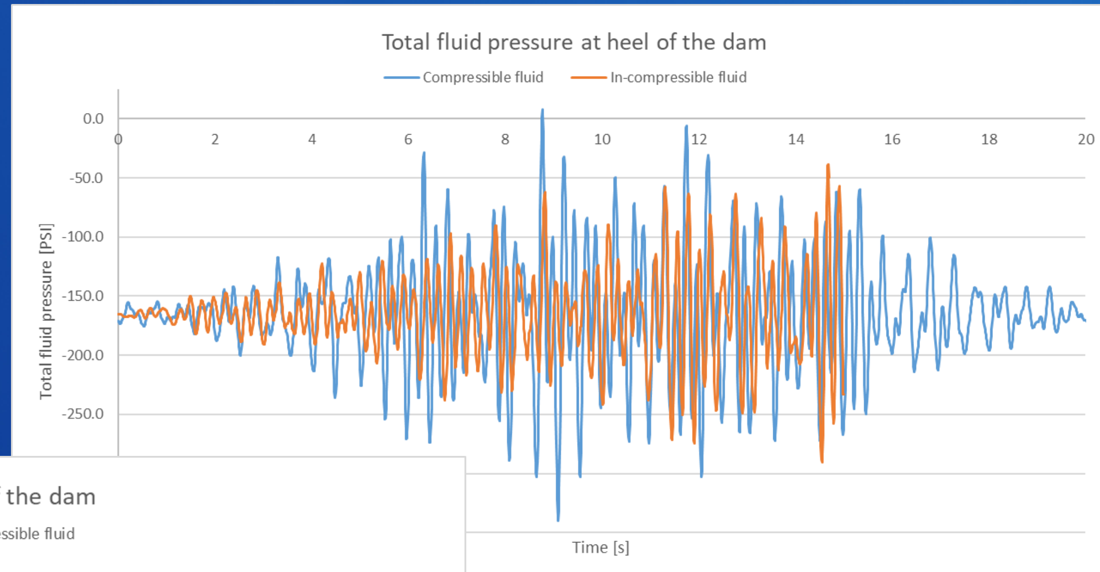

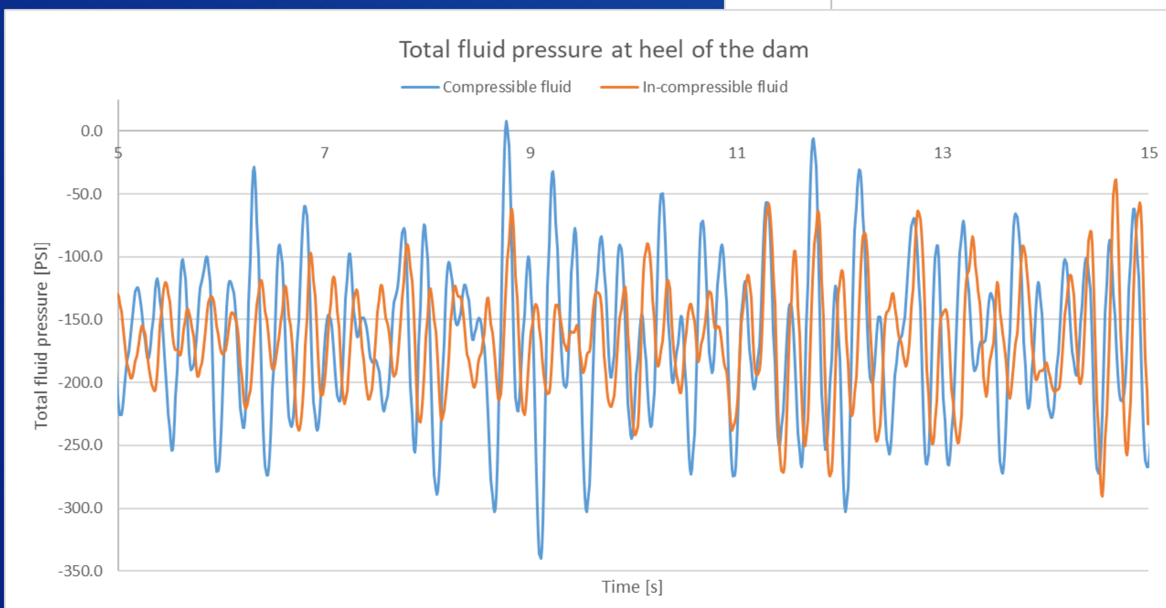

Compressible vs in-compressible fluid

Case D for - ETAF signal
Vertical Stress at dam heel:

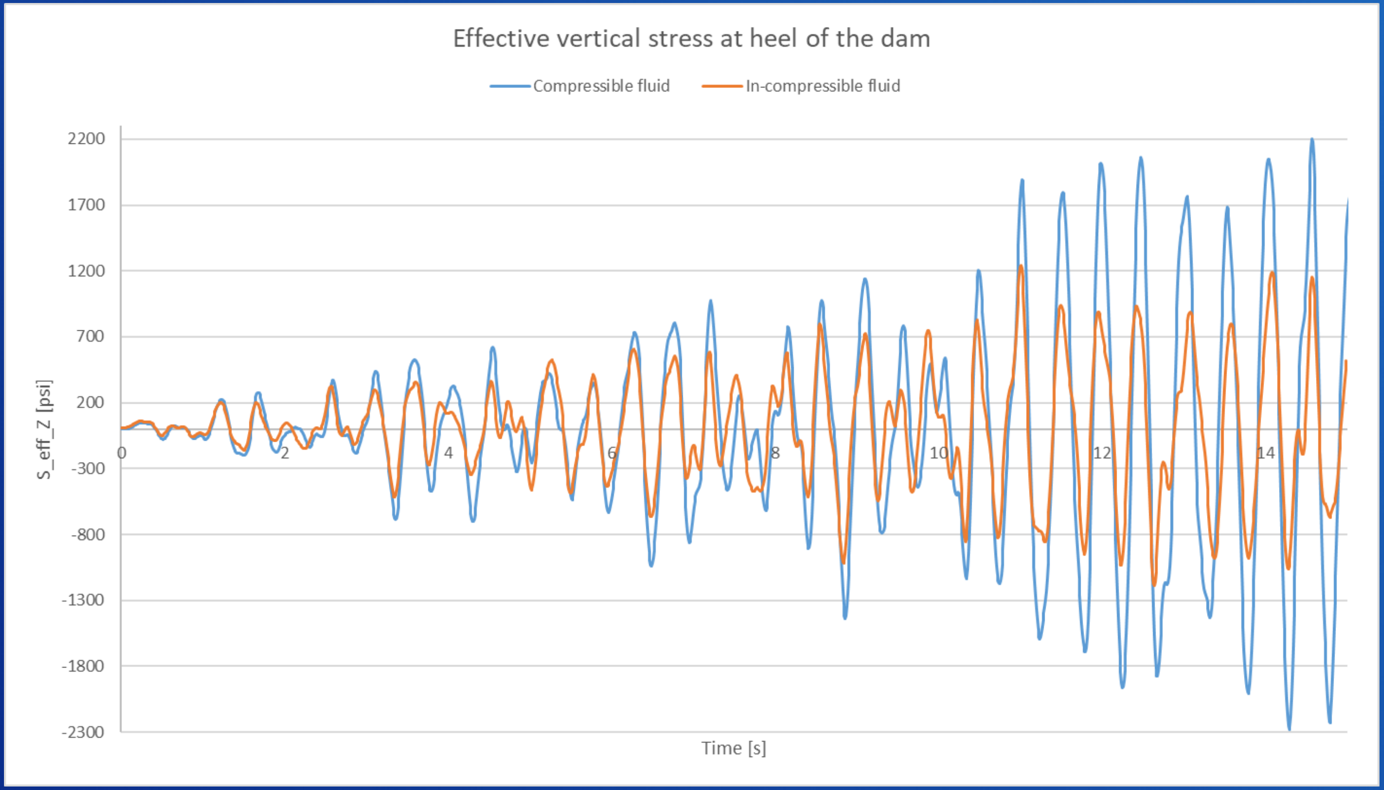

DIANA FEA

RECLAMATION

Summary

- Eigenfrequencies of the dam-reservoir-foundation system vary significantly with the type of assumptions made for the analyzed physical model

- Compressibility of the fluid influences the analysis results

- Computed hydrodynamic pressure at the face of the dam is related to the method used in the analysis

Conclusions

- Compressibility of water is the primary factor that influences the hydrodynamic pressure distribution in the reservoir.

- The time analysis with an "incompressible fluid" material model provides significantly different results when compressibility of the fluid is considered

- It appears that a hybrid frequency-time domain (HFTD) analysis should be implemented in the seismic simulations of the dam-reservoir-foundation system

Questions?

2018 USSD Miami conference

Evaluation of Plaxis 3D Analysis of Pine Flat Dam

Yixing Yuan, Ph.D.
Matthew A. Taylor, P.E.
May 3, 2018

Introduction

- **Evaluate performance of Plaxis 3D with Dynamic Module**
  - which is widely used in analyzing soil-structure interaction
  - but not popular in modeling dam-water-foundation system

- **FE model includes**
  - 10-noded tetrahedra elements with averaged size ≤ minimum wave length/8
  - Rayleigh damping leading to 5% damping for frequency between 2Hz and 6Hz
  - Dynamic signal applied at the base of the foundation

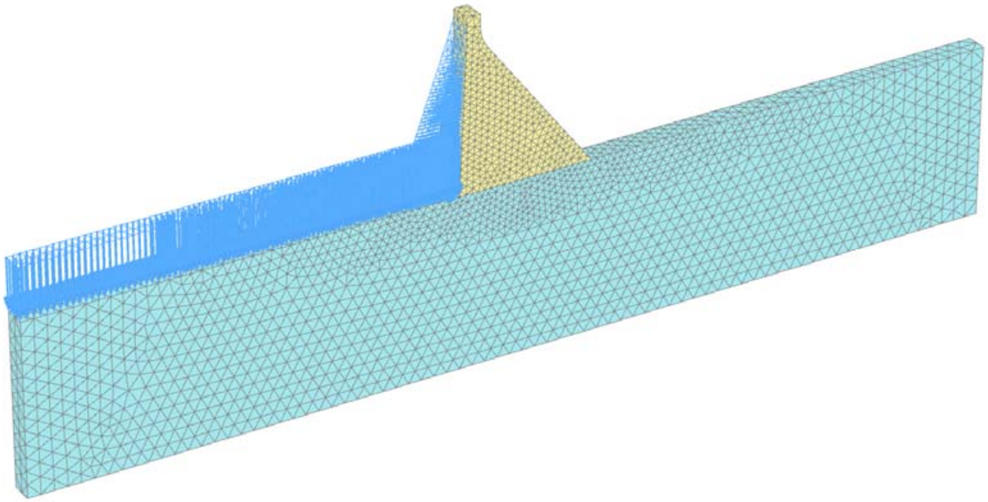

Assumptions of plane stress and plane strain

- **Assumptions following Chopra et al. (1980)**
  - **Plane stress => dam monolith**
  - **Plane strain => rock foundation**
- **Simplified plane strain analysis (e.g., with Plaxis 2D) may not be representative for dam monolith**

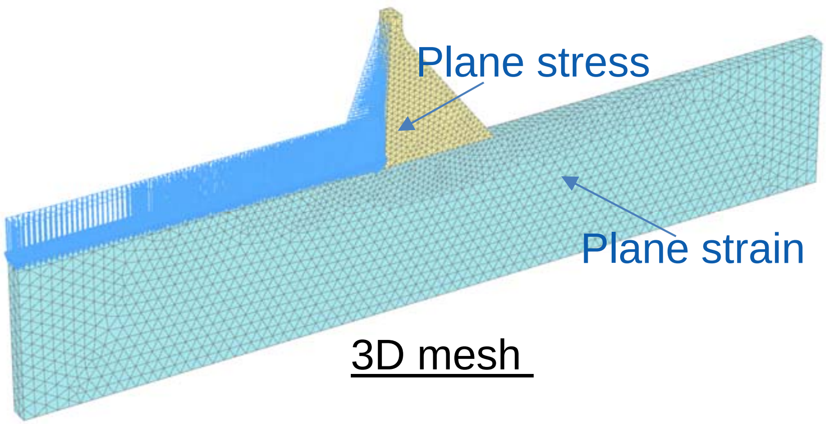

3D mesh

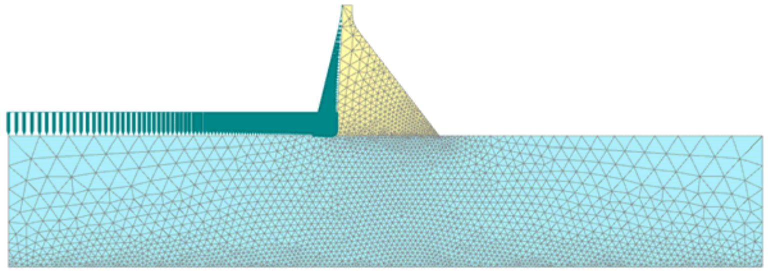

2D plane strain mesh

Challenges of using Plaxis 3D in dynamic analyses

- **There is no built-in function for modal analyses**

Workaround:

- Free vibration after removal of concentrated force at crest => natural frequency
- Force vibration under a harmonic excitation at base at a selected natural frequency => mode shape

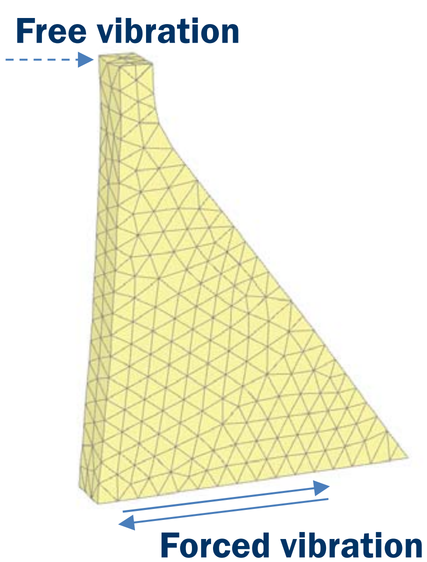

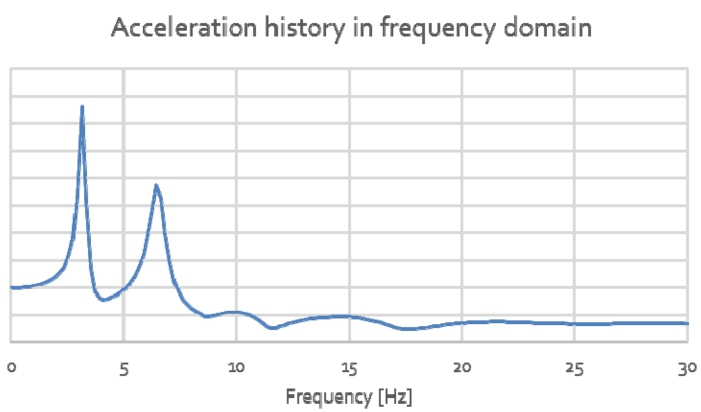

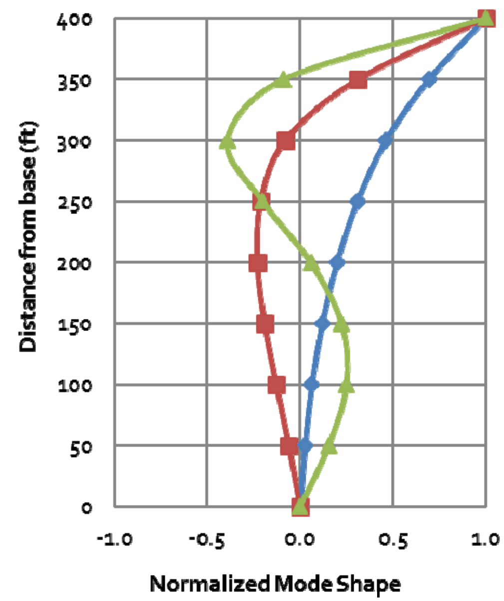

Challenges of using Plaxis 3D in dynamic analyses

- **Not able to capture dynamic effects of water pressure on upstream face of dam**

Workaround:

Model reservoir with continuum elements with unit weight of water, a Poisson's ratio close to 0.5 and a negligible shear strength to emulate fluid-like behavior

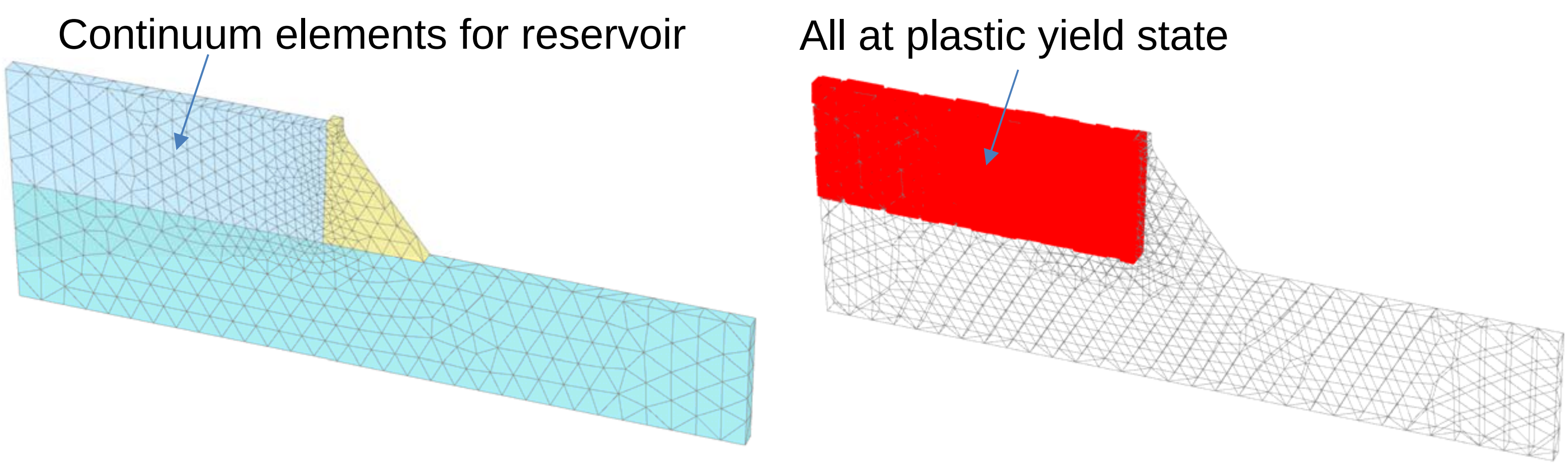

Key findings

- **Case B**
  - Extending far field boundary mitigates the influence of lateral boundaries
- **Case C**
  - The 1st natural frequencies for dam monolith and dam-reservoir system are 3.183 and 2.539 Hz, close to the values in Chopra et al (1980)
- **Case D**
  - Hydrodynamic effect of reservoir and flexible foundation reduces 1st natural frequencies.

Lessons learned

- Workaround solutions were needed for modal analyses with Plaxis 3D
- Current version of Plaxis 3D ignores hydrodynamic effects of reservoir under earthquake loading; Modeling water with continuum elements led to numerical difficulties.
- Mesh size was iteratively examined and adjusted to achieve convergence with acceptable computation time
- The option of using constant time step was preferred to facilitate debugging and post-processing

Future investigations

- Interface along dam base allowing sliding and overturning of dam monolith, and gap occurring between dam base and foundation
- Impact of fractures in concrete dam
- Hybrid analysis = particle based method for fluid phase + mesh based method for dam and foundation

Thanks!
Questions?

Yixing Yuan, Ph.D.
Yixing.Yuan@gza.com

Matthew A. Taylor, P.E.
Matthew.Taylor@gza.com

Numerical analysis of concrete dams
Workshop presentation

Brent Bergman, P. Eng.
Osmar Penner, Ph.D., P. Eng.
Mina Shahbazi, Ph.D., EIT
Jeff Yathon, EIT

3 May 2018

BC Hydro
Power smart

Contents

BC Hydro
Power smart

Model overview

BC Hydro
Power smart

Model overview

- LS-DYNA

BC Hydro
Power smart

Model overview

- LS-DYNA
- Explicit integration scheme

BC Hydro
Power smart

Model overview

- LS-DYNA
- Explicit integration scheme

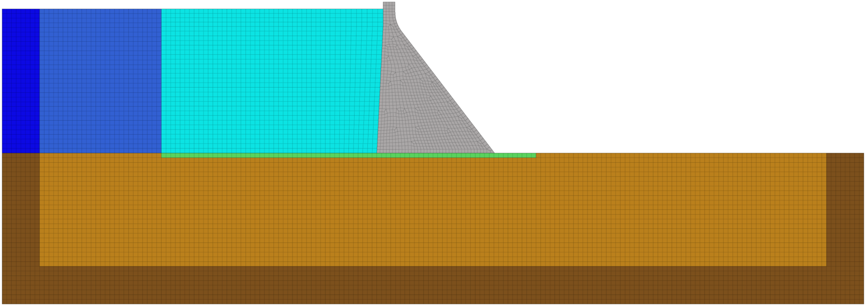

BC Hydro
Power smart

Model overview

- LS-DYNA
- Explicit integration scheme

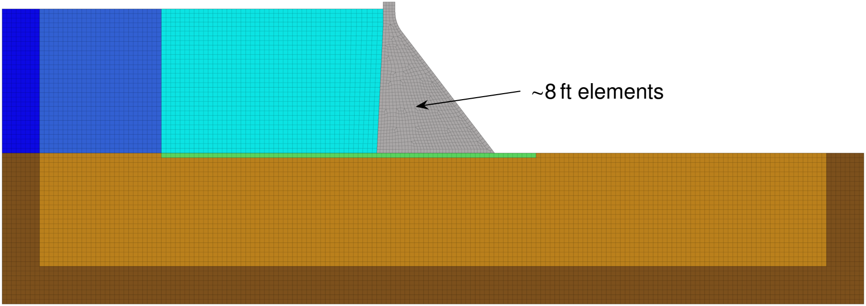

BC Hydro
Power smart

Model overview

- LS-DYNA
- Explicit integration scheme

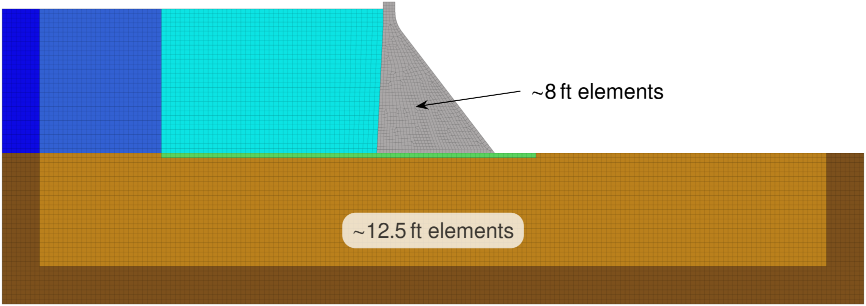

BC Hydro
Power smart

Model overview

- LS-DYNA
- Explicit integration scheme

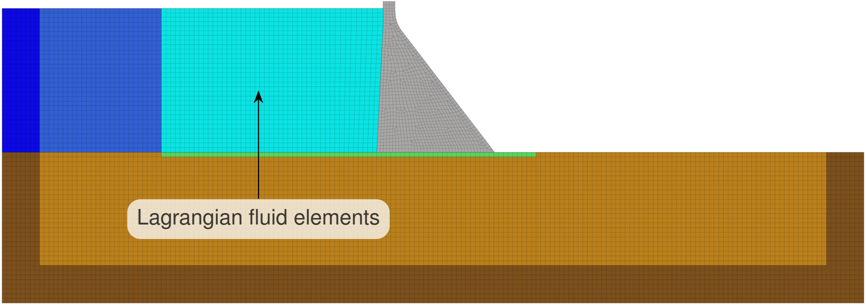

BC Hydro
Power smart

Model overview

- LS-DYNA
- Explicit integration scheme

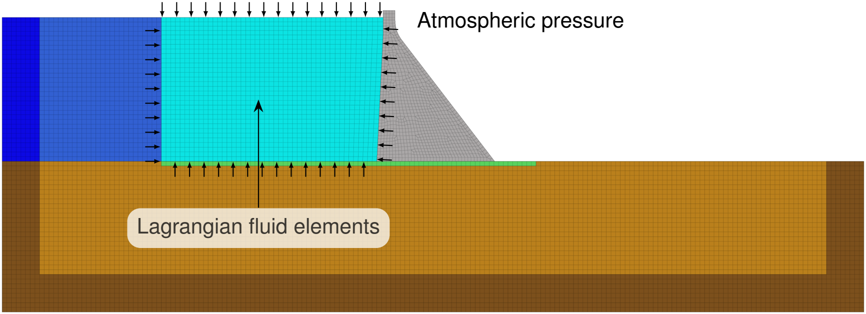

BC Hydro
Power smart

Model overview

- LS-DYNA
- Explicit integration scheme

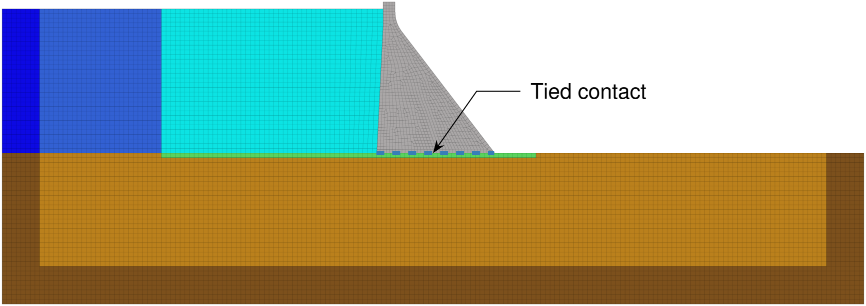

Model overview

- LS-DYNA
- Explicit integration scheme

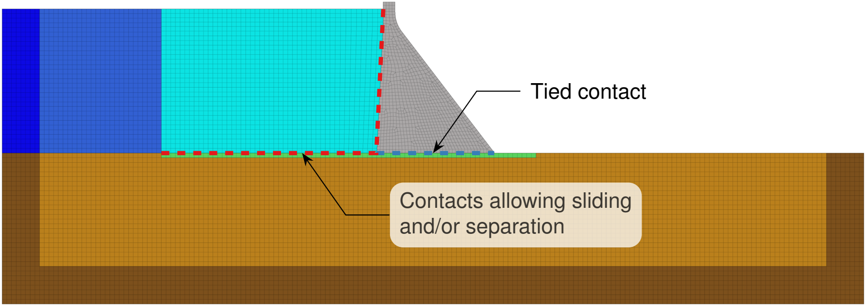

BC Hydro
Power smart

Model overview—effective seismic input method

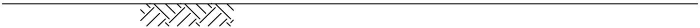

BC Hydro
Power smart

Model overview—effective seismic input method

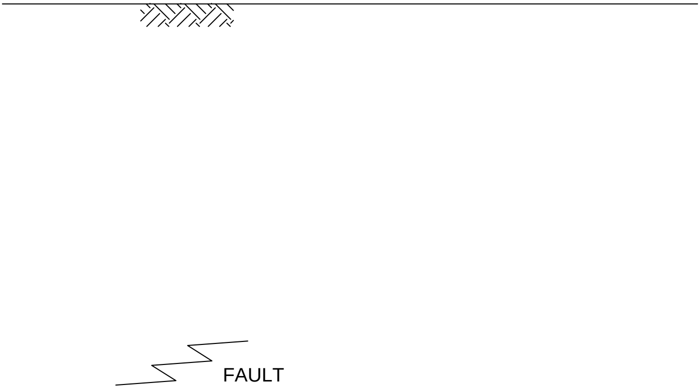

BC Hydro
Power smart

Model overview—effective seismic input method

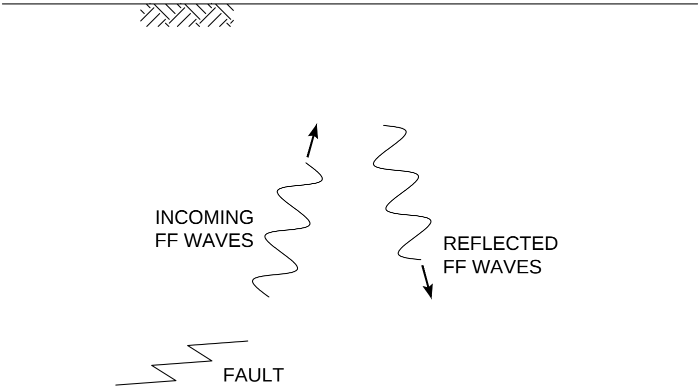

BC Hydro
Power smart

Model overview—effective seismic input method

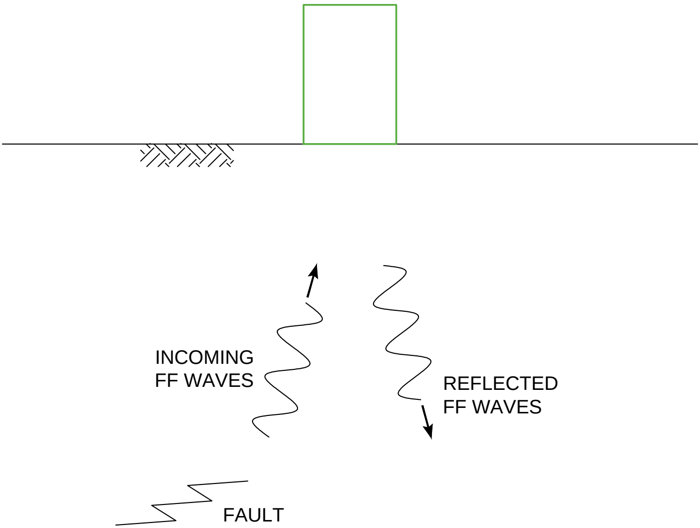

BC Hydro
Power smart

Model overview—effective seismic input method

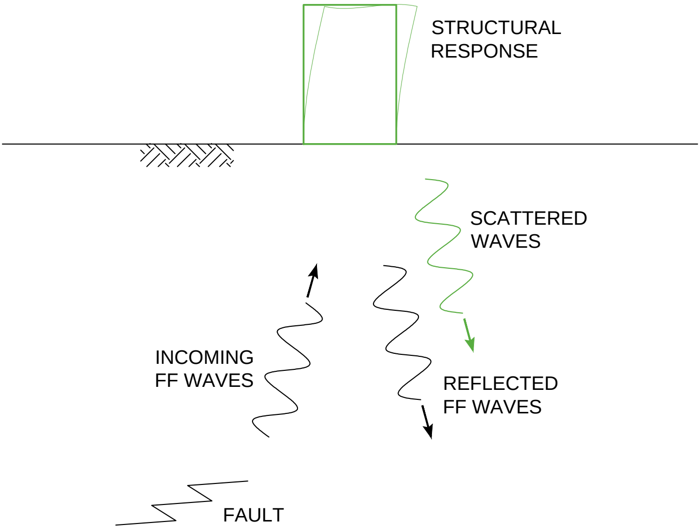

BC Hydro
Power smart

Model overview—effective seismic input method

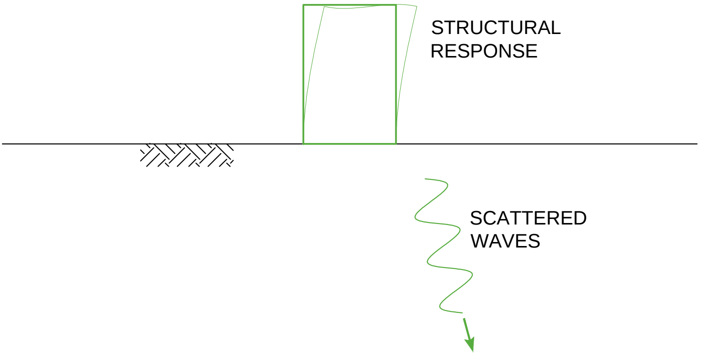

BC Hydro
Power smart

Model overview—effective seismic input method

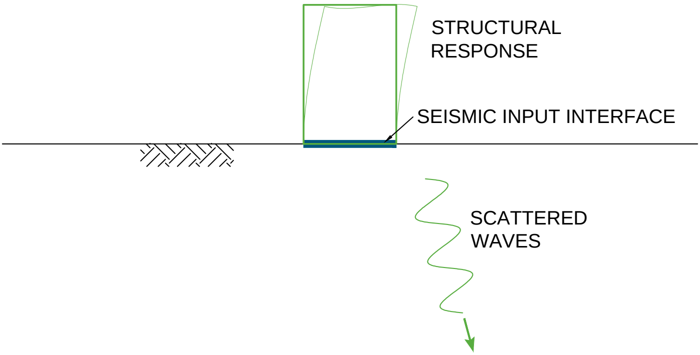

BC Hydro
Power smart

Model overview—effective seismic input method

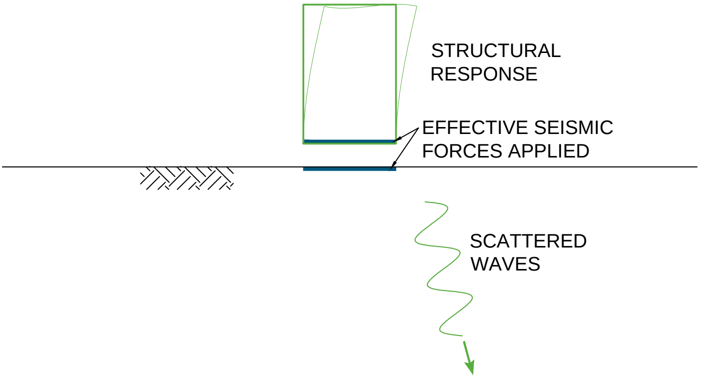

BC Hydro
Power smart

Model overview—effective seismic input method

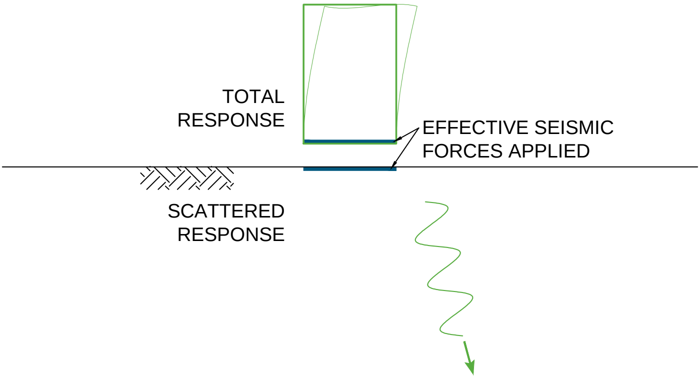

Model overview—effective seismic input method

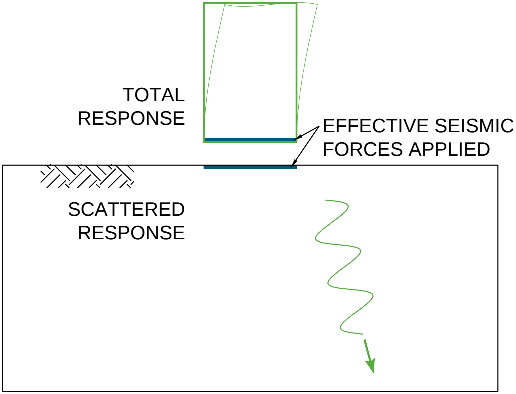

Model overview—effective seismic input method

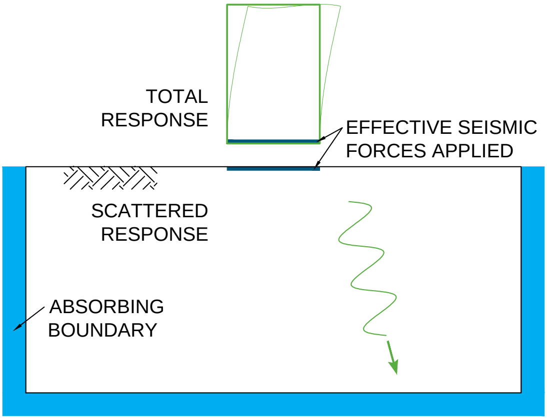

BC Hydro
Power smart

Model overview—effective seismic input method

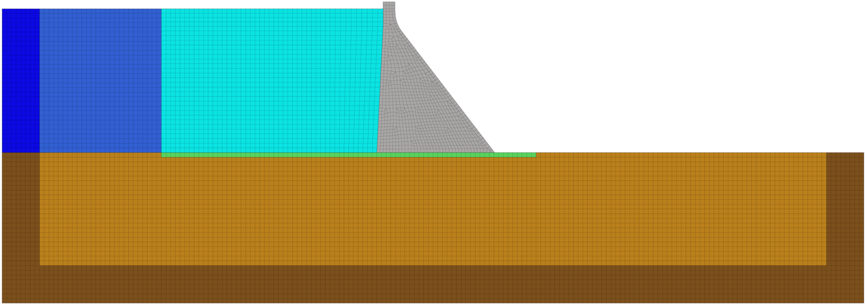

BC Hydro
Power smart

Model overview—effective seismic input method

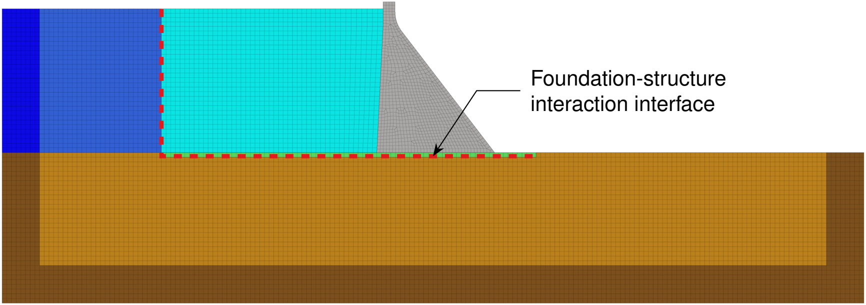

BC Hydro
Power smart

Model overview—effective seismic input method

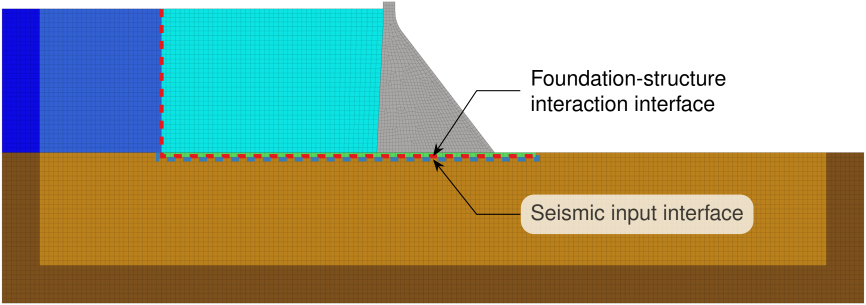

BC Hydro
Power smart

Model overview—effective seismic input method

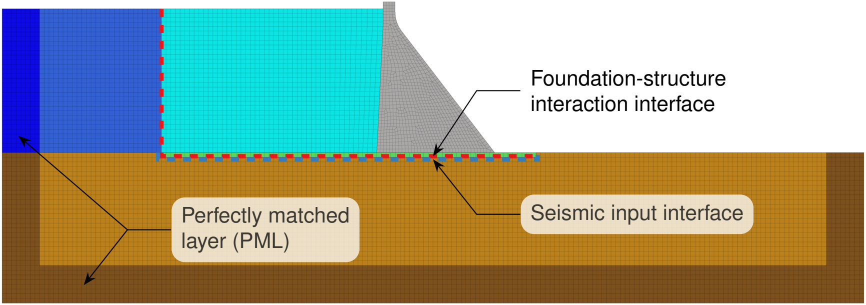

Frequency and damping

Frequency and damping

- PML does not permit solution of eigenvalues

BC Hydro
Power smart

Frequency and damping

- PML does not permit solution of eigenvalues
- Borrow from experimental modal analysis

BC Hydro
Power smart

Frequency and damping

- PML does not permit solution of eigenvalues
- Borrow from experimental modal analysis

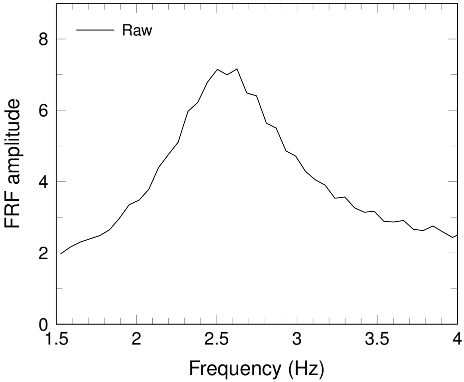

Frequency and damping

- PML does not permit solution of eigenvalues
- Borrow from experimental modal analysis

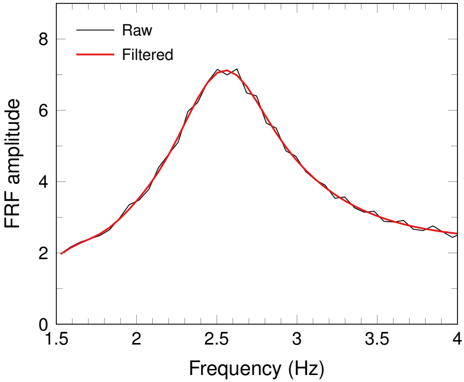

BC Hydro
Power smart

Frequency and damping

- PML does not permit solution of eigenvalues
- Borrow from experimental modal analysis

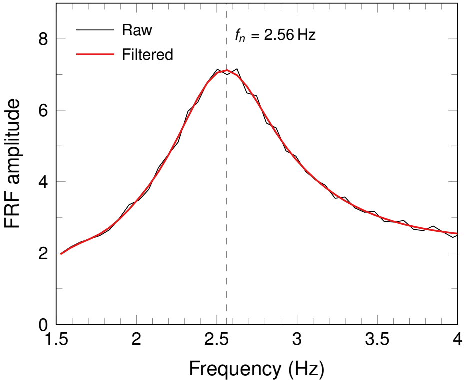

Frequency and damping

- PML does not permit solution of eigenvalues
- Borrow from experimental modal analysis

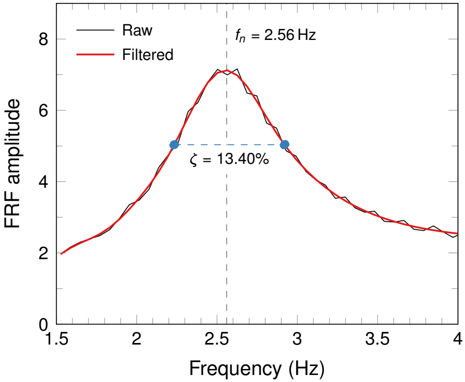

BC Hydro
Power smart

Frequency and damping

Frequency and damping

- Can determine total damping

BC Hydro
Power smart

Frequency and damping

- Can determine total damping
- Specify ~5% damping

BC Hydro
Power smart

Frequency and damping

- Can determine total damping
- Specify ~5% damping
  - Remainder due to radiation damping

BC Hydro
Power smart

Frequency and damping

- Can determine total damping
- Specify ∼5% damping
  - Remainder due to radiation damping

	No reservoir		
	f_n (Hz)	ζ (%)	
$E_f = E_c$	2.6	13.4	

BC Hydro
Power smart

Frequency and damping

- Can determine total damping
- Specify ∼5% damping
    - Remainder due to radiation damping

	No reservoir		
	f_n (Hz)	ζ (%)	
$E_f = E_c$	2.6	13.4	
$E_f = 3E_c$	3.1	7.4	
$E_f = \infty$	3.4	5.5	

Frequency and damping

- Can determine total damping
- Specify ~5% damping
    - Remainder due to radiation damping

	No reservoir		With reservoir	
	f_n (Hz)	ζ (%)	f_n (Hz)	ζ (%)
$E_f = E_c$	2.6	13.4	2.1	13.0
$E_f = 3E_c$	3.1	7.4	2.4	8.2
$E_f = \infty$	3.4	5.5	2.7	6.1

BC Hydro
Power smart

2D seismic input

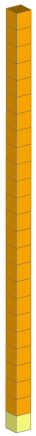

BC Hydro
Power smart

2D seismic input

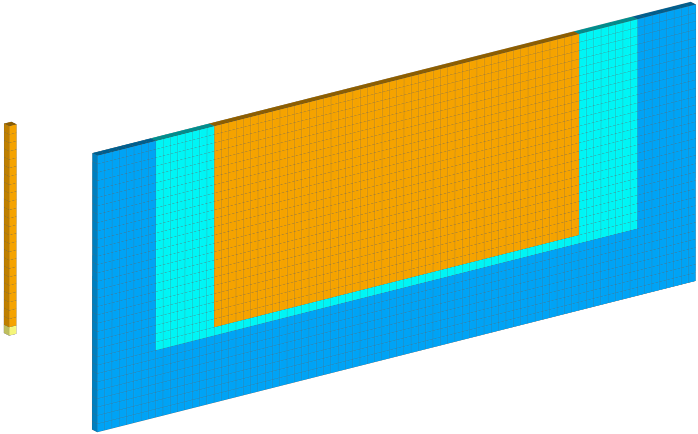

BC Hydro
Power smart

2D seismic input

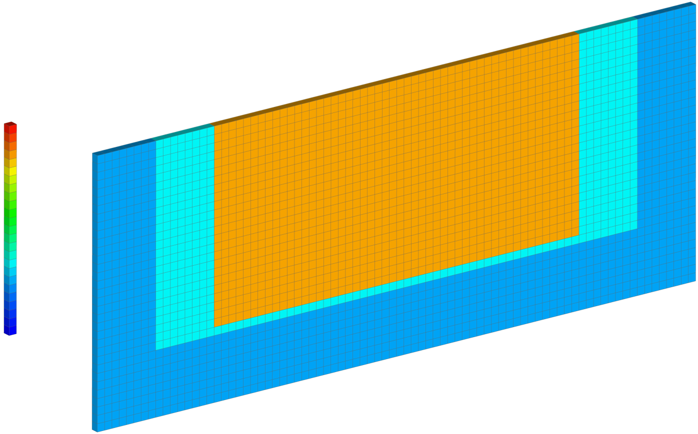

BC Hydro
Power smart

2D seismic input

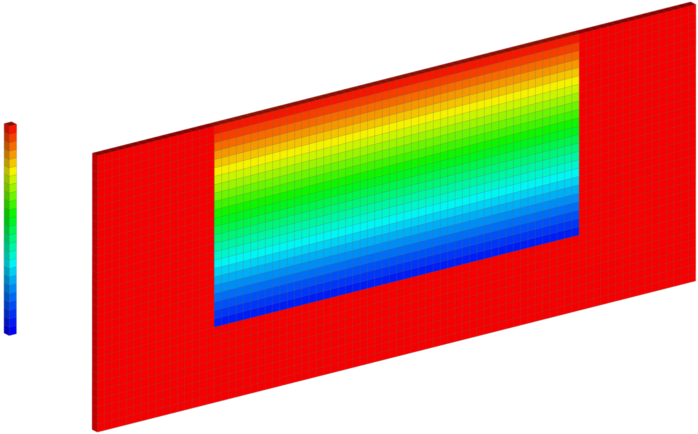

2D seismic input

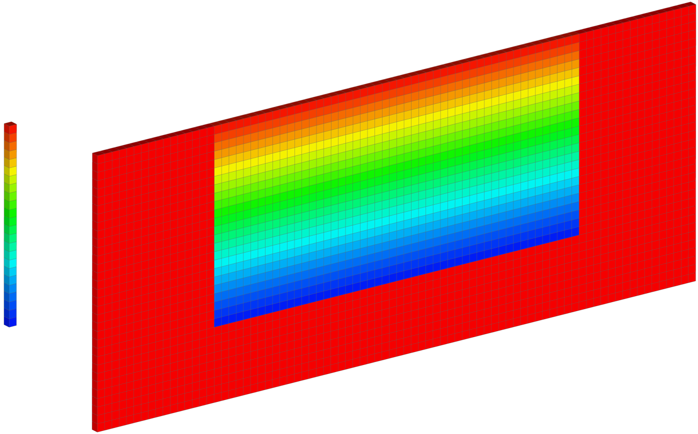

BC Hydro
Power smart

2D seismic input

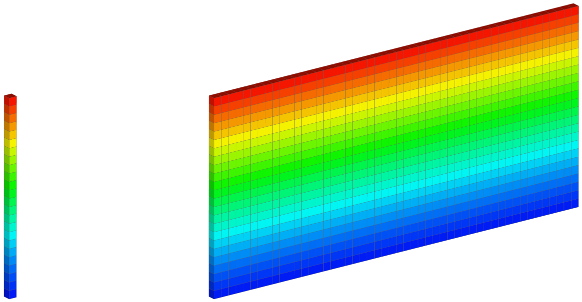

BC Hydro
Power smart

2D seismic input

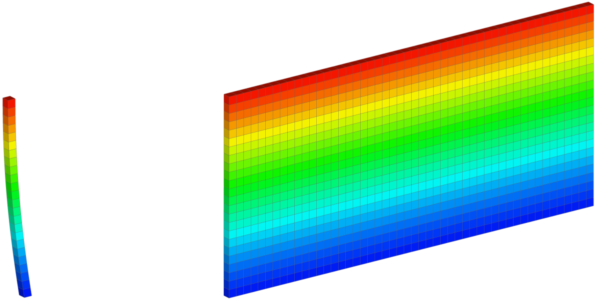

BC Hydro
Power smart

2D seismic input

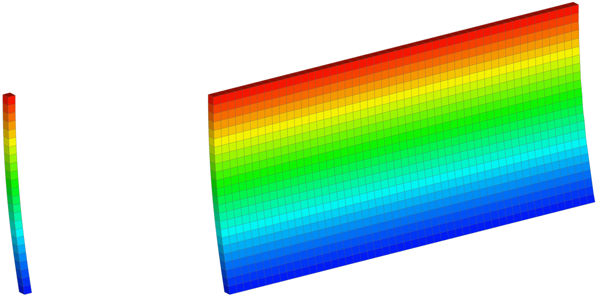

BC Hydro
Power smart

2D seismic input

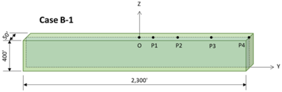

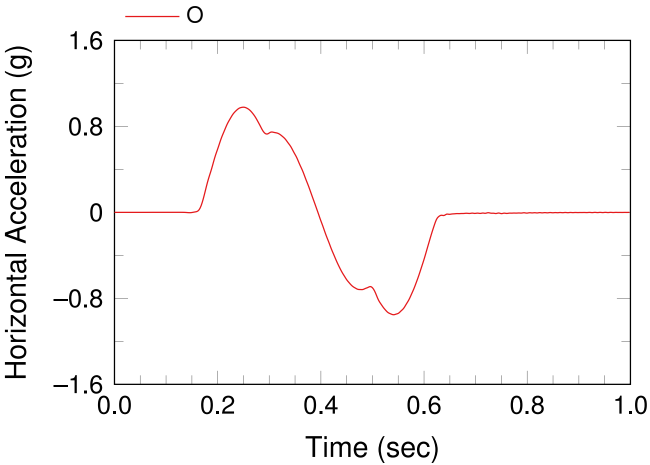

BC Hydro
Power smart

2D seismic input

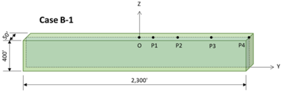

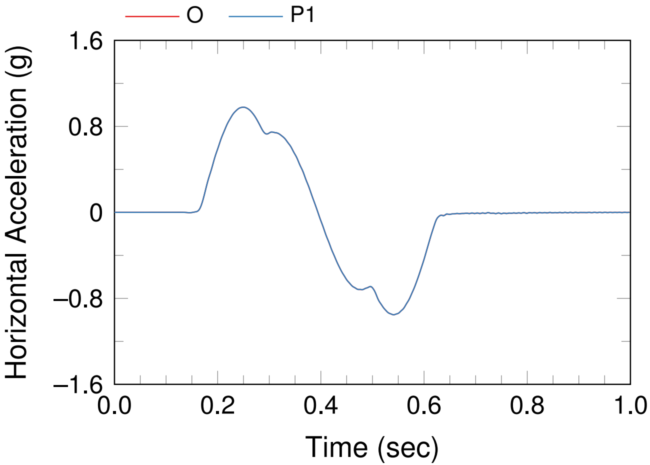

BC Hydro
Power smart

2D seismic input

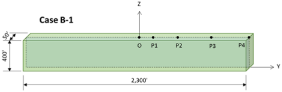

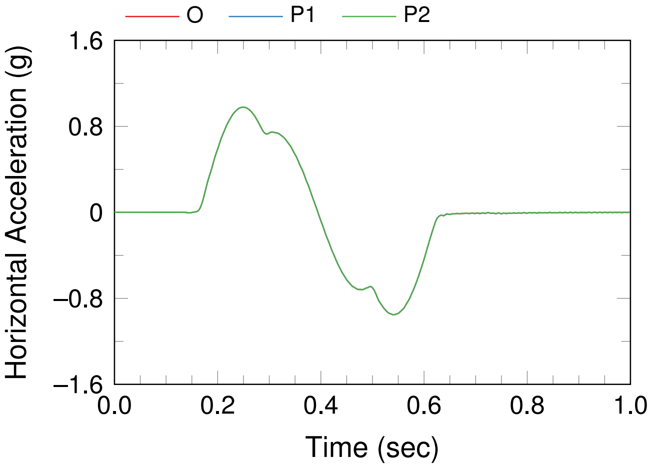

BC Hydro
Power smart

2D seismic input

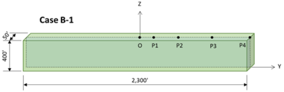

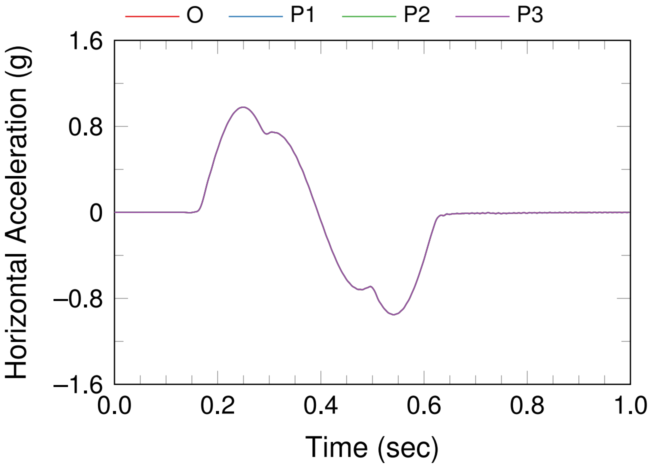

BC Hydro
Power smart

Foundation extent

Foundation extent

- Foundation extent was fixed in the workshop

Foundation extent

- Foundation extent was fixed in the workshop
- Displacement reported, but not a good measure for ESIM

BC Hydro
Power smart

Foundation extent

- Foundation extent was fixed in the workshop
- Displacement reported, but not a good measure for ESIM
  - Look at stress convergence instead

BC Hydro
Power smart

Foundation extent

- Foundation extent was fixed in the workshop
- Displacement reported, but not a good measure for ESIM
  - Look at stress convergence instead

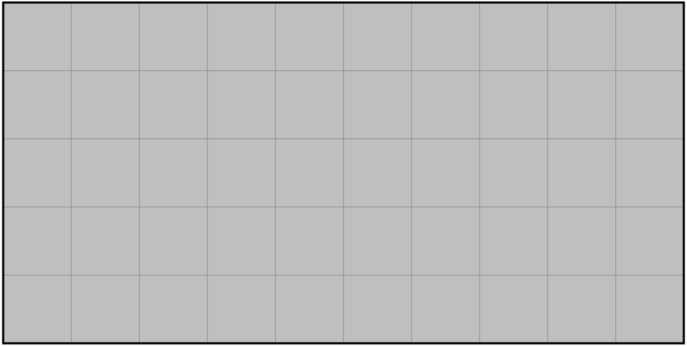

BC Hydro
Power smart

Foundation extent

- Foundation extent was fixed in the workshop
- Displacement reported, but not a good measure for ESIM
  - Look at stress convergence instead

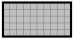

BC Hydro Power smart

Foundation extent

- Foundation extent was fixed in the workshop
- Displacement reported, but not a good measure for ESIM
  - Look at stress convergence instead

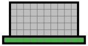

BC Hydro
Power smart

Foundation extent

- Foundation extent was fixed in the workshop
- Displacement reported, but not a good measure for ESIM
    - Look at stress convergence instead

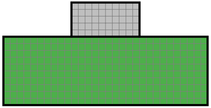

BC Hydro
Power smart

Foundation extent

- Foundation extent was fixed in the workshop
- Displacement reported, but not a good measure for ESIM
  - Look at stress convergence instead

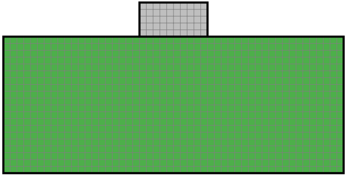

BC Hydro
Power smart

Foundation extent

- Foundation extent was fixed in the workshop
- Displacement reported, but not a good measure for ESIM
    - Look at stress convergence instead

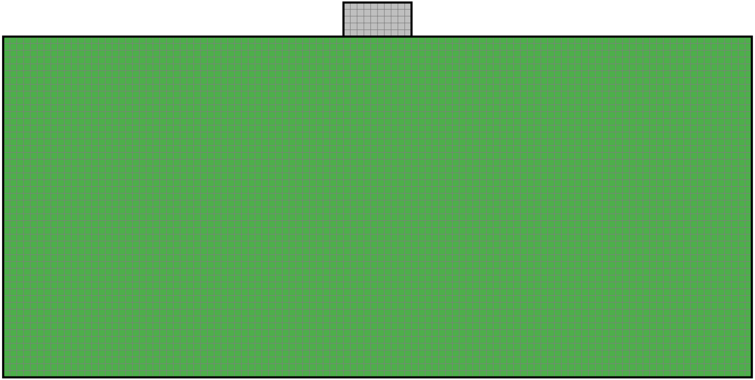

Foundation extent

- Foundation extent was fixed in the workshop
- Displacement reported, but not a good measure for ESIM
  - Look at stress convergence instead

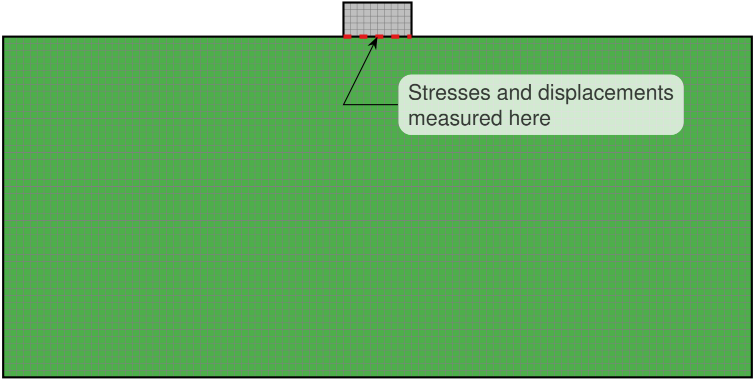

BC Hydro
Power smart

Foundation extent

- Foundation extent was fixed in the workshop
- Displacement reported, but not a good measure for ESIM
  - Look at stress convergence instead

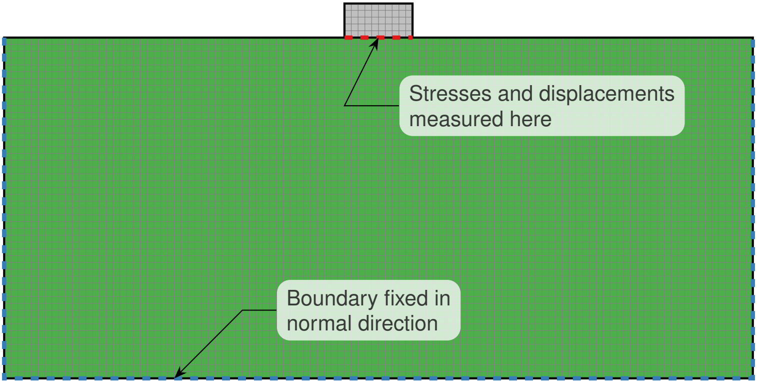

BC Hydro
Power smart

Foundation extent

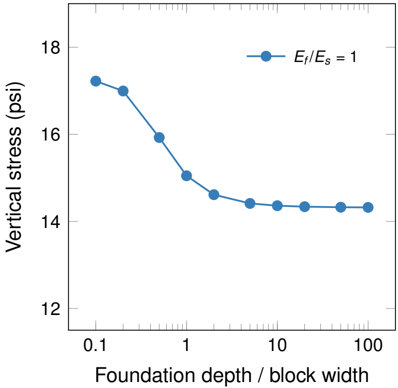

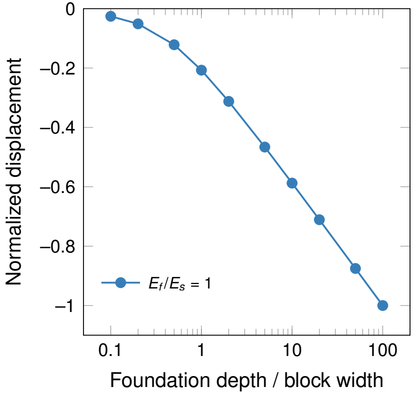

BC Hydro
Power smart

Foundation extent

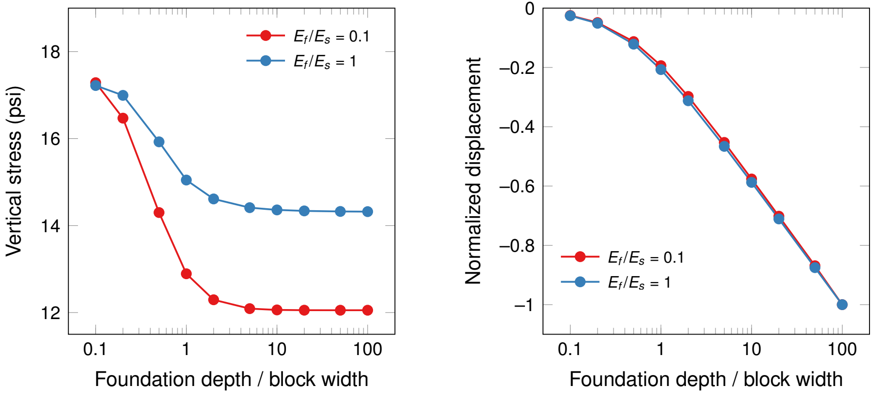

BC Hydro
Power smart

Foundation extent

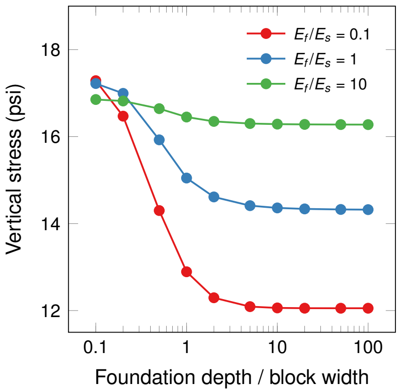

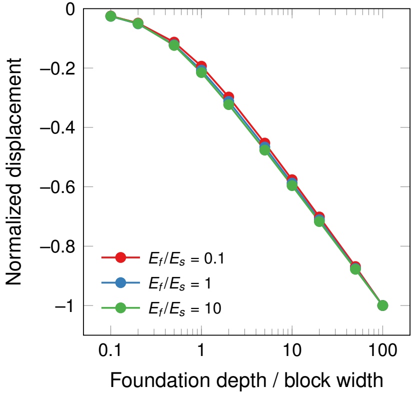

BC Hydro
Power smart

Foundation extent

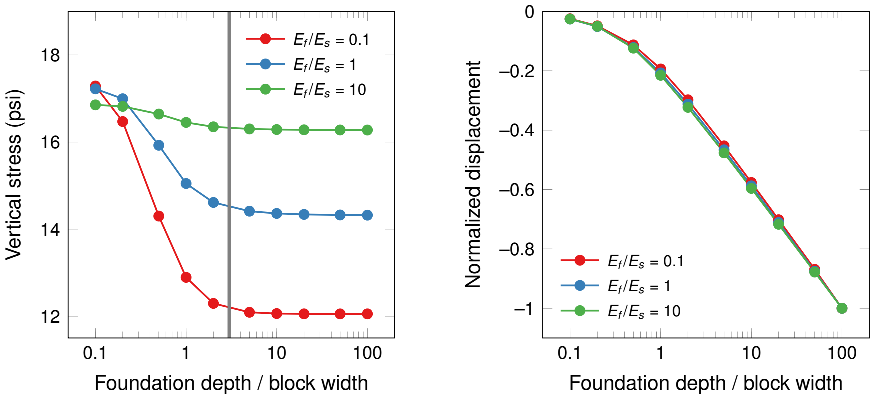

BC Hydro
Power smart

Future work—fracture and sliding

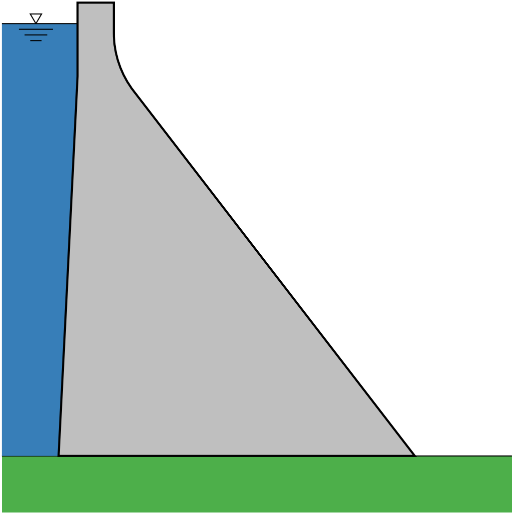

BC Hydro
Power smart

Future work—fracture and sliding

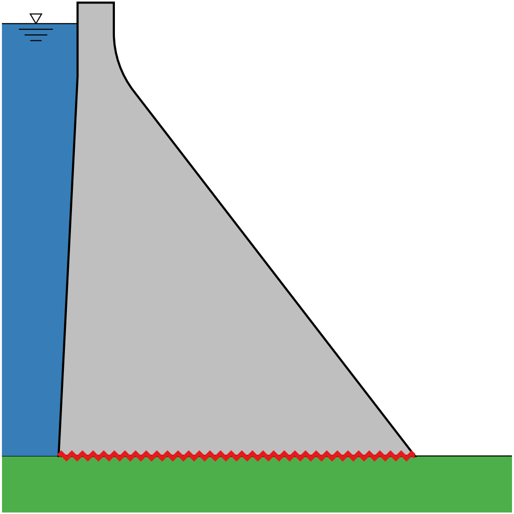

BC Hydro
Power smart

Future work—fracture and sliding

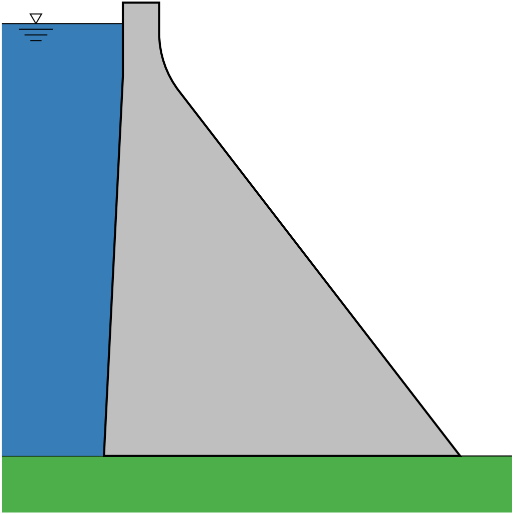

BC Hydro
Power smart

Future work—fracture and sliding

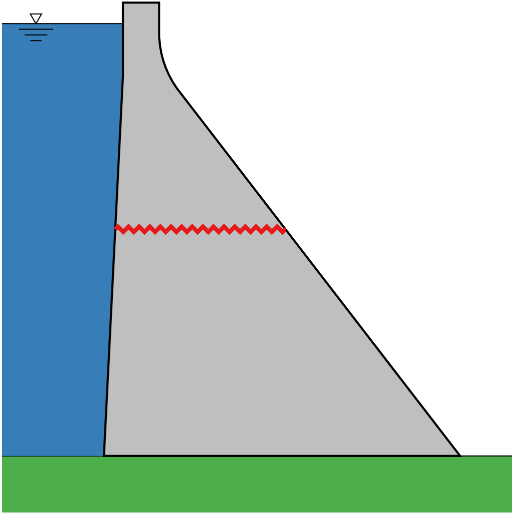

BC Hydro
Power smart

Future work—fracture and sliding

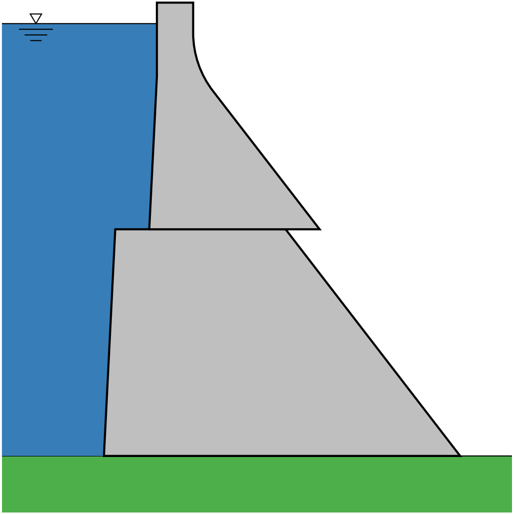

Future work—fracture and sliding

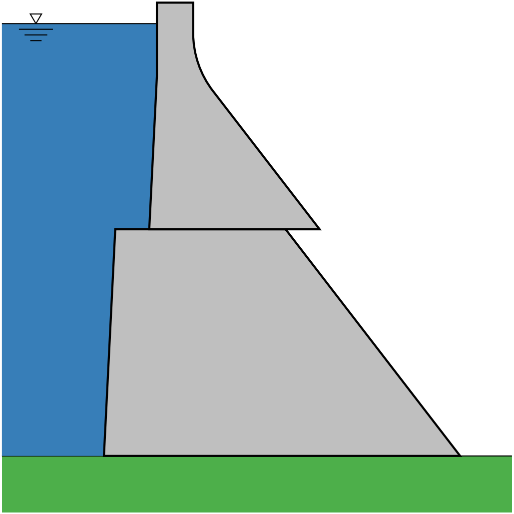

Main issues:

BC Hydro
Power smart

Future work—fracture and sliding

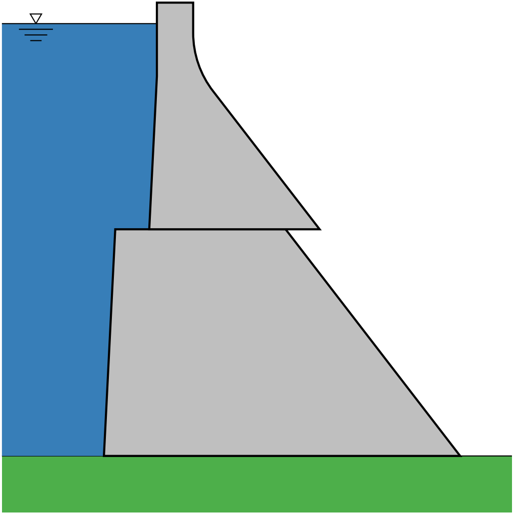

Main issues:

- Bond strength

BC Hydro
Power smart

Future work—fracture and sliding

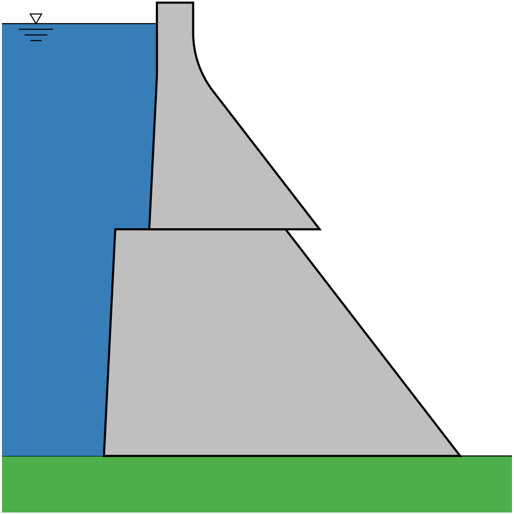

Main issues:

- Bond strength
- Fracture

BC Hydro
Power smart

Future work—fracture and sliding

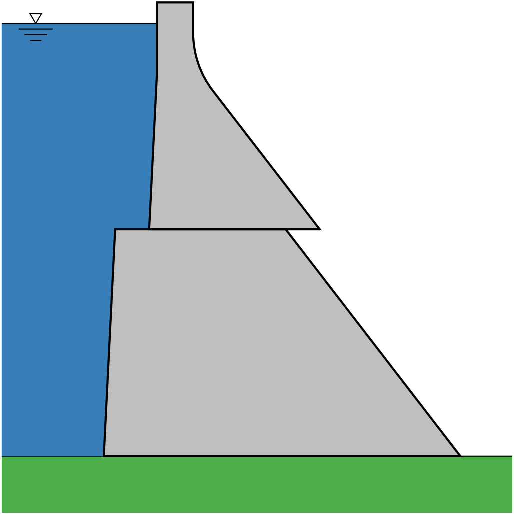

Main issues:

- Bond strength
- Fracture
- Friction parameters

BC Hydro
Power smart

Future work—fracture and sliding

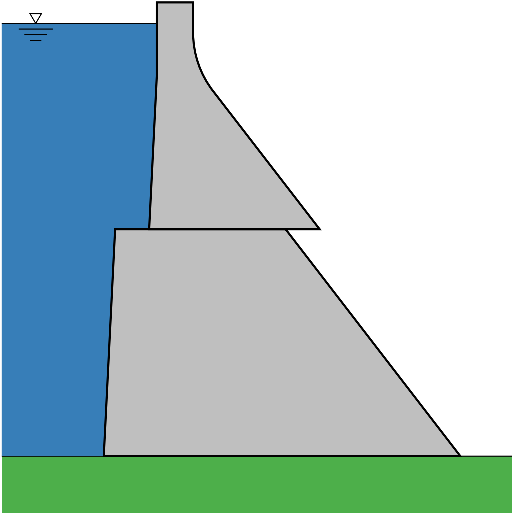

Main issues:

- Bond strength
- Fracture
- Friction parameters
- Stick-slip

BC Hydro
Power smart

Future work—3D seismic input

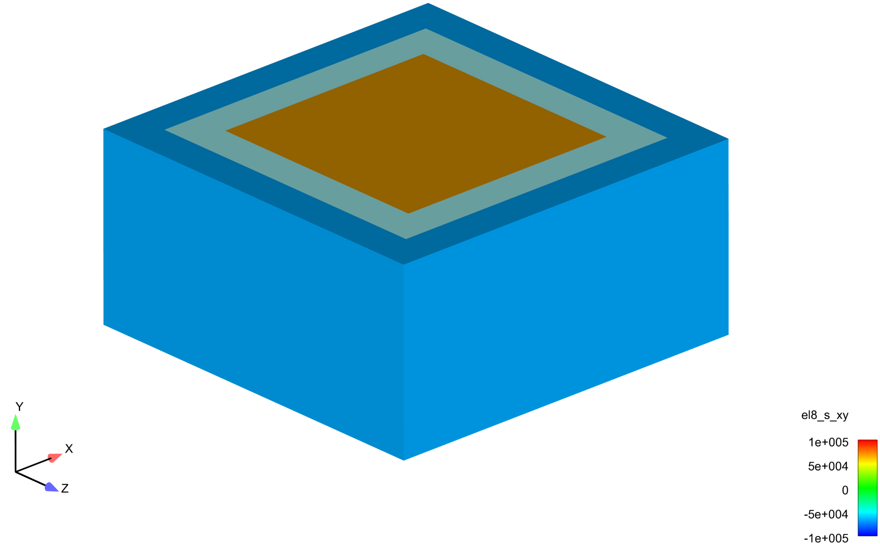

BC Hydro
Power smart

Future work—3D seismic input

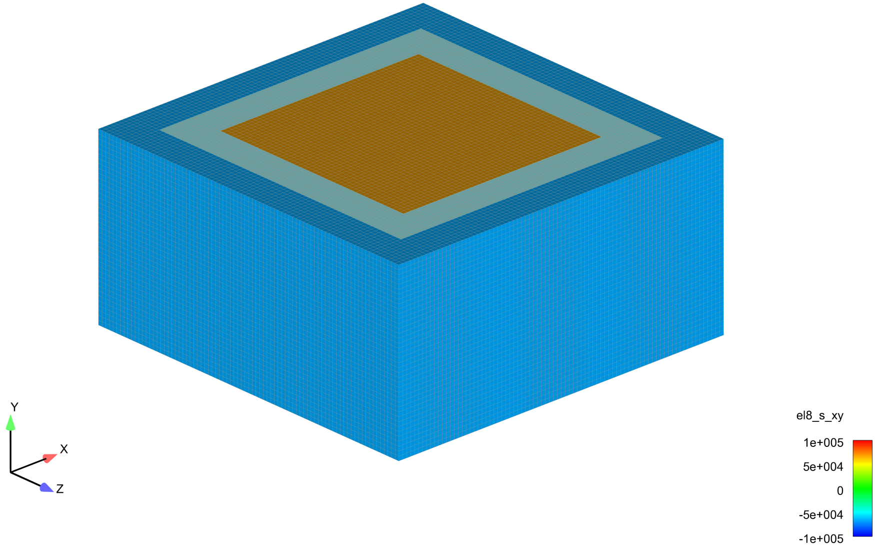

BC Hydro
Power smart

Future work—3D seismic input

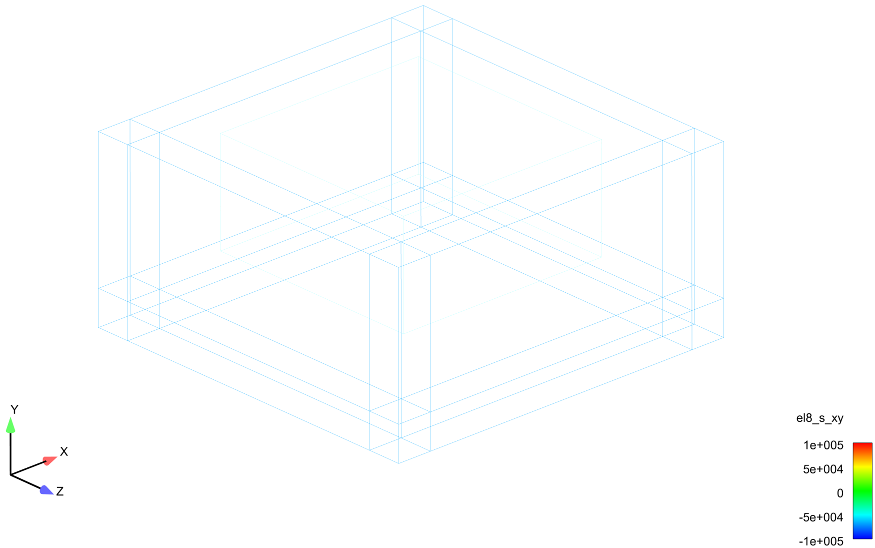

BC Hydro
Power smart

Future work—3D seismic input

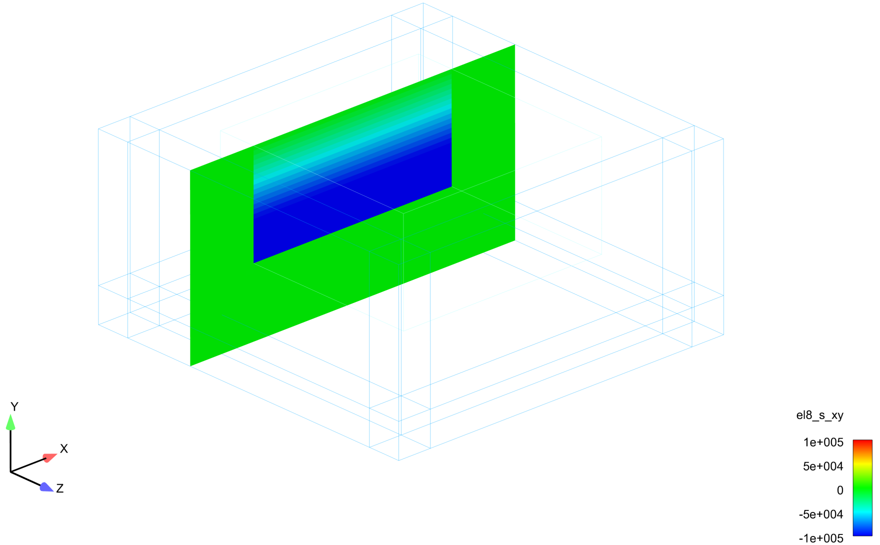

BC Hydro
Power smart

Future work—3D seismic input

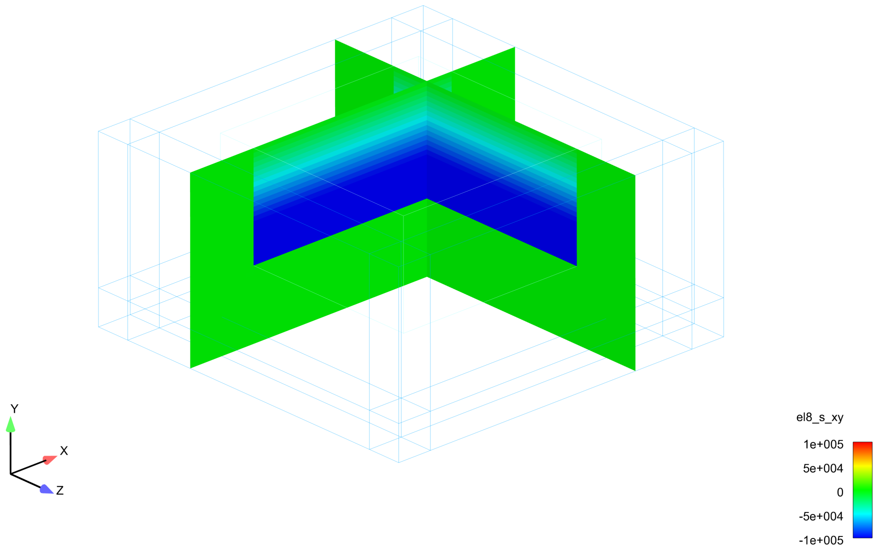

BC Hydro
Power smart

Future work—3D seismic input

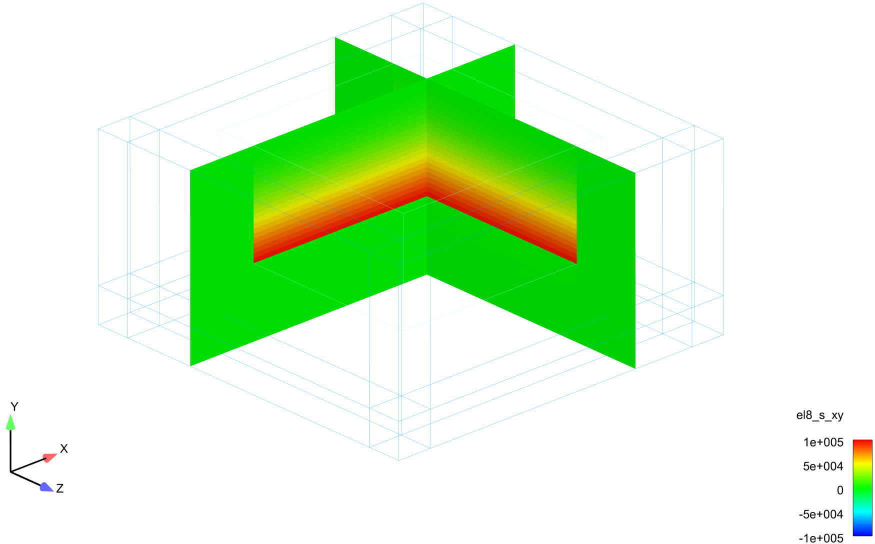

BC Hydro
Power smart

Future work—3D seismic input

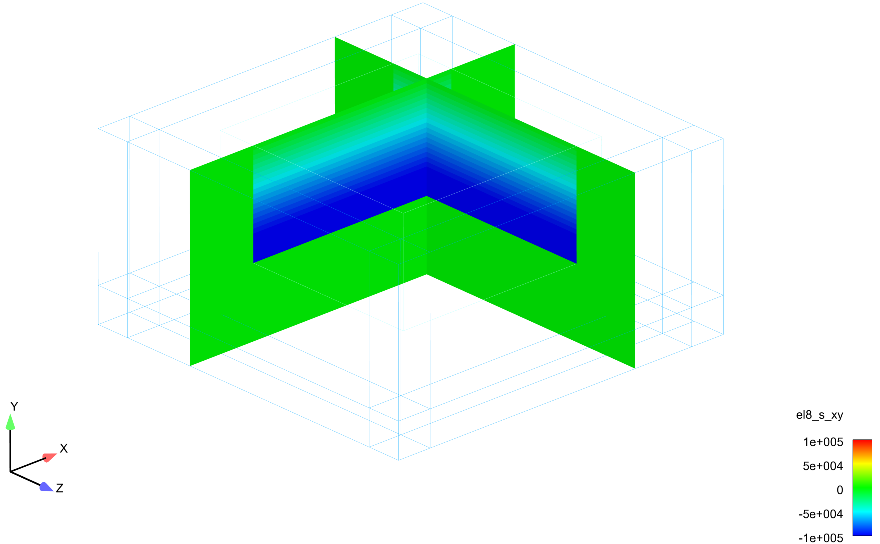

BC Hydro
Power smart

Future work—3D seismic input

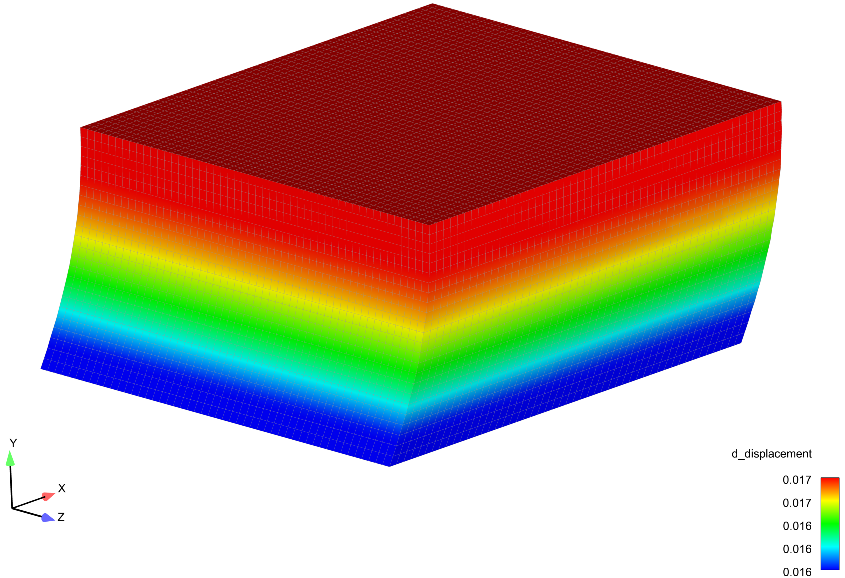

BC Hydro
Power smart

Future work—3D seismic input

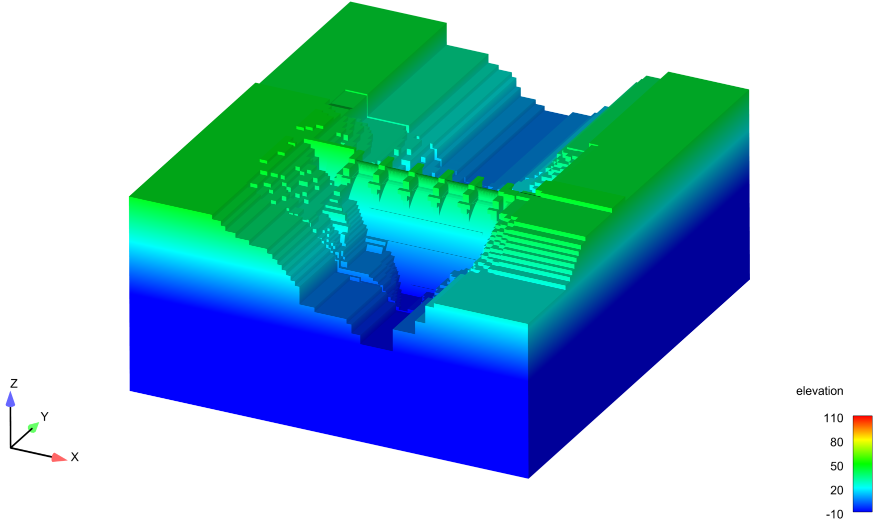

Future work—3D seismic input

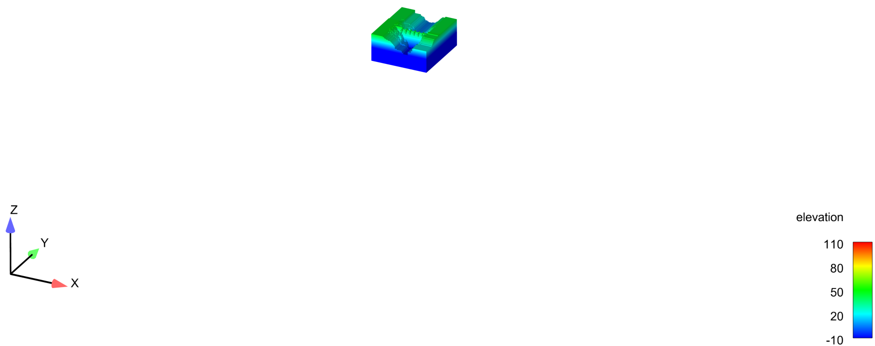

BC Hydro
Power smart

Future work—3D seismic input

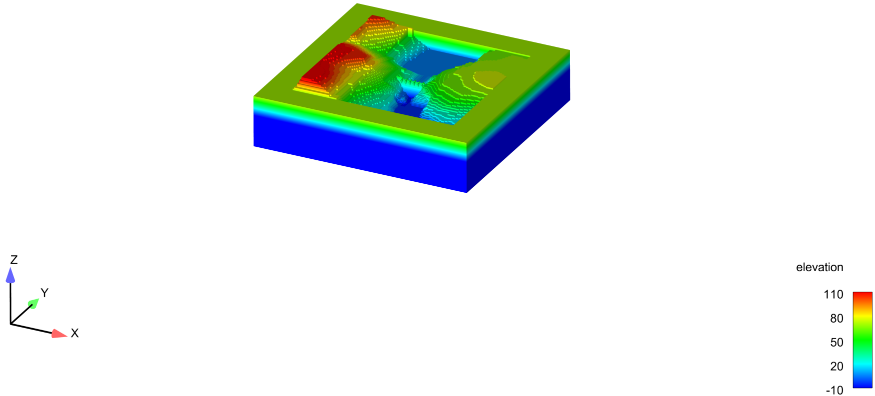

BC Hydro
Power smart

Future work—3D seismic input

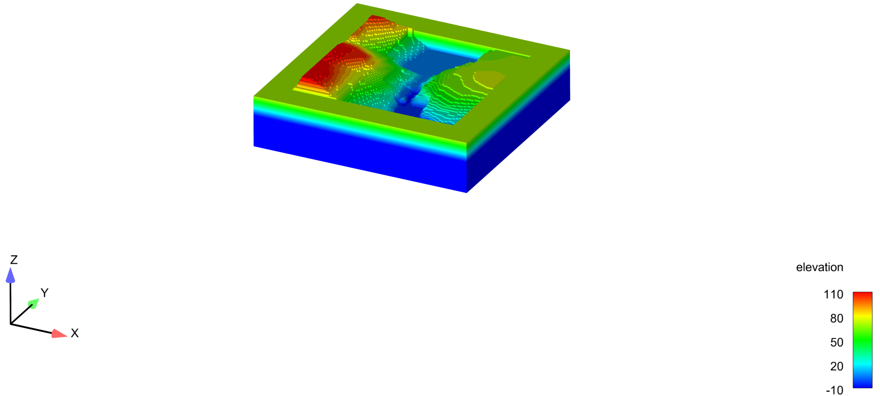

BC Hydro
Power smart

Future work—3D seismic input

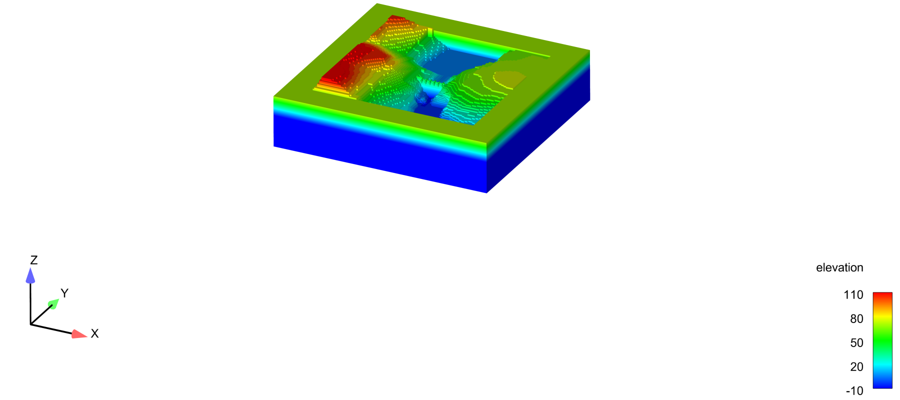

BC Hydro
Power smart

Future work—3D seismic input

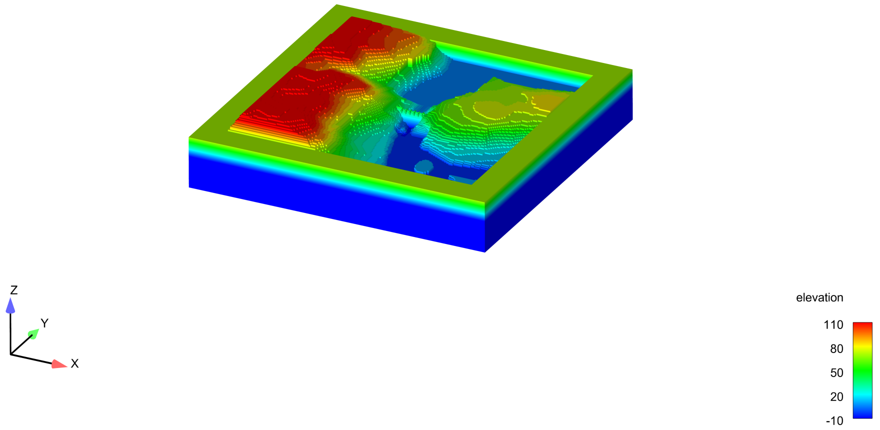

BC Hydro
Power smart

Future work—3D seismic input

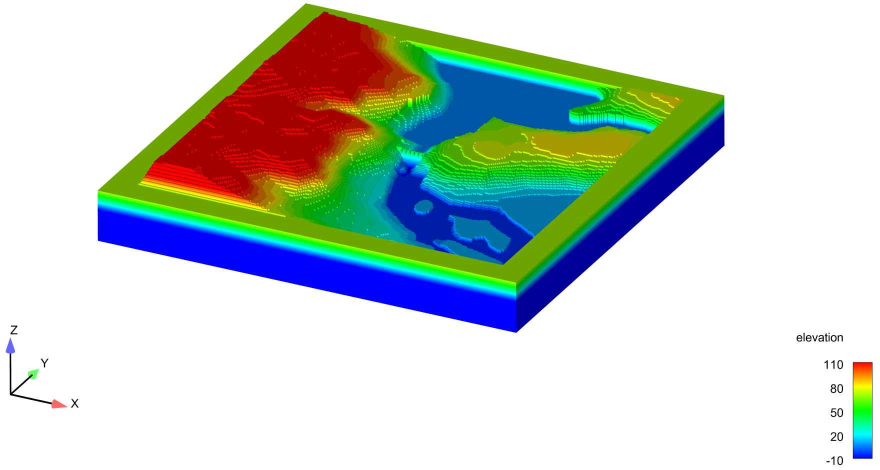

BC Hydro
Power smart

Future work—3D seismic input

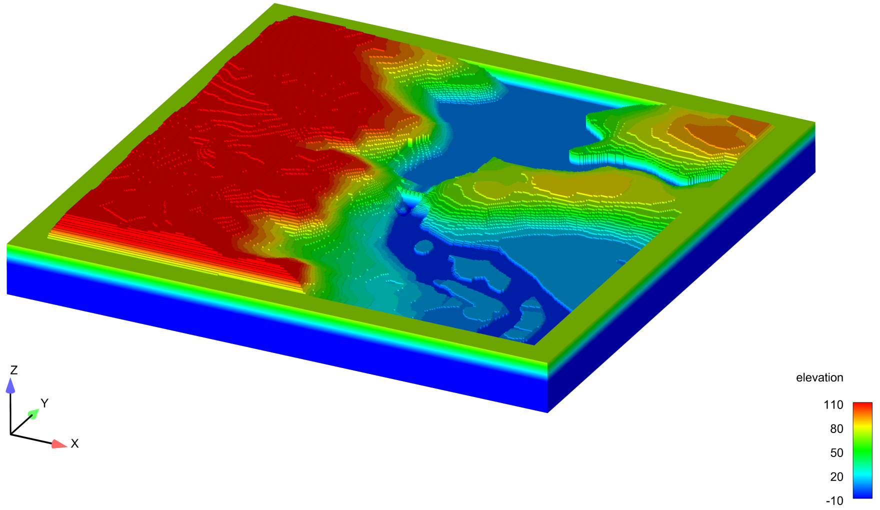

BC Hydro
Power smart

Future work—shear keys

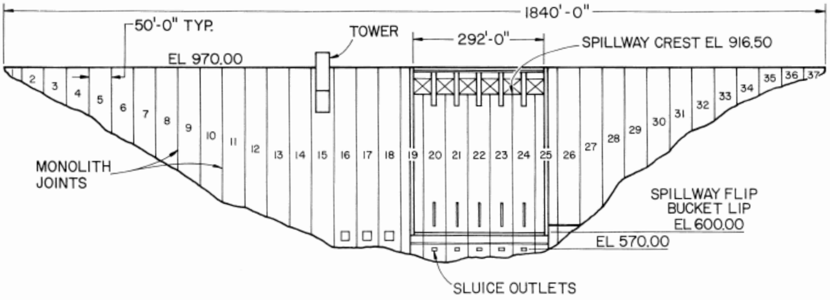

BC Hydro
Power smart

Future work—shear keys

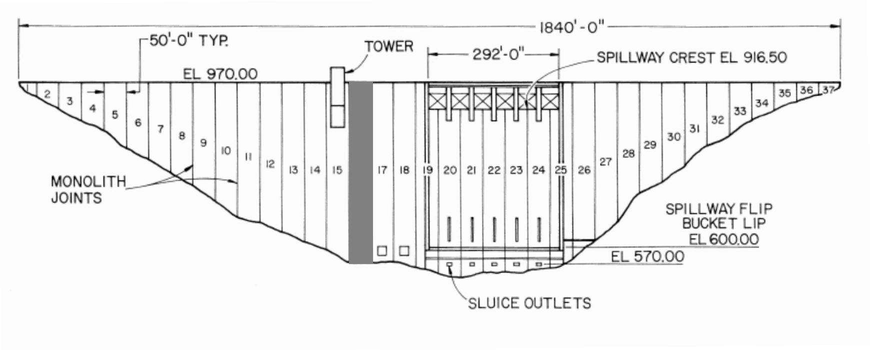

BC Hydro
Power smart

Future work—shear keys

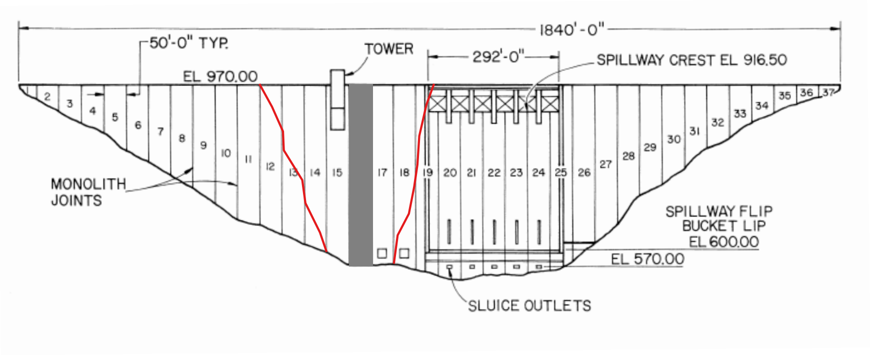

BC Hydro
Power smart

Questions?

BC Hydro
Power smart

RECLAMATION

Managing Water in the West

Workshop Discussion on

EVALUATION OF NUMERICAL MODELS AND INPUT PARAMETERS IN THE ANALYSIS OF CONCRETE DAMS

USSD 2018 Annual Conference, Miami

U.S. Department of the Interior
Bureau of Reclamation

Team members

- Roman Koltuniuk
- Sherry Hamedian
- Lan Nguyen

RECLAMATION

Model information, boundary conditions

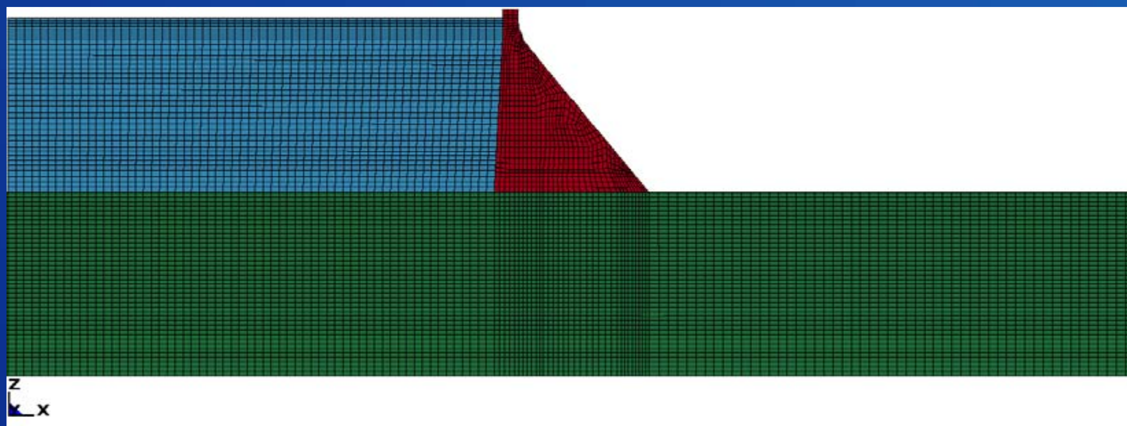

<u>Model detail</u>

* 63,490 nodes

* 53,148 solid elements

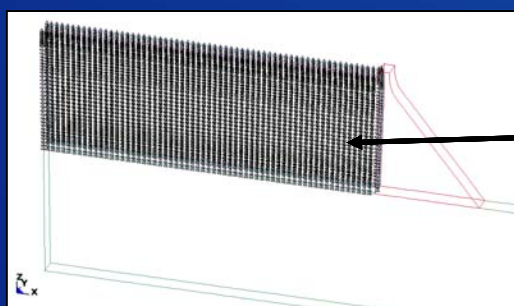

Restrains in cross canyon for reservoir

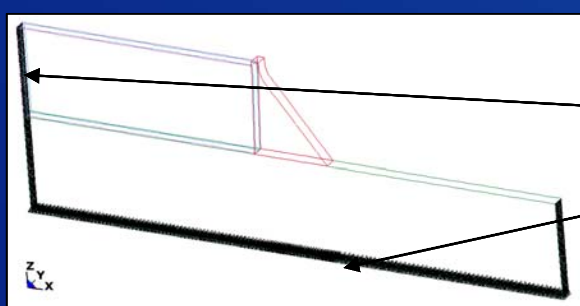

Boundary conditions at the base of foundation

And locations of non-reflecting boundary conditions

RECLAMATION

Submitted results for cases

- **Case A: static analysis**

- **Case C: rigid foundation**

  ***Modal analysis**

  ***Dynamic analysis with Harmonic load and ETAFT load**

- **Case D: soft foundation**

  ***Modal analysis**

  ***Dynamic analysis with ETAFT and TAFT loads**

- **Case E: stiff foundation**

  *** Dynamic analysis with ETAFT and TAFT loads**

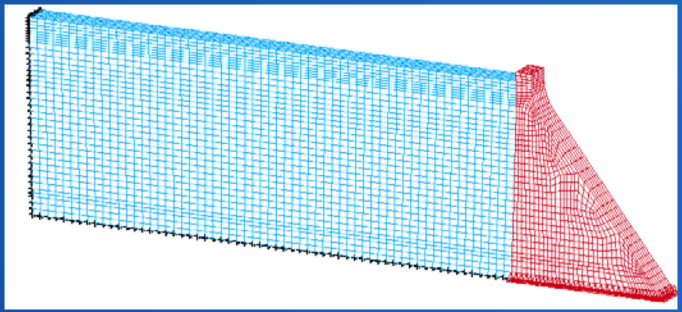

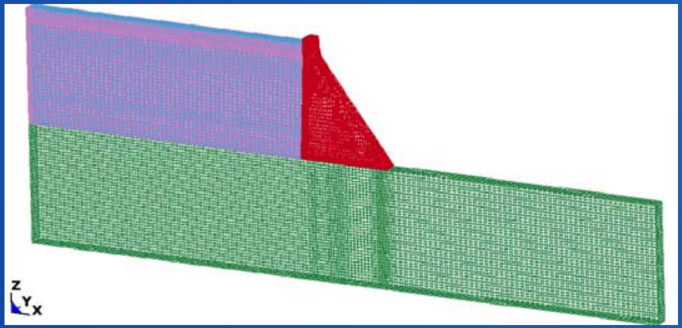

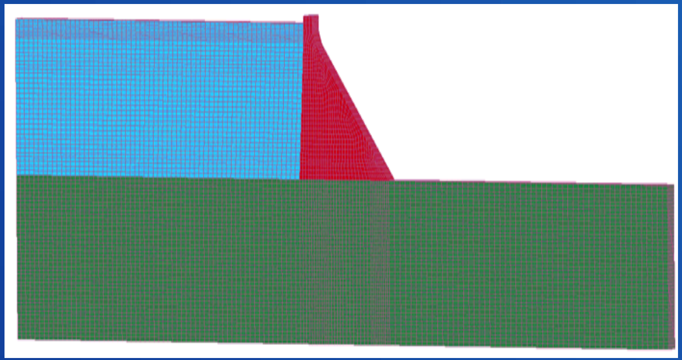

RECLAMATION

Results/Findings

1. Deconvolution, loading verification from full 3D to 2D sectional models

2. Natural frequencies, vertical stresses at upstream dam face and foundation stiffness.

3. Effect of frequencies and non-reflecting BCs to the pressure profiles.

4. Effect of damping to the stress time history.

Deconvolution, loading verification from full 3D to 2D sectional models

Free field response spectrum and deconvolved response spectrum for full 3D foundation model

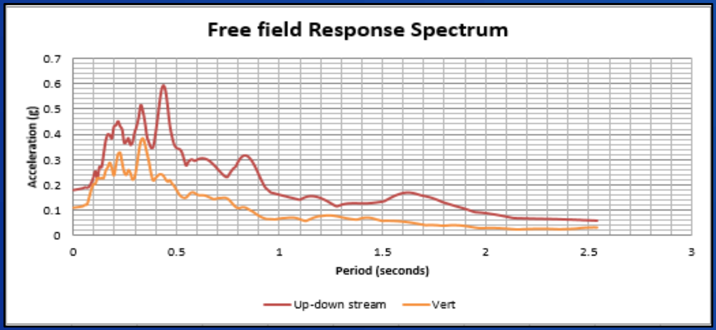

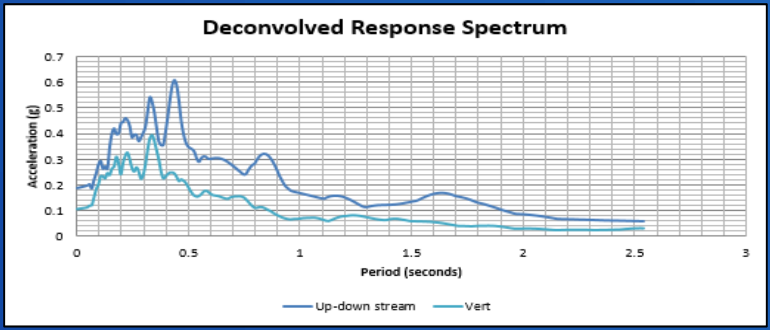

Free field response spectrum and deconvolved response spectrum for 50 foot section of foundation model

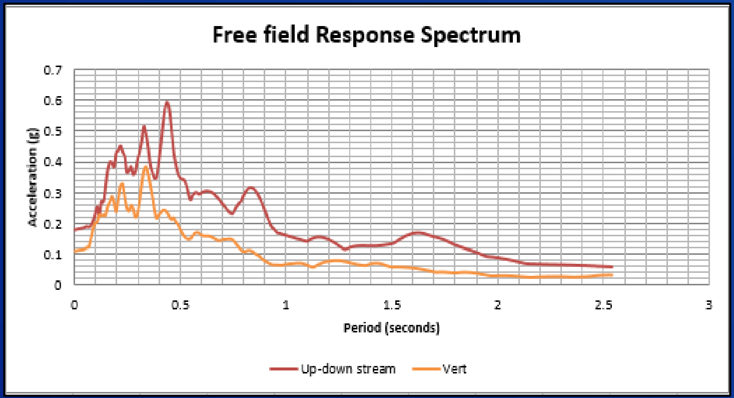

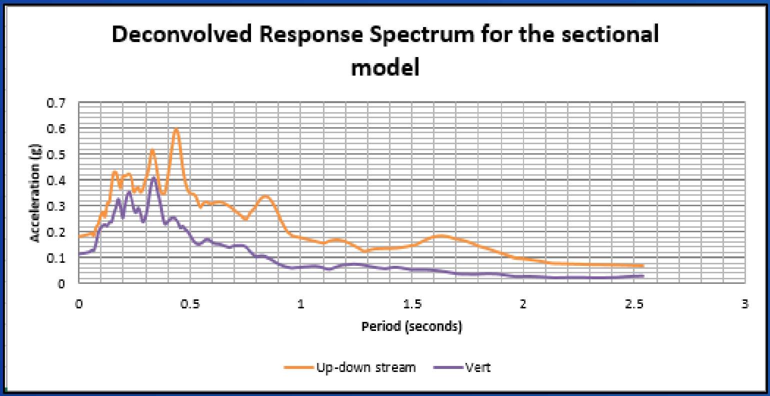

RECLAMATION

Natural Frequencies and Foundation (FDN) Stiffness

Dam and Foundation

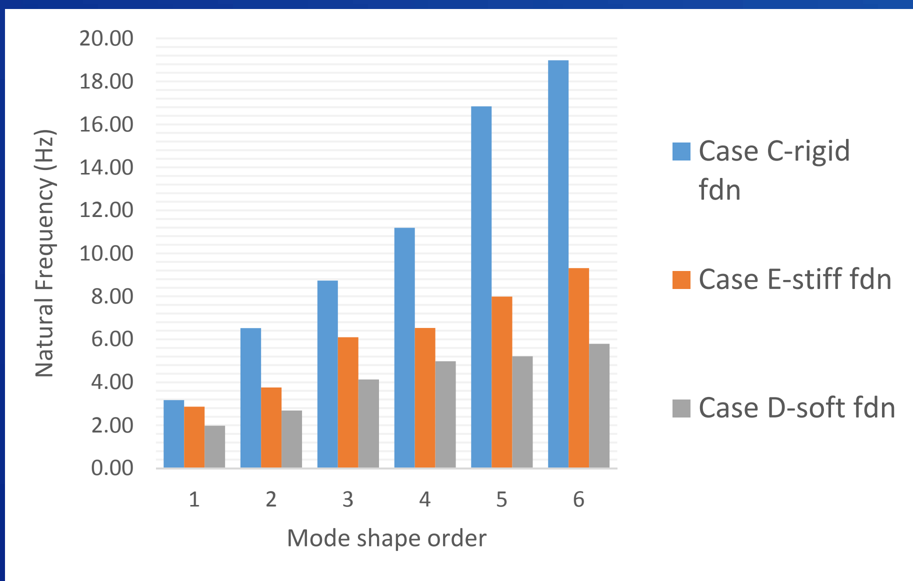

Dam, Foundation, and Reservoir

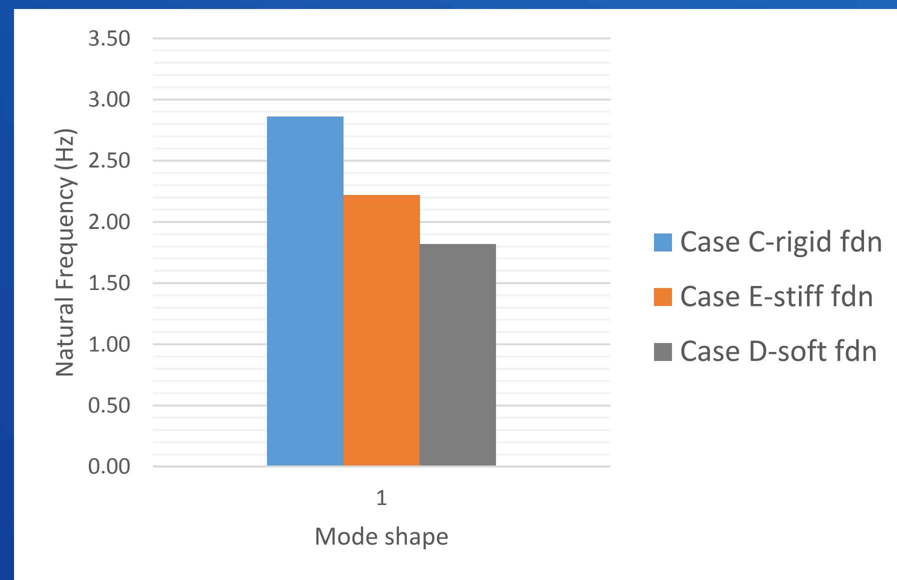

RECLAMATION

Vertical stress at dam heel and Foundation (FDN) Stiffness

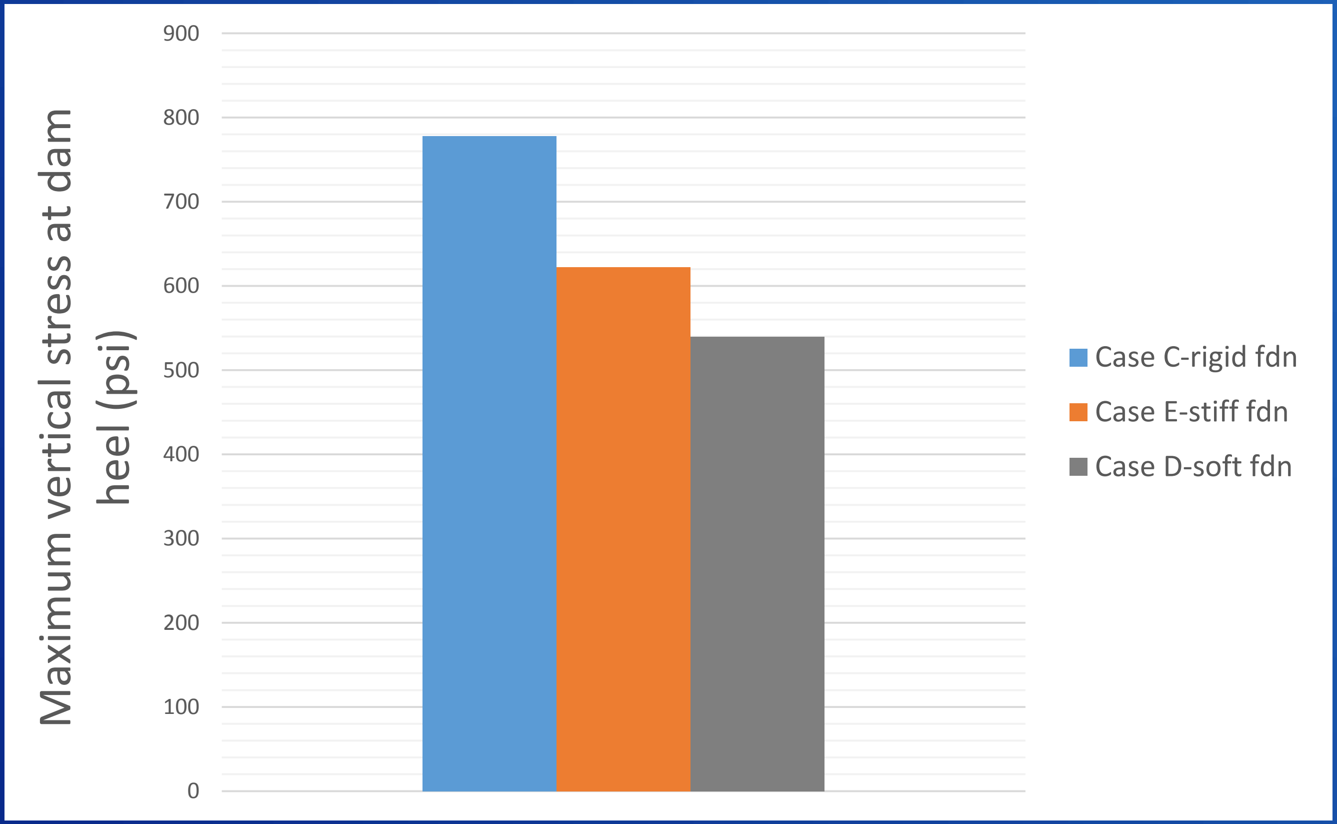

RECLAMATION

Effects of frequencies and non-reflecting boundary conditions to the pressure profiles.

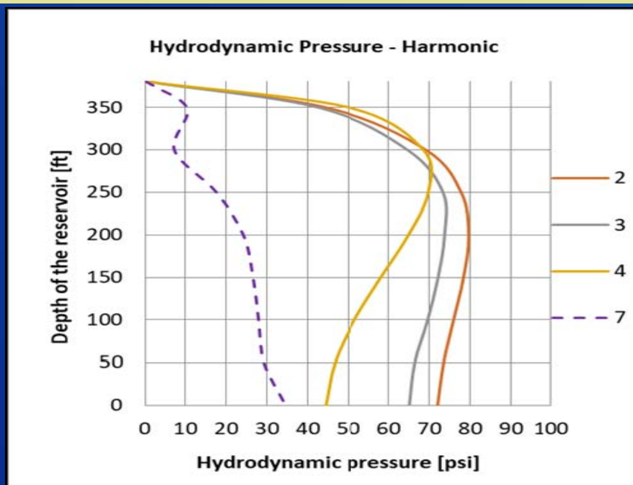

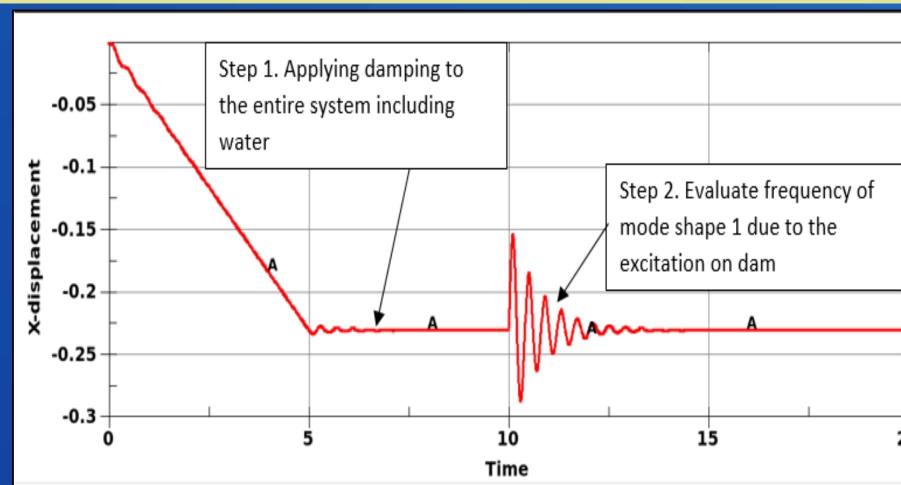

	Amplitude=	0.1	g
	Frequency =	2.82	Hz
	Offset =	0	seconds
	Time increment=	0.01	seconds
	Time =	5	seonds
Time		Time funciton	
0.000	10.000	0	
0.010	10.010	0.017626016	
0.020	10.020	0.034700113	
0.030	10.030	0.050687653	
0.040	10.040	0.065088023	

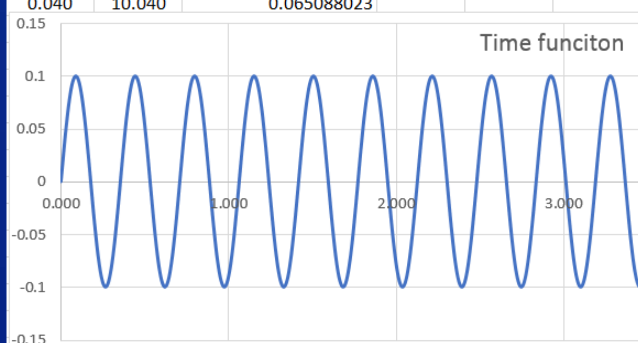

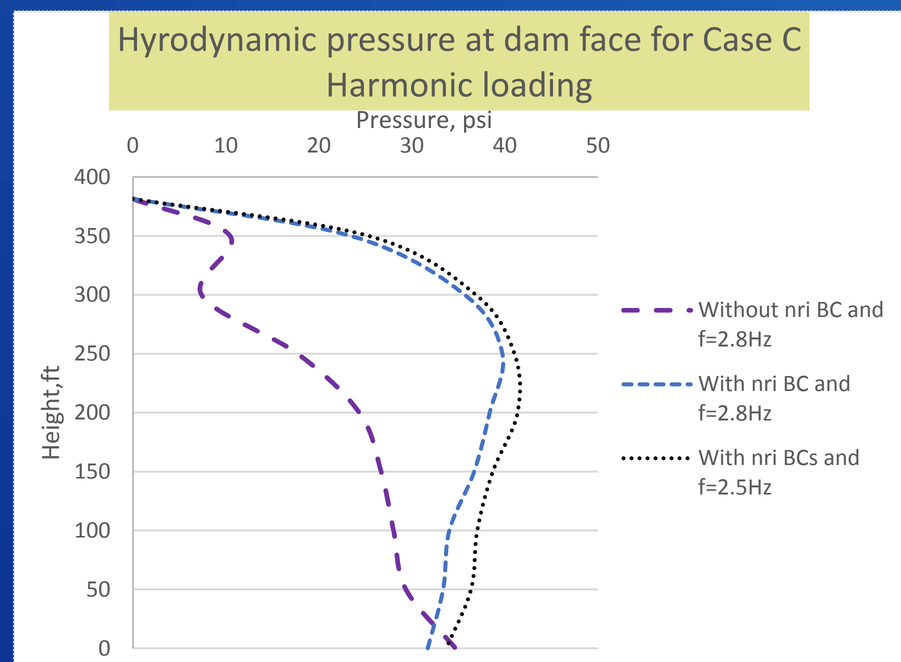

Effects of frequency and non-reflecting boundary conditions to the pressure profiles.

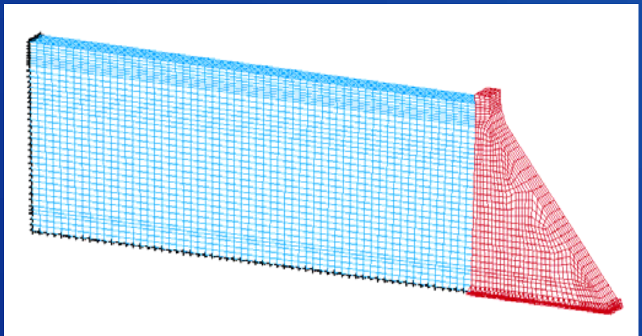

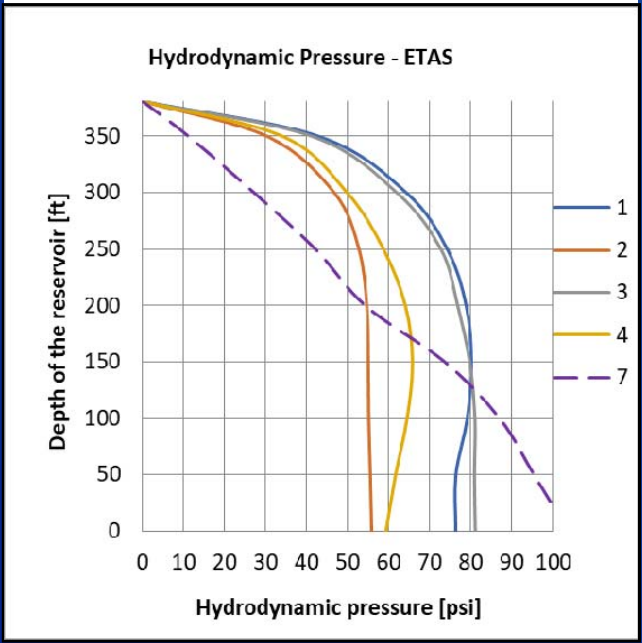

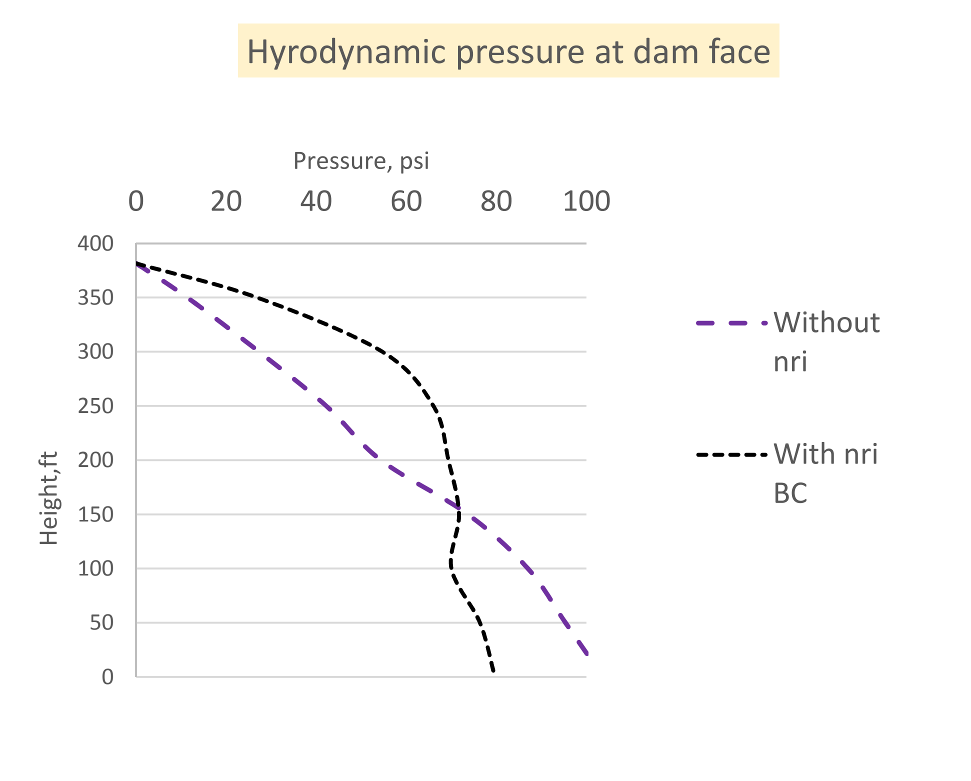

RECLAMATION

Effect of damping

α value in Rayleigh damping equation	Damping in {Dam+foundation+reservoir}	Damping in {Dam+foundation}
1.5	9.3%	8.4%
1.1	8.6%	7.5%
0.75	8.4%	6.4%
0.60	7.5%	5.3%

RECLAMATION

Effect of damping

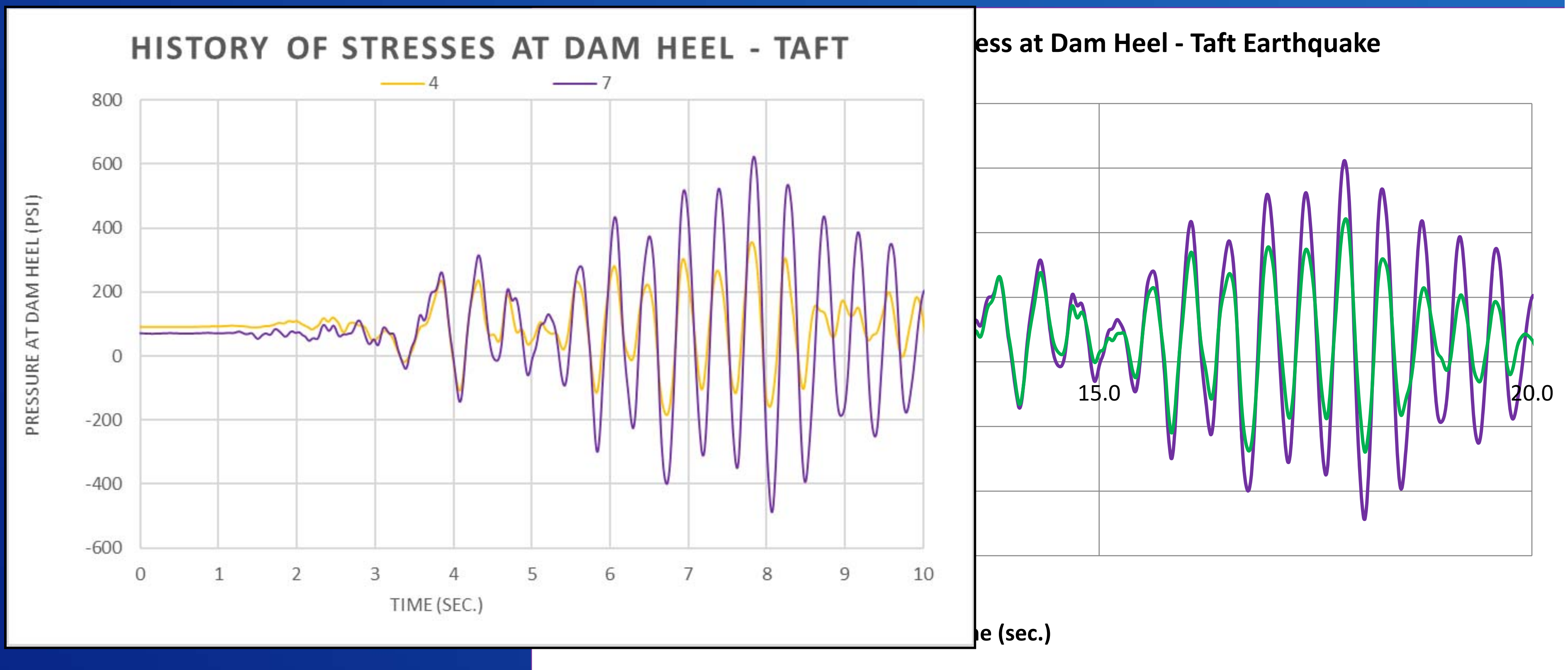

RECLAMATION

Effect of damping

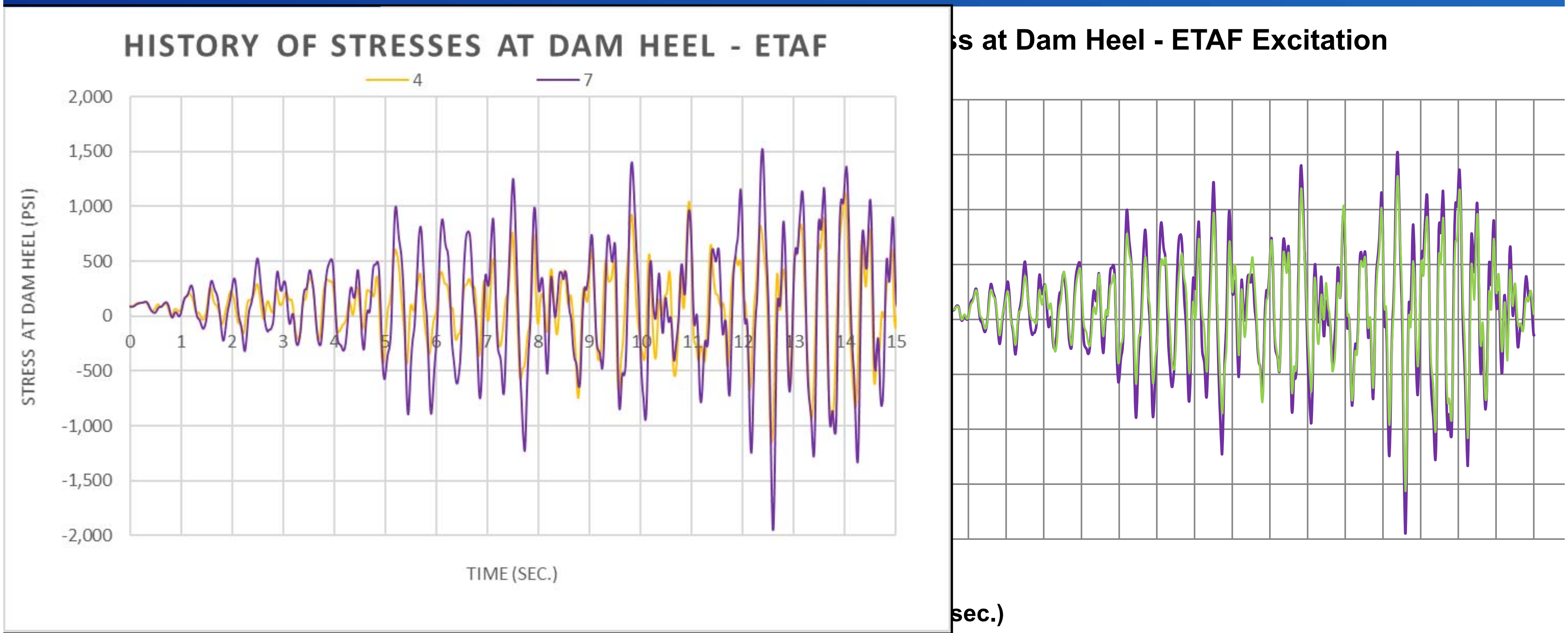

RECLAMATION

USSD Numerical Workshop

Evaluation of Numerical models and input parameters in the analysis of concrete dams

Yusof Ghanaat

Zachary Harper

Quest Structures, Inc.

Orinda, California

Finite Element Model

Case A – Static Analysis

- 1,664 3D 8-node concrete elements
- 10,880 3D 8-node fluid elements
- 23,552 3D 8-node rock elements
- 46,335 nodes

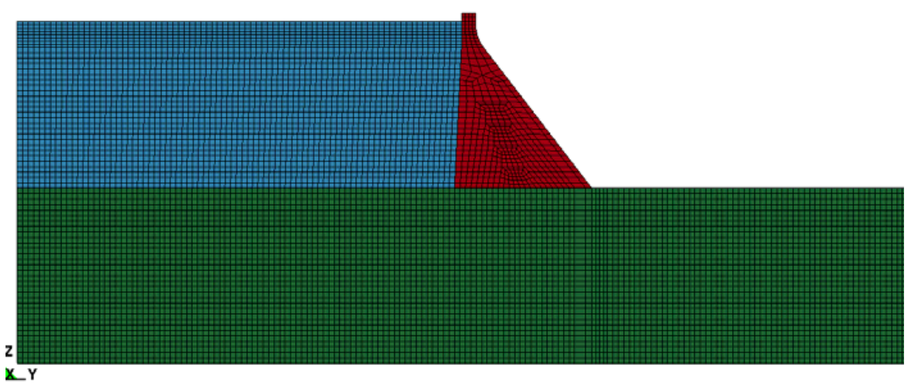

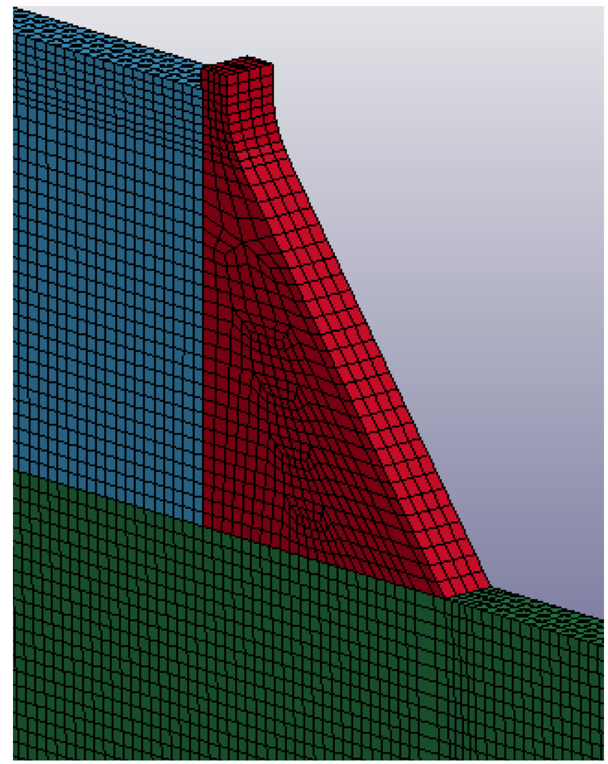

Why Does Stiffer Foundation Generate Identical or Slightly Higher D/S Relative Displacement?

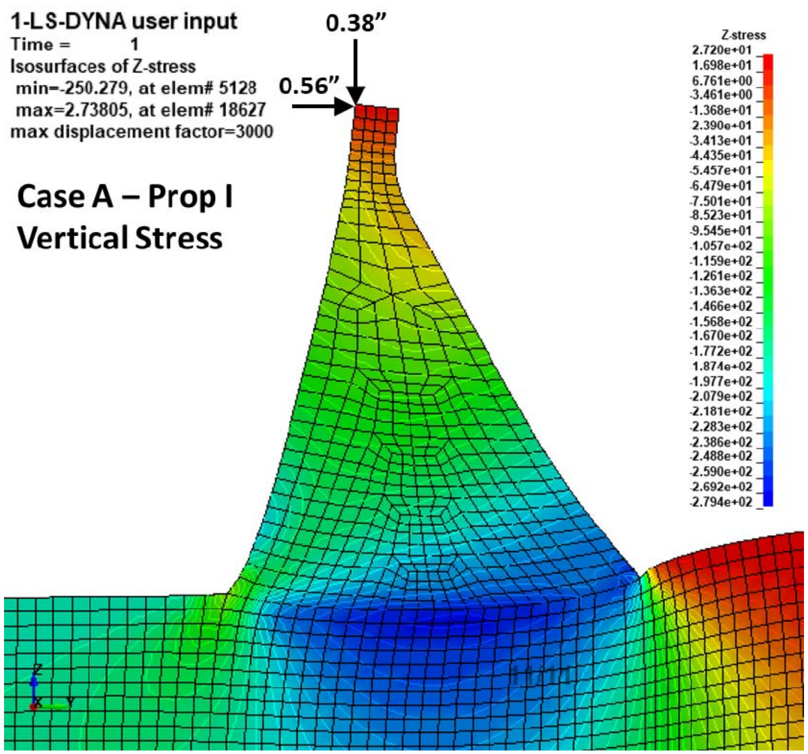

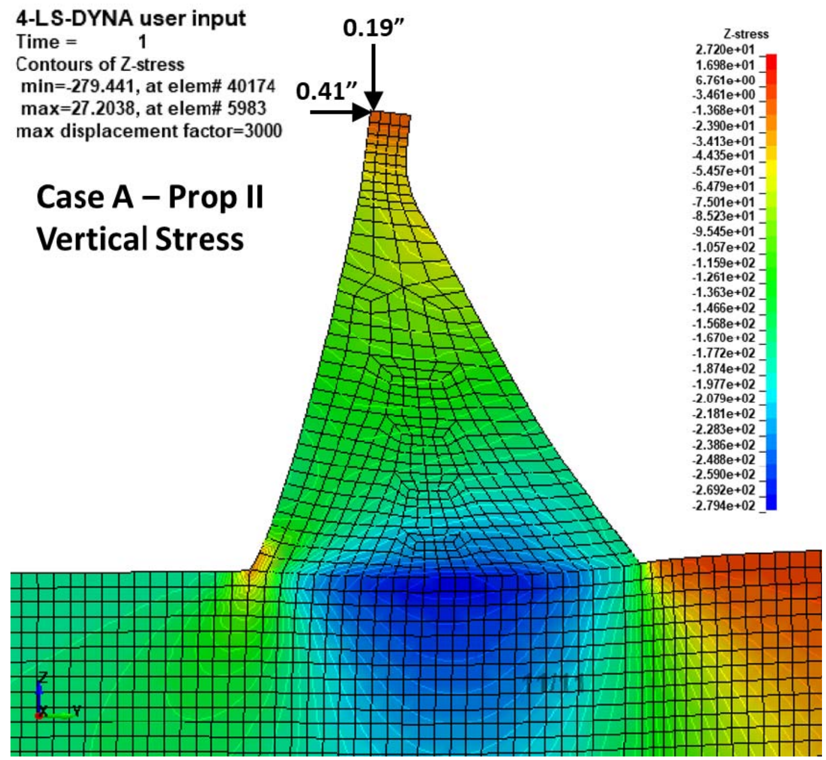

Sinking and rotation of dam on more flexible foundation results in slightly smaller relative D/S movement

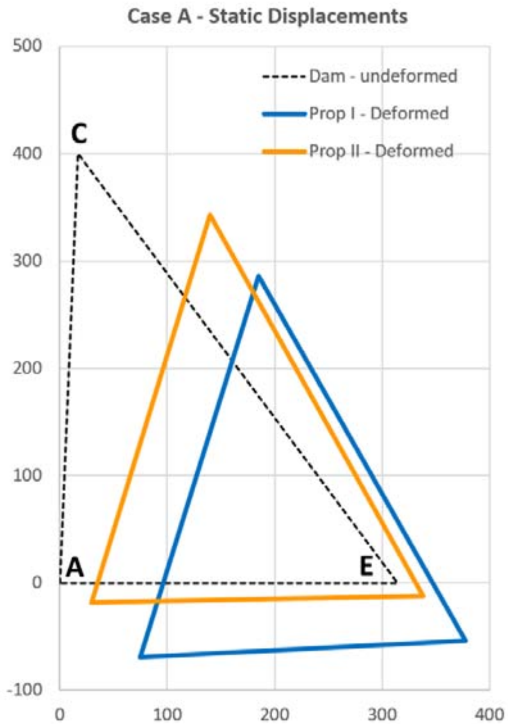

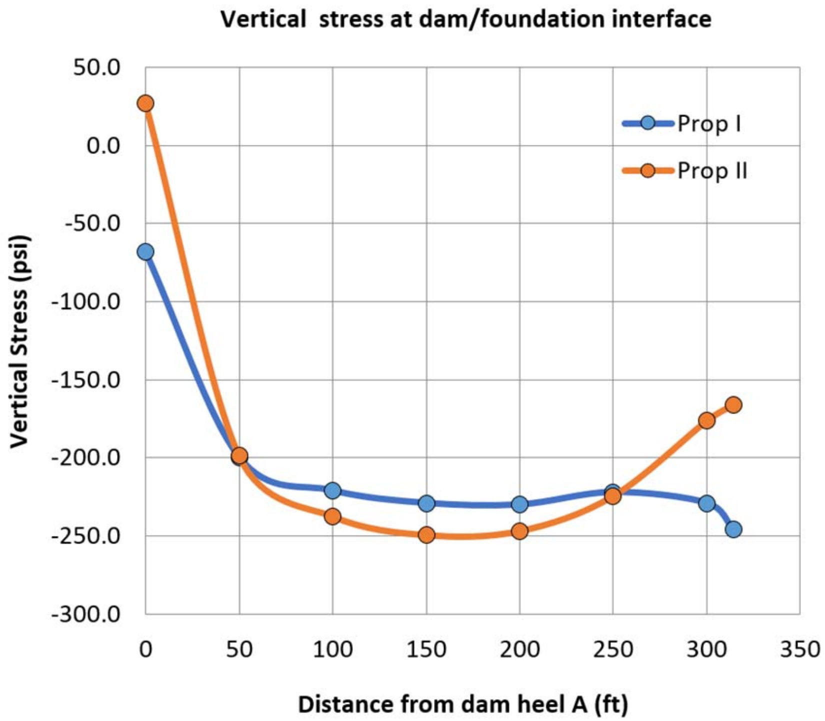

Case B
Comparison with 1D Site Response Analysis (Deconvolution)

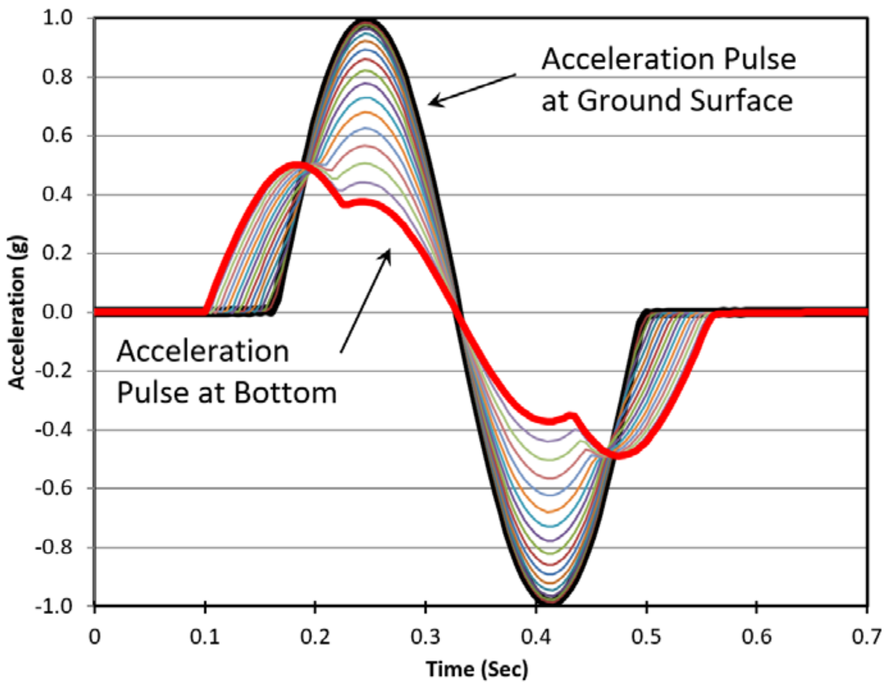

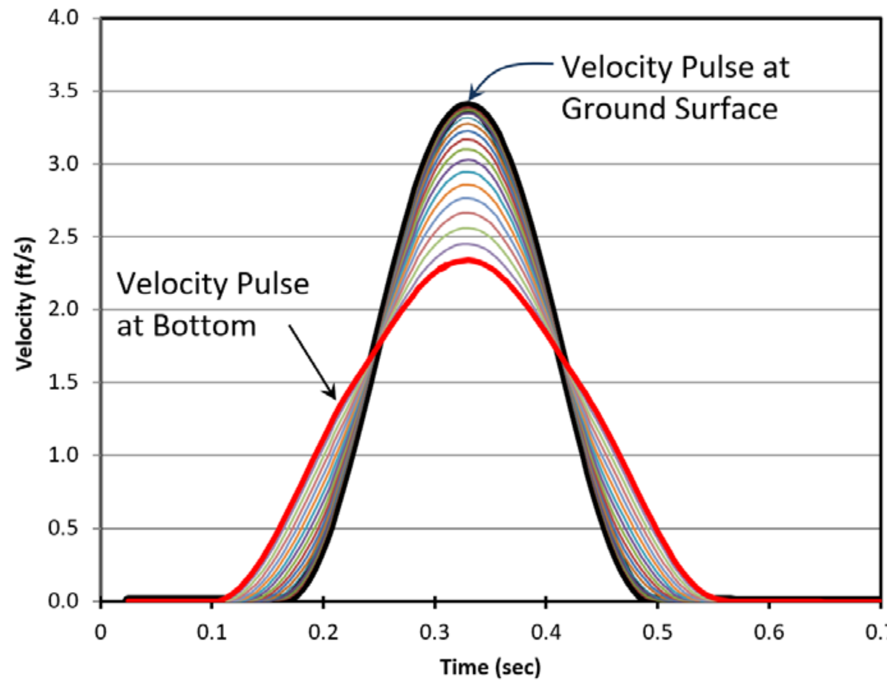

Horizontal Excitation

- Amplitudes close to 1D response for intermediate and long models
- But wave forms are not

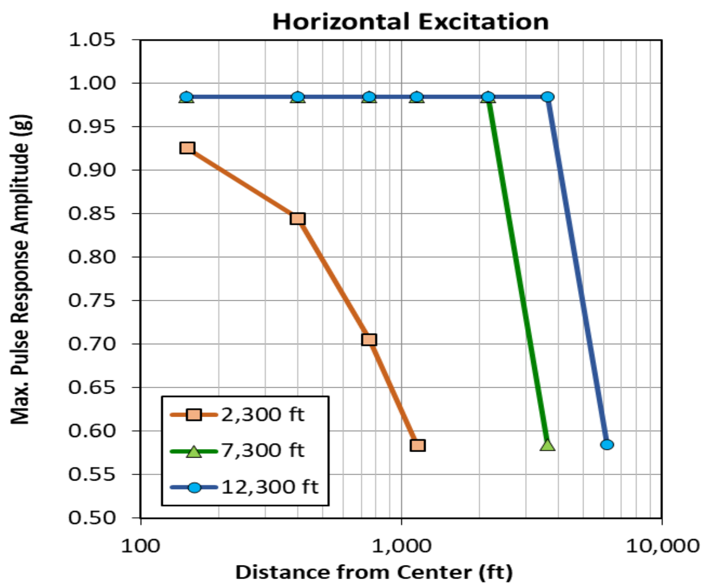

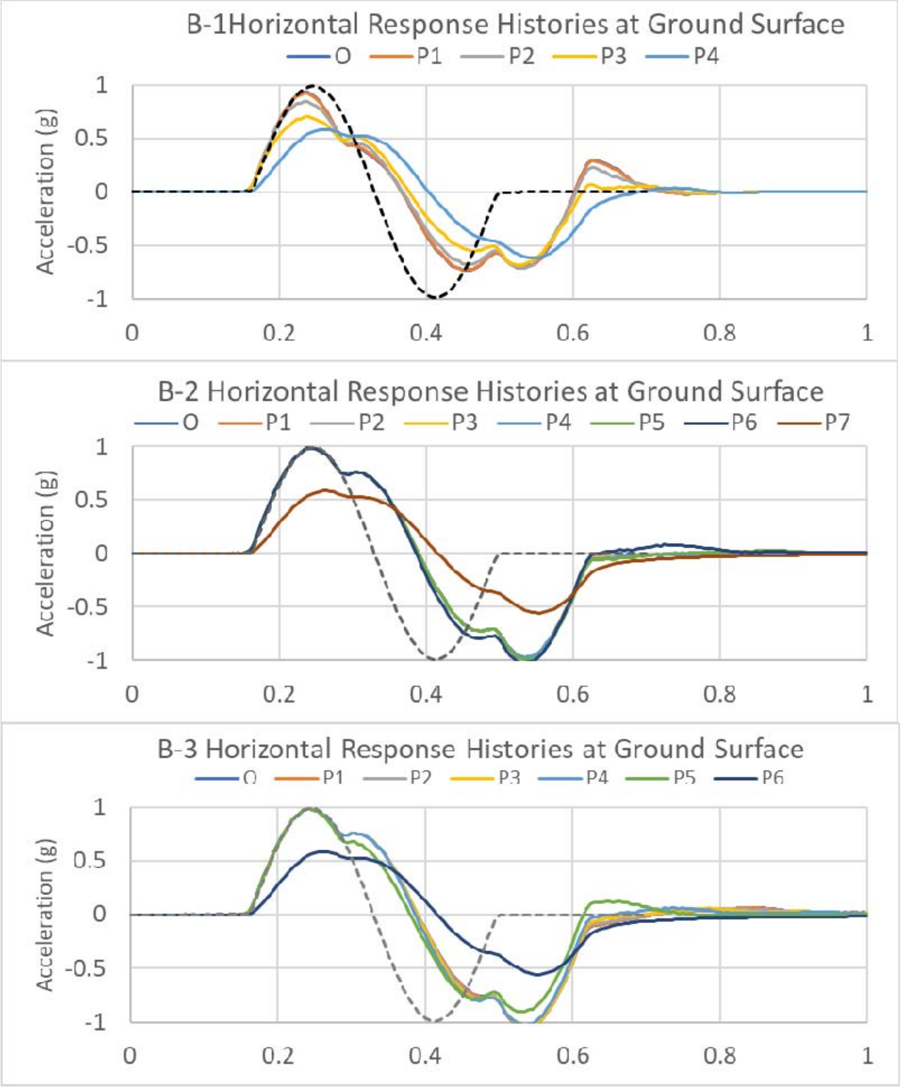

Vertical Excitation

- Response amplitudes are 35% higher
- Wave forms have improved

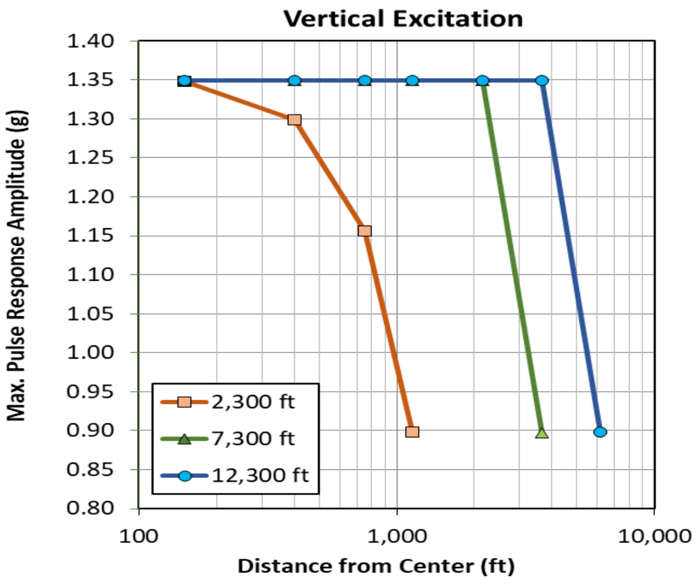

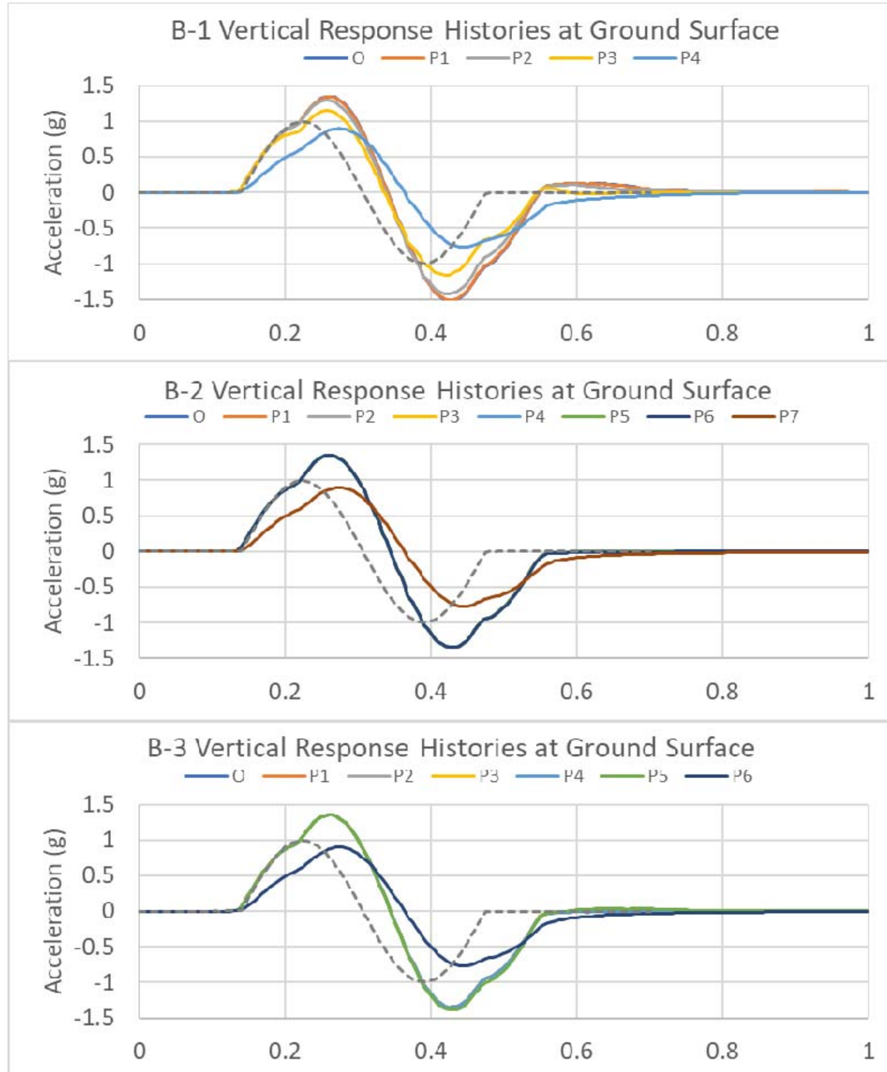

For dams on flexible foundations, addition of Water May not always reduce natural frequencies

Case D-1a

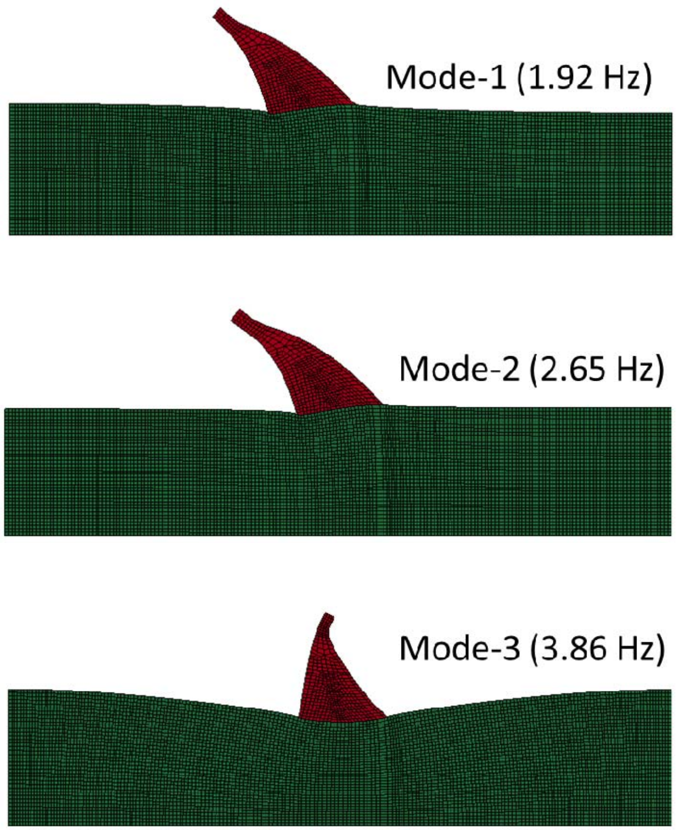

Case D-2a

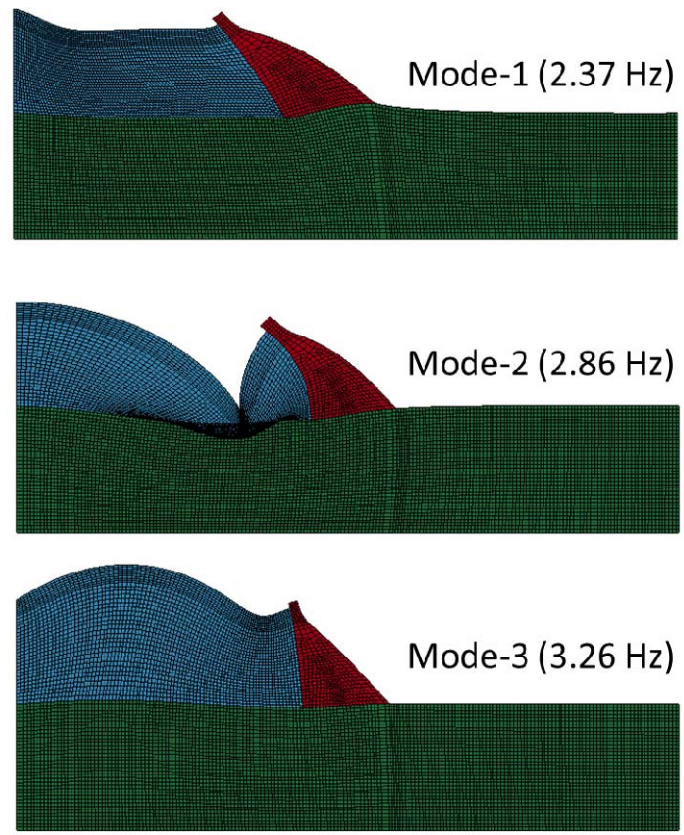

For dams on stiff foundation, addition of Water expected to reduce natural frequencies

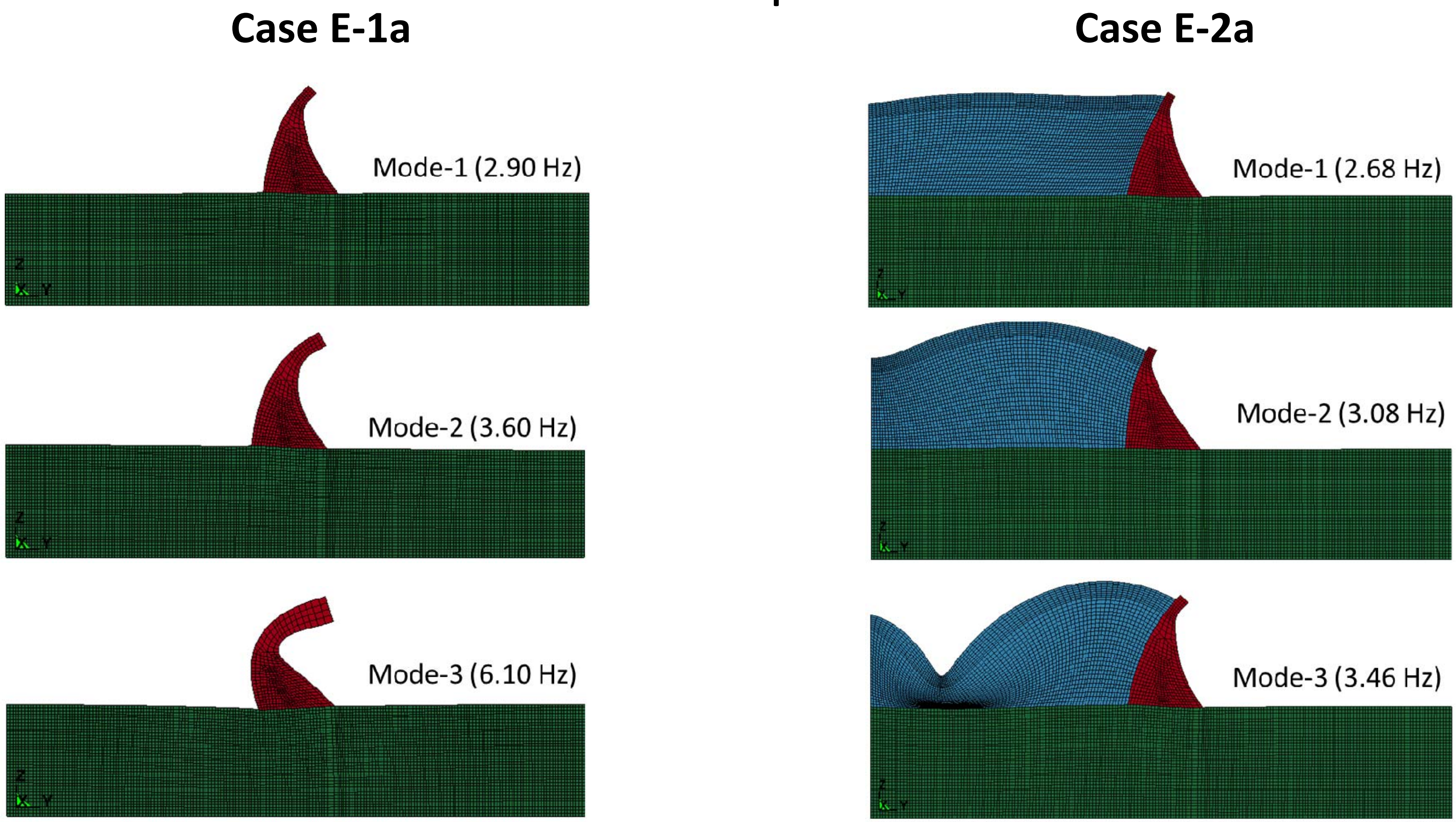

Case D & E

Dam, Foundation, and Water with PML

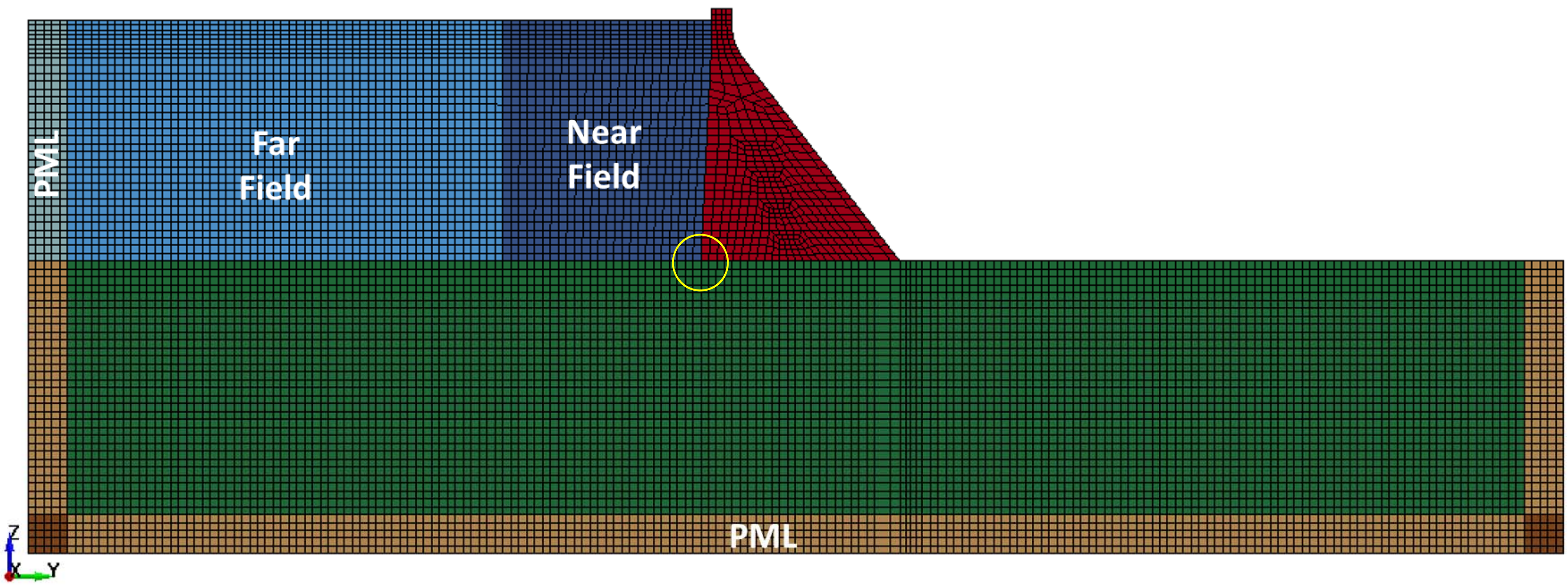

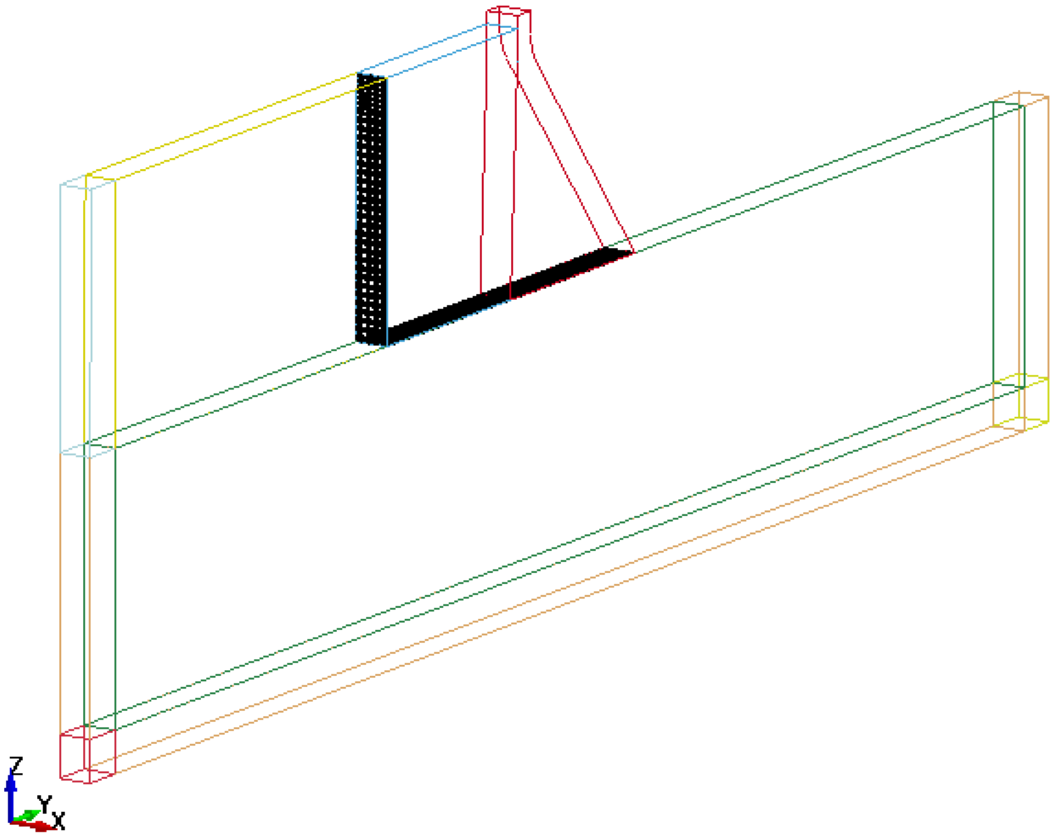

Case D-2: Transient Run

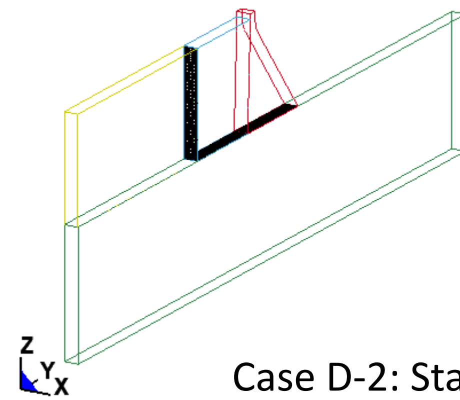

Case D-2: Static Run

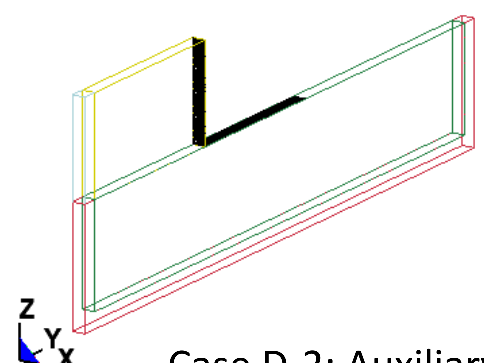

Case D-2: Auxiliary Run

Suggestions for Future Workshops

- Formulate benchmark problems to investigate and compare fluid modeling approaches
- Expand Case-B foundation response analysis considering various boundary conditions and seismic input for flat and canyon sites
- Formulate benchmark problems to address significant nonlinear mechanisms such as contraction joint opening/closing and cracking followed by sliding and overturning